PHARMACOLOGICAL CONTROL OF MEMBRANE CURRENTS GENERATING THE AFTER-HYPERPOLARIZATION OF RAT SYMPATHETIC NEURONES

by

Stephen Mark Duffy

A thesis presented for the degree of Doctor of Philosophy

University of London

Department of Pharmacology,

University College London,

Gower Street,

London, WC1E 6BT.

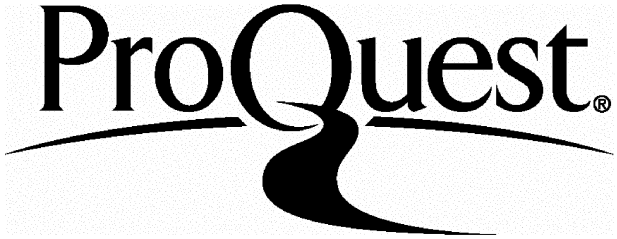

Abstract

Sympathetic neurones show a calcium-dependent after-hyperpolarization (a.h.p.) following action potentials. This study has investigated the currents responsible for generating the a.h.p. in the rat superior cervical ganglion (s.c.g.), and their inhibition by pharmacological agents.

The calcium current (I_{Ca}) was recorded from voltage-clamped dissociated s.c.g. neurones using Cs^+ filled electrodes. I_{Ca} was abolished by removal of external Ca^{2+}, and blocked by inorganic divalent cations (IC_{50}):- Cd^{2+}(3.3μM), Cu^{2+}(87μM), Zn^{2+}(190μM), Ni^{2+}(520μM), Mn^{2+}(580μM) and Co^{2+}(1.1mM) and trivalent cations:- Gd^{3+}(2.6μM), Lu^{3+}(72μM) and La^{3+}(3.0μM). Noradrenaline suppressed I_{Ca} by approximately 50% (EC_{50}; 87nM) and slowed the rising phase of the current. I_{Ca} was also reduced by the α_2-adrenergic agonists, UK14304, clonidine and oxymetazoline (EC_{50}; 37,57 and 27nM respectively) whilst α_1- and ß-adrenergic agonists had no effect in low concentrations. The inhibition by noradrenaline was antagonised by phentolamine, yohimbine and prazosin with pK_B values of 8.0, 7.5 and 5.4 respectively, indicating that adrenergic suppression of I_{Ca} is mediated by an α_2-receptor. I_{Ca} was also reduced by the muscarinic agonist methacholine.

The current underlying the a.h.p. (I_{AHP}) was investigated in intact and dissociated neurones using both intracellular and whole-cell electrodes. The current was characterised as a small slowly decaying outward current following depolarizing voltage commands. A 37mV shift in reversal potential was observed as extracellular potassium was raised from 4.8 to 20mM confirming that I_{AHP} was carried by potassium ions. Calcium dependence was shown by removal of extracellular calcium and block by Cd^{2+}. The current was blocked by d-tubocurarine (dTC) and apamin but was insensitive to tetraethylammonium ions, distinguishing it from the fast calcium-activated potassium current, I_C. Noradrenaline and methacholine suppressed I_{AHP}.

Control of I_{AHP} by calcium was investigated further. Reducing the calcium load (by reducing extracellular calcium, blocking Ca^{2+} entry with Cd^{2+} or decreasing the duration of the voltage commands) increased the rate of decay. dTC (which blocked I_{AHP} without effect on I_{Ca}) had no effect upon the rate of decay of I_{AHP}. These observations suggest that the rate of decay of I_{AHP} is dependent upon the size of calcium load. Inhibition of I_{AHP} by both noradrenaline and methacholine showed, in addition to reduction of peak amplitude, an increase in rate of decay suggesting that the inhibition of I_{AHP} is due to suppression of I_{Ca}.

It is concluded that (1) The adrenergic suppression of I_{Ca} is mediated by α_2-receptors. (2) The a.h.p. is generated by a calcium-activated potassium current that is similar to the I_{AHP} of bullfrog sympathetic neurones. (3) The kinetics of I_{AHP} decay are determined by the calcium load. (4) Noradrenaline and methacholine inhibit I_{AHP} by reduction of the preceding calcium entry.

Acknowledgments

I am very grateful to Professor D.A. Brown for allowing me to work in his department, and for his guidance, encouragement and patience during the course of this work.

I would like to thank Dr Steve Marsh for his invaluable technical expertise, advice and moral support.

I wish to thank Pearline Benjamin and Yvonne Vallis for help with the preparation of dissociated neurones.

I also wish to thank Drs. Tim Allen, Malcolm Caulfield, Reg Docherty, Ian McFadzean, Jon Robbins and Joan Sim for encouragement and helpful discussions.

I would like to thank Sarah Davis for encouraging me to finish this thesis and for all her support.

Finally, I am very grateful to the Medical Research Council for providing financial support for this study.

Contents

List of Figures

List of tables

Chapter 1.

Introduction.

The long after-hyperpolarization of rat sympathetic ganglion cells.

The first report of a prolonged after-hyperpolarization (a.h.p.) following action potentials in rat sympathetic neurones was made by Yarowsky and McAfee (1977). It was subsequently further investigated by McAfee and Yarowsky, (1979) and Horn and McAfee (1979). In these studies, the a.h.p. was shown to have the following characteristics:

(1) It had a peak amplitude of about 12mV with a total duration around 300ms, the decay from peak amplitude varying between different cells.

(2) It reversed at -90mV and was inversely proportional in both magnitude and reversal potential to the extracellular potassium (K^+) concentration, indicating that the a.h.p. was generated by an increased K^+ conductance.

(3) The amplitude of the a.h.p. was proportional to the external calcium (Ca^{2+}) concentration, and reduced by cobalt and manganese ions, indicating a dependence upon Ca^{2+}. In addition, the a.h.p. was still recorded in the presence of tetrodotoxin (TTX) which blocks the sodium current (leaving a calcium spike), and augmented by tetraethylammonium (TEA), which also increased the duration of the calcium spike.

(4) Both the a.h.p. and the calcium spike were reversibly inhibited in a similar manner by noradrenaline.

From these observations it was suggested that the a.h.p. of rat sympathetic neurones was generated by a calcium-dependent potassium conductance. In addition, inhibition of this calcium-dependent potassium conductance by noradrenaline was suggested to be via inhibition of a voltage-dependent calcium current. In the rat sympathetic ganglion, the role of the a.h.p. is to regulate cell excitability, increasing the threshold following an

action potential, and it has been demonstrated that inhibition of the a.h.p. leads to repetitive firing of the neurone (Kawai et al, 1985; Kawai and Watanabe, 1986).

The aim of this project was to investigate the pharmacological control of the membrane currents responsible for generation of the a.h.p. in the rat superior cervical ganglion (s.c.g.). In order to achieve this, the calcium current, and the potassium current underlying the a.h.p. were recorded separately under voltage-clamp, and the effects of drugs on the two currents studied. In particular, the suppression of these currents by noradrenaline was investigated.

As two different membrane currents were investigated separately, this introduction is divided into two sections considering (A) calcium currents, and (B) calcium-activated potassium conductances.

(A) Calcium currents.

Regenerative calcium action potentials (calcium spikes) were originally recorded from crayfish muscle fibres in a recording solution containing K^+ channel blockers (Fatt and Ginsborg, 1958). Such calcium spikes have been widely described in both invertebrate neurones, for example Aplysia giant neurones (Geduldig and Junge, 1968), Helix pomata neurones (Eckert and Lux, 1976), and in mammalian neurones, for example hippocampal neurones (Schwartzkroin and Slawsky, 1977), myenteric neurones (Hirst and Spence, 1973), and dorsal root ganglion (DRG) cells (Matsuda et al, 1976). Early reports of calcium spikes recorded from sympathetic neurones include bullfrog sympathetic neurones (Koketsu and Nishi, 1969; Minota and Koketsu, 1977), and rat sympathetic neurones (Yarowsky and McAfee, 1977; McAfee and Yarowsky, 1979).

Following on from these early studies of calcium spikes, much work has been directed at investigating the calcium current (I_{Ca}) of sympathetic neurones. The initial descriptions of I_{Ca} recorded from voltage-clamped rat s.c.g. neurones were by Adams (1981), and Galvan and Adams (1982), who used TTX to block the sodium current, and

TEA and caesium (Cs^+) to block potassium currents. I_{Ca} was characterized as an inward current, activated during depolarizing voltage commands from a hyperpolarized holding potential. Activation occurred at command potentials positive to -40mV and peaked at about 0mV. This current was also shown to be dependent upon external Ca^{2+} and was blocked by cadmium (Cd^{2+}). I_{Ca} has since been more thoroughly characterized in dissociated rat sympathetic neurones using whole-cell voltage-clamp techniques (Wanke et al, 1987; Marrion et al, 1987; Hirning et al, 1988; Schofield and Ikeda, 1988). The biophysical properties of I_{Ca} in intact rat s.c.g. neurones have been determined using two electrode voltage-clamp (Belluzzi and Sacchi, 1989). I_{Ca} has also been investigated in dissociated bullfrog sympathetic neurones (Jones and Marks, 1989a,b; Lipscombe et al, 1988).

Heterogeneity of calcium currents.

Analysis of neuronal calcium currents has shown the existence of multiple types of Ca^{2+} channels. Voltage recordings from central neurones (Llinas and Yarom, 1981) revealed the coexistence of two types of calcium channels, 'low threshold' and 'high threshold' channels. Subsequent voltage-clamp recordings in chick DRG neurones demonstrated corresponding low voltage-activated (LVA) and high voltage-activated (HVA) channels (Carbone and Lux, 1984). LVA channels showed a low threshold of activation ($<$-50mV) and inactivated quickly in a voltage dependent manner. HVA channels exhibited a higher threshold of activation (about -20mV) and inactivated slowly. Investigation of LVA and HVA calcium channels in various neurones has suggested channel conductances (using Ba^{2+} as the charge carrier) of 5 to 8pS and 20 to 25pS respectively (reviewed by Bean, 1989a).

Nowycky et al (1985) further divided calcium channels into 'T', 'N', and 'L' subtypes. The 'T' channel corresponded to the LVA subtype of earlier studies. HVA channels could however be divided into the 'N' and 'L' subtypes. 'L' type channels showed a large unitary slope conductance (about 25pS) and could be activated from

relatively depolarized potentials, and inactivated slowly (as previously demonstrated for HVA channels). The 'L' type channels showed a pattern of long openings separated by short closures (Fox et al, 1987b). Characteristics of 'L' type channels are also consistent between different types of neurones (Tsien et al, 1988). The 'N' type channel exhibited characteristics between those of 'T' and 'L' type channels (Nowycky et al, 1985). Like the 'T' channel, 'N' channels require hyperpolarized holding potentials for removal of inactivation, but also showed a high threshold of activation, similar to the 'L' channel. The channel conductance was also intermediate between the 'T' and 'L' type channels, at about 13ps, using Ba^{2+} as the charge carrier (Nowycky et al, 1985). 'N' type channels show some heterogeneity between different neurones, showing differing inactivation. In the rat s.c.g., inactivation occurs with a time constant of about 500ms (Hirning et al, 1988) whilst in chick DRG neurones it is only about 70ms (Fox et al, 1987a). Similarly, single channel conductance varies between different neurones (Bean, 1989a).

The various types of calcium channels have also been distinguished in terms of their selective modulation by pharmacological agents. LVA ('T') channels show a different sensitivity to inorganic ions than HVA ('N' and 'L') channels. Low concentrations of cadmium selectively block HVA channels (Fox et al, 1987a), while nickel selectively blocks LVA channels in various preparations (Carbone et al, 1987; Fox et al, 1987a; Crunelli et al, 1989). However such ions have failed to differentially inhibit separate HVA components.

HVA currents can be separated on the basis of their differing sensitivity to Ω-conotoxin (Ω-CgTx), a 27 amino acid peptide purified from marine snail 'Conus geographus' venom (Olivera et al, 1984). Initial reports showed that Ω-CgTx selectively blocked HVA calcium channels (McCleskey et al, 1987), but failed to distinguish the 'N' and 'L' components since both the transient and steady-state components of the current were blocked (Nowycky et al, 1985). More recent work indicates a selective inhibition of an 'N' like current, rather than the 'L' type current (Kasai et al, 1987; Kasai and Aosaki, 1989; Plummer et al, 1989), although the Ω-CgTx sensitive channels

determined in these studies show different kinetic properties to the 'N' type channel of chick DRG neurones (Nowycky et al, 1985). The use of Ω-CgTx has illustrated differences between calcium currents recorded from central and peripheral neurones. In peripheral neurones, up to 90% of I_{Ca} is blocked by saturating concentrations, for example rat s.c.g. cells (Plummer et al, 1989) and bullfrog sympathetic neurones (Jones and Marks, 1989a), whist in central neurones only 40-50% of I_{Ca} is blocked (Sah et al, 1989).

Selective inhibition of the 'L' type calcium channels has been demonstrated by dihydropyridine (DHP) antagonists, for example in rat sympathetic ganglion cells (Hirning et al, 1988) where nifedipine strongly suppressed 'L' type channels without any effect on the activity of 'N' type channels. Similar results have been demonstrated in DRG neurones (Nowycky et al, 1985) where the DHP agonist BayK8644 increased the opening of 'L' type channels.

Several studies have characterized the subtypes of calcium channel contributing to I_{Ca} in sympathetic neurones. In the rat s.c.g. the current is activated at potentials positive to -35mV indicating the absence of a 'T' component (Marrion et al, 1987; Wanke et al, 1987; Schofield and Ikeda, 1988). The whole-cell current shows a transient 'N' like component and longer lasting 'L' type component (Wanke et al, 1987), although Schofield and Ikeda (1988) found no evidence for the 'N' type current since inactivation of the current was slow. Hirning et al (1988) provided clear evidence for the existence of both 'N' and 'L' type currents by recording single channels with conductances of 11 and 27pS respectively. The 'L' type channels were blocked by nitrendipine, indicating DHP sensitivity, but both 'N' and 'L' components of the whole-cell current appeared to be equally blocked by Ω-CgTx (Hirning et al, 1988). Plummer et al (1989) investigated the sensitivity of I_{Ca} to Ω-CgTx more thoroughly, showing that Ω-CgTx irreversibly blocked 80% of I_{Ca}, the current being blocked corresponding to the 'N' type current. The 'L' type current was unaffected, indicating that 'N' type channels accounted for at least 80% of I_{Ca} in rat s.c.g. cells. It was also suggested that Ω-CgTx revealed two components of the 'N' type current. This was subsequently proved

by Plummer and Hess (1991) who demonstrated that 'N' type channels exhibited two kinetically distinct components of current, a rapidly inactivating component, and a non-inactivating one, both of which were sensitive to Ω-CgTx. Individual 'N' type channels could show either type of behaviour. These observations also explain the apparent non-specificity of Ω-CgTx on whole-cell HVA currents in sympathetic neurones reported by Hirning et al (1988), since the non-inactivating component of the 'N' type current is kinetically similar to the 'L' type current, and the 'L' type component only contributes about 20% of the total current.

Recent research in sympathetic neurones has investigated 'N' type channel gating kinetics more closely, and it now appears that 'N' type channels display considerable variations in activity. In rat sympathetic neurones it has been demonstrated that 'N' type calcium channels exhibit three types of activity (Rittenhouse and Hess, 1994), in addition to the inactivating and non-inactivating components described previously. These additional patterns (modes) of activity were described as (1) large unitary current amplitude and low open probability (LLP); (2) small unitary current and low open probability (SLP); and (3) small unitary current and higher open probability (SHP). These modes were present in both inactivating and non-inactivating recordings. Bullfrog sympathetic neurones demonstrate a comparable heterogeneity of 'N' type channel activity, with at least three modes present, characterized as low-P_o, medium-P_o and high-P_o according to their probability of being open at -10mV (Delcour et al, 1993).

Transmitter modulation of calcium currents.

The inhibition of neuronal calcium currents was first reported by Dunlap and Fischbach (1978), who demonstrated that noradrenaline, γ-aminobutyric acid (GABA) and 5-hydroxytryptamine (5-HT) reduced the calcium component of the action potential. Many examples of transmitter modulation of calcium currents have since been published (reviewed by Anwyl, 1991; Dolphin, 1991 for example).

In sympathetic neurones, I_{Ca} has been shown to be suppressed by several different

neurotransmitters: noradrenaline (Galvan and Adams, 1982), acetylcholine (Wanke et al, 1987), dopamine (Marchetti et al, 1986), substance P (Bley and Tsien, 1990), somatostatin (Ikeda et al, 1987), LHRH (Bley and Tsien, 1990), and neuropeptide Y (Schofield and Ikeda, 1988). (Note, these examples present only a small proportion of the available literature describing transmitter modulation of I_{Ca} in sympathetic neurones.)

Noradrenergic suppression of calcium currents in the rat s.c.g. was first suggested by Horn and McAfee (1979) who showed inhibition of the calcium spike. These findings were confirmed by Galvan and Adams (1982) who demonstrated inhibition of I_{Ca} by noradrenaline, recorded under voltage clamp. Inhibition was mediated by an α-receptor (Horn and McAfee, 1979), a consistent feature of noradrenergic suppression of calcium currents in various neurones (see chapter 4 for a more comprehensive discussion of the type of adrenoceptor mediating inhibition of the calcium current). Noradrenergic suppression of I_{Ca} in the rat s.c.g. has more recently been demonstrated using whole-cell recordings (Song et al, 1989; Schofield, 1990), and it appears that inhibition is specific for 'N' type channels since dihydropyridine induced tail-currents are unaffected (Plummer et al, 1991). There have been no reports of the ß-enhancement of whole-cell I_{Ca} which has been observed in other preparations, for example frog sympathetic neurones (Lipscombe and Tsien, 1987), but in the absence of full investigation this can not be ruled out. A small enhancement of patch currents has been observed during cell-attached recordings (Beech et al, 1990).

Muscarinic inhibition of I_{Ca} in rat sympathetic neurones is also well documented, and was initially demonstrated in intact neurones using intracellular electrodes by Belluzzi et al (1985b). Inhibition of whole-cell calcium currents in dissociated neurones was subsequently shown (Marrion et al, 1987; Wanke et al, 1987), and was suggested to be specific for the 'N' type current since only the rapidly inactivating component was inhibited (Wanke et al, 1987) and, similarly to noradrenaline, dihydropyridine enhanced tail-currents were unaffected (Plummer et al, 1991). However, another study contradicted this showing that the sustained current was preferentially inhibited

(Logethetis et al, 1989). Recent work has clarified the situation, showing that both 'N' and 'L' type channels can be inhibited by muscarinic agonists (Mathie et al, 1992), via M_4 and M_1 receptors respectively (Bernheim et al, 1992).

The mechanism by which neurotransmitters inhibit I_{Ca} has been extensively studied, and models have been proposed to account for their action. Many studies have demonstrated that in addition to inhibiting peak current, the activation of I_{Ca} is slowed, for example by Marchetti et al (1986), Bean (1989b), Grassi and Lux (1989). This was initially attributed to a specific block of 'N' type currents revealing a slowly activating 'L' type component, but more recent reports suggest an inhibition of a single HVA component (reviewed by Swandulla et al, 1991). In addition, inhibition is unaffected by positive holding potentials at which 'N' type channels would be expected to be inactivated (Kasai and Aosaki, 1989). Also, inhibition is removed by large positive voltages (Bean 1989b; Marchetti et al, 1986), or by conditioning prepulses (Grassi and Lux, 1989), indicating that inhibition can not be a simple blocking of a proportion of open channels. Models have been proposed, for example by Bean (1989b), Grassi and Lux (1989), Swandulla et al (1991), suggesting that the slowed activation of I_{Ca} in the presence of transmitter is caused by a time and voltage dependent recovery of transmitter inhibited channels (see chapter 3 for a discussion of these models).

The signal transduction mechanisms by which neurotransmitters suppress I_{Ca} have also been studied. Initial reports, for example, in chick DRG cells (Holz et al, 1986) and rat DRG cells (Dolphin and Scott, 1987) showed a role for guanosine 5'-triphosphate-binding proteins (G-proteins), and it has subsequently been established that suppression of I_{Ca} in many neurones is mediated by G-proteins (reviewed by Carbone and Swandulla, 1989; Anwyl, 1991; Dolphin, 1991). In rat sympathetic cells, early reports showed muscarinic inhibition of I_{Ca} to be mediated by a pertussis toxin-sensitive G-protein (Wanke et al, 1987; Song et al, 1989), though there was conflicting evidence regarding the mechanism of noradrenaline's inhibition, with Song et al (1989) reporting a pertussis toxin-insensitive block and Schofield (1991) reporting a pertussis toxin-sensitive block. More recent studies investigating muscarinic and adrenergic suppression

of I_{Ca} have revealed the existence of multiple transduction mechanisms (Beech et al, 1991; Bernheim et al, 1991; Beech et al, 1992; Mathie et al, 1992). Muscarinic inhibition of 'N' type channels is proposed to be mediated by three pathways, two of which are rapid and membrane delimited and the other is slow and via a diffusable second messenger (Beech et al, 1992). The slow pathway is pertussis toxin-insensitive and voltage independent (Beech et al, 1992) and is blocked by BAPTA in the recording pipette (Bernheim et al, 1992). The two fast pathways can be distinguished on the basis that one is pertussis toxin-sensitive and voltage-dependent, while the other is pertussis toxin-insensitive and is not voltage-dependent (Beech et al, 1992). Adrenergic suppression is proposed to be mediated via the two fast membrane delimited pathways, explaining the previous conflicting reports on the pertussis toxin-sensitivity of adrenergic receptors. Mathie et al (1992) have also demonstrated that the slow muscarinic pathway inhibits 'L' type channels as well as 'N' type channels. It is therefore apparent that neurotransmitters inhibit I_{Ca} in rat sympathetic neurones by multiple mechanisms. Experiments in bullfrog sympathetic neurones indicate that neurotransmitter suppression of I_{Ca} is similarly complicated with at least two G-proteins involved (Elmslie, 1992)

Functional role of I_{Ca}.

Although the role of I_{Ca} in generating the a.h.p. in sympathetic neurones is of primary interest in this study, neuronal calcium currents serve many functions such as mediating transmitter release (Katz, 1969), controlling excitability (Tsien et al, 1988), and playing a role in regulating neuronal growth (Kater et al, 1988). The various responses generated by calcium entry also appear to be mediated by specific subtypes of calcium channel (Tsien et al, 1988). For example, 'T' type channels contribute to the generation of regular (pace-maker) depolarizations in cardiac muscle cells (Hagiwara et al, 1988) and in central neurones (Llinas and Yarom, 1981; Jahnsen and Llinas, 1984; Burlhis and Aghajanian, 1987). 'N' type channels have been suggested to be

predominantly responsible for transmitter release from nerve terminals (Miller, 1987) since calcium influx in synaptosomal preparations is inhibited by Ω-CgTx, but is resistant to dihydropyridines (Reynolds et al, 1986). 'L' type channels have also been demonstrated to contribute to transmitter release, for example release of substance P from DRG neurones (Perney et al, 1986; Rane et al, 1987), and it has been suggested (Hirning et al,1988) that 'L' type channels may predominate in release of large peptide containing vesicles from nerve terminals.

In sympathetic neurones, calcium entry via voltage activated calcium channels appears to have two main functions:

(1) Facilitation of transmitter release. The role of 'N' type channels has been shown in rat s.c.g. neurones by inhibition by Ω-CgTx and insensitivity to DHP antagonists (Hirning et al, 1988). In addition, inhibition of I_{Ca} has been proposed to be the mechanism by which transmitters reduce noradrenaline release from sympathetic neurones (Starke, 1987), and adrenergic inhibition of noradrenaline release from frog sympathetic neurones has been shown to be mediated via inhibition of 'N' type channels (Lipscombe et al, 1989).

(2) Activation of calcium-dependent potassium conductances. Such conductances have been proposed to play a role in spike repolarization (Adams et al, 1982a), generation of the a.h.p. (McAfee and Yarowsky, 1979) and modulation of firing characteristics (Kawai et al, 1985; Kawai and Watanabe, 1986; Goh and Pennefather, 1987).

It is this second consequence of calcium entry that will be considered in the second part of this chapter.

(B) Calcium-activated potassium conductances.

The first observation of a potassium conductance dependent upon intracellular calcium was made in human erythrocytes by Gardos (1958). Later experiments (Meech and Strumwasser, 1970) in Aplysia neurones demonstrated that microinjection of

calcium hyperpolarized the cell, via an increase in potassium conductance, leading to the proposal of a calcium-activated potassium conductance, $G_{K(Ca)}$. Such conductances have since been reported in a variety of neurones, for example in rat sympathetic ganglion cells (McAfee and Yarowsky, 1979; Brown et al, 1982), bullfrog sympathetic ganglion cells (Adams et al, 1982a; Pennefather et al, 1985; Kuba et al, 1983), guinea-pig myenteric neurones (Morita et al, 1982), in central neurones (Seagar et al, 1984; Zhang and Krnjevic, 1986; Lancaster and Adams, 1986), and also in non-neuronal preparations, for example in hepatocytes (Cook and Haylett, 1985), smooth muscle cell (Gater et al, 1985) and skeletal muscle (Romey and Lazdunski, 1984; Traore et al, 1986).

$G_{K(Ca)}$ in peripheral ganglion cells.

In peripheral ganglion cells there appear to be at least three types of $G_{K(Ca)}$, which can be distinguished in terms of their voltage sensitivity, their time-course and their pharmacological characteristics.

(1) In sympathetic ganglion cells a large rapidly activated Ca^{2+}-activated K^+ current (designated I_C) has been observed (Adams et al, 1982a; MacDermott and Weight, 1982; Brown et al, 1983). I_C shows a strong voltage dependence (independent of the voltage sensitivity of calcium channels) demonstrated by intracellular injection of Ca^{2+} to bypass the calcium channels (Adams et al, 1982a). This current also activates and de-activates rapidly, with de-activation being very rapid at normal resting potentials. I_C is blocked by TEA, with 5mM TEA causing a virtually complete block, but has proved insensitive to 1mM 4-aminopyridine (4-AP) (Adams et al, 1982a). I_C is also insensitive to apamin (Brown et al, 1983). The single channels generating I_C have been characterized (Smart, 1987) and have a slope conductance of about 200pS (using an external K^+ concentration of 150mM). These channels were blocked by TEA, quinine and d-tubocurarine (dTC), but were insensitive to apamin. I_C has been suggested to play

an important role in spike repolarization (Adams et al, 1982a; Lancaster and Pennefather, 1987).

(2) Sympathetic neurones also possess a slowly decaying $G_{K(Ca)}$ generating the a.h.p. described at the beginning of this chapter. The current underlying this slow conductance has been investigated in bullfrog sympathetic ganglion cells where it has been designated I_{AHP} (Pennefather et al, 1985), and showed the following characteristics:

(a) The current was activated by either action potentials recorded using a 'hybrid clamp' technique which switched from current clamp to voltage clamp immediately following an action potential, or by depolarizing voltage commands in voltage-clamped neurones.

(b) Decay of I_{AHP} was slow (time constant approximately 200-300ms) and was independent of voltage over a wide range of membrane potentials.

(c) Calcium dependence was shown by removal of Ca^{2+}.

(d) The current was insensitive to TEA but was reduced by apamin.

Other studies have also indicated inhibition of this slow $G_{K(Ca)}$ by apamin (Kawai and Watanabe, 1986), dTC (Nohmi and Kuba, 1984), hexamethonium (Kawai et al, 1985) and leiurotoxin I (Goh et al, 1992a). Partially purified charybdotoxin has been shown to block I_{AHP} (Goh and Pennefather, 1987), though a later study using low concentrations of a more highly purified sample of charybdotoxin demonstrated a selective block of I_C (Goh et al, 1992a).

It has also been suggested (Goh and Pennefather, 1987) that the time-course of I_{AHP} is controlled by intracellular calcium (see below).

The single channels underlying I_{AHP} in sympathetic neurones have not been described, but the channels generating a similar current in cultured rat skeletal muscle have been observed (Blatz and Magleby, 1986) and have a single channel conductance of 10-14pS with the necessary properties to account for the a.h.p., for example high calcium sensitivity and block by apamin.

(3) Another type of $G_{K(Ca)}$ has been observed in myenteric ganglion cells (Hirst et al, 1985) which has a slow activation and lasts several seconds (much longer than the a.h.p. described above). This current is insensitive to dTC and low concentrations of TEA (North and Tokimasa, 1987) but is blocked by 4-AP (Hirst et al, 1985).

The available evidence suggests that the a.h.p. of rat sympathetic neurones is most likely to be generated by a current comparable to the slow $G_{K(Ca)}$ (I_{AHP}) of bullfrog sympathetic neurones. The rest of this chapter will therefore concentrate upon this subtype of $G_{K(Ca)}$, although the other types are mentioned where relevant.

Calcium dependence of I_{AHP}.

Although the calcium dependence of the a.h.p. has been established, there still remains the question of where the calcium that activates the a.h.p. comes from. The origin of the calcium was initially thought to be influx through calcium channels during membrane excitation, which was subsequently taken up into intracellular stores or extruded through the cell membrane (Meech 1978; Smith et al, 1983; Neering and McBurney, 1984). It has also been shown, however, that caffeine (which causes release of calcium from intracellular stores; Endo 1977) generated slow rhythmic membrane hyperpolarizations, for example in bullfrog ganglion cells (Kuba 1980; Kuba and Nishi, 1976), suggesting that intracellular release of calcium may contribute to the generation of the a.h.p. Further experiments (Kuba et al, 1983; Nohmi et al, 1983) provided possible evidence for this. An a.h.p. of longer duration was recorded using an electrode filled with K_3-citrate (originally suggested to promote intracellular release; Morita and Koketsu, 1980; but see below), than by using KCl filled electrodes. In addition, application of caffeine prolonged the a.h.p. recorded using the KCl electrode (presumably via release of intracellular calcium), but showed little effect when using a K_3-citrate electrode, when intracellular release of calcium was already being initiated. More recent evidence suggests, however, that the action of citrate is to buffer

intracellular Mg^{2+} thereby removing an inhibition of $I_{K(Ca)}$ by Mg^{2+} (Robbins et al, 1992).

However, although intracellular release of calcium by caffeine can contribute to generation of the a.h.p. under specific experimental conditions, it does not necessarily imply that this mechanism occurs during normal cell activity. More conclusive evidence was provided by Kawai and Watanabe (1989) who showed that ryanodine (which inhibits release of intracellular calcium; Sutko et al, 1985) significantly shortened the a.h.p. in rat sympathetic neurones. Thus the origin of the calcium that activates the a.h.p. appears to be both influx during the action potential and release from intracellular stores.

There is also the question of the role of calcium in controlling the size and duration of the a.h.p. In bullfrog sympathetic ganglion cells, an increased calcium influx, caused either by increasing the number of action potentials, or by increasing the extracellular calcium concentration, significantly prolonged I_{AHP} such that the rate of decay was reduced (Goh and Pennefather, 1987). Peak amplitude of I_{AHP} only showed a small increase. Similarly, when extracellular calcium was lowered, the duration of I_{AHP} became shorter, with an associated increase in the rate of decay. A comparable effect of calcium has been observed on the slow calcium-activated potassium conductance of guinea-pig myenteric neurones (Morita et al, 1982) in which the mean time constant of decay increased from 1.5 to 6 seconds as the number of action potentials was increased from 1 to 6. A similar role for calcium has been described for other physiological systems, for example the relationship between calcium load and relaxation in frog skeletal muscle (Cannell, 1986).

Comparison of intracellular calcium signals with simultaneous intracellular recordings of membrane potentials in bullfrog sympathetic neurones (Smith et al, 1983) show that the decay of the a.h.p. closely reflects the decay of intracellular calcium. Thus the available data suggests that the rate of decay of I_{AHP} is inversely related to the size of the calcium load, and reflects the removal of intracellular calcium rather than the

open time of individual channels.

Goh and Pennefather (1987) also demonstrated that pharmacological agents that inhibit the I_{AHP} channels directly without any effect on the calcium current (for example apamin), reduce only the amplitude, without affecting the rate of decay of I_{AHP}. This therefore provides a simple method of testing whether inhibition of I_{AHP} by pharmacological agents is direct or via inhibition of the preceding calcium current. Any agent which, in addition to reducing the amplitude, also increases the rate of decay of I_{AHP} is likely to do so via inhibition of I_{Ca}. Conversely any drug which inhibits I_{AHP} without also increasing the rate of decay, probably blocks the I_{AHP} channels directly.

Transmitter modulation of I_{AHP}.

Compared to I_{Ca}, reports of transmitter modulation of I_{AHP} are limited. I_{AHP} in bullfrog sympathetic ganglion cells is reduced by muscarine (Tokimasa, 1985, Tanaka and Kuba, 1987; Goh and Pennefather, 1987), though the effect is small (maximum inhibition is about 30%; Goh and Pennefather, 1987) compared to muscarine's inhibition of the M-current in the same cells (Adams et al, 1982b). Muscarine has been shown to significantly inhibit a.h.p.s in bullfrog sympathetic neurones (Tokimasa, 1984) but this large inhibition is mainly due to a reduced input resistance caused by a muscarinic-induced leak current (Jones, 1985)

Goh and Pennefather (1987) also reported that inhibition of I_{AHP} by muscarine occurred without altering the time-course of I_{AHP} suggesting that muscarinic suppression of I_{AHP} in bullfrog neurones is not mediated via inhibition of the calcium influx. This is, however, in contrast to Tokimasa (1985) who reported that muscarinic agonists did increase the rate of decay of I_{AHP}, so the action of muscarine on I_{AHP} still needs to be clarified.

Inhibition of I_{AHP}-like conductances by muscarine in other cells is variable. In myenteric neurones, the slow $G_{K(Ca)}$ is reduced, and the a.h.p. in hippocampal

neurones is completely blocked. Notably the a.h.p. in rat s.c.g. neurones has been shown to be relatively insensitive to muscarine (Brown et al, 1986), although this has not been studied in detail.

Inhibition of I_{AHP} by noradrenaline in sympathetic neurones has not been reported, although inhibition of the a.h.p. in the rat s.c.g. is well established (Horn and McAfee, 1979). Since this inhibition is accompanied by a comparable inhibition of the calcium spike (Horn and McAfee, 1979) and inhibition of I_{Ca} has been demonstrated (see earlier) it is likely that inhibition of the a.h.p. current in the rat s.c.g. is via inhibition of I_{Ca}.

Functional role of I_{AHP}.

The principle effect of I_{AHP} is the generation of the after-hyperpolarization, which reduces neuronal excitability following action potentials. The effect this has on firing characteristics is most clearly illustrated by the use of pharmacological agents to block I_{AHP}. Goh and Pennefather (1987) demonstrated that block of I_{AHP} in bullfrog neurones by dTC increased the number of spikes evoked during current commands in current-clamp, and also increased the time over which adaptation occurred. Similar observations have been made on the a.h.p. in the rat s.c.g. using hexamethonium (Kawai et al, 1895) and apamin (Kawai and Watanabe, 1986). It was also shown that apamin prevented transmission failure to submaximal stimuli during the a.h.p., and it was concluded that the function of the a.h.p. was to suppress subsequent activity following an initial action potential (Kawai and Watanabe, 1986).

Aims of this thesis.

The a.h.p. of rat sympathetic neurones has been characterized, and its role in controlling cell excitability, and modulation by neurotransmitters previously shown (see earlier). The general aim of this thesis is to investigate the currents underlying the a.h.p.

in the rat s.c.g. and to study the pharmacological modulation of these currents. In order to achieve this, the calcium current, and the potassium current underlying the a.h.p. were recorded separately under voltage-clamp. More specifically, the objectives of this project were as follows:-

(1) To record I_{Ca}, investigate suppression by noradrenaline and to determine what subtype of adrenoceptor is responsible for mediating the action of noradrenaline. Investigation of calcium-dependent potentials suggested an α_2-receptor (McAfee et al, 1981), but at the time the experiments in this project were performed, this had not been confirmed for I_{Ca} recorded in isolation. Furthermore no detailed evaluation of agonist and antagonist potencies has been attempted, and investigation in this project was considered relevant since the receptor mediating suppression of I_{Ca} in other preparations does not in all cases conform to classical α_2-receptors. This is considered further in chapter 4.

(2) To record the current underlying the a.h.p. and characterize the properties of this current. It is important to be able to distinguish the current from the other potassium currents present in sympathetic neurones. The current underlying a similar a.h.p. in bullfrog sympathetic neurones (I_{AHP}) has been characterized (Pennefather et al, 1985), and it is interesting to determine if the current in rat sympathetic neurones is similar. The current underlying the a.h.p. in dissociated rat s.c.g. neurones has been recorded (Marrion et al, 1987), but has not been investigated in detail.

(3) Investigate the importance of calcium influx on the a.h.p. current, and to determine how the calcium load affects the magnitude and rate of decay of the current. Rate of decay of I_{AHP} in bullfrog neurones decreases as calcium load is increased (Goh and Pennefather, 1987). Does a similar relationship exist in rat s.c.g. neurones, and what relationship exists between calcium influx and current amplitude? It is also possible that intracellular release of calcium can contribute to the a.h.p. current.

(4) To study the pharmacology of the a.h.p. current and to distinguish direct and indirect (via modulation of calcium entry) inhibition of the a.h.p. current. Noradrenergic inhibition of calcium-dependent potentials has been demonstrated (see earlier), but has not been investigated using voltage-clamp to record the a.h.p. current. The amplitude and duration of the a.h.p. itself are extremely sensitive to changes in resting membrane potential and conductance (because the underlying current is small: Adams and Galvan, 1986). By recording under voltage-clamp conditions, the effect that subtle changes in steady-state membrane conductance have on the a.h.p. is avoided, allowing clearer observation of I_{AHP} inhibition. Similarly, any action of muscarinic agonists can be determined. Assuming that calcium load does affect decay of the a.h.p. current, then it should be possible to distinguish between direct and indirect inhibition of the a.h.p. current as suggested by Goh and Pennefather (1987), thus eliminating the need to record the current directly after by-passing activation of I_{Ca}.

Chapter 2.

Methods.

A. Preparation of neurones for recording.

(1) Intact superior cervical ganglion.

Dissection of ganglia.

Male Sprague-Dawley rats (140-160g) were killed by nitrous oxide inhalation, and tied to a cork dissecting board. The skin over the throat was cut away, and the muscles around the carotid artery removed, taking care not to cause bleeding. With a fine pair of forceps, the carotid artery was separated from the superior cervical ganglion (s.c.g.) and vagus nerve, allowing the s.c.g. to be easily viewed under a binocular dissecting microscope (Prior). The s.c.g. was then carefully dissected free from the surrounding tissue and placed in freshly bubbled Krebs' solution. Under a higher magnification, the connective tissue sheath was removed from around the ganglion using fine forceps.

Experimental arrangements.

Recordings were carried out in a perspex bath (see Fig. 2.1A). The desheathed ganglia were pinned to the Sylgard (Dow-Corning)-coated base of the central recording chamber using fine insect pins. The s.c.g. preparation was viewed using a binocular microscope (Nikon) and illuminated from a light source via a fibre optic light pipe (Barr and Stroud).

The recording chamber was continuously perfused with Krebs' solution (freshly bubbled with 95% O_2/5% CO_2) at a rate of 5-10 ml/min, under gravity feed from 50ml

reservoirs above the recording bath. Drug solutions were placed in these reservoirs, and selected by the use of three-way taps. Care was taken not to cause fluctuations in the flow rate, or to introduce air bubbles into the chamber; both these could adversely affect recording conditions. The superfusing solution was removed by a peristaltic pump (Watson-Marlow 5025) and either re-circulated, or put to waste as appropriate. Removal of superfusing solutions was carried out at a rate sufficient to maintain a fluid depth of 2-3mm in the chamber. The earth reference electrode, consisting of a silver/silver chloride pellet (Clark Electromedical Co), was housed in a small side chamber adjacent to the central recording chamber. Junction potentials were not compensated.

Experiments were normally carried out at room temperature (20-25^{o}C), but when ambient temperature fell below this, or the effect of changed temperature was investigated, the temperature was regulated using a heat-exchange unit (designed by C.Courtice and J.V.Halliwell).

(2) Dissociated s.c.g. neurones.

Tissue culture.

Ganglia were isolated from 16-17 day old Sprague-Dawley rats, killed using nitrous oxide as described previously, and placed in L-15 medium (Gibco) kept on ice. The ganglia were desheathed, taking care to remove all connective tissue, and cut into several pieces using iridectomy scissors. The pieces were then transferred into 2 ml Hanks (Ca^{2+} and Mg^{2+} free) saline (Gibco) containing 315 μg/ml collagenase (type 1A, Sigma) and 6 mg/ml albumin (Sigma), for incubation at 37^{o}C for 15 minutes. The incubation was terminated by removing the medium and washing with 2 ml unsupplemented Hanks (Ca^{2+} and Mg^{2+} free) saline. This was then removed and the tissue incubated in a further 2 ml Hanks (Ca^{2+} and Mg^{2+} free) saline with 2.5 mg/ml trypsin (Sigma) and 6 mg/ml albumin for 30 minutes. The enzymatic incubation was

terminated by addition of 1 ml of growth medium. The pieces of tissue were then mechanically titurated through glass pasteur pipettes. The pipettes had previously been heated over a flame to constrict their tips to a diameter just sufficiently large to allow the pieces of ganglia to pass through. Usually two pipettes were used, the first having a slightly larger tip diameter than the second. The tissue suspension was triturated through each pasteur pipette 4 times. The resulting cell suspension was centrifuged through 5 ml Horse serum (Gibco) at 1000 r.p.m. for 3 minutes. The supernatant was removed, and the pellet resuspended in growth medium (0.3 ml per plate); several drops of the suspension were put into the centre of plastic culture plates (Cell Cult) which had been previously coated with laminin (Sigma) to encourage adherence of the cells to the plate.

The dissociated s.c.g. neurones were maintained in culture using a growth medium consisting of L-15 medium supplemented with 10% foetal calf serum (Gibco), 0.2 mM glutamine (Gibco), 0.6% (w/v) D-glucose (B.D.H.), 0.19% (w/v) $NaHCO_3$ (B.D.H.), 100 μg/ml penicillin-G , 100 μg/ml streptomycin (Gibco) and 1 μg/ml nerve growth factor (mouse; Sigma). The cells were kept at 37^{o}C in an atmosphere of 5% CO_2 and high humidity to prevent evaporation from the growth medium. On the day following dissociation, a further 1 ml of growth medium was added to cover each plate, and every following 3 days, 0.5 ml of the medium was removed by aspiration and replaced with fresh medium. In this way, cells could be successfully maintained in culture for many days.

The s.c.g. neurones usually adhered to the laminin coated plate within 4 hours of dissociation, and at this time appeared spherical. By the following day, the neurones showed characteristic multipolar appearance with neuritic processes which continued to grow over several days. Fig. 2.2 shows photographs taken of s.c.g. neurones 1 day and 4 days after dissociation. Investigation of calcium currents was carried out on neurones no more than 2 days after dissociation, since the growth of the neuritic processes severely hindered voltage control of the neurones resulting in poor space-clamp (see later). In an attempt to reduce neuritic growth, the amount of nerve growth factor in the medium was reduced, but this appeared to be of little help. In contrast, neurones were

left in culture for at least 3-4 days before the study of I_{AHP}. The size of the recorded current increased over this time; the current was usually too small to use until 3 days after dissociation.

Experimental arrangements.

Plates of neurones were secured in the perspex recording bath, illustrated in Fig. 2.1B, and placed on the stage of an inverted microscope (Nikon TMS, 10x eyepiece with 10x and 40x objectives). The culture plate was continuously perfused under gravity feed from reservoirs at a flow rate of 5-10 ml/min, and the perfusate re-circulated or disposed of by a Watson-Marlow 5025 peristaltic pump. The stainless steel inflow and outflow tubes were adjusted so that the neurones were covered at a constant depth of 1-2mm, the outflow tube being kept firmly against the side of the dish to prevent constant surging of the level of the Krebs' solution. The temperature of the superfusion medium was regulated, when necessary, by a heat exchange unit (see above), otherwise experiments were carried out at room temperature (20-25^{o}C). The Krebs' solution in the bath was connected to the reference electrode using an agar bridge. This consisted of a 1.5mm glass tube, containing 4% agar in 3M KCl solution. The reference electrode was a silver/silver chloride pellet set in a louer fitting (Clark Electromedical Co), in a chamber containing 3M KCl.

B. Composition of external solutions.

(1) Calcium currents.

The normal Krebs' solution for recording I_{Ca} was of the following composition (mM): NaCl (96), KCl (4.8), KH_2PO_4 (1.18), $MgSO_4$ (1.2), $CaCl_2$ (2.5), $NaHCO_3$ (25), glucose (11), TEACl (20), CsCl (2). The Krebs' solution was continuously

bubbled with a mixture of 95% O_2, 5% CO_2, and the pH adjusted to 7.4 using NaOH or HCl as appropriate. Tetrodotoxin (TTX; 0.5μM) was routinely added to the Krebs' solution to block the sodium current (I_{Na})

In experiments where Ca^{2+} was omitted, the concentration of Mg^{2+} was, in some experiments, raised to 10mM (to minimize voltage shifts due to changes in surface potential (Blaustein and Goldman, 1968). However, since this concentration of Mg^{2+} partially suppresses I_{Ca} (see Results), the concentration of Mg^{2+} was raised in an equimolar manner to replace Ca^{2+} in other experiments. This did not affect the results. To prevent precipitation of insoluble salts during investigation of inorganic blockers, $MgSO_4$ and KH_2PO_4 were replaced by $MgCl_2$ and KCl respectively.

(2) Potassium currents.

The normal Krebs' solution for recording I_{AHP} was as follows (mM): NaCl (118), KCl (4.8), KH_2PO_4 (1.18), $MgSO_4$ (1.2), $CaCl_2$ (2.5), $NaHCO_3$ (25), glucose (11). The pH was adjusted and the solution gassed as described above. Ca^{2+}-free Krebs' was modified by raising Mg^{2+} to 10 mM (see above). In experiments where high potassium Krebs' solution was used, the K^+ concentration was increased by addition of KCl and KH_2PO_4 was omitted, giving an initial K^+ concentration of 4.8mM. 0.5μM TTX (which blocks I_{Na}) and 5mM TEA (which reduces outward currents) were sometimes added to improve voltage-clamp during the depolarizing voltage commands used to evoke I_{AHP}.

C. Electrophysiological recording.

(1) Preparation of electrodes.

Impalement electrodes.

Impalement electrodes were constructed from boro-silicate fibre-containing capillary

glass (1.2mm outside diameter, Clark Electromedical Instruments) using a Brown-Flaming horizontal micropipette puller (Sutter Instruments). The electrodes were designed to have a short rigid shank, to enable electrodes to easily impale neurones rather than bending or breaking on contact. The micro-electrodes were filled with 4M potassium acetate (titrated to pH 6.9 using acetic acid), resulting in d.c. resistances of 50-100MΩ. Electrodes which had higher resistances, or which showed a varying resistance (indicating blocking of the electrode) were rejected. All electrodes were dipped in dimethlydichlorosilane (silane) to prevent creep of the Krebs' solution up the outside of the electrode, reducing electrical capacitance. Electrodes were connected to the amplifier headstage via a chlorided silver wire.

Whole-cell electrodes.

Whole-cell electrodes were constructed from boro-silicate fibre-containing capillary glass (1.5mm outside diameter, Clark Electromedical Instruments) using a two-stage horizontal micropipette puller (Campden Instruments Limited). Electrodes were coated with Sylgard (Dow-Corning) to reduce capacitance, and were heat-polished to aid the formation of high-resistance seals. For recording of potassium currents, whole-cell electrodes were usually filled with the following solution: KGluconate (120mM), KCl (50mM), $MgCl_2$ (1mM), Hepes (5mM), NaOH (3mM), Na_2ATP (1mM), at pH 6.9 (free Ca^{2+} < 10nM). For some experiments 0.5mM EGTA was included, with $CaCl_2$ added to give a free Ca^{2+} concentration of 100 nM.

For investigation of calcium currents, whole cell electrodes were filled with the following solution: CsCl (150mM), EGTA (3mM), Hepes (10mM), NaOH (2mM), at pH 6.9. For some experiments, 10mM TEA was included in an attempt to reduce contaminating potassium currents; 1mM Na_2ATP and 0.1mM GTP were also sometimes included to reduce run-down of the calcium current.

The whole cell electrodes had d.c. resistances of 4-8MΩ when filled with the filling solutions described above.

(2) Impalement and whole-cell patch formation of neurones.

Impalement electrodes were fastened to a perspex rod and lowered into either the intact ganglion or towards a cultured neurone by a 3-dimensional hydraulic micromanipulator (Narishige). Electrodes were set at vertical for the intact s.c.g., and at about 45^{o} for dissociated neurones; this was to allow clear visualization of the electrode tip with the different optics used for the different types of preparation, and had no effect on the actual impalement. Cells were impaled by lightly pressing the electrode tip against the membrane of the dissociated neurone, or the surface of the intact ganglion (with the optics used for intact ganglion recording, individual cells could not easily be visualized), and briefly over-compensating the negative capacity neutralization. To aid impalement, 0.2nA hyperpolarizing pulses of 0.2s duration were applied to the electrode. Contact with a cell was hence indicated by an apparent increase in electrode resistance. A successful impalement was shown by a drop in the potential recorded, and the development of a slow membrane capacitance. Upon impaling a cell, a hyperpolarizing current (up to 1nA) was applied and maintained for several minutes. This procedure appeared to promote the increase in membrane potential, resistance and capacitance as the membrane sealed around the microelectrode. The amount of hyperpolarizing current was continually reduced as the quality of the impalement improved. Successful impalements generally resulted in a membrane potential of -60 to -70mV, and an input resistance of 100-200MΩ.

Whole-cell electrodes were used to gain access to the interior of neurones using the method of Hamill et al (1981). Electrodes were mounted in a perspex microelectrode holder (Clark Electromedical Instruments), and gently lowered towards dissociated neurones using the Narishige micromanipulator. Prior to making contact with a neurone, positive pressure was sometimes applied to the electrode to remove debris from the surface of the neurone. The electrode tip was then slowly lowered until it was touching the membrane of a cell; this was usually characterized by a slight increase in electrode

resistance. Gentle suction was applied to the electrode to form a seal between the cell membrane and the tip of the electrode. Seal formation was characterized by a large increase in electrode resistance, usually of 1 to 10GΩ (cells with electrode seals of less than 1GΩ were rejected). Once the seal had reached a maximum, further suction was applied to break through the membrane; this was indicated by a sudden drop in electrode resistance and the development of typical membrane charging characteristics.

(3) Voltage-clamp recording.

Intracellular and whole-cell voltage-clamp recordings were made using an Axoclamp 2A amplifier (Axon Instruments) via a x0.1 headstage. The amplifier was operated in a discontinuous (switched) 'single-electrode voltage-clamp' mode, allowing both voltage-recording and current passing to be performed on a time-share basis (Wilson and Goldner, 1975). The headstage output was viewed on an oscilloscope, and the gain, capacitance neutralization and phase were adjusted for optimal performance (see Finkel and Redman, 1984). Once correctly adjusted, the switching frequency was raised to the maximum possible while still allowing the electrode voltage to decay to zero. Switching frequency was approximately 3kHz for intracellular electrodes, and between 5-7kHz for whole-cell electrodes. A duty cycle of 30% current passing, 70% voltage-recording was used.

The headstage output was continually monitored during experiments, this being important because minor variations in the bath fluid level alter electrode capacitance (adjustment of capacitance neutralization compensated for this). Also, an increase in electrode resistance (common with intracellular electrodes) was detrimental to clamp performance, although this was more difficult to compensate for and recordings often had to be aborted.

(4) Space-clamp conditions.

The electrotonic length of intact rat s.c.g. neurones has been estimated to be 1.2-2.2 (Belluzzi et al. 1985a) suggesting that intact neurones are electrically compact. During dissociation, however, the dendritic processes are cleaved leaving neurones appearing spherical. Once dissociated neurones have adhered to the culture plate, dendritic growth resumes, such that the processes are far more extensive after several days in culture compared to 1 day. Since cells were used at both 1 day and several days following dissociation, space-clamp conditions were investigated for both recording conditions. The electrotonic length of neurones at 1 day and 6 days following dissociation was calculated on the basis of the lumped soma, finite-length equivalent model of Rall (1977). Electrotonic potentials, evoked by hyperpolarizing current injections were recorded using whole-cell electrodes, and the passive membrane time constant, and superimposed faster time-constant calculated. The electrotonic length, L, was calculated using the following formula:

$$L = n\pi / (\tau_0/\tau_n - 1)^{1/2}$$

where:

τ_0 = passive membrane time constant

τ_n = faster superimposed time constant (n can be any positive integer).

Calculated mean values for 'L' were 1.2 $\pm$ 0.08 and 1.5 $\pm$ 0.05 for 1 day and 6 day old neurones respectively, similar to the values reported in intact neurones (Belluzzi et al. 1985a), and suggesting that dissociated neurones were quite compact. These values correspond to a recorded steady-state voltage of 55% and 42% respectively at the end of the dendrites compared to the electrode potential. Consequently, full voltage control of the dendrites will not be achieved, the situation being worse for I_{AHP} experiments on several day old neurones. This means that the relationship between membrane currents

and potential will be distorted, and that direct quantitative comparisons between I_{AHP} and I_{Ca} voltage-dependence can-not really be made. Poor space-clamp was illustrated in experiments by badly distorted current shapes, even though the recorded voltage indicated adequate clamp.

(5) Data acquisition and analysis.

Membrane currents and voltage protocols were routinely recorded onto a Gould 2400S chart recorder. This gave limited resolution, so for analysis of fast currents and for preparation of figures, current records from some experiments were digitized (typical sampling frequencies 1-2kHz) on-line using a Labmaster (TL-1) DMA interface (Axon Instruments) and recorded on computer (Ness PC-286). The currents were usually filtered at 0.3KHz (for recording I_{AHP}) and 1KHz (for recording I_{Ca}) prior to digitizing. Acquisition, and the subsequent analysis and plotting of the digitized data was performed using 'pClamp' software (Axon Instruments). Curve-fitting and plots of analysed data were carried out using 'Graphpad Inplot' computer software (Graphpad, California).

D. Drugs and solutions.

The following drugs were obtained from commercial sources: Sigma Chemical Corporation - (-)noradrenaline (arterenol) bitartrate, (-)adrenaline bitartrate, clonidine hydrochloride, (-)isoprenaline hydrochloride, phenylephrine hydrochloride, yohimbine hydrocloride, phentolamine hydrochloride, prazosin hydrochloride, (±)propranolol hydrochloride, tetraethylammonium chloride, tetrodotoxin, hepes, EGTA, ATP (sodium salt), d-tubocurarine chloride, methacholine chloride. UK14304 (tartrate salt) was obtained from Pfizer.

The constituents of the Krebs' solution and other inorganic salts were obtained from

BDH and were of 'Analar' grade.

Fig. 2.1 Recording baths used for electrophysiological study of neurones.

A. Illustrates the bath used for the intact ganglion preparation. The ganglion was viewed from above.

B. Illustrates the bath used for dissociated neurones. Cells were viewed from below using an inverting microscope.

A.

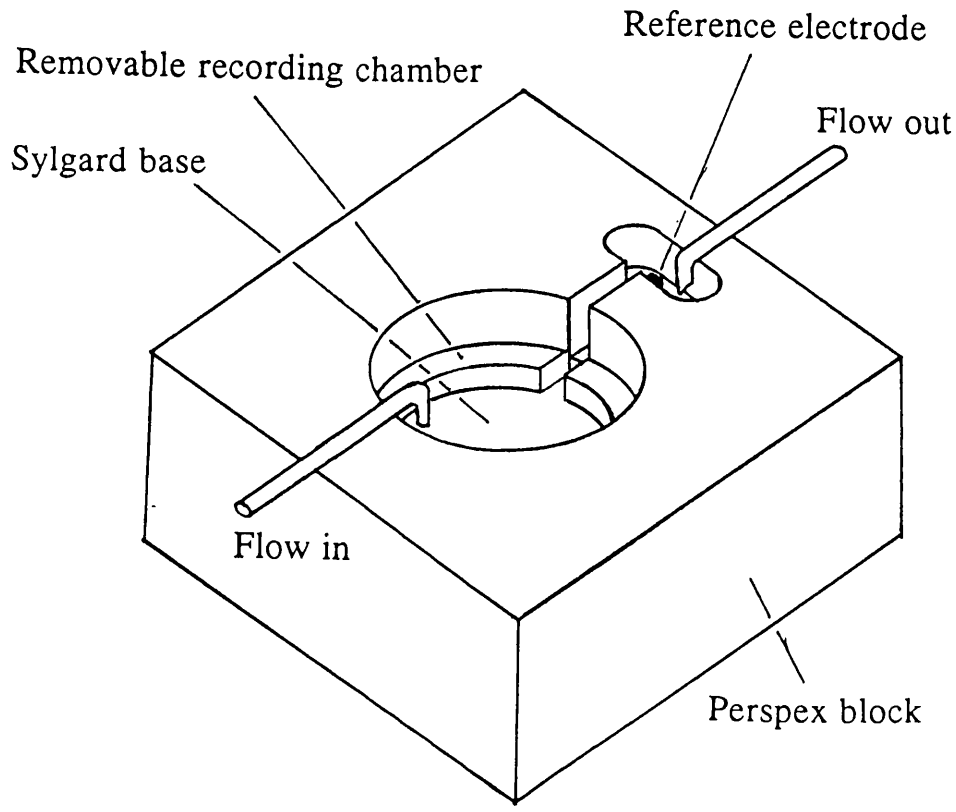
Reference electrode
Removable recording chamber
Flow out
Sylgard base
Flow in
Perspex block

B.

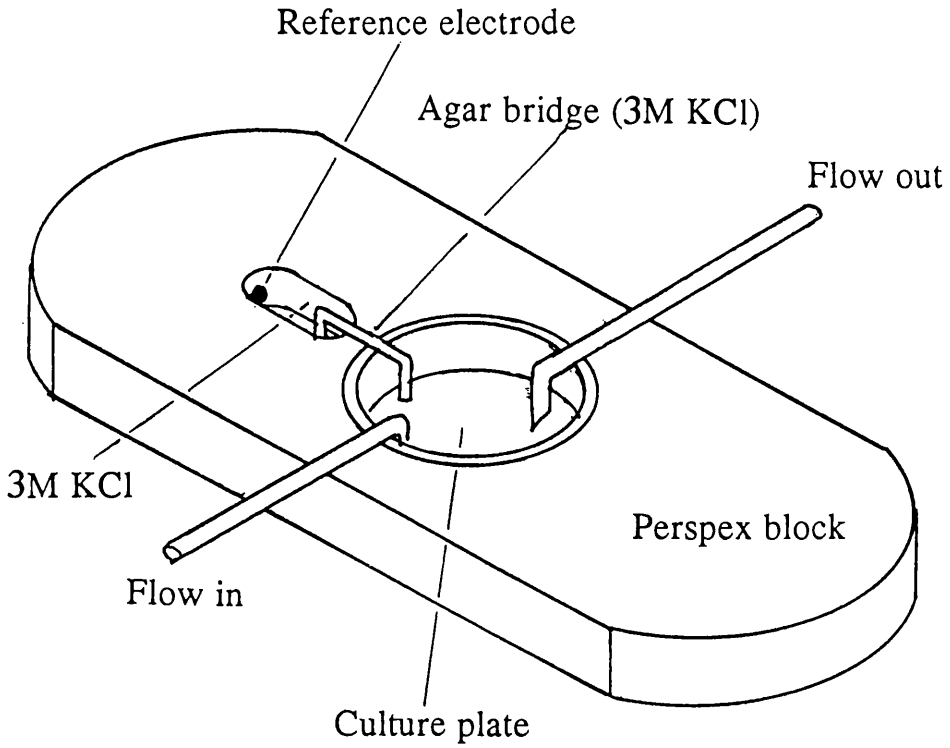
Reference electrode
Agar bridge (3M KCl)
Flow out
3M KCl
Perspex block
Flow in
Culture plate

Fig. 2.2 Photographs of dissociated s.c.g. neurones maintained in culture.

A. Shows neurones 1 day following culture, the typical age at which recordings of I_{Ca} were made.

B. Shows neurones 4 days following culture (different plate). Recordings of I_{AHP} were usually made from neurones at least this age. Beyond this time neurones appeared similar but there was greater growth of non-neuronal cells.

A.

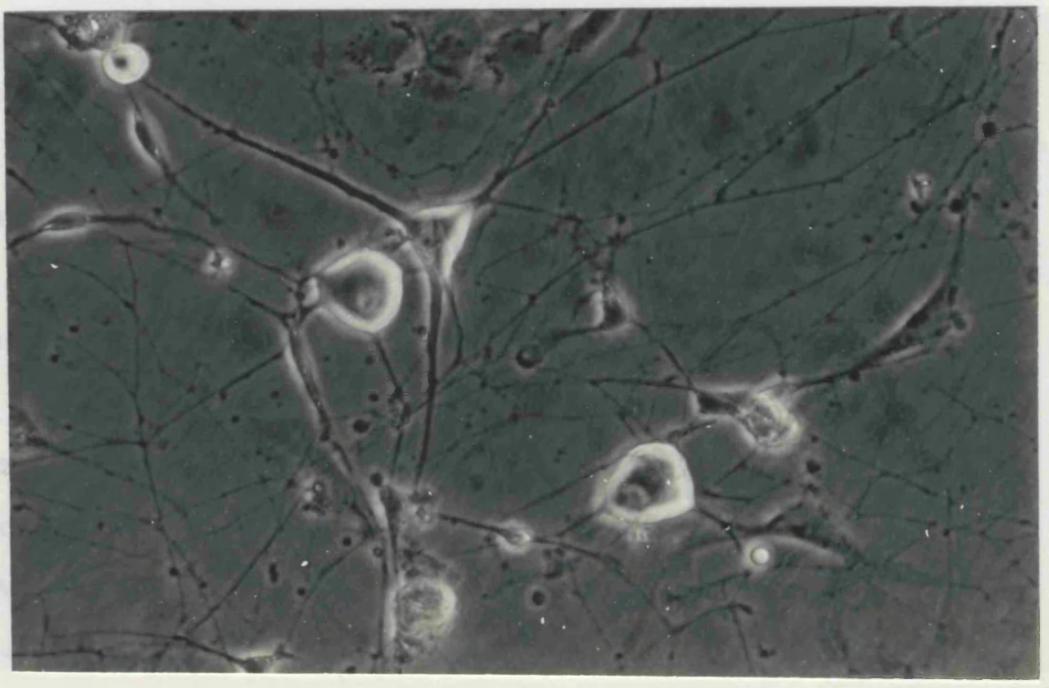

B.

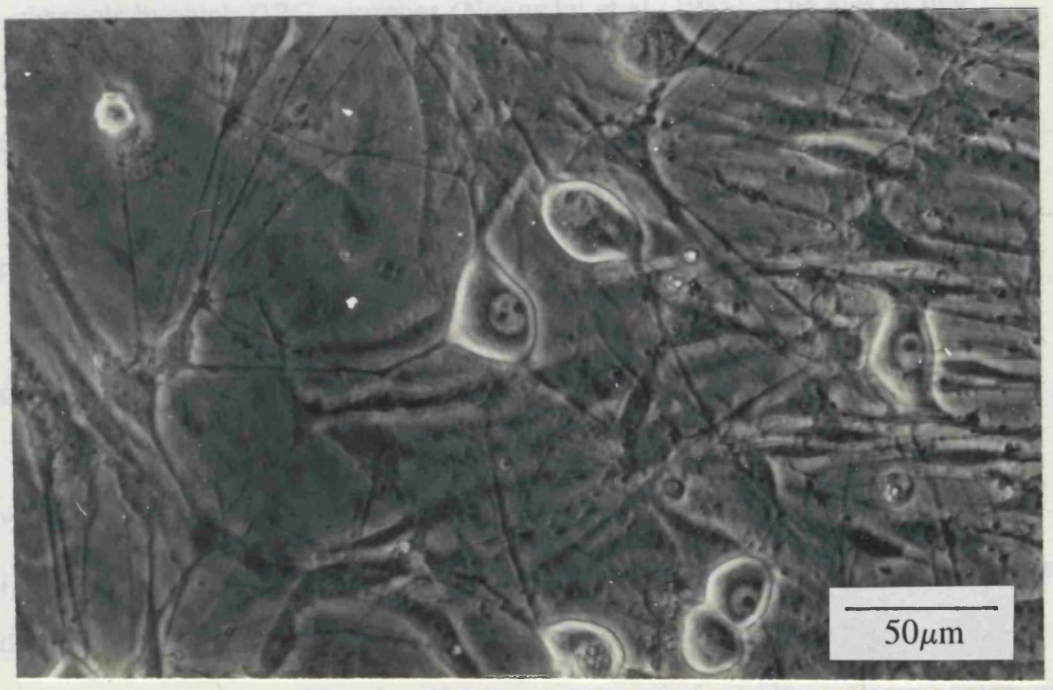

Chapter 3.

Characterization and inhibition of the calcium current.

A. Initial observations.

Introduction.

The calcium current (I_{Ca}) recorded from isolated rat sympathetic neurones is activated at potentials positive to -35mV, and is maximal around 0mV (Marrion et al, 1987; Wanke et al, 1987; Schofield and Ikeda, 1988). Once activated, the current decays slowly (Schofield and Ikeda, 1988; Hirning et al, 1988). Cell-attached patch recordings have revealed two distinct calcium channels with slope conductances of 11pS and 27pS respectively (Hirning et al, 1988) corresponding to the 'N' and 'L' type calcium channels in chick DRG neurones (Nowycky et al, 1985). The aim of this section is to isolate, and record under stable conditions I_{Ca} from dissociated rat s.c.g. neurones. Since the properties of I_{Ca} in the rat s.c.g. have already been extensively studied (see chapter 1), no attempt was made to dissect the components contributing to the current.

Methods.

Voltage-clamp recordings were made from dissociated superior cervical ganglion (s.c.g.) neurones, using whole-cell patch pipettes (see Chapter 2, Methods). Cells were selected to be spatially compact, in that they appeared spherical and had a minimal growth of neuritic processes. The aim of this was to maximise voltage-clamp control of the cells so that the recorded voltage was an accurate measure of the membrane potential across the whole cell.

Cells were voltage-clamped at hyperpolarized potentials (usually -80 to -90mV), and calcium currents were evoked by depolarizing voltage commands to approximately 0mV, of 0.1- 1 seconds duration. Before recordings could be made, the pipette solution had to fully dialyse with the intracellular contents of the cell. This was assumed to be the point at which I_{Ca} reached a steady amplitude, as Cs^+ ions replaced K^+ ions. This usually took between 5 and 15 minutes.

Current-voltage relationships were constructed by evoking voltage-clamp commands to a wide range of potentials from constant holding potentials. Unless otherwise stated, calcium currents were measured at peak amplitude.

Results.

Fig. 3.1 shows an example of the calcium current recorded from an s.c.g. neurone, evoked by a voltage-clamp command to 10mV from a holding potential of -80mV. The calcium current is characterized by a rapidly developing inward current, which peaks within about 10ms, and then decays slowly during the 100ms voltage command. Although this decay varied between different cells, even with long depolarizations (0.5-1 seconds) the current relaxation rarely reached a true steady-state. Any measurements of 'steady-state' calcium currents were therefore arbitrarily made at the end of 0.5 or 1 second depolarizations.

At the end of the depolarizing command, in Fig. 3.1, the membrane current rapidly returned to its original value. The absence of an outward tail-current following repolarization indicates a successful block of K^+ channels by the internal and external solutions used. However in many cells, slow inward tail-currents were observed. These were occasionally larger than the calcium current evoked during the depolarizing command. These tail-currents probably indicate poor voltage control, leading to regenerative activity in the dendrites. Alternatively they might suggest the presence of a Ca^{2+}-dependent Cl^- current which has been identified in other cells, for example rat

DRG neurones where it generates an after-depolarization (Mayer, 1985). Because of this, cells showing large tail-currents were rejected from use in experiments.

Stability of I_{Ca} during long experiments was variable. A constant current amplitude could in some cells be maintained for up to an hour, whilst in others the current ran down to less than 50% of its original amplitude within 20 minutes, and the variability was such that run-down was not possible to quantitate. Fig. 3.2 shows that stable currents could be maintained for sufficient time to allow investigation of I_{Ca}. However, the only reliable method of checking stability of I_{Ca} during an experiment was to compare the current recorded at the end of an experiment with that obtained initially. The addition of 3mM ATP to the pipette solution failed to noticeably reduce run-down. A creatine phosphate/creatine phosphokinase nucleotide regeneration system (Forscher and Oxford, 1985) was also tried but no successful calcium currents were recorded, although this was possibly due to the tip of the pipette being contaminated with the solution, preventing adequate seal formation.

Current-voltage relationship.

Fig. 3.3 illustrates the experimental protocol for investigating the current-voltage relationship of I_{Ca}. Neurones were voltage-clamped at a hyperpolarized level (-90mV), and subjected to increasing voltage commands, with intervals of 30s to allow for removal of inactivation.

From potentials of -90 to about -30mV, the voltage steps produced outward currents. These increased as a linear function of command potential (ohmic) from -90 to -70mV, but between -70 and -30mV the currents were of similar amplitude. Voltage commands to more positive potentials produced inward currents, peaking at around 0mV. Increasing the voltage commands further produced progressively smaller inward currents until outward currents predominated. Fig. 3.3B also shows the data presented in the form of a current-voltage plot. The relatively positive activation of I_{Ca} implies the absence of a transient (T) component of I_{Ca} (Hirning et al, 1988; Wanke et al,

1987). The slow rate of rise of I_{Ca} (Fig.3.1) also indicates this, but a frequent problem of studying the rise of I_{Ca} in many neurones was the presence of a rapidly inactivating outward current, which with a similar time-course to the rise of I_{Ca} masked the actual rise of I_{Ca}. The characteristics of this contaminating outward current, which was evoked by stepping positive from potentials negative to -50mV, and inactivated at holding potentials more positive than -50 mV, might indicate this current to be I_A, previously characterized in s.c.g. neurones (Belluzzi et al, 1985a; Galvan and Sedlmeir, 1984; Marrion et al, 1987). Small inward currents were often observed between commands to -50 and -30mV (see Fig. 3.3) but it is unlikely that these currents represented a low threshold calcium current because this component of inward current was not increased in high Ca^{2+} containing solution, unlike the larger inward currents recorded at higher potentials, and was only partially reduced by 300μM cadmium. However, 'T' type currents are relatively unaffected by Cd^{2+} (Fox et al, 1987a), and are preferentially blocked by Ni^{2+} (Fox et al, 1987a; Carbone et al, 1987). Consequentially, two cells were tested with 3mM Ni^{2+}, but again only showed a partial reduction of this inward current even though the calcium current recorded at 0mV is completely blocked at this concentration (see later).

Fig. 3.3 also shows the current-voltage relationship from a holding potential of -50mV. The calcium current is activated at command potentials more positive than -30mV. Despite being very much smaller than the currents recorded from -90, the shape of the current-voltage relationship is otherwise similar (other than the smaller inward current between -50 and -30mV.)

Dependence of I_{Ca} on external Ca^{2+}.

Assuming that Ca^{2+} is the only cation contributing to the inward current evoked, then removal of Ca^{2+} from the external solution should eliminate the inward current. Fig. 3.4 illustrates a neurone subjected to a brief superfusion of Krebs' solution

containing no added Ca^{2+}. This resulted in almost total loss of the inward current. Once the normal Ca^{2+}-containing medium had been replaced, the inward current returned to near its control value. This implies that the current observed is due to Ca^{2+} ions entering the cell, rather than, for example, by Na^{+} ions entering via Ca^{2+} channels.

Discussion.

The current recorded here appears similar to the calcium currents reported for dissociated adult s.c.g. neurones (Marrion et al, 1987; Schofield and Ikeda, 1988). Dependence of the inward current on external Ca^{2+} strongly suggests the current to be I_{Ca}. The current was activated at potentials positive to -30 mV, and was maximal at about 0mV, again characteristic of I_{Ca} in s.c.g. neurones. One problem in this study was the large contaminating outward currents recorded during voltage commands to positive potentials. These were possibly potassium currents activated by depolarization such as the delayed rectifier (Galvan and Sedlmeir, 1984; Schofield and Ikeda, 1989) which may not have been completely blocked by the Cs^{+} and TEA ions. The concentration (20mM) of TEA used was, for example, probably insufficient, since the EC_{50} for $I_{K(DR)}$ inhibition by TEA is at least 10 mM (Marsh and Brown, 1991). In addition, a rapidly inactivating outward current was occasionally observed resembling I_A recorded from dissociated s.c.g. neurones (Marrion et al, 1987). 4-aminopyridine (4-AP) is an effective blocker of I_A, but was not tested in this study.

B. Block of I_{Ca} by inorganic ions.

Introduction.

Inorganic ions are potent calcium channel blockers in a variety of preparations

(Hagiwara and Byerly, 1981); this has been demonstrated in s.c.g. neurones by the block of I_{Ca} by 500μM Cd^{2+}; Schofield and Ikeda, 1988). Such ions can prove a useful tool for separating calcium current components, for example low concentrations of Cd^{2+} selectively block 'N' and 'L' type currents leaving the 'T' type current unaffected (Fox et al, 1987a). Low concentrations of Ni^{2+} selectively inhibit 'T' type currents in some preparations (Carbone et al; 1987, Fox et al, 1987a; Crunelli et al, 1989). However, these ions can not distinguish 'N' from 'L' type channels. Selective inhibition of the 'N' type current by gadolinium ions (Gd^{3+}) has been suggested in NG108-15 cells by Docherty (1988) who demonstrated that the Gd^{3+} sensitive component had a time-course very similar to the 'N' type current of s.c.g. neurones. Lansman (1990) however failed to demonstrate a selective action of Gd^{3+} in cardiac cells.

In this study a variety of divalent and trivalent inorganic ions were tested for their ability to block I_{Ca} in dissociated rat s.c.g. neurones.

Methods.

Dissociated rat s.c.g. neurones were whole-cell voltage-clamped at about -90mV and calcium currents evoked by depolarizing commands to 0mV. Depolarizing commands were usually 100ms in duration to minimise current run-down during experiments to determine dose-response relationships, but were occasionally increased to 500ms, to compare peak with steady-state currents. Cells were only used if I_{Ca} showed no appreciable run-down prior to addition of drug. Inorganic cations were added directly to the perfusion chamber, and applied until the response had reached steady-state. Dose-response relationships were constructed by cumulative applications of cations. Following each experiment, I_{Ca} was allowed to recover fully. When using some ions, from which recovery was only partial or did not occur, a fresh plate of cells was used for each experiment.

A modified Krebs' solution was used for these experiments because of the poor

solubility of the salts of some of the cations used. $MgSO_4$ was replaced by $MgCl_2$, and KH_2PO_4replaced by KCl. However, at the highest concentrations used, precipitates were occasionally seen with some of the cations.

Results.

Divalent cations.

Fig. 3.5 illustrates inhibition of I_{Ca} by Cd^{2+}. The current is inhibited in a concentration-dependent manner with complete block occurring at about 300μM. Fig. 3.5 also indicates that Cd^{2+} did not noticeably alter the kinetics of I_{Ca} inactivation, giving no indication of sub-populations of calcium channels differentially sensitive to Cd^{2+}. Cd^{2+} did however reduce the inward holding current observed at negative potentials in many cells (not present in Fig. 3.5). The identity of this inward current is uncertain; though it may be an outward chloride current (E_{Cl} was approximately 4mV) which has been shown to be Cd^{2+} sensitive (Selyanko, 1984).

Fig. 3.6 shows concentration-response curves to a range of divalent cations. Concentration-response curves were constructed by applying cumulative concentrations of each divalent ion, and finally adding a maximal concentration of Cd^{2+} (300μM) to determine the total amount of blockable current. All the divalent cations used were effective at blocking I_{Ca}, producing similarly shaped dose-response curves to that seen with Cd^{2+}. However, Cd^{2+} was far more potent than the other divalent cations used. The order of potency (approximate IC_{50})in blocking peak I_{Ca} was Cd^{2+} (3.3μM), Cu^{2+} (87μM), Zn^{2+} (190μM), Ni^{2+} (520μM), Mn^{2+} (580μM), Co^{2+} (1.1mM), Mg^{2+} (approximately 10mM). All the divalent cations appeared to block I_{Ca} without any obvious alteration in the kinetics of the current. It was noted that the block of I_{Ca} by each divalent cation showed no relationship to the suppression of the steady-state inward current at the hyperpolarized holding potential. For example Co^{2+} and Ni^{2+} both had virtually no effect upon this current at concentrations which completely

blocked I_{Ca}. Subsequent addition of Cd^{2+} had no further effect upon I_{Ca}, but reduced this holding current.

Trivalent cations.

Trivalent cations were also investigated for their ability to block I_{Ca}. Gadolinium (Gd^{3+}) caused a dose-dependent inhibition of I_{Ca} (Fig. 3.7A). Gd^{3+} produced a half-maximal block of I_{Ca} at 2.6μM showing it to be a potent blocker of the calcium current. However unlike the divalent cations which produced a complete block of I_{Ca}, Gd^{3+} only blocked about 55% of total I_{Ca} at concentrations of 10 to 30μM. Higher concentrations had no further effect. Gadolinium also appeared to alter the kinetics of I_{Ca} relaxation. In the presence of Gd^{3+} the current inactivated more rapidly than the control current. This is more clearly shown in Fig. 3.7B where the effects of Gd^{3+} are compared to Cd^{2+} on the same cell. At the concentrations used, Cd^{2+} had a greater effect on the peak current than Gd^{3+}, but the initial rate of inactivation of the Gd^{3+} resistant current is much faster than the Cd^{2+} resistant current. As a result Gd^{3+} had a greater effect on the sustained current.

Fig. 3.8 illustrates the dose-response curves for Gd^{3+}, Lu^{3+} and La^{3+} ions. Their relative potency (approximate IC_{50}) for block of I_{Ca} was Gd^{3+} (2.6μM), Lu^{3+} (72μM), La^{3+} (3.0mM). Whilst Gd^{3+} only blocked about 55% of the current, Lu^{3+} reliably blocked I_{Ca} by up to 80% at 300μM (higher concentrations formed a precipitate so could not be tested). La^{3+} caused only a small inhibition of I_{Ca} at concentrations of up to 1mM. Although a greater block could be seen at higher concentrations, the results were very variable and were irreversible. In contrast to Gd^{3+}, La^{3+} did not cause any obvious effect upon the shape of the calcium current, although the limited resolution of the Gould chart recorder, used for routine acquisition of data, may have obscured any small effect. Lu^{3+} increased the initial rate of current relaxation similarly to Gd^{3+}, but the effect was small. The trivalent cations tested were all less effective as calcium current blockers than the divalent cations, and it was noted that addition of 300μM

Cd^{2+} to maximal concentrations of the trivalent ions produced a more complete block of I_{Ca}.

Discussion.

This study showed that inorganic cations were potent blockers of I_{Ca} in rat s.c.g. neurones. All the divalent ions tested produced a complete block of I_{Ca}, and did not appear to distinguish between peak and sustained current. Block by the trivalent ions was less complete, particularly noticeable with Gd^{3+} which also altered the decay kinetics. The similar block reported in NG108-15 cells (Docherty 1988), was suggested to be due to selective block of the 'N' type current leaving the 'T' and 'L' currents intact. However, s.c.g. neurones do not show an obvious 'T' type current, and Gd^{3+} appears to block the sustained current more than the peak current, inconsistent with the preferential block of 'N' type current in NG108-15 cells. Similarly in rat pituitary GH_4C_1 cells, low concentrations of Gd^{3+} blocked 'T' and 'L' type currents preferentially to 'N' type channels (Biagi and Enyeart, 1990).

It is not clear why Gd^{3+} altered the decay of I_{Ca}, and may be due to an alteration in the inactivation properties of a single subtype of channel. Alternatively, it has been suggested that Gd^{3+} preferentially blocks open channels (Biagi and Enyeart, 1990), such that greater block of the sustained current reflects entry and block of the calcium channels by Gd^{3+} during the voltage command.

This study also revealed the probable identity of the large inward current at hyperpolarized holding potentials as the chloride current identified by Selyanko (1984) in s.c.g. neurones. Similarly to the current recorded by Selyanko, the steady-state current observed here was blocked by Cd^{2+} but resistant to Co^{2+}. Since there was no correlation between the block of I_{Ca} and the holding current, it is unlikely that there is any link between the two effects of inorganic cations observed in this study.

C. The effect of noradrenaline on I_{Ca}.

Introduction.

Inhibition of calcium currents in the rat s.c.g. was originally suggested by Horn and McAfee (1979) who demonstrated that noradrenaline antagonised the calcium spike, along with other calcium dependent potentials via an action on α-receptors (see chapter 4). I_{Ca} recorded from voltage-clamped intact s.c.g. neurones, was subsequently shown to be suppressed by noradrenaline (Galvan and Adams, 1982). Inhibition was shown to occur without any obvious change to the voltage dependence, and appeared to be due to suppression of I_{Ca} rather than activation of an outward current (Galvan and Adams, 1982).

Suppression of I_{Ca} has more recently been reported in dissociated s.c.g. neurones (Song et al, 1989; Schofield, 1990) and it appears that inhibition is selective for the 'N' type current, since dihydropyridine (DHP)-induced tail currents are unaffected (Plummer et al, 1991). Investigation of noradrenaline's suppression of I_{Ca} in various neurones has also revealed, as with other transmitters, the time-course of activation of I_{Ca} is slowed, for example in chick DRG neurones (Marchetti et al, 1986).

The aim of this study is to investigate the effects of noradrenaline on I_{Ca} in rat s.c.g. neurones and to determine any changes to the voltage dependence and activation kinetics.

Methods.

Voltage-clamp recordings were made in the absence and presence of noradrenaline. Cells were only used provided the calcium current showed little or no run-down during several consecutive control records before addition of noradrenaline. The application of noradrenaline was maintained for at least 1 minute to allow the response to stabilise. Where appropriate, leak subtraction was performed by subtracting the current remaining following addition of high concentrations of Cd^{2+} (usually 100μM) from the currents

recorded in the presence and absence of noradrenaline. The currents illustrated in the figures have not been leak subtracted unless otherwise stated.

Results.

Noradrenaline was a potent and reversible inhibitor of the calcium current in s.c.g. neurones. Fig. 3.9A illustrates current records from an s.c.g. neurone. Addition of 1μM noradrenaline to the superfusing solution caused a rapid reduction of the peak amplitude of I_{Ca}. Maximal inhibition was observed within 1 minute of noradrenaline being added, the time taken for noradrenaline to reach and fill the bath accounting for this delay. Following removal of noradrenaline the response was fully restored. Also shown is the complete block of I_{Ca} by 100μM Cd^{2+}. Noradrenaline reduced the amplitude of the calcium current in all cells tested, although the extent to which the current was inhibited was variable (mean inhibition by 10μM = 51.2 $\pm$ 2.4%, n=16). Noradrenaline had no effect on the residual outward current following block of I_{Ca} by Cd^{2+}, indicating that the apparent inhibition of I_{Ca} by noradrenaline was genuine rather than representing the appearance of an outward current activated by the depolarizing voltage commands in the presence of noradrenaline.

Although noradrenaline reduced the amplitude of the peak calcium current, the effect of noradrenaline on the shape of the current trajectory during the voltage-command was variable. Fig. 3.9 illustrates two different types of response obtained. Some cells gave a response to noradrenaline which showed inhibition of the peak current but with little change to the time of peak current (Fig. 3.9A). Fig. 3.9B illustrates calcium currents recorded from another cell under the same conditions showing a different response where, in addition to reduction of peak current, the time at which peak current occurs is visibly delayed with a slowed rate of rise of I_{Ca}. Most cells showed responses which varied between the two extremes shown here.

The effect of noradrenaline on the time-course of the calcium current was

investigated further. Fig. 3.10A shows calcium currents recorded in the absence and presence of 1μM noradrenaline illustrating the slowed activation of I_{Ca}, the peak current being delayed from 12 to 70ms. Fig. 3.10B shows the same data plotted as log amplitude current against time. The rise of the calcium current in the absence of noradrenaline was fitted to a single exponential with a time constant (τ) of 1.7ms. In the presence of noradrenaline the rise of the calcium current was fitted to two exponentials, a fast component (τ= 2.1ms) and a slow component (τ= 16.8ms).

During longer voltage commands it was also noticed that noradrenaline often caused greater inhibition of peak calcium current than the steady-state current although this was difficult to quantify because the time-course of calcium current relaxation often varied during an experiment.

Effect of membrane potential.

Current-voltage curves were constructed in the absence and presence of noradrenaline to determine any effect of noradrenaline on the voltage dependence of I_{Ca}. Fig. 3.11 illustrates records from an experiment in which the effect of 1μM noradrenaline on I_{Ca} at different command potentials was investigated. Fig. 3.11B illustrates the data shown in A as a current-voltage relationship. In the absence of noradrenaline, the leak current was linear at potentials between -130 and -80mV. At more positive potentials a small inward current was observed (see earlier). The calcium current was activated at potentials more positive than -30mV and reached a peak at 0mV. Addition of noradrenaline had no effect upon the leak current, or the small inward current, but inhibited I_{Ca} at all potentials between -30mV and 30mV. There was no obvious selectivity by noradrenaline on any part of the current-voltage relationship between these potentials, although maximum inhibition was observed around 0mV. Above +30mV, noradrenaline appeared to produce very little effect but this was difficult to determine accurately because of the large contaminating outward currents.

The effect of noradrenaline on I_{Ca} at different holding potentials.

Fig. 3.12 shows calcium currents evoked by commands to 10mV from holding potentials of -80 and -40mV in the absence and presence of 1μM noradrenaline. The calcium current recorded under these conditions shows considerable inactivation at a holding potential of -40mV, particularly the loss of an initial rapidly decaying component. At both holding potentials, however, noradrenaline inhibited a similar proportion of the recorded calcium current, although the slowing of the calcium current rising phase was more pronounced at the holding potential of -40mV. In similar experiments performed at holding potentials of -90 and -40mV the proportion of I_{Ca} inhibited by 1μM noradrenaline was 60.5 ± 1.6% and 57.7 ± 1.6% (mean ± s.e.m., n=3) respectively. Fig. 3.12B also shows steady-state inactivation curves obtained in the absence and presence of noradrenaline. At each holding potential, noradrenaline blocked almost the same proportion of current.

Duration of inhibition by noradrenaline.

The effect of a prolonged single application of noradrenaline was investigated. This was important because of the method used to construct dose-response curves for noradrenaline by cumulative additions (see chapter 4). In order for this method to be suitable, the inhibition by noradrenaline needed to reach a maximum rapidly and then show no fading of response for at least ten minutes (the time taken to construct a complete dose-response curve for noradrenaline). Fig. 3.13A shows peak I_{Ca} plotted against time for a voltage-clamped neurone, with noradrenaline producing maximal inhibition of I_{Ca} within one minute . The application of noradrenaline was maintained for 30 minutes with very little fading of response, but with recovery following removal. It therefore seems valid to construct dose-response curves by cumulative additions.

Even when the calcium current ran down, it was possible to obtain reproducible

responses to brief applications of noradrenaline.. Fig. 3.13B illustrates the inhibition by noradrenaline on calcium currents recorded 25 minutes apart. A small decrease with time was noticed, but this could be due to deterioration of the cell rather than any alteration to the receptors or transduction pathway involved. Run-down of the current during long experiments was therefore not a problem provided that the current was still measurable and that adequate control records of I_{Ca} were made prior to each addition of noradrenaline.

Discussion.

The inhibition of I_{Ca} observed in this study confirms the inhibition of calcium action potentials reported by Horn and McAfee (1979), and the inhibition of I_{Ca} described by Galvan and Adams (1982), and is also consistent with the inhibition more recently described in acutely dissociated s.c.g. neurones (Schofield, 1990). The current-voltage relationship indicated that noradrenaline did not alter the threshold for activation of I_{Ca}, and that inhibition occurred at all potentials up to around +40mV. At higher command potentials, the contaminating outward currents hindered investigation, but inhibition by noradrenaline appeared to be negligible, consistent with the suggestion by Bean (1989b) that strong depolarization removes inhibition of I_{Ca} (see below for discussion of models of transmitter action). Similarly, it has been reported that the size of modulated calcium currents is increased by preceding the command pulse with a positive conditioning pre-pulse (Grassi and Lux, 1989, Elmslie et al, 1990). Inhibition by noradrenaline was also independent of the holding potential, with steady-state inactivation curves appearing similar under both control conditions and with noradrenaline present. This is in contrast to frog sympathetic neurones, where very little inhibition was observed from a holding potential of -40mV, indicating the selective inhibition of 'N' type channels (Lipscombe et al, 1989). However, the action of noradrenaline observed here agrees with Schofield (1990), and it has been suggested that both 'N' and 'L' type channels show similar steady-state inactivation (Wanke et al,

1987) such that investigation of steady-state inactivation would be unlikely to reveal selective inhibition of either 'N' or 'L' type currents.

The other observed action of noradrenaline was the slowing of the calcium current rising phase. The same effect was observed by Schofield (1990) and has been reported in a variety of neurones. It is possible that this slowing of the rise of I_{Ca} represents the unmasking of a slowly activating 'L' type component which is relatively resistant to noradrenaline. However most available evidence suggests a different mechanism by which the slow rise of I_{Ca} is caused by a time and voltage dependent recovery of inhibited channels of a single HVA component (see below).

Bean (1989b) proposed a model in which calcium channels can exist in either 'willing' or 'reluctant' states, which are in equilibrium with each other. Channels in the 'willing' state are opened by moderate depolarizations, while channels in the 'reluctant' state are unlikely to be opened by moderate depolarizations and require large depolarizations to open. In the absence of transmitter most channels are in the 'willing' state, and therefore open easily upon depolarization. However, in the presence of transmitter, the equilibrium is shifted to the 'reluctant' state so that upon depolarization fewer channels open. Strong depolarization still cause all the channels to open, this explaining the small inhibition noticed above +40mV. In addition, this model also explains the slow rise of I_{Ca} in the presence of transmitter. Following a moderate depolarization, all the 'willing' channels are opened, so that channels in the closed 'reluctant' state are converted to the 'willing' state to maintain the equilibrium, thus themselves becoming available for activation, and therefore increasing total current with a time-course that represents the conversion from 'reluctant' to 'willing' states. The results obtained in this study are consistent with this. Under control conditions there is a single fast component of the rise of I_{Ca} (τ=1.7ms) representing the opening of channels from the 'willing' state. In the presence of noradrenaline there are two components, a fast component (τ=2.1ms) representing the opening of channels from the 'willing' state, and a slow component (τ=16.8ms) representing conversion from the 'reluctant' to 'willing' state and subsequent activation. This model therefore explains both the voltage

dependence of inhibition and the slowing of the rising phase observed in this study.

Other similar mechanisms for the action of neurotransmitters on I_{Ca} have been suggested indicating that a G-protein subunit interacts in a voltage-dependent manner with a closed state of the channel to give a closed-inhibited conformation, the two states equilibrating in a time and voltage dependent manner during depolarizing commands (Grassi and Lux, 1989; Kasai and Aosaki, 1989, Carbone and Swandulla 1989). The role of G-proteins has been demonstrated by the similarity of inhibition by GTP-γ-S compared with neurotransmitters (for example, Dolphin and Scott, 1987; Wanke et al, 1987, Ikeda and Schofield, 1989; Grassi and Lux, 1989) , and the involvement of G-proteins in the noradrenergic suppression of I_{Ca} has been established (Schofield, 1990 for example). A model has been proposed (Carbone and Swandulla, 1989; Swandulla et al, 1991) which suggests that under control conditions, the calcium channel opens and closes in a simple voltage dependent manner. In the presence of transmitter, the receptor/G-protein complex couples to the channel inhibiting current flow during depolarization. Once depolarized, charged groups of the G-protein re-orientate, leading to a relief of inhibition so that the channels open, the time this takes causing the apparent slowed activation. In addition, larger depolarizations will cause greater dissociation of the G-protein from the channel, consistent with the reduced inhibition at higher command potentials observed in this study.

Both the models described above adequately account for the inhibition of I_{Ca} investigated in this study, though these models may both be oversimplified now that it has been established that there are multiple modes of 'N' type channel activity in sympathetic neurones (Delcour et al, 1993; Rittenhouse and Hess, 1994). It has been demonstrated in bullfrog neurones that noradrenaline decreases high-P_o behaviour whilst increasing low-P_o behaviour (Delcour and Tsien, 1993) suggesting that neurotransmitters act by altering the balance between the different modes, though this is still consistent with a willing-reluctant hypothesis. It remains to be seen how neurotransmitters effect the multiple modes of 'N' type channels observed in rat s.c.g. neurones, and it is likely that this will prove valuable in determining the mechanism of

noradrenaline's inhibition of I_{Ca}.

Fig. 3.1 Calcium current recorded from an s.c.g. neurone.

Membrane currents recorded from a dissociated s.c.g. neurone during depolarizing voltage commands from a holding potential of -80mV. Upper records, voltage; lower records, current. The records on the left show a voltage command (V_C) to a subthreshold potential for activation of I_{Ca} (-40mV). The records on the right show a calcium current evoked by a command to +10mV (the clamp potential at which the largest inward current was observed in this cell).

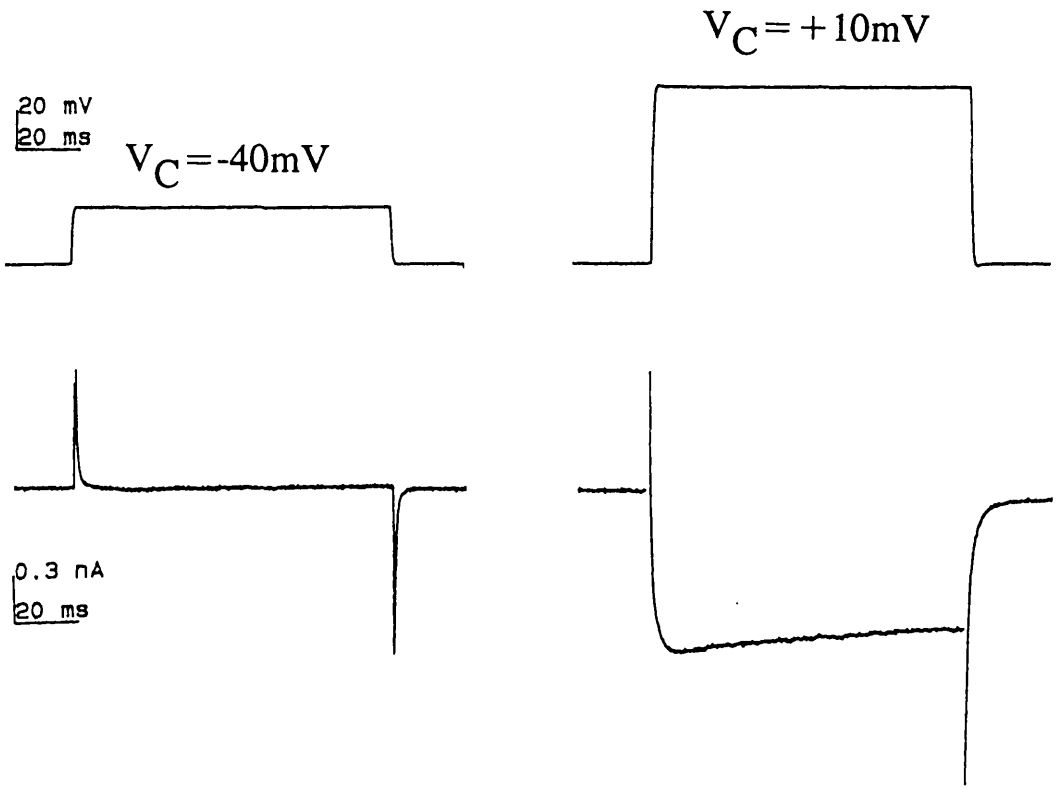
V_C = +10mV
20 mV
20 ms
V_C = -40mV
0.3 nA
20 ms

Fig. 3.2 Stability of I_{Ca} during long experiments.

Records obtained at the times shown illustrating stability of I_{Ca} during long experiments. Currents were evoked by 100ms voltage-commands to 0mV from a holding-potential of -90mV with intervals of 30s between commands. The first record shown was obtained approximately 12 minutes after formation of the whole-cell patch, once the cell had dialyzed with the whole-cell pipette solution. Initial holding current was -0.04nA.

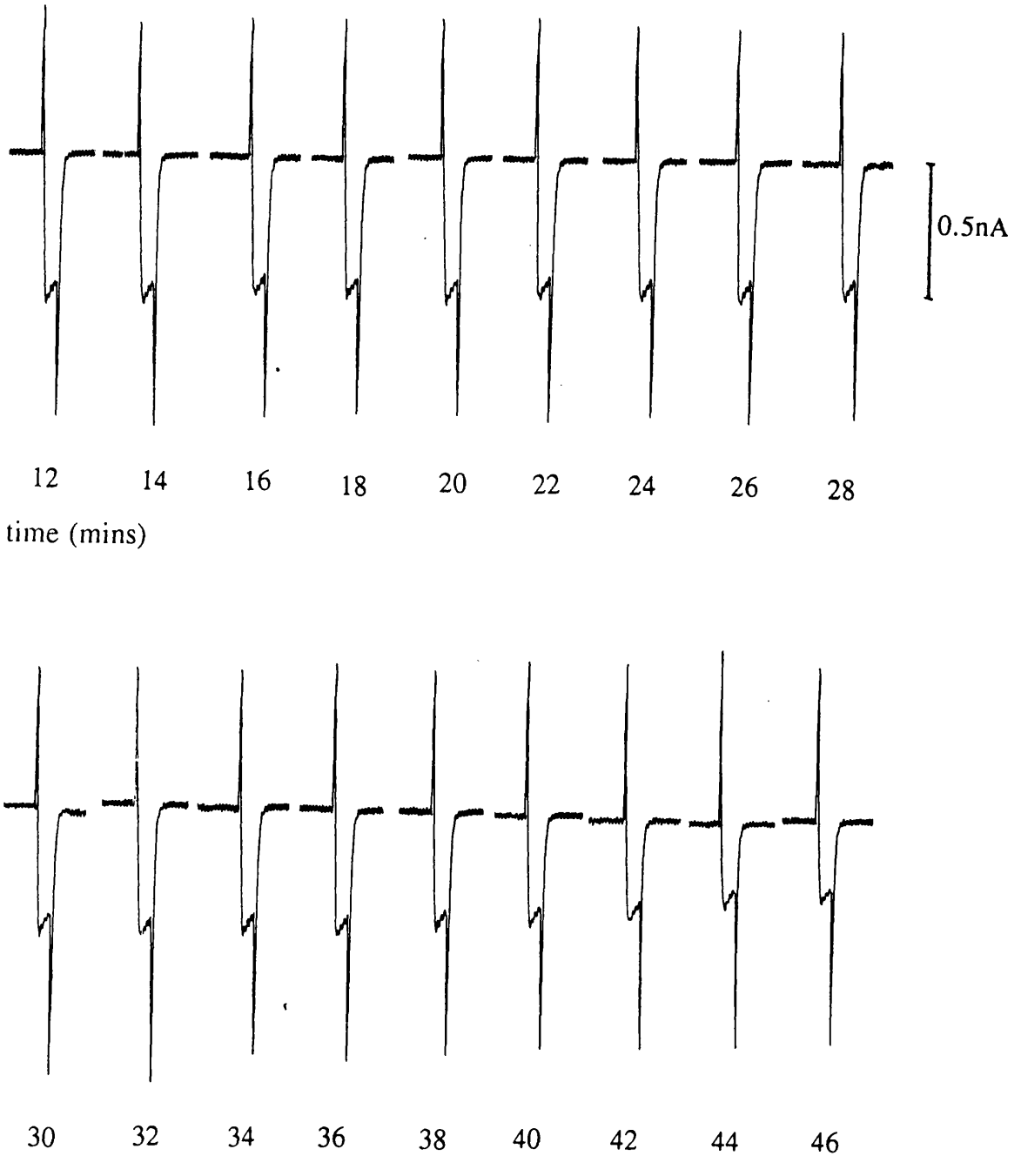
0.5nA
12
14
16
18
20
22
24
26
28
time (mins)
30
32
34
36
38
40
42
44
46

Fig. 3.3 Current-voltage relationship for an s.c.g. neurone.

A. Membrane currents recorded during 100mS depolarizing voltage commands from a holding potential of -90mV (above) and -50mV (below).

B. Current-voltage plot of the records shown in A (●V_H -90;○V_H -50). The data presentedhavebeen leak subtracted by extrapolation of the leak current at potentials negative to activation of the calcium current, assuming that the leak was a linear function of potential (probably not true at positive command potentials). Measurements were made of initial current. This is illustrated on current records at -40, 0 and +60mV in A., where the current measured is indicated by a dashed line.

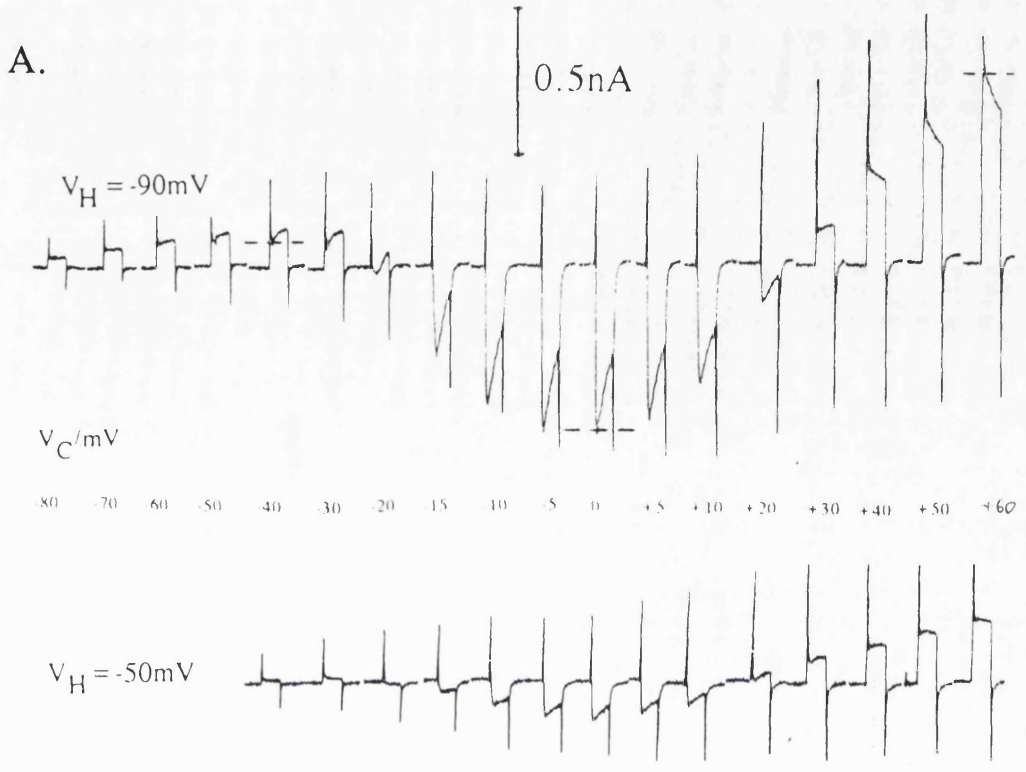
A.
0.5nA
V_H = -90mV
V_C/mV
-80 -70 -60 -50 -40 -30 -20 -15 -10 -5 0 +5 +10 +20 +30 +40 +50 +60
V_H = -50mV

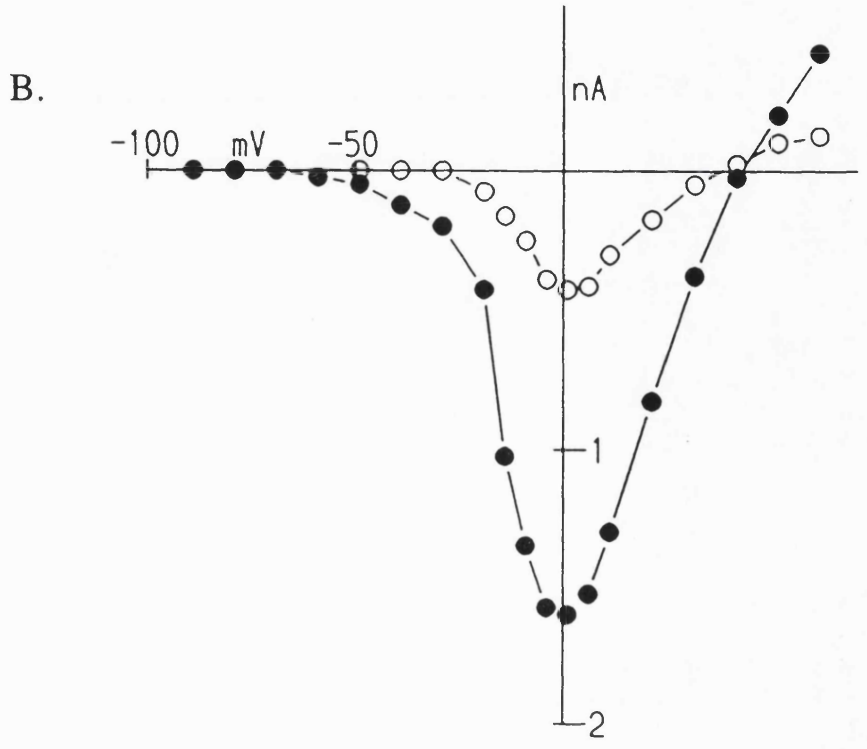
B.
nA
-100 mV -50
1
2

Fig. 3.4 Dependence of the calcium current on extracelullar calcium.

Calcium currents recorded from an s.c.g. neurone clamped at -80mV and evoked by jumps to 0mV showing records (a) before and (b) during perfusion with Ca^{2+} free Krebs' solution, and (c) after return to normal Krebs' solution.

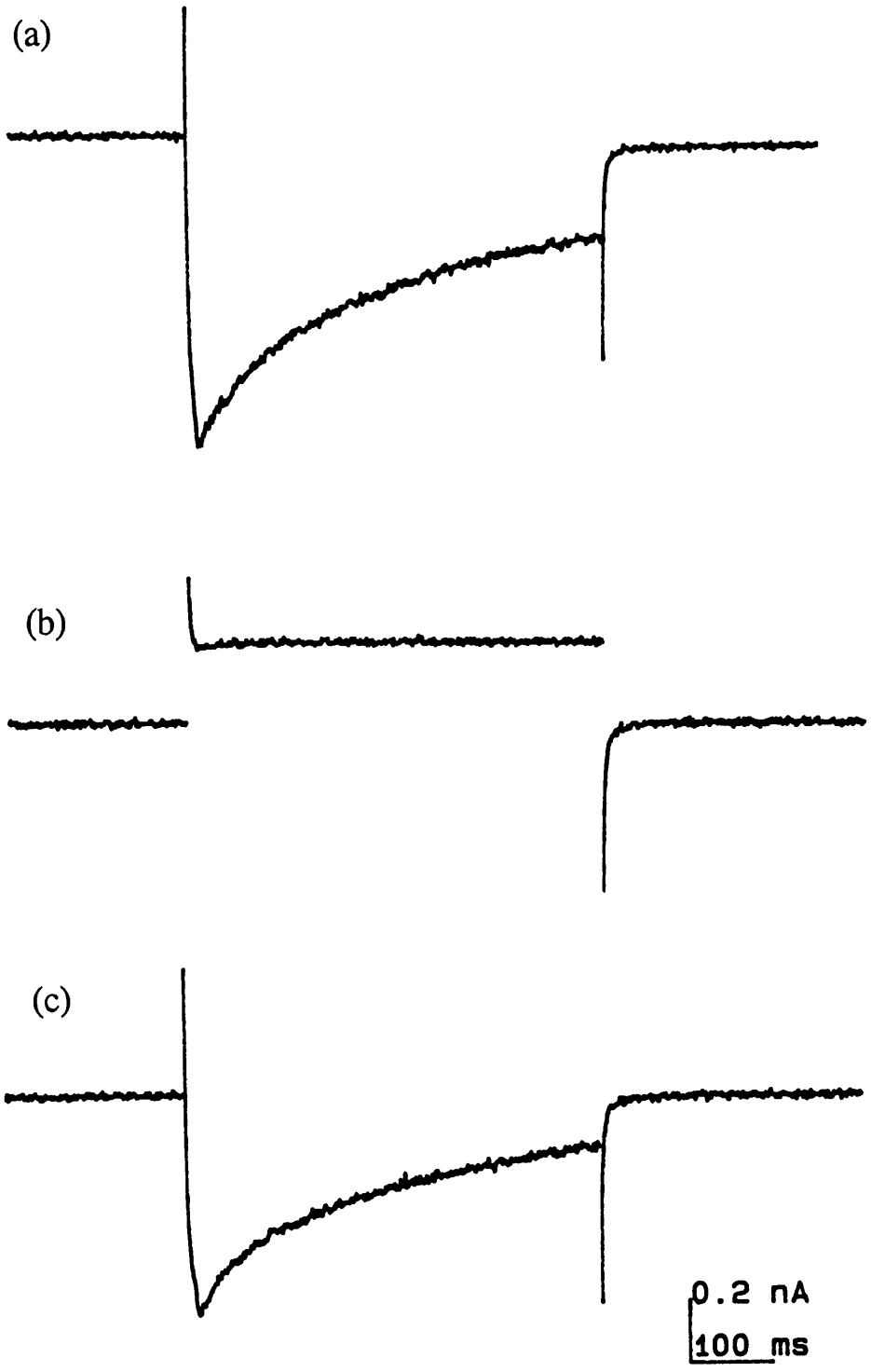
(a)
(b)
(c)
0.2 nA
100 ms

Fig. 3.5 Effect of cadmium on the calcium current.

Superimposed calcium current records (V_H=-80, V_C=0mV) showing the inhibition of I_{Ca} by cumulative additions of $CdCl_2$ (control current, 0.03, 0.1, 0.3, 1.0, 3.0, 10, 30, 100, 300μM Cd^{2+}). Recovery from Cd^{2+} was not recorded.

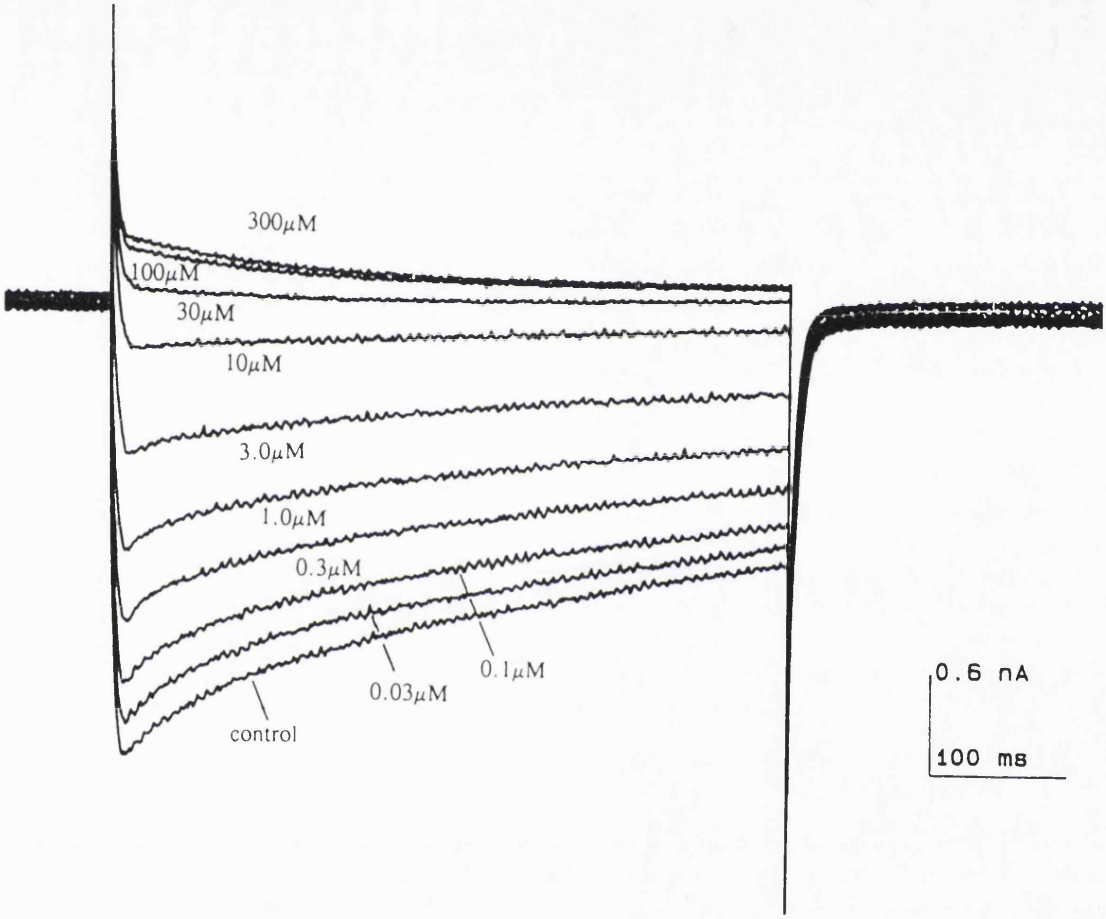
300μM
100μM
30μM
10μM
3.0μM
1.0μM
0.3μM
0.1μM
0.03μM
control
0.6 nA
100 ms

Fig. 3.6 Inhibition of I_{Ca} by divalent cations.

Dose-response relationships for the inhibition of I_{Ca} by cadmium (n=4,■), copper (n=3,○), zinc (n=3,●), nickel (n=4,◆), cobalt (n=3,□), and magnesium (n=3,▲). The curve for manganese is omitted for clarity, but had a half maximal block of I_{Ca} at 580μM (n=3). Data represents mean $\pm$ s.e.m.

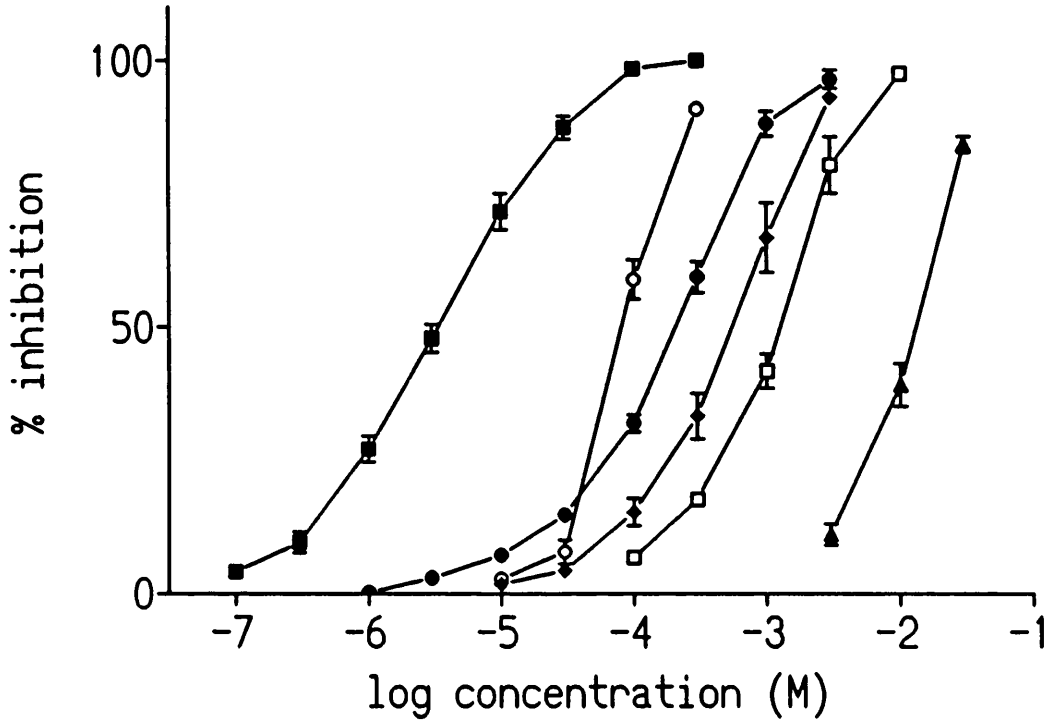
100
50
0
% inhibition
-7
-6
-5
-4
-3
-2
-1
log concentration (M)

Fig. 3.7 Effect of gadolinium on I_{Ca}

A. Calcium currents (V_H=-80mV, V_C=0mV) recorded before and after addition of increasing concentrations of gadolinium (Gd^{3+}).

B. Calcium currents (V_H=-80mV, V_C=0mV) recorded from another cell comparing the effects of Gd^{3+} with Cd^{2+}. The records illustrate responses obtained before and after addition of 10μM Gd^{3+}, and following recovery, subsequent addition of 2μM Cd^{2+}.

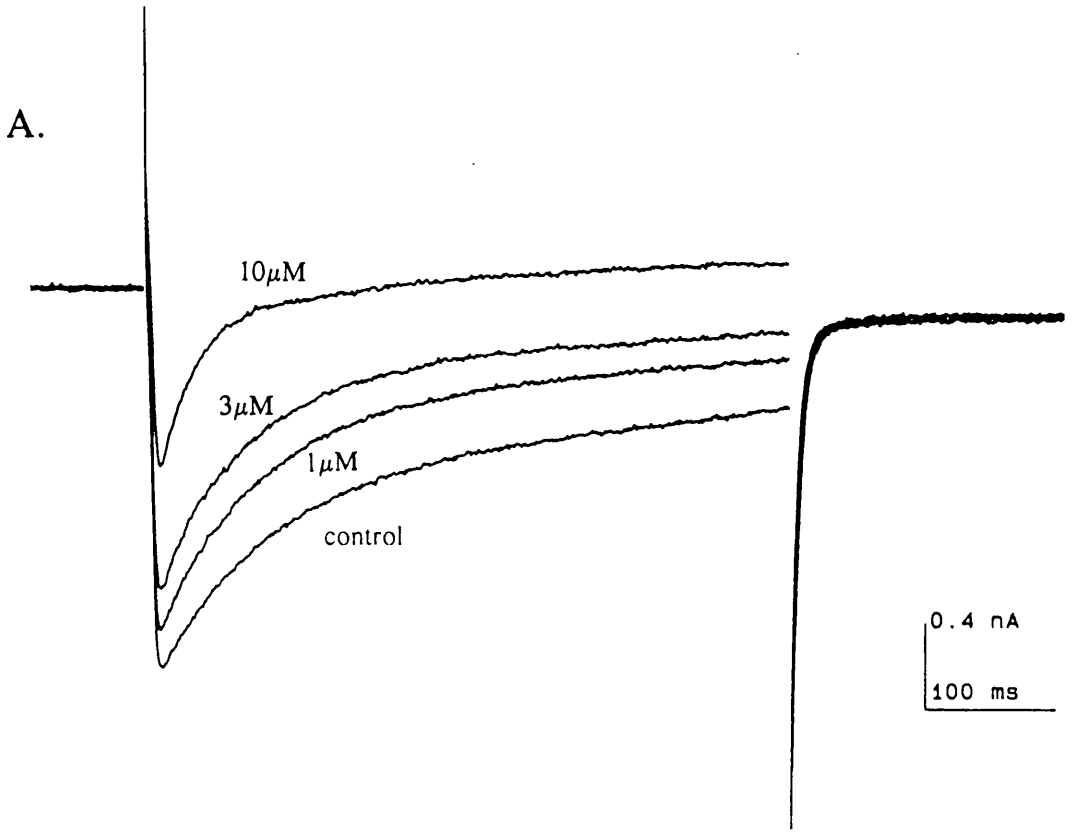
A.
10μM
3μM
1μM
control
0.4 nA
100 ms

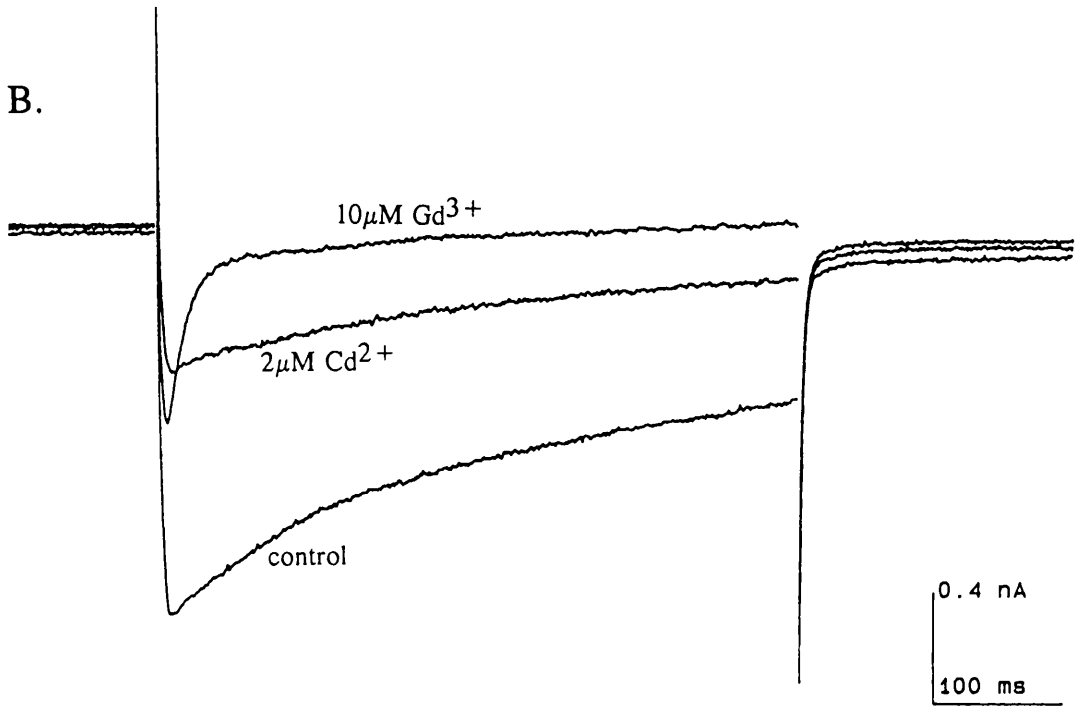
B.
10μM Gd3+
2μM Cd2+
control
0.4 nA
100 ms

Fig. 3.8 Inhibition of I_{Ca} by trivalent cations.

Dose-response relationships for the inhibition of I_{Ca} by gadolinium (■), lutetium (▲) and lanthanum (●). Complete block of I_{Ca} was induced by 300μM Cd^{2+} in each experiment. Measurements were of peak current and data is presented as mean ± s.e.m (n=4 for all data except for 10 and 100mM La^{3+} where n=3).

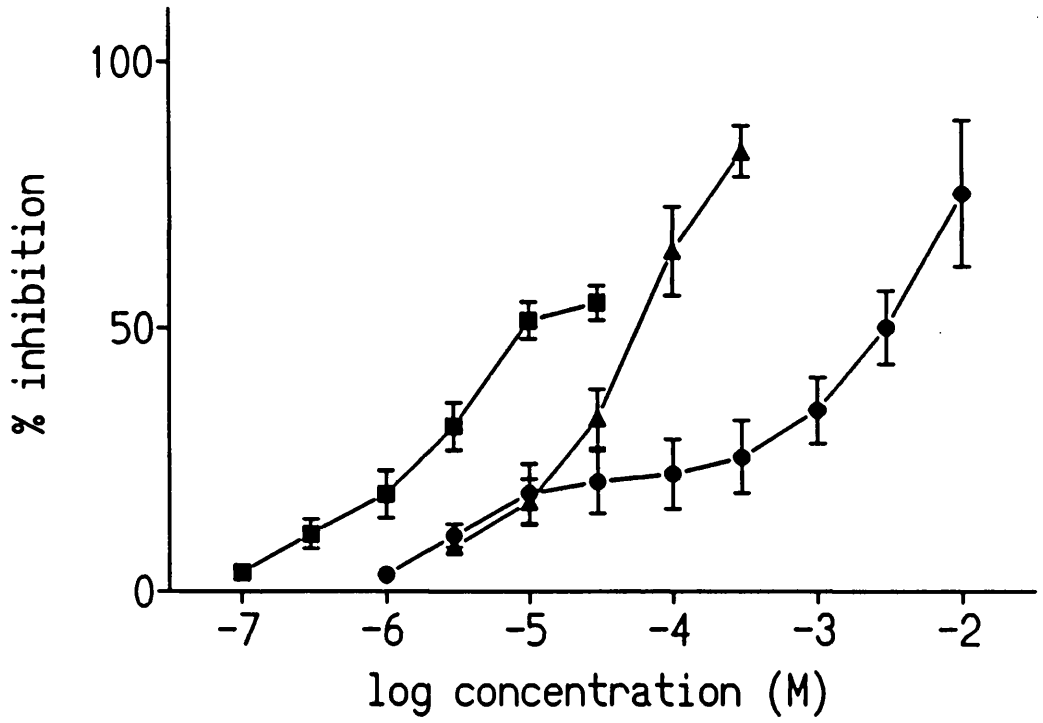
100
50
0
% inhibition
-7
-6
-5
-4
-3
-2
log concentration (M)

Fig. 3.9 Inhibition of I_{Ca} by noradrenaline.

A. Calcium currents recorded from a voltage-clamped s.c.g. neurone (V_H=-90, V_H=0mV) showing the inhibition of I_{Ca} by 1μM noradrenaline. Also shown is the complete block of I_{Ca} by 100μM Cd^{2+}.

B. Inhibition of I_{Ca} (V_H=-90, V_H=0mV) by 1μM noradrenaline illustrating a different response than that in A, in that the time of peak inward current is clearly delayed by noradrenaline.

A.

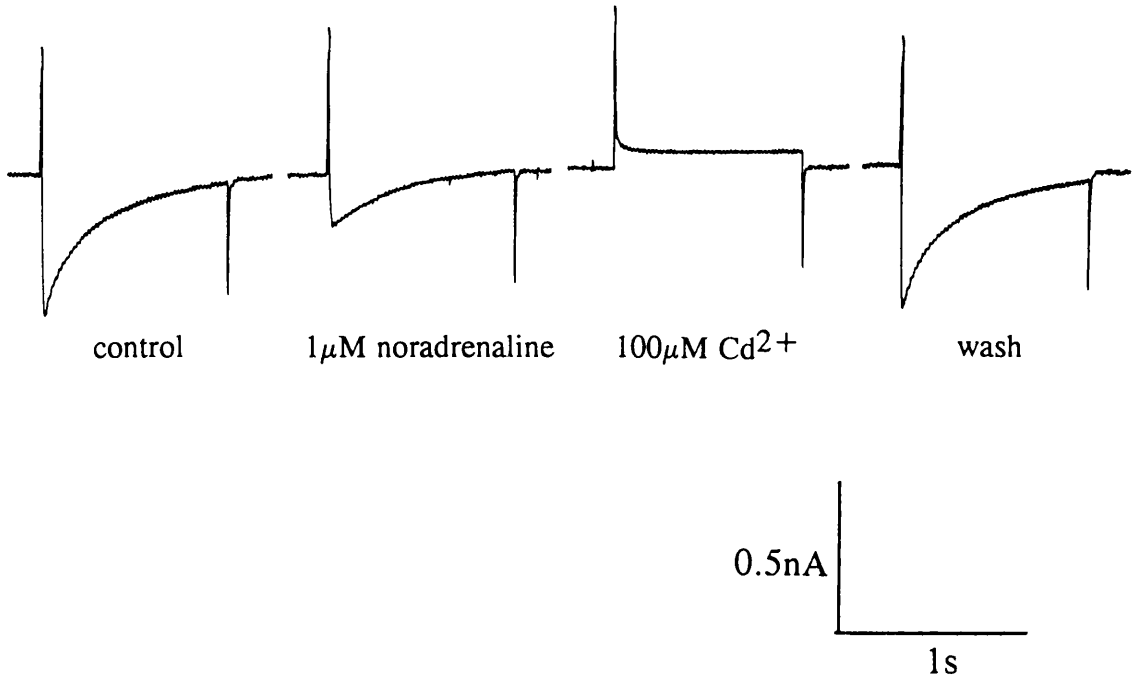
control
1μM noradrenaline
100μM Cd2+
wash
0.5nA
1s

B.

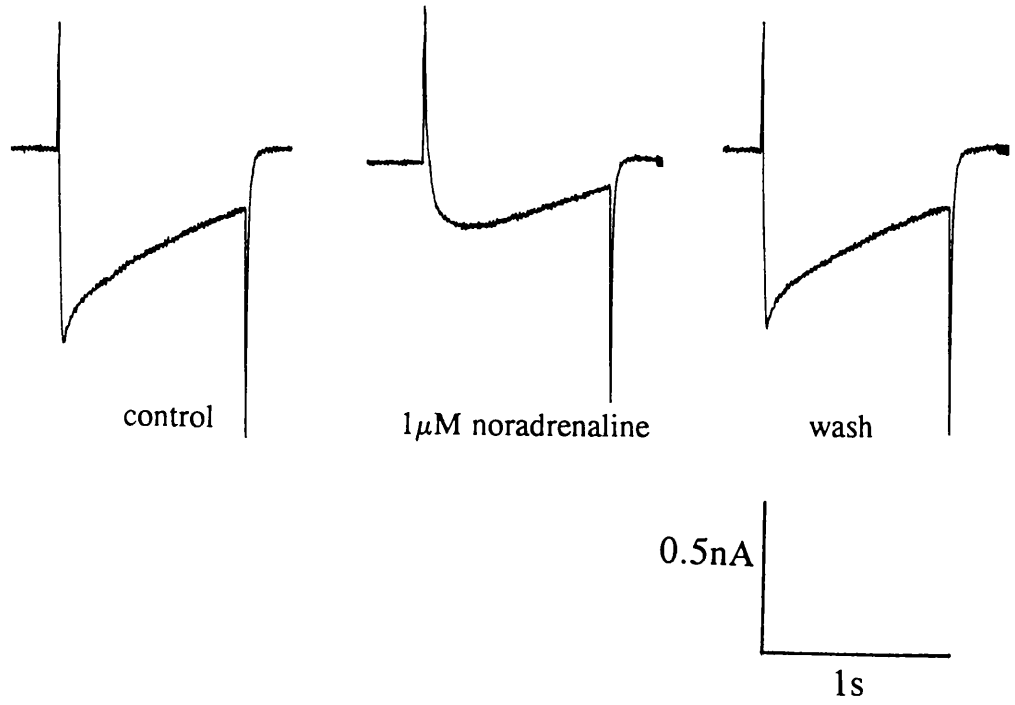
control
1μM noradrenaline
wash
0.5nA
1s

Fig. 3.10 Effect of noradrenaline on I_{Ca} rising phase.

A. Calcium current records during 100ms commands to 0 from -80mV in the absence and presence of 1μM noradrenaline, illustrating the slowing of the rise of I_{Ca} by noradrenaline.
Note that noradrenaline also shortens the tail-current.

B. Semi-logarithmic plot of I_{Ca} amplitude against time for the records shown in A. Data was fitted by least-squares regression analysis. The control values (●) give a time constant (τ) of 1.7ms for the rise in I_{Ca}. The noradrenaline data is best fitted by the sum of two exponentials, a fast component (□) of 2.1ms and a slow component (■) of 16.8ms.

A.

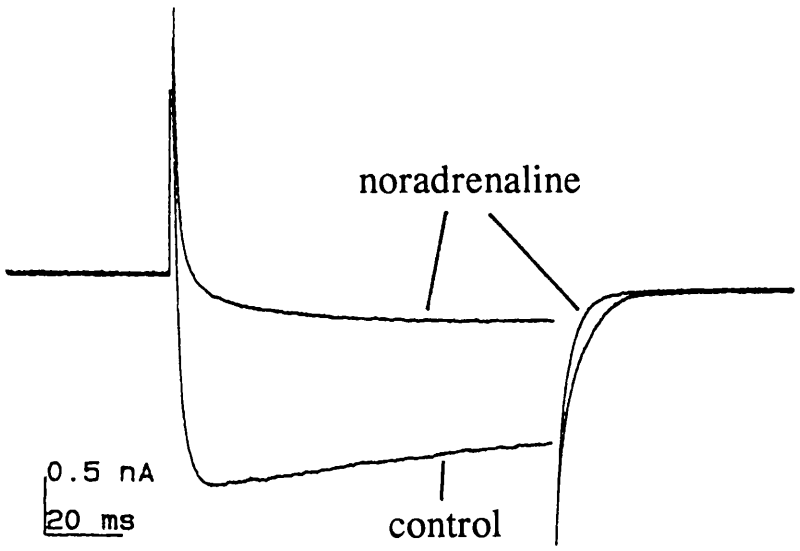
noradrenaline
0.5 nA
20 ms
control

B.

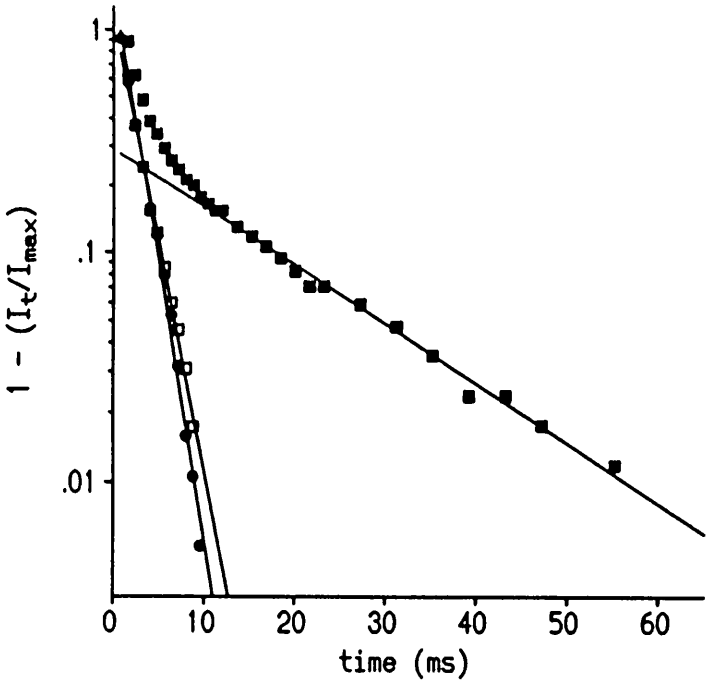
1
.1
.01
1 - (It/Imax)
0
10
20
30
40
50
60
time (ms)

Fig. 3.11 Effect of noradrenaline on the current-voltage relationship.

A. Calcium currents recorded from a voltage-clamped s.c.g. neurone during commands to the potentials indicated from a holding potential of -90mV in the absence (above) and presence (below) of 1μM noradrenaline.

B. Current-voltage relationship from the calcium currents shown in A. Measurement was made of peak current, and the plot illustrates absolute current with no leak correction applied.

A.

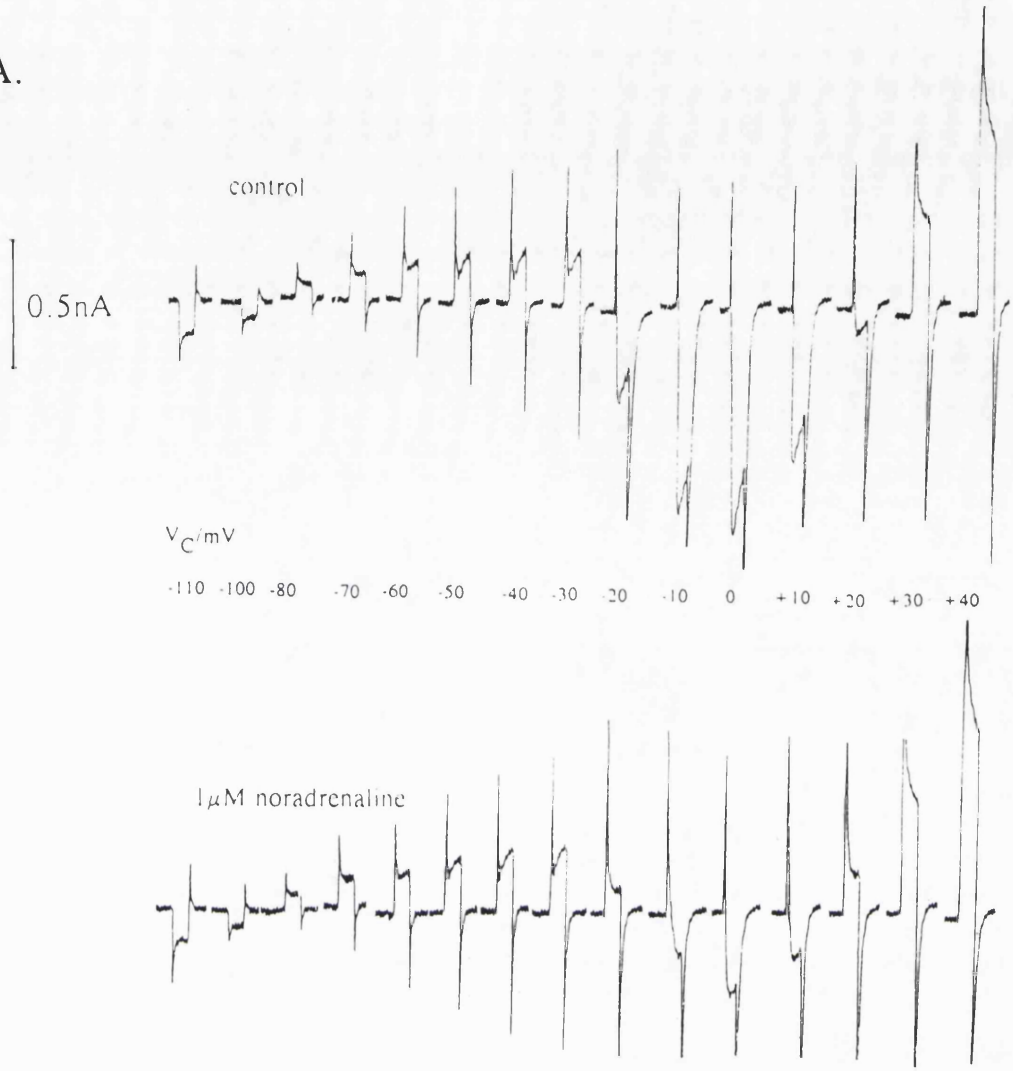
control
0.5nA
V_C/mV
-110 -100 -80 -70 -60 -50 -40 -30 -20 -10 0 +10 +20 +30 +40
1μM noradrenaline

B.

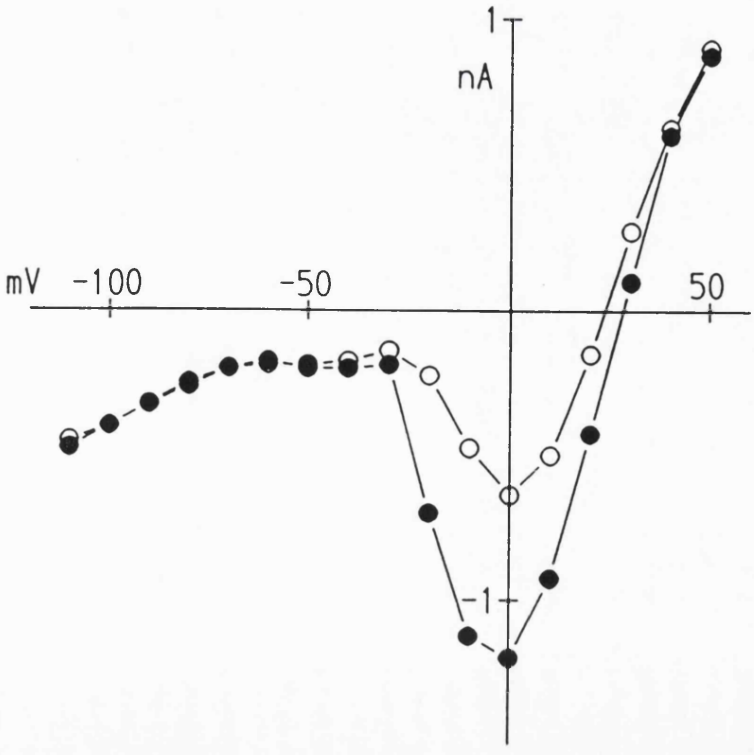
1
nA
mV -100
-50
50
-1

Fig. 3.12 Effect of noradrenaline at different holding potentials.

A. Calcium current records evoked by commands to 0mV from two different holding potentials (-80mV, above; and -40mV, below) showing the effect of 1μM noradrenaline. The records have been leak subtracted using records obtained in the presence of Cd^{2+}.

B. Effect of noradrenaline on the steady-state inactivation of the calcium current. Records were obtained by commands to 0mV from a range of holding potentials in the absence and presence of 1μM noradrenaline (same cell as above). One minute was allowed at each potential to attain steady-state. Currents were leak subtracted using 100μM Cd^{2+}.

A.

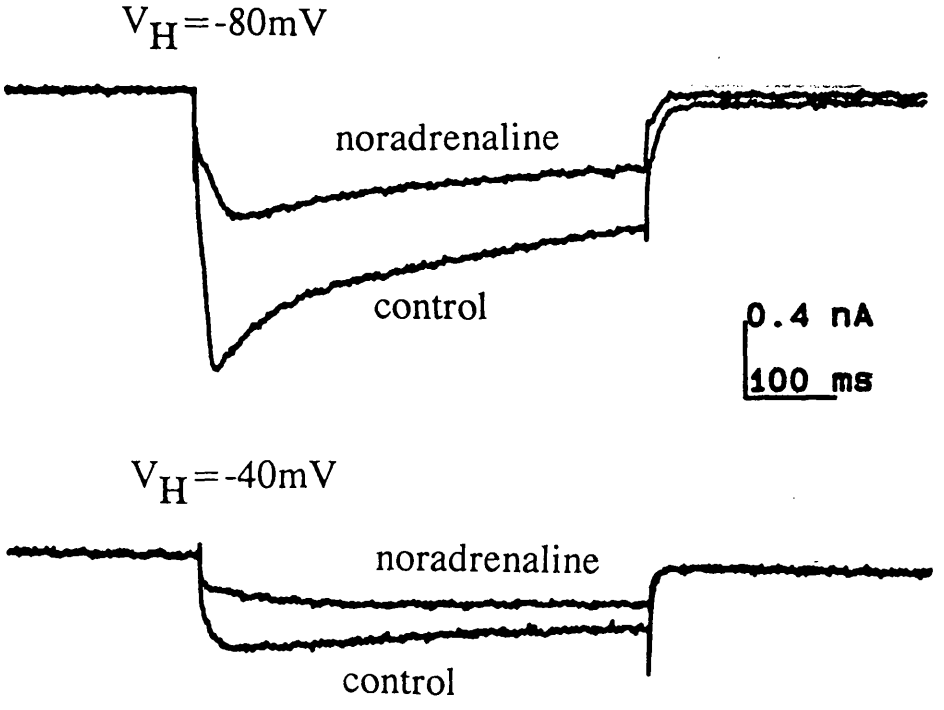
V_H=-80mV
noradrenaline
control
0.4 nA
100 ms
V_H=-40mV
noradrenaline
control

B.

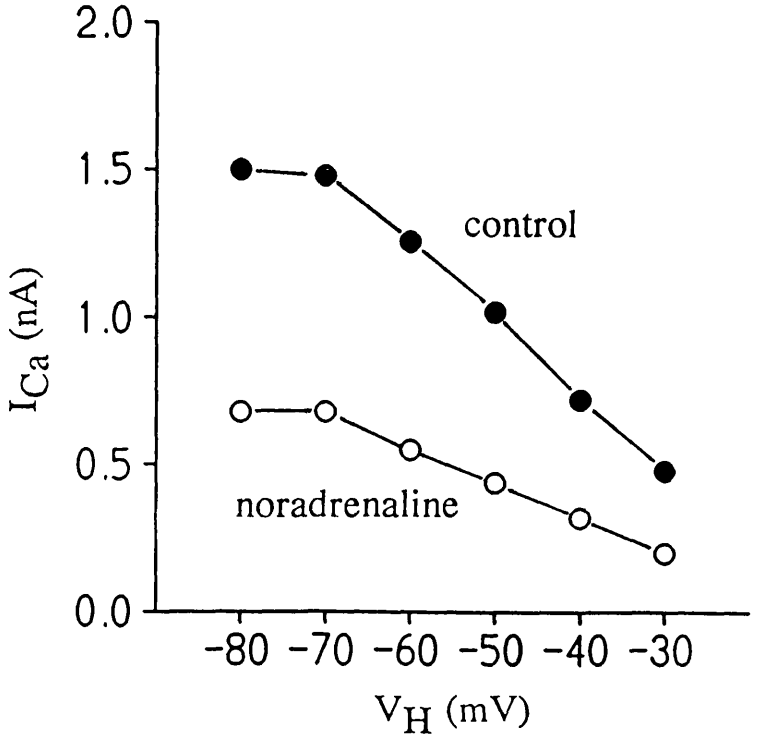
2.0
1.5
1.0
0.5
0.0
I_{Ca} (nA)
control
noradrenaline
-80 -70 -60 -50 -40 -30
V_H (mV)

Fig. 3.13 Calcium current inhibition by sustained and repeated application of noradrenaline.

A. Calcium current amplitude plotted against time. 1μM noradrenaline was present during the time indicated. Data has been leak subtracted using records obtained, at the end of the experiment, in the presence of Cd^{2+}. The calcium currents shown are the uncorrected records obtained at the times indicated.

B. Inhibition of the calcium current by repeated application of noradrenaline with an interval of 25 minutes between the two sets of records. Although the current has partially run down a similar proportion (51% and 45% respectively) of current is blocked by noradrenaline.
Records show (a) control current, (b) suppression by 1μM noradrenaline, (c) complete block with 100μM Cd^{2+}, (d) recovery.

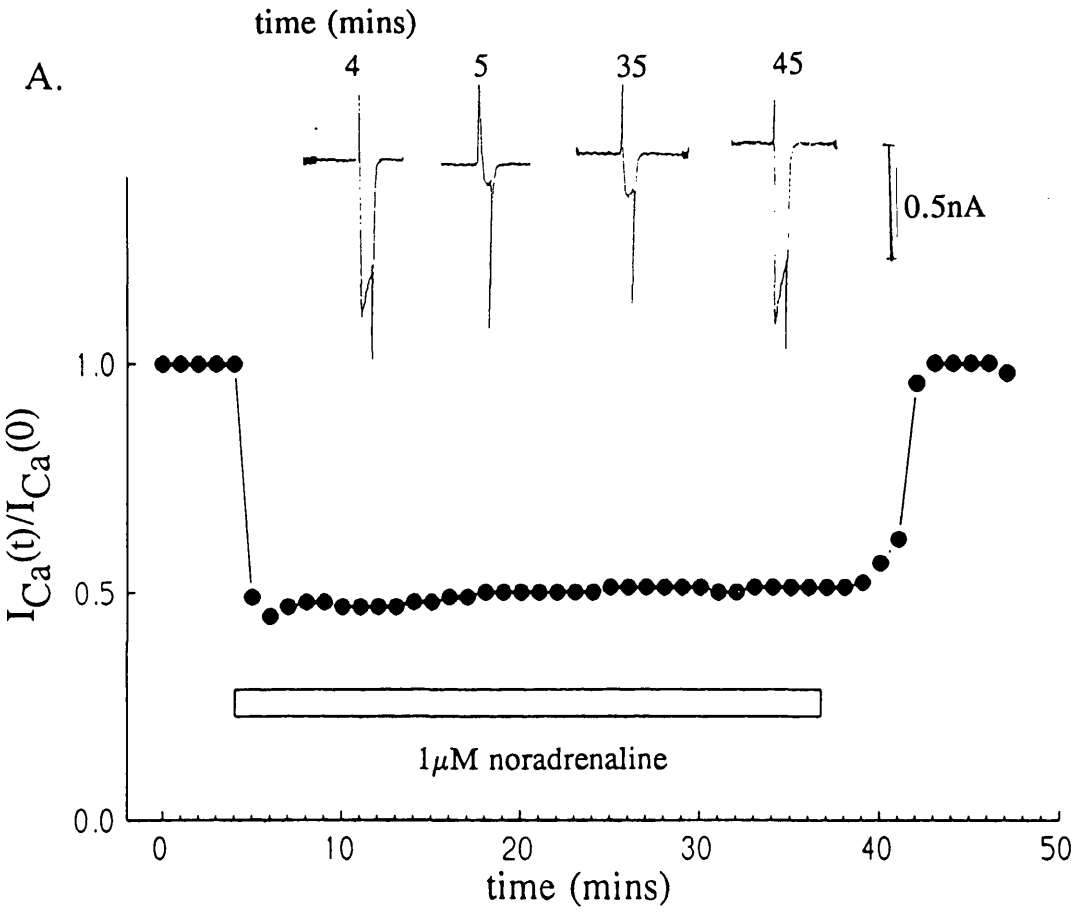
A.
time (mins)
4
5
35
45
0.5nA
1.0
0.5
0.0
$I_{Ca}(t)/I_{Ca}(0)$
1μM noradrenaline
0
10
20
30
40
50
time (mins)

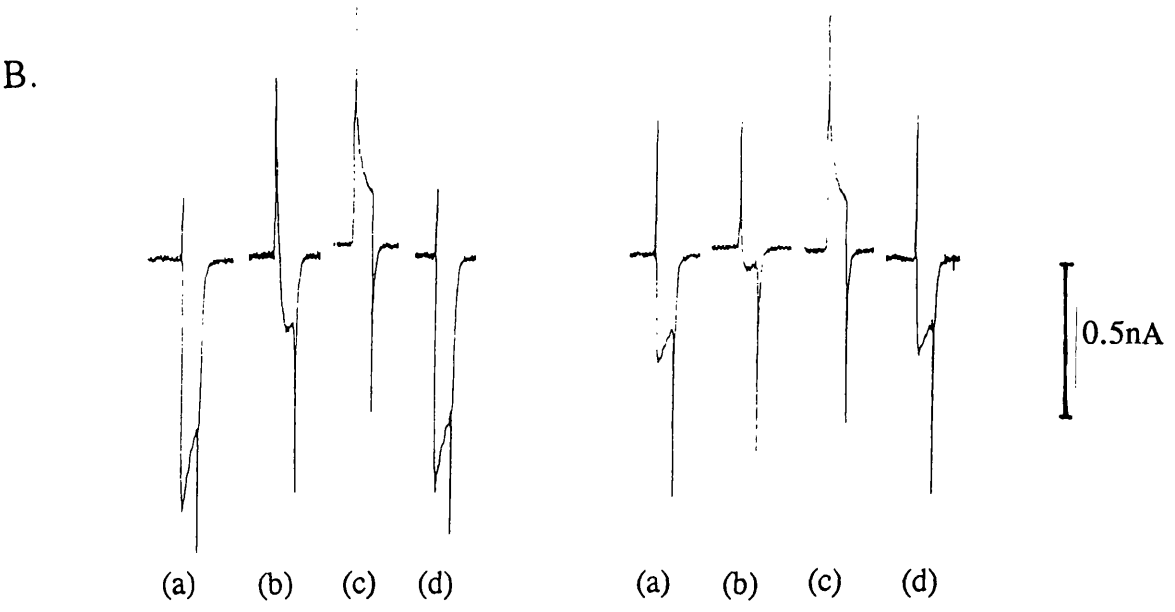
B.
0.5nA
(a)
(b)
(c)
(d)
(a)
(b)
(c)
(d)

Chapter 4.

Pharmacology of noradrenaline's suppression of I_{Ca}.

Introduction.

The species of adrenoceptor responsible for mediating the effect of noradrenaline on the calcium current has been pharmacologically evaluated in various neurones (see below). The high potency of noradrenaline's inhibition of I_{Ca} observed in the previous chapter suggests that noradrenaline too acts via a specific adrenoceptor in rat s.c.g. neurones.

Adrenoceptors have been divided into subtypes based on their pharmacological characteristics, the initial differentiation into α- and ß-subtypes being described by Ahlquist (1948). Subsequent studies divided ß-receptors into $ß_1$- and $ß_2$-receptor subtypes (Lands et al, 1967), and α-receptors into α_1- and α_2-subtypes (Langer, 1974; Berthelson and Pettinger, 1977; and more convincingly by Starke and Langer, 1979).

Previous investigations of the calcium current in neurones have shown that inhibition by noradrenaline is mediated by α-receptors, although doubt remains of the subtype of α-receptor. In the rat sympathetic ganglion inhibition of the calcium spike by noradrenaline in postganglionic neurones was reduced by the α-antagonist phentolamine (Horn and McAfee, 1980). Further experiments showed the effects of noradrenaline were mimicked by the α_2-agonist clonidine, and blocked by the α_2-antagonist yohimbine but not by the α_1-antagonist prazosin (McAfee et al, 1981), suggesting the involvement of the α_2-receptor. In rat preganglionic sympathetic neurones, however, the failure of 1μM yohimbine to antagonise the inhibition of the calcium spike by noradrenaline suggested an α-receptor which did not correspond to either α_1- or α_2-subtypes (Elliott et al, 1989). In frog sympathetic neurones inhibition of whole-cell calcium currents by noradrenaline was also shown to be mediated via a distinct type of

α_2-receptor at which clonidine was inactive (Lipscombe et al, 1989). Similarly NG108-15 neuroblastoma/glioma hybrid cells showed no response to clonidine, though yohimbine and phentolamine antagonised inhibition by noradrenaline (Docherty and McFadzean, 1989).

The pharmacology of the receptors mediating inhibition of I_{Ca} by noradrenaline in other neurones is not uniform either. The receptor has been described as α_2 in guinea-pig submucosal neurones (Surprenant et al, 1990) and in rabbit vesical parasympathetic neurones (Akasu et al, 1990) on the basis of sensitivity to clonidine and antagonism by yohimbine. In chick dorsal root ganglion neurones inhibition of the calcium action potential by noradrenaline was mimicked by phenylephrine and antagonised by phentolamine suggesting an α-receptor (Dunlap and Fischbach, 1978). Although a later study (Canfield and Dunlap, 1984) indicated an α_2-like receptor (being antagonised by yohimbine but not by prazosin), both clonidine and xylazine (an α_2-agonist) were without effect. Furthermore, inhibition of the calcium action potential by dopamine and 5-hydroxytryptamine showed a similar sensitivity to antagonists compared with noradrenaline, suggesting that a general amine receptor was responsible (Canfield and Dunlap, 1984). In rat locus coeruleus neurones the receptor mediating inhibition of the calcium action potential proved insensitive to both yohimbine and prazosin, though was antagonised by high concentrations of phentolamine (Williams and North, 1985). In addition clonidine showed no effect, implying that α_2-receptors were not involved (Williams and North, 1985), particularly since the catecholamine-induced outward potassium current observed in the same cells showed classical α_2-pharmacology (Williams et al, 1985). In general though, most of the available evidence does implicate the role of α-receptors in mediating noradrenergic inhibition of neuronal calcium currents.

Facilitation of I_{Ca} is observed in some preparations, an action which is due to stimulation of ß-receptors, as demonstrated by the action of isoprenaline on frog sympathetic neurones (Lipscombe and Tsien, 1987). The role of ß-receptors in

enhancement of I_{Ca} has also been demonstrated in hippocampal neurones (Gray and Johnston, 1987) and in heart cells (Reuter, 1983; Kameyama et al, 1985; Tsien et al, 1986). A similar enhancement of I_{Ca} in rat sympathetic neurones is possible, and it has been observed that noradrenaline causes a small increase in patch currents during cell-attached recordings (Beech et al, 1990). There have been no reports of ß-adrenergic enhancement of whole-cell I_{Ca}, but this does not exclude the possibility of a small enhancement being hidden by a dominant α-inhibition.

Although the adrenoceptor mediating the inhibition of I_{Ca} by noradrenaline in the rat s.c.g. has not been fully characterized, convincing descriptions of receptors mediating other effects of catecholamines are available. The catecholamine-induced hyperpolarization is mediated by α_2-receptors: clonidine and oxymetazoline were potent agonists, and the receptors were blocked by yohimbine (pA_2 for block of noradrenaline was 8.7; Caulfield, 1978) but not by prazosin (Brown and Caulfield, 1979). It is possible that the same receptors mediate the action of noradrenaline on I_{Ca}, but the failure of yohimbine to block inhibition of preganglionic calcium spikes at concentrations which block the postsynaptic hyperpolarization (Elliott et al, 1989) indicate the receptor is different, at least in preganglionic neurones. Other actions of catecholamines in the rat s.c.g. are mediated by ß-receptors, for example the $ß_2$-mediated ganglionic depolarization and facilitation of submaximal transmission (Brown and Dunn, 1983a).

Since catecholamines produce numerous effects in the rat s.c.g., it is necessary for the adrenergic pharmacology of I_{Ca} suppression to be determined under conditions where I_{Ca} can be studied in isolation. The aim of this section is to attempt a detailed pharmacological characterization of the adrenoceptor responsible for the inhibition of I_{Ca} in isolated rat s.c.g. neurones, using selective agonists and antagonists.

A. Agonists.

Methods.

Dissociated rat s.c.g. neurones were voltage-clamped at between -80 and -90mV, and calcium currents evoked by depolarizing voltage commands to 0mV. The duration of the voltage command was usually limited to 100ms, with intervals of 30 seconds between commands to minimise run-down of I_{Ca}. Cells which showed noticeable run-down were rejected.

Agonists were applied in the bath, and each concentration of agonist was maintained until the response had reached a steady-state. Increasing concentrations of agonist were applied cumulatively until a maximal inhibition was reached. Previous tests (see chapter 3) showed no significant fade of the response (see earlier results). In addition, some run-down of I_{Ca} was likely during the time-course of the experiment, so experiments needed to be carried out quickly. If there was no recovery from the agonist-evoked response, the experiment was rejected on the basis that run-down may have contributed to the response. At the end of each experiment, cadmium (usually 100μM) was applied to the cell, to determine the total calcium current. Also, in some cells, 10μM noradrenaline was applied following complete wash, so that direct comparisons of agonist and noradrenaline efficacy could be made.

Measurements of peak I_{Ca} were made, regardless of any agonist-induced shift in the time of peak current. The percentage inhibition by each concentration of agonist was calculated using the following formula:

$$(1 - I_{Ca}{}^{*}/I_{Ca}) \times 100$$

where I_{Ca} = peak amplitude of control calcium current (using residual current in Cd^{2+} as baseline)

$I_{Ca}{}^{*}$ = peak amplitude of calcium current in presence of agonist.

The data obtained was used to construct dose-response relationships by plotting % inhibition against log concentration.

Some of the agonists were also tested for antagonist behaviour. The potential partial agonists were briefly applied during continuous exposure to noradrenaline. It was assumed that noradrenaline was itself a full agonist. EC_{50} values are expressed as mean (95% confidence limits). All other results are expressed as mean $\pm$ s.e.m. The data obtained from curve-fitting is summarised in Table 1.

Results.

(a) Noradrenaline.

The suppression of I_{Ca} by noradrenaline was concentration dependent. Fig. 4.1A shows a typical experiment illustrating the effect of cumulative application of noradrenaline. Noradrenaline suppressed I_{Ca} at concentrations as low as 10nM, and produced a maximal response at about 10μM. The data for each experiment was fitted (using an iterative curve-fitting routine) to the hyperbolic function below :-

$$Y = Y_{max} \cdot X^n / (X^n + EC_{50}{}^n)$$

where Y = %inhibition

Y_{max} = maximum inhibition

X = agonist concentration

EC_{50} = concentration producing half maximal inhibition

n = molecular ratio of ligand to receptor

Free estimates of Y_{max}, EC_{50}, and n were allowed, and the results obtained plotted on a log-concentration scale producing the sigmoidal derivative of the hyperbolic

function shown above.

Separate fits were calculated for each experiment and the combined results used to calculate mean values. The mean EC_{50} (n=16) for noradrenaline was 86.5nM (71.9-104.7nM), assuming a log-normal distribution of EC_{50} values (see Hancock et al, 1988), although actual analysis of the distribution in this study was not possible because of the low number of determinations. The maximal inhibition of I_{Ca} by noradrenaline varied from 31 to 69% (mean = 51.2 $\pm$ 2.4%). There was no correlation between maximum inhibition and EC_{50} between different cells. The value of 'n' was calculated as 1.08 $\pm$ 0.05 suggesting that calcium current inhibition is mediated by noradrenaline interacting with a receptor on a one-to-one basis.

The data was also plotted in the form of a Hill plot (log (r/1-r) against log concentration, where r = fractional response). Using least-squares linear regression, a slope of 1.04 $\pm$ 0.04 was obtained again indicating a molecular ratio of ligand to receptor of 1 (plot not shown).

Fig. 4.1B shows the dose-response relationship constructed from combined data from 16 experiments, clearly illustrating that the data obtained was accurately fitted by the equation described above.

(b) Adrenaline.

Suppression of I_{Ca} by adrenaline produced similar dose-response relationships to those of noradrenaline (Fig. 4.2). Using the same method of analysis as for noradrenaline, the mean EC_{50} (n=4) was calculated as 52.6nM (29.8-93.2nM), and maximal inhibition was 45.9 $\pm$ 6.6%.

(c) α_2-agonists.

Using the same procedure as for noradrenaline, dose-response relationships were obtained for the selective α_2-agonists oxymetazoline (n=5), UK14304 (n=9) and

clonidine (n=4), see Fig. 4.2. The EC_{50} values obtained for the three agonists were 26.9nM (14.7-49.0nM), 37.3nM (23.0-60.6nM) and 57.1nM (25.5-127nM) respectively. The dose-response relationships obtained for both oxymetazoline and clonidine showed a much lower maximal suppression of I_{Ca}, compared with that seen with noradrenaline (22.1 $\pm$ 3.1%, 21.5 $\pm$ 3.4% respectively), suggesting that clonidine and oxymetazoline were partial agonists compared to noradrenaline. This was investigated further, and Fig. 4.3 illustrates antagonism of noradrenaline's suppression of I_{Ca} by oxymetazoline. A similar effect was produced by clonidine (not shown).

The dose-response relationship obtained with UK 14304 showed a maximal inhibition more comparable to that seen with noradrenaline (40.5 $\pm$ 3.7%). Although this value is lower, suggesting partial agonist activity, UK 14304 displayed the greatest efficacy of the α_2-selective agonists tested.

(d) Other agonists.

Phenylephrine, an α_1-agonist, showed no suppression of I_{Ca} at concentrations below 1μM (Fig 4.2). At 1 mM, phenylephrine reduced I_{Ca} by only 22 $\pm$ 1.7% (n=3). The shallow slope also suggested that phenylephrine was a partial agonist, but with no clear maximal response, this was not certain.

Isoprenaline, a ß-agonist, exerted no significant effect on I_{Ca} at concentrations below 10μM (Fig 4.2). At higher concentrations of isoprenaline, when α-receptor activation would be expected, there was some reduction of I_{Ca}. Facilitation of I_{Ca} was never observed.

Table 1. Results obtained by non-linear regression analysis of I_{Ca} suppression by adrenergic agonists.

Agonist	max. inhibition (% ± s.e.m.)	EC_{50}/nM (95% limits)	n
oxymetazoline	22.1 ± 3.1	26.9 (14.7-49.0)	5
UK 14304	40.5 ± 3.7	37.3 (22.9-60.6)	9
adrenaline	45.9 ± 6.6	52.6 (29.8-93.2)	4
clonidine	21.5 ± 3.4	57.1 (25.5-127)	4
noradrenaline	51.2 ± 2.4	86.5 (71.9-104)	16

B. Antagonists.

Methods.

As described for agonists (see above), dissociated s.c.g. neurones were voltage-clamped at -90mV, and calcium currents usually evoked by 100ms voltage commands to 0mV at 30 second intervals. Initial determination of antagonist activity was made by application of a single concentration of noradrenaline in the presence and absence of the antagonist.

A more detailed investigation of antagonist properties was then attempted, in order to estimate pA_2 values. Ideally, dose-response curves to noradrenaline should be constructed in the presence of increasing concentrations of antagonist on each individual cell. However, in order to achieve an adequate number of dose-response curves to agonist in the presence of different antagonist concentrations, a cell needs to remain viable for up to several hours. This was impractical because of the gradual run-down of I_{Ca}. Instead, therefore, dose-response curves to noradrenaline were constructed in the presence of a single concentration of antagonist, using several different cells. The

concentration of antagonist was then altered, and, after allowing 30 minutes for equilibration of antagonist, dose-response curves to noradrenaline were redetermined in previously unused cells. Each fresh plate of cells was initially tested with noradrenaline to ensure that the preparation responded similarly to noradrenaline, before antagonists were added. The dose-response relationships obtained to noradrenaline alone during the course of this study were pooled and used as the control data for all the antagonists used.

This method yielded consistent results (see below), and the dose-responses obtained were used to make estimates of pA_2 and pK_B values (as defined by Jenkinson, 1991) for the antagonists used, using the method of Arunlakshana and Schild (1959).
Data obtained from the Schild plots is expressed as mean (95% confidence limits).
Other data is expressed as mean $\pm$ s.e.m.

Results.

(a) Phentolamine.

Phentolamine, an α-antagonist, was an effective antagonist of the noradrenergic suppression of I_{Ca}. Fig. 4.4 illustrates an experiment in which the suppression of I_{Ca} by 0.1μM noradrenaline is reduced by 1μM phentolamine. It was also noted that phentolamine alone had no effect on I_{Ca} (not shown).

Dose-response curves were constructed for noradrenaline in the presence of different concentrations of phentolamine, as described above. Fig. 4.5A shows the pooled data for all of these experiments. There was an increasing rightward shift in the dose-response curve for noradrenaline, for each increasing dose of phentolamine. The shifts in the dose-response produced by 0.01 and 0.1μM phentolamine appeared to be parallel, though the dose-response obtained in the presence of 1μM phentolamine was comparatively shallow. The data was fitted to a sigmoidal function (see agonists), a separate fit being made for each experiment. There was no significant change to the maximal inhibition produced by noradrenaline (control, 51.2 $\pm$ 2.4%; 1μM

phentolamine, 56.2 ± 5.2%). The EC_{50} values obtained were used to calculate dose-ratios, and these were plotted in the form of a Schild plot (Fig 4.5B). The least-squares regression line had a slope of 0.871 (0.681-1.062), intercepting the abscissa at a point giving an apparent pA_2 value of 8.12 (7.95-8.30), corresponding to a phentolamine concentration of 7.5nM (5.0-11.4nM).

Assuming the antagonism by phentolamine is of a competitive nature, then the line can be represented by the equation:

$$\textbf{Log [DR-1] = log [B] - log } K_B$$

where [B] = antagonist concentration

[DR] = dose-ratio of the antagonist

K_B = antagonist dissociation constant

The intercept on the abscissa therefore provides an estimate of the dissociation constant (K_B) for the antagonist.

Schild analysis of a competitive antagonist should, however, yield a slope of unity (Schild, 1949). Accordingly the regression line was constrained to satisfy this requirement (see Jenkinson, 1991), and yielded an intercept (pK_B) value of 7.97 (7.80-8.13), corresponding to an apparent K_B value of 10.8nM (7.4-15.8nM).

(b) Yohimbine.

Experiments investigating the antagonist properties of the α_2-selective antagonist, yohimbine, were performed using the same methods as for phentolamine. Fig. 4.6 illustrates the antagonism by 1μM yohimbine on the suppression of I_{Ca} by 1μM yohimbine. Yohimbine was an effective antagonist, though less potent than phentolamine. Dose-response curves to noradrenaline were constructed in the presence of different yohimbine concentrations (see Fig. 4.7A); again, a rightward parallel shift

of the dose-response curve was seen. The Schild plot for this data (Fig. 4.7B) gave a least-squares regression line of slope 0.739 (0.502-0.959), and a pA_2 of 7.65 (7.42-7.89). Constraining the slope to unity yielded an apparent pK_B value of 7.46 (7.24-7.68), apparent K_B for yohimbine of 34.8nM (20.9-58.5nM).

(c) Prazosin.

The α_1-selective antagonist prazosin was tested for its ability to block the effect of noradrenaline on I_{Ca}. The noradrenergic suppression of I_{Ca} proved insensitive to prazosin at concentrations below 1μM. At higher concentrations however, prazosin caused a rightward shift in the agonist dose-response curve (Fig. 4.8A).The Schild plot (Fig 4.8B) for this data had a unconstrained slope of 0.709 (0.439-0.979), and a pA_2 of 5.44 (5.15-5.73). Constraining the slope to unity provided a pK_B value of 5.36 (5.16-5.57), apparent K_B of 43.7μM (26.9-69.2μM).

(d) Propranolol.

The ß-antagonist propranolol was used to determine whether any ß-receptors were involved in the effect of noradrenaline on I_{Ca}. At concentrations as high as 10μM, propranolol showed no significant antagonism of the noradrenergic suppression of I_{Ca} (n=3), implying that ß-receptors were not involved and was therefore not further investigated.

The possibility of ß-facilitation of I_{Ca} was considered, in which case block of ß-receptors by propranolol should potentiate noradrenaline's suppression of I_{Ca}. This was not observed (n=3). In addition, block of α-receptors by phentolamine did not reveal facilitation I_{Ca} by isoprenaline (n=3).

Discussion.

The inhibition of I_{Ca} was concentration dependent with an EC_{50} of approximately 86nM. This was lower than the value obtained (200nM) in a recent study of the adrenergic suppression of I_{Ca} of acutely dissociated rat s.c.g. neurones (Schofield, 1990), although inhibition was otherwise similar with a maximal blockade of 51% and 57% by noradrenaline, respectively for the two studies. The EC_{50} obtained was also lower than that reported in NG108-15 cells (Docherty and McFadzean, 1989; 177nM). Noradrenaline's inhibition of calcium spikes recorded from intact rat preganglionic sympathetic nerves yielded an EC_{50} of 1.5μM (Elliott et al, 1989), much higher than that recorded for inhibition of I_{Ca} in isolated postganglionic neurones (although the EC_{50} in intact postganglionic neurones was also probably at least 1μM). This does not imply a different receptor since the apparent low potency in the study by Elliott et al (1989) was probably caused by uptake of noradrenaline into the intact ganglion preparation used. Such an effect has been clearly demonstrated for the adrenergic hyperpolarization recorded from amphibian sympathetic ganglia where an uptake blocker, desmethylimipramine, lowered the EC_{50} for adrenaline from 1.65μM to 0.30μM (Rafuse and Smith, 1986). Uptake blockers were not tested in this study but the low EC_{50} suggests that uptake of noradrenaline is unlikely to be a significant problem. Furthermore since there were only a small number of isolated cells in each culture dish compared to the intact ganglion, and a rapid perfusion of Krebs' solution, any uptake would have only a small effect. Previous investigation of uptake blockers on the adrenergic hyperpolarization of the intact rat s.c.g. failed to show potentiation (Brown and Caulfield, 1979) though this was probably due to α-receptor blockade. The phenomenon of noradrenaline uptake into the rat s.c.g. has however been well documented (Fischer and Snyder, 1965; Hanbauer et al, 1972; Burton and Bunge, 1975).

The use of selective agonists and antagonists in this study allowed the subtype of adrenoceptor to be determined, the results suggesting an α_2-receptor. The selective α_2-

agonists, clonidine and oxymetazoline, both inhibited I_{Ca} in low concentrations, the action of clonidine being in agreement with Schofield (1990). However because of the low maximum of the dose-response relationships shown by both agonists, with some cells showing a very small response to the agonists, raised doubt to the subtype of α-receptor. This discrepancy was probably due to the partial agonist behaviour of clonidine and oxymetazoline, illustrated by the ability of these agonists to antagonise noradrenaline: the partial agonist nature of these agonists has been well documented (e.g. Medgett, 1978). It is possible that this effect is responsible for some of the confusion over the subtype of α-receptor mediating I_{Ca} inhibition in other tissues, for example in frog sympathetic ganglia where clonidine's lack of effect suggested a distinct type of α_2-receptor (Lipscombe et al, 1989).

UK14304, which has been described as a full agonist at α_2-receptors (Grant and Scrutton, 1979), proved useful in this study, proving both to be potent, and to produce a maximal response similar to noradrenaline. Therefore UK14304 is probably a much better agonist to determine α_2-receptor stimulation than more commonly used agonists such as clonidine.

In contrast to α_2-agonists, the α_1-agonist phenylephrine and the ß-agonist isoprenaline inhibited I_{Ca} only at very high concentrations suggesting that activation of α_1- and ß-receptors did not contribute to the adrenergic inhibition of I_{Ca} in s.c.g. neurones.

The quantitative determination of antagonist affinities provided further evidence for the subtype of adrenoceptor. The α-antagonist phentolamine inhibited noradrenaline's suppression of I_{Ca} with a pK_B of 7.97 comparable to values for phentolamine on various α-receptor responses (Furchgott, 1970; Besse and Furchgott, 1976). This is also in agreement with the reported blockade of the noradrenergic suppression of calcium spikes in s.c.g. neurones (Horn and McAfee, 1980) although a quantitative evaluation was not made. Interestingly, the pA_2 obtained in the present study was different from the value obtained for the noradrenergic suppression of calcium spikes in preganglionic s.c.g. neurones (Elliott et al, 1989) although this does not necessarily imply a different

type of receptor because antagonist activity can be distorted by agonist uptake (see below).

The α_2-antagonist yohimbine also showed an effective block of noradrenaline's response with a pK_B of 7.46, consistent with yohimbine's block of α_2-receptors in other preparations (for example Starke et al, 1975). These experiments also confirm the block of noradrenaline's suppression of calcium spikes in the intact s.c.g. (McAfee et al, 1981) and appeared similar to the action of yohimbine against adrenergic inhibition of calcium currents in frog sympathetic neurones (Lipscombe et al, 1989). However , as with phentolamine, yohimbine was far more potent in this study than in preganglionic s.c.g. neurones where yohimbine was only effective at very high concentrations (Elliott et al, 1989).

In contrast prazosin, which is a selective α_1-blocker, showed no block of the noradrenergic suppression of I_{Ca} at low concentrations, although it did show antagonist action at higher concentrations (pK_B of 5.36). The experiments using antagonists therefore agree with the agonist studies, and suggest that the α_2-subtype of receptor is responsible for mediating the effects of noradrenaline.

Accurate estimation of pA_2 values was difficult for the antagonists used in this study because the slopes of the Schild plots were less than unity (phentolamine, 0.87; yohimbine, 0.74; prazosin, 0.71 without constraint). Since Schild analysis of a competitive antagonist yields a slope of unity (Schild, 1949), the values obtained here suggest either the antagonists were not fully competitive, or there were other factors distorting antagonist activity. The possibility that the antagonists were not competitive was considered unlikely since these drugs have been extensively used to characterize adrenoceptors making use of their competitive nature. Furthermore the parallel shifts of dose-response curves are consistent with a competitive block, although it is possible that the antagonists produced both a competitive and non-competitive block. Alternatively more than one type of receptor could have contributed to the block of I_{Ca} although since both α_1- and ß-selective drugs were ineffective any additional receptor involved is

unlikely to be a classical adrenoceptor.

Another possible explanation for the non-ideal behaviour shown by the antagonists is the influence of noradrenaline uptake. Reduced dose-ratio shifts have been reported for agonists (including noradrenaline) which are substrates for uptake (Blinks, 1967; Furchgott, 1967). Such an effect which has been demonstrated in the intact rat s.c.g. for phentolamine's block of the ganglionic hyperpolarization (Brown and Caulfield, 1979), where isoprenaline (not taken up) and phenylephrine (only poorly taken up) were more effectively antagonised than noradrenaline. The role of uptake has been demonstrated by its elimination by uptake blockers (Moore and O'Donnell, 1970). It has been proposed (Langer and Trendelenburg, 1969) that this reduction in dose-ratio is due to a lack of proportion between the applied concentration of an agonist and the effective concentration (the effective concentration only being a proportion of the applied concentration). As the applied agonist concentration is increased (necessary during antagonist experiments), the uptake mechanism becomes saturated so that further increase results in a disproportionate increase in the effective concentration. This has the apparent effect of reducing the potency of a competitive antagonist, hence the smaller dose-ratios than expected. Although uptake was not considered a significant problem in this study (see earlier), it was not investigated, so can not be totally discounted as the cause of the non-ideal antagonist behaviour. In conclusion further investigation is necessary before the cause of the low slopes of the Schild plots can be determined.

Despite the potential errors in the antagonist affinities presented in this chapter, the size of these errors are probably small. Constraining the slopes of the Schild plots to unity (see results) has only a small effect on the pA_2 values obtained, mainly because the antagonist concentrations used were close to the pA_2 values at which point slope differences are minimal (see Tallarida et al, 1979). The data, therefore, still provide a good estimate of antagonist potency and selectivity and does not alter the conclusions from the experiments.

The pharmacological characteristics observed allow comparison with other investigations of noradrenergic suppression of I_{Ca}. This work is in agreement with the

suppression of calcium spikes in intact rat sympathetic ganglia (Horn and McAfee, 1980; McAfee et al, 1981) and I_{Ca} in acutely dissociated s.c.g. neurones (Schofield, 1990) both studies indicating an α_2-receptor. The receptor mediating suppression in preganglionic sympathetic neurones appears different (Elliott et al, 1989) but the low antagonist potencies are possibly due to distortion by uptake (see earlier).

Suppression of I_{Ca} in other neurones indicates that the receptor characterized here most closely resembles the receptor described in guinea-pig submucosal neurones (Surprenant et al, 1990) where both α_2-agonists and antagonists were effective. Inhibition of I_{Ca} in NG108-15 cells (Docherty and McFadzean, 1989) and frog sympathetic neurones (Lipscombe et al, 1989) was also similar except for the inactivity of clonidine. The receptor described in this study, however, appears appreciably different to the receptors described in avian DRG neurones (Canfield and Dunlap, 1984) and locus coeruleus neurones (Williams and North, 1985).

It is also interesting to compare the receptor characterized here to the α_2-receptor responsible for generating the adrenergic hyperpolarization observed in the rat s.c.g. (Brown and Caulfield, 1979). Noradrenaline and adrenaline were both much more potent in this study (approximately 10 fold and 5 fold respectively) as would be expected since agonist responses were affected by uptake in the previous study. Clonidine and oxymetazoline were partial agonists in both studies. Surprisingly though, both phenylephrine and isoprenaline were potent agonists generating the hyperpolarization (EC_{50} values of approximately 4.2 and 3.2μM respectively), whilst these agonists inhibited I_{Ca} only at much higher concentrations. The effects of antagonists were similar, though not identical, in the two studies, with yohimbine being approximately 10 times more potent at preventing the hyperpolarization, and phentolamine twice as potent at blocking suppression of I_{Ca}. Given this evidence, it appears that the two receptors may not be the same, implying the coexistence of different types of α_2-receptor in the s.c.g. Caution must be applied, though, since experimental conditions were different, particularly since different strains and age of rat were used, and the dissociation and culture techniques used in this study may possibly

alter receptor characteristics. Ideally, a direct comparison needs to be made using the same cells under the same experimental conditions. This was not possible here because the conditions necessary to record I_{Ca} also block other membrane currents, including the outward current (representing the hyperpolarization) generated by noradrenaline (see chapter 5).

Despite doubt whether the receptor characterized in this study is identical to the hyperpolarizing α_2-receptor, the results still suggest a strong similarity to the α_2-autoreceptors proposed for noradrenergic neurones (reviewed by Starke, 1987). One mechanism by which autoreceptors are proposed to reduce transmitter release is via inhibition of I_{Ca} (Starke, 1987) and, since the role of 'N'-type calcium channels in release of noradrenaline from rat s.c.g. neurones has been shown (Hirning et al, 1988), it is likely that the receptor investigated here is typical of noradrenergic autoreceptors.

There was no evidence for a ß-adrenergic enhancement of I_{Ca}. Isoprenaline was without effect, other than suppression at high concentrations. In addition, α-receptor blockade failed to reveal any facilitation of I_{Ca} that might have been obscured by the dominant α-inhibition. This is in contrast to frog sympathetic neurones where facilitation was observed in response to isoprenaline (Lipscombe and Tsien, 1987), an effect which was reproduced by 8-bromocyclic AMP indicating the involvement of cAMP. Since ß-adrenergic stimulation also increases cAMP in the rat s.c.g. (Brown and Dunn, 1983b) it is tempting to speculate that an enhancement of I_{Ca}, similar to that observed in frog neurones, might be expected. Furthermore, facilitation of noradrenaline release by ß-receptors has been widely reported (reviewed by Langer, 1981), notably in cultured rat s.c.g. neurones (Weinstock et al, 1978). It is possible that facilitation of I_{Ca} can occur in the rat s.c.g. but was not observed in this study because of the washout of soluble intracellular messengers during the whole-cell recording. Evidence for this is provided by the observation that noradrenaline facilitated patch barium currents during cell-attached recordings from s.c.g. neurones (Beech et al, 1990). Use of this recording method prevents both washout of intracellular molecules, and eliminates the dominant α-inhibition which has been shown to be membrane

delimited (Beech et al, 1991; Bernheim et al, 1991), and it is possible that only under specific recording conditions such as these will enhancement be observable. Using intracellular electrodes, no effects of isoprenaline, other than those replicating the actions of noradrenaline, were observed against Ca^{2+} dependent potentials in intact s.c.g. neurones (Horn and McAfee, 1979). The physiological relevance of such a small and virtually unobservable enhancement is likely to be negligible when compared to the α-inhibition. However, since the recordings described above have all been made from the soma, it is possible that ß-enhancement of I_{Ca} plays a more important role at the nerve terminal, where control of noradrenaline release is important.

In conclusion, the results from this chapter indicate that the noradrenergic suppression of I_{Ca} in rat s.c.g. neurones is mediated by the α_2-subtype of receptor.

During the course of this study it has become increasingly apparent that there are multiple subtypes of α_2-receptors, evidence for this being provided from both pharmacological and molecular cloning studies. Thus whilst the conclusion that an α_2-receptor mediates I_{Ca} suppression in s.c.g. neurones is still valid, further work will be necessary to determine the identity of the sub-type of α_2-receptor involved. The question of α_2-receptor subtypes is discussed further in chapter 6.

Fig. 4.1 Concentration-dependence of the inhibition of I_{Ca} by noradrenaline.

A. Membrane currents recorded from a voltage-clamped s.c.g. neurone (V_H = -80, V_C = 0mV) showing inhibition of I_{Ca} by cumulative increases in noradrenaline concentration (records show control, 0.01, 0.03, 0.1, 1, 10μM). Each concentration of noradrenaline was allowed one minute to equilibrate with the recording chamber.

B. Log-concentration response relationship for the inhibition of I_{Ca} by noradrenaline. Inhibition was determined by measurement of peak I_{Ca}. Results are plotted as mean ± s.e.m. The numbers in parentheses are the number of determinations (from 16 cells). Non-linear regression was used to fit the combined data to the hyperbolic function below, the sigmoidal derivative shown here being the result of plotting log agonist concentration on the abscissa.

$$Y = \frac{Y_{max} \cdot X^n}{X^n + EC_{50}{}^n}$$

where Y = inhibition of I_{Ca}

Y_{max} = maximum inhibition of I_{Ca}

X = agonist concentration

n = molecular ratio of agonist to receptor

EC_{50} = agonist concentration at half maximal inhibition

EC_{50}, Y_{max} and n were variables and yielded values of 81.5nM, 52% and 0.93 respectively. Note these values are slightly different to the values obtained by calculating a separate fit to each experiment (see text).

A.

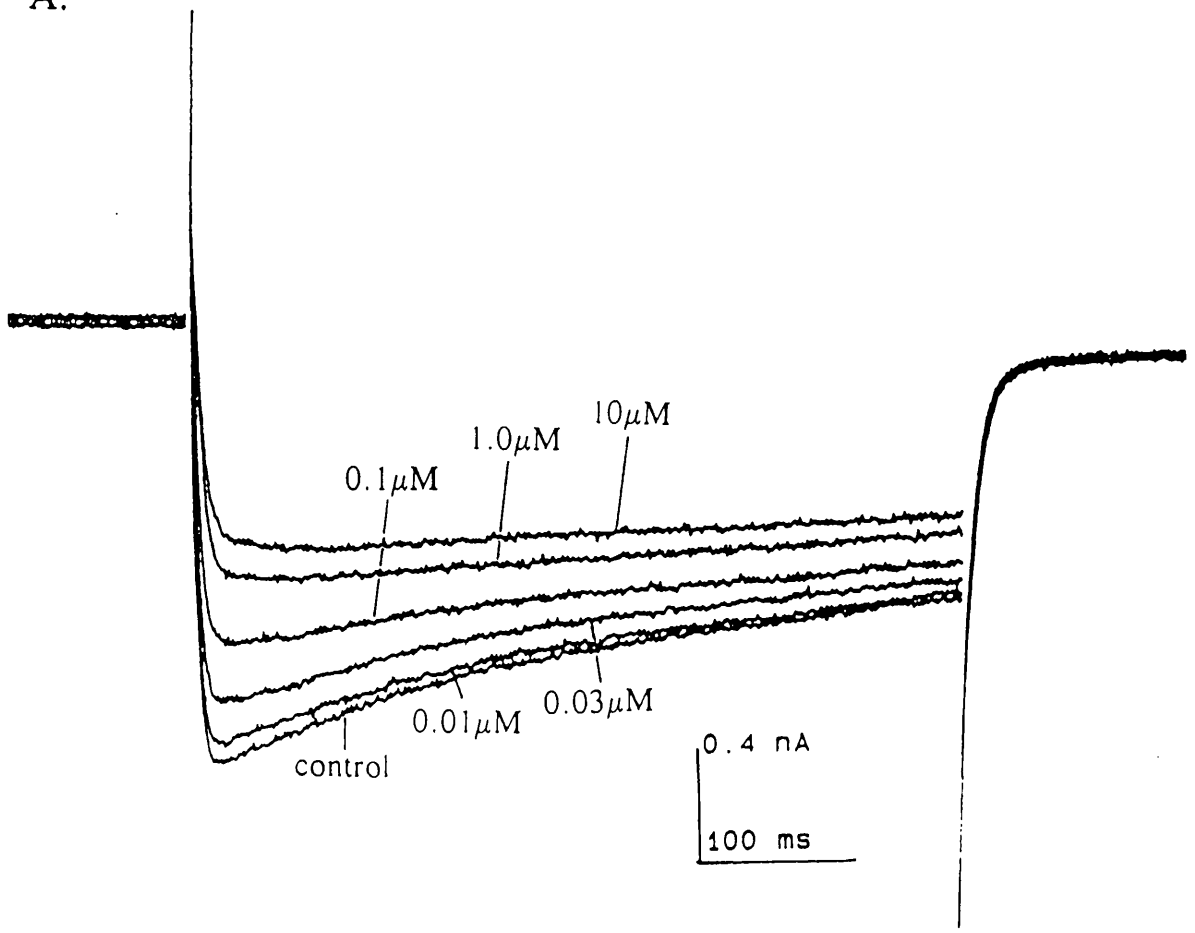
10μM
1.0μM
0.1μM
0.03μM
0.01μM
control
0.4 nA
100 ms

B.

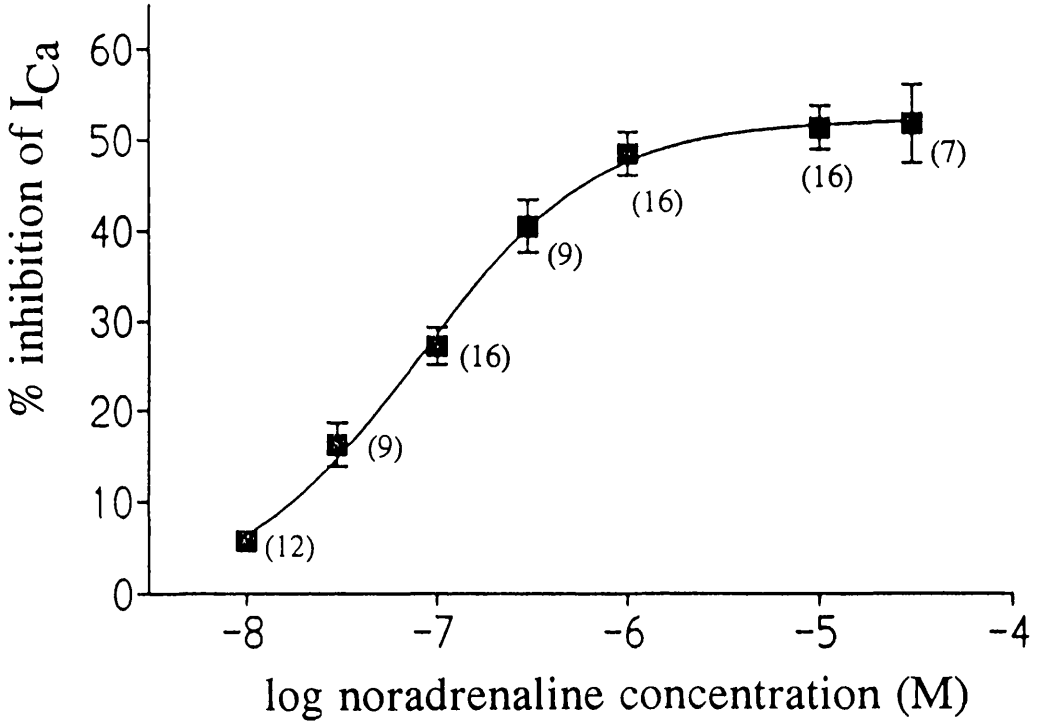
% inhibition of I_{Ca}
60
50
40
30
20
10
0
-8
-7
-6
-5
-4
log noradrenaline concentration (M)
(12)
(9)
(16)
(9)
(16)
(16)
(7)

Fig. 4.2 Inhibition of I_{Ca} by adrenergic agonists.

Dose-response relationships for the inhibition of I_{Ca} by adrenaline (□), UK14304 (○), clonidine (■), oxymetazoline (▲), phenylephrine (◆) and isoprenaline (△). Results plotted as mean ± s.e.m. The numbers in parentheses are the number of determinations.

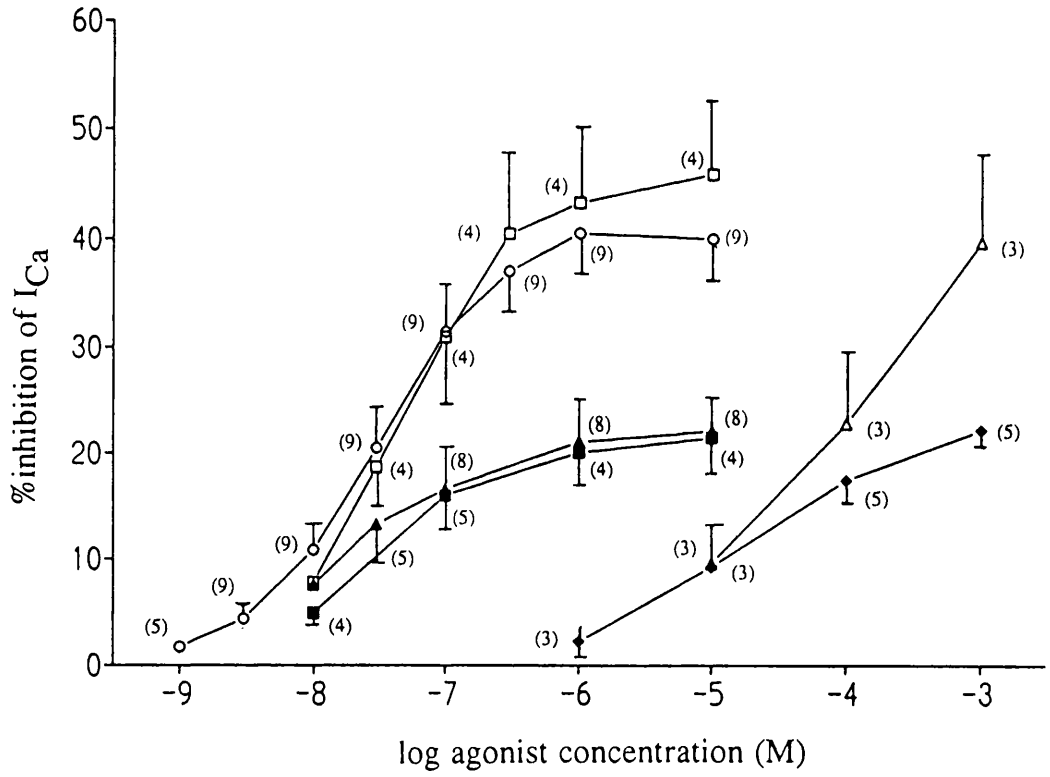
60
50
40
30
20
10
0
%inhibition of I_{Ca}
-9
-8
-7
-6
-5
-4
-3
log agonist concentration (M)

Fig. 4.3 Partial agonist activity of oxymetazoline.

A. Records showing inhibition of I_{Ca} by 1μM oxymetazoline (V_H=-90, V_C=0mV)

B. Records obtained from the same cell as above showing antagonism of noradrenaline's suppression of I_{Ca} by oxymetazoline. Records show (a) control current, (b) 1μM noradrenaline, (c) 1μM oxymetazoline (noradrenaline still present), (d) removal of oxymetazoline, (e) complete wash.

A.

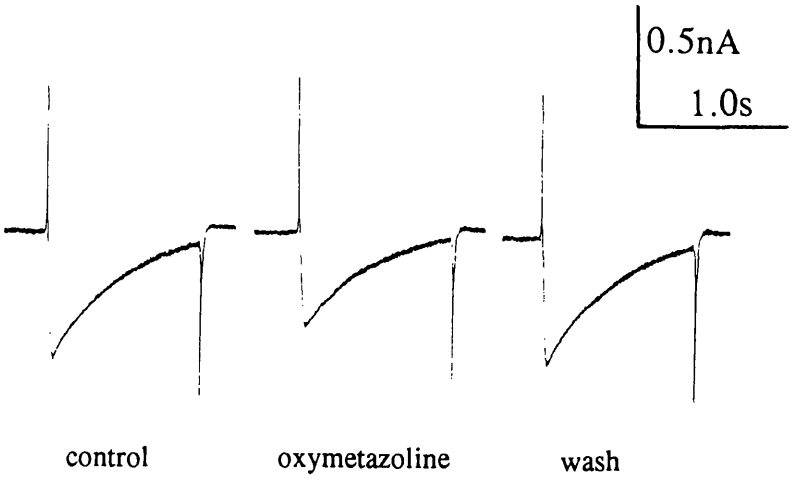
0.5nA
1.0s
control
oxymetazoline
wash

B.

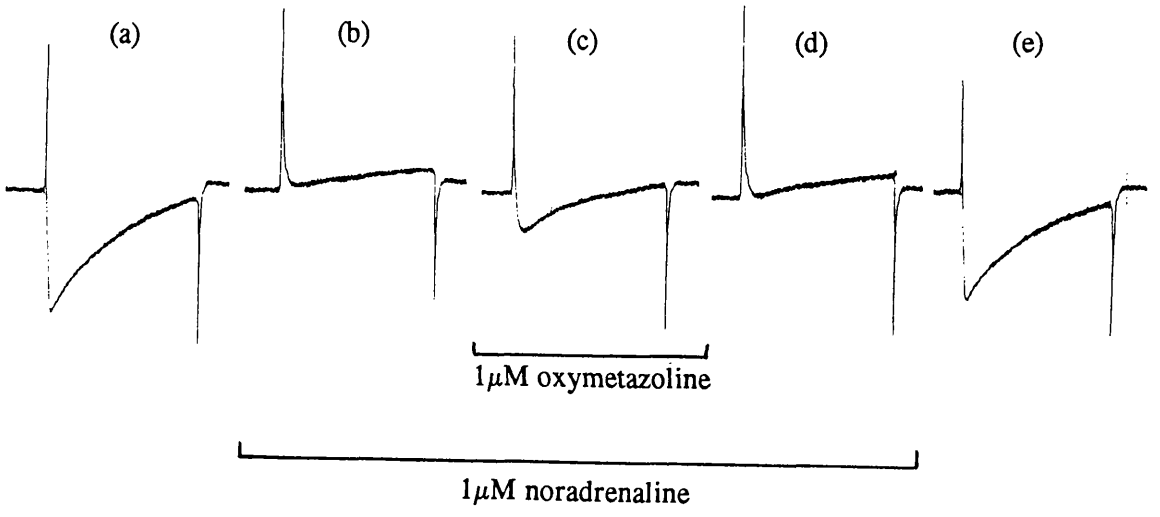
(a)
(b)
(c)
(d)
(e)
1μM oxymetazoline
1μM noradrenaline

Fig. 4.4 Effect of phentolamine on inhibition of I_{Ca} by noradrenaline.

Membrane currents recorded from a s.c.g. neurone (V_H = -80, V_C = 0mV) showing inhibition of I_{Ca} by 0.1μM noradrenaline in (a) the absence, and (b) 10 minutes after adding 1μM phentolamine.

(a)

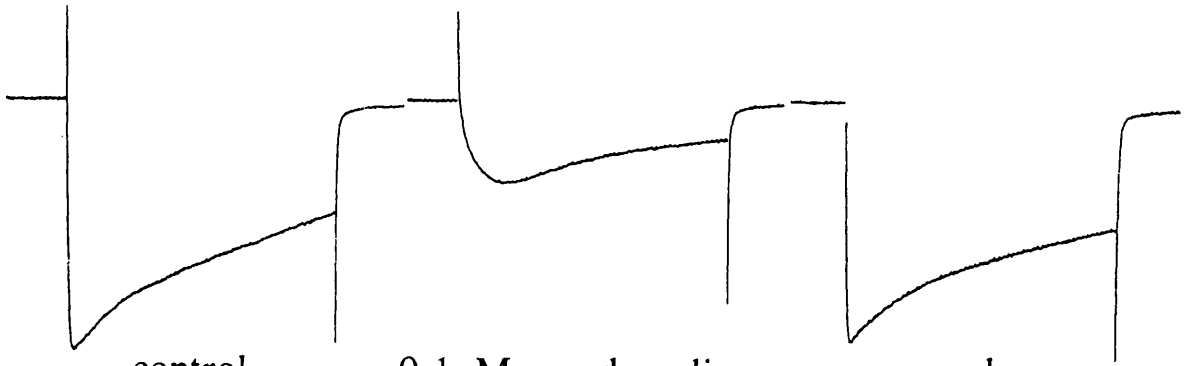

(b) +1μM phentolamine

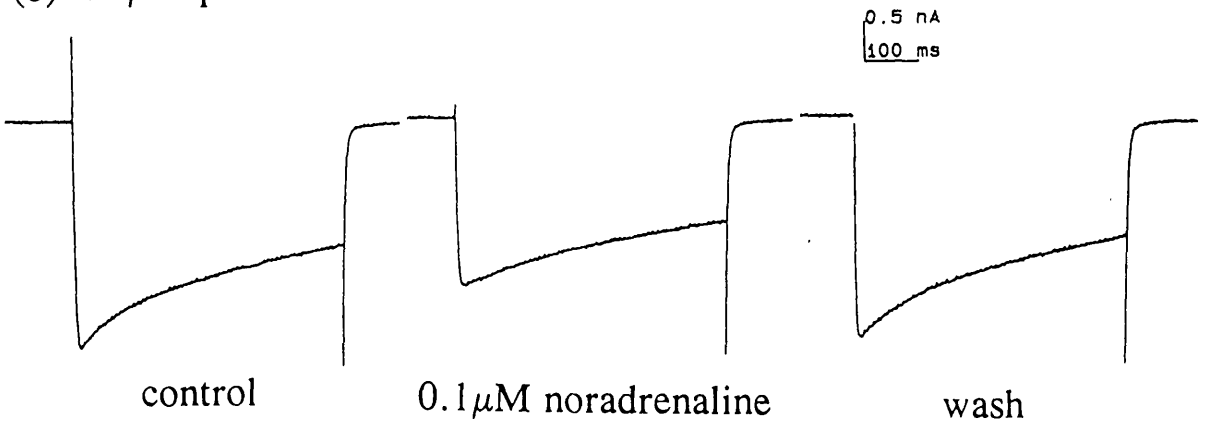

Fig. 4.5 Analysis of antagonism of noradrenaline's suppression of I_{Ca} by phentolamine.

A. Combined dose-response curves illustrating the shift in dose-response relationship for noradrenaline's inhibition of I_{Ca} by increasing concentrations of phentolamine. The curves show data obtained in the absence (●), and the presence of 10nM (n=3,■), 100nM (n=4,▲) and 1μM (n=4,◆) phentolamine. The results are plotted as mean ± s.e.m.

Note that for use in calculations, the data from each experiment was analysed separately.

B. Schild plot using data from the experiments illustrated above. The log (dose-ratio - 1) for the shift in noradrenaline response is plotted against log (phentolamine concentration). Dose-ratios were measured at 50% maximal inhibition of current, assuming that phentolamine did not alter the maximum inhibition.

The solid line represents the fit obtained by least-squares regression analysis to the equation $y = mx + c$, where m (slope) and c (y-axis intercept) are variables. The dashed line represents the solution to the same equation when the slope is constrained to unity.

A.

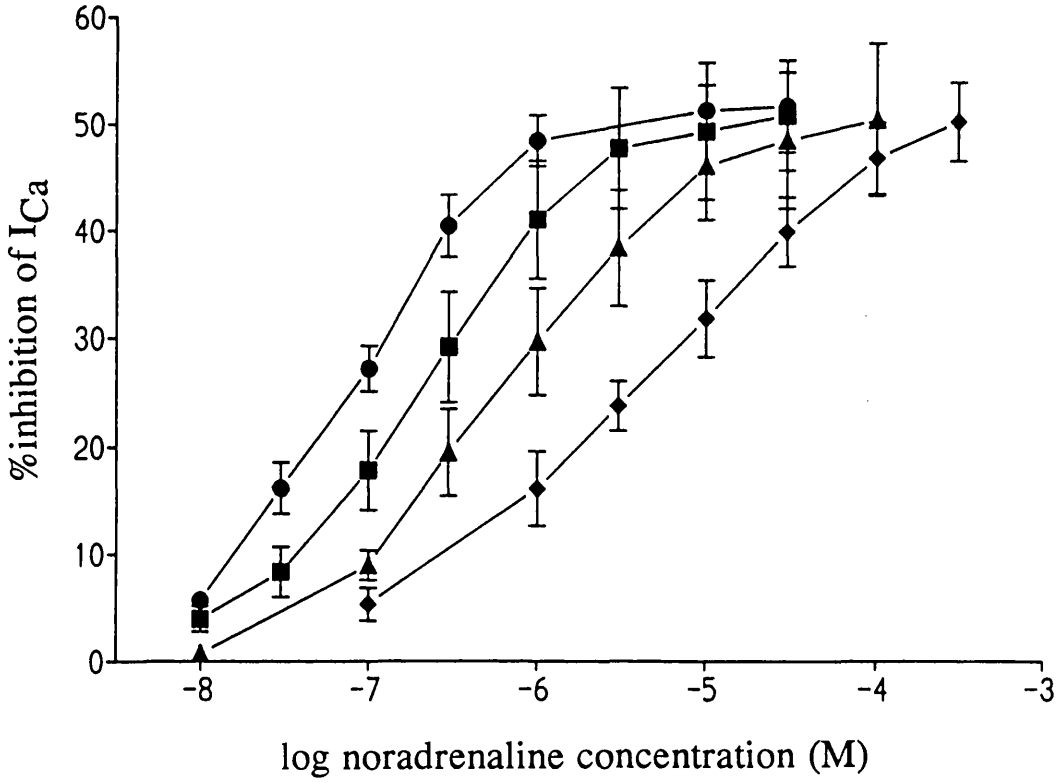
60
50
40
30
20
10
0
%inhibition of I_{Ca}
-8
-7
-6
-5
-4
-3
log noradrenaline concentration (M)

B.

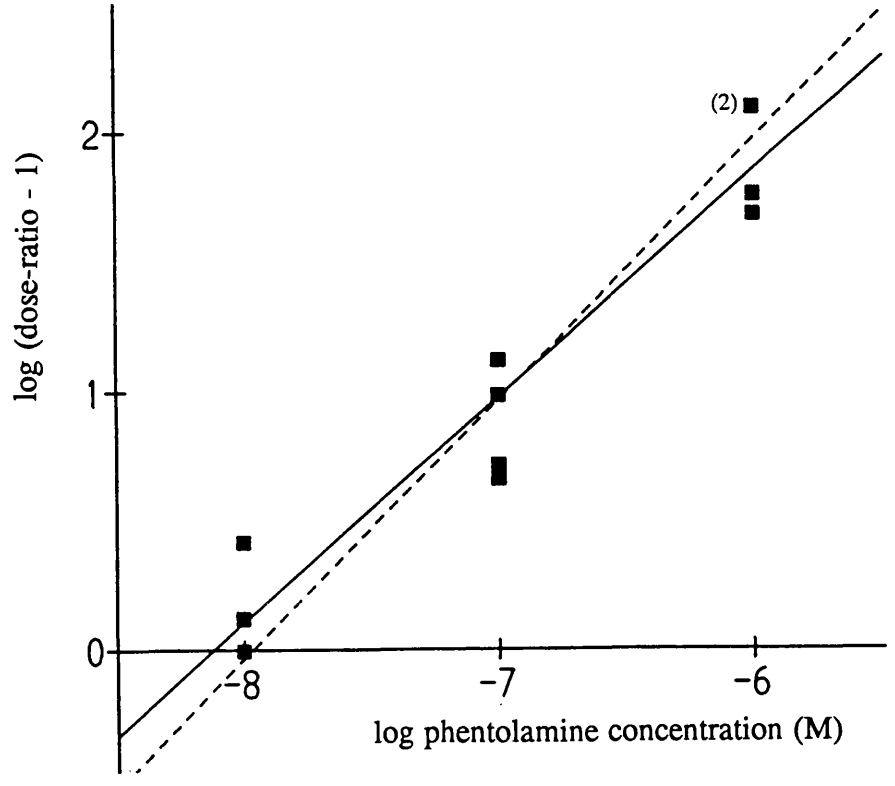
2
1
0
log (dose-ratio - 1)
(2)
-8
-7
-6
log phentolamine concentration (M)

Fig. 4.6 Effect of yohimbine on inhibition of I_{Ca} by noradrenaline.

Inhibition of I_{Ca} by 1μM noradrenaline recorded (a) before, and (b) 10 minutes after adding 1μM yohimbine. Currents were evoked by 500ms steps to 0mV from -80mV.

(a)

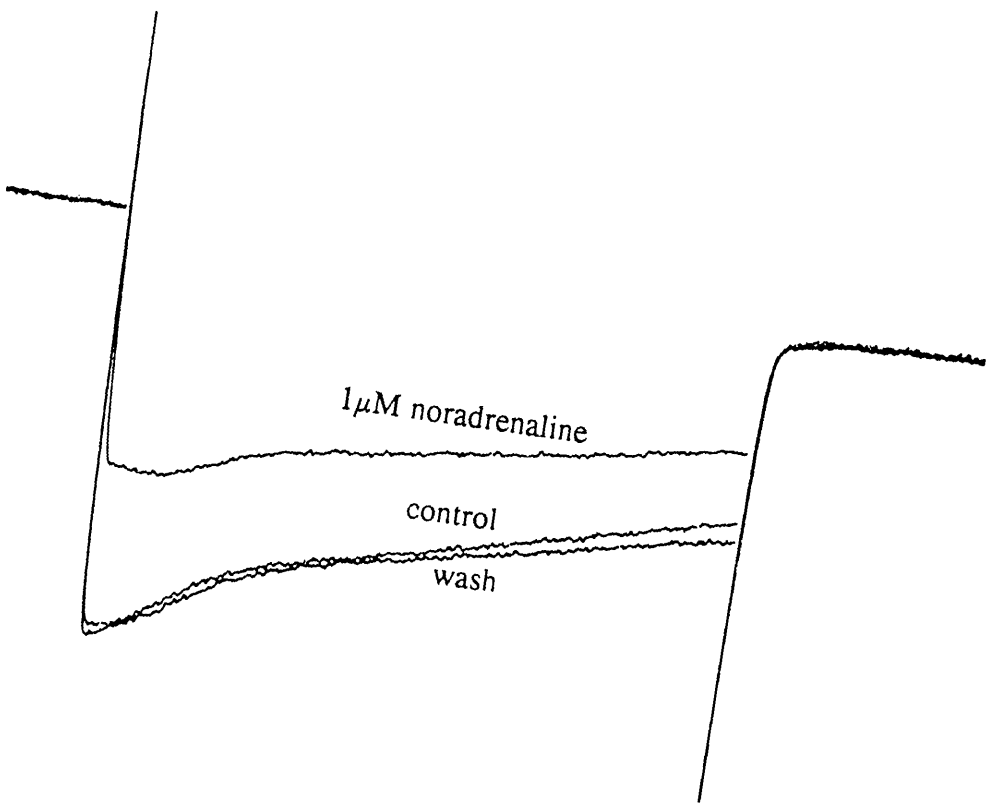
1μM noradrenaline
control
wash

(b)

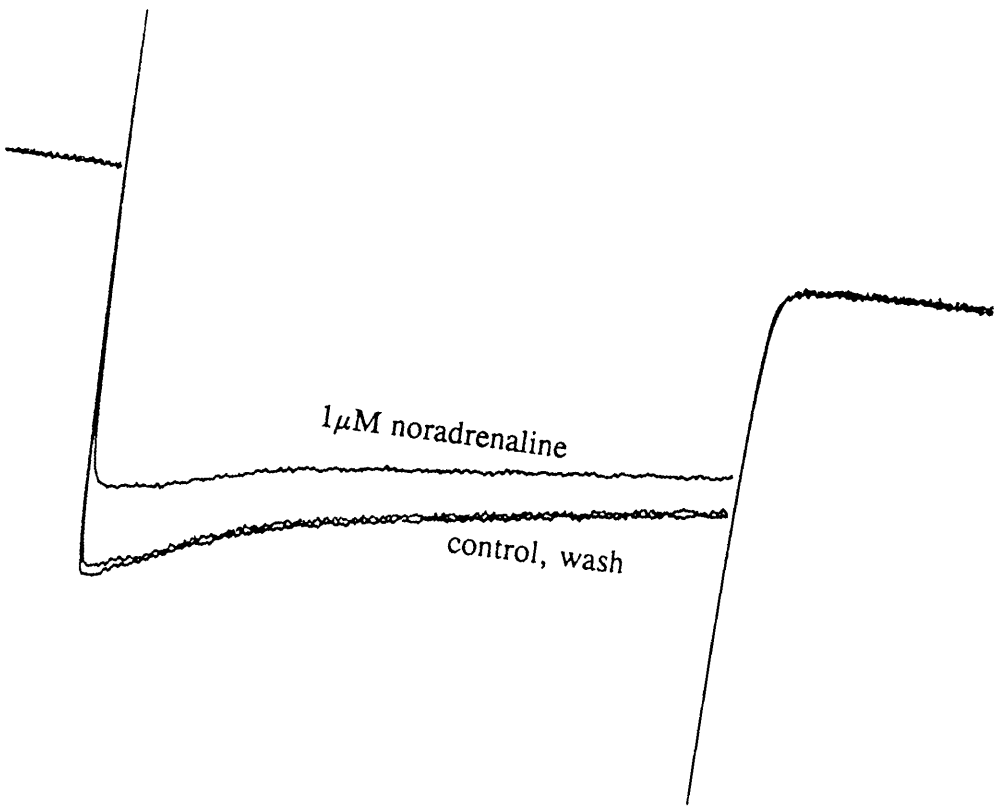
1μM noradrenaline
control, wash
0.6 nA
100 ms

Fig. 4.7 Analysis of antagonism of noradrenaline's suppression of I_{Ca} by yohimbine.

A. Combined dose-response relationships illustrating the inhibition of I_{Ca} by noradrenaline in the absence (●) and the presence of 10nM (n=3,■), 100nM (n=4,▲) and 1μM (n=4,◆) yohimbine. Data plotted as mean ± s.e.m.

B. Schild analysis of the data shown above. See fig. 4.5 for details.

A.

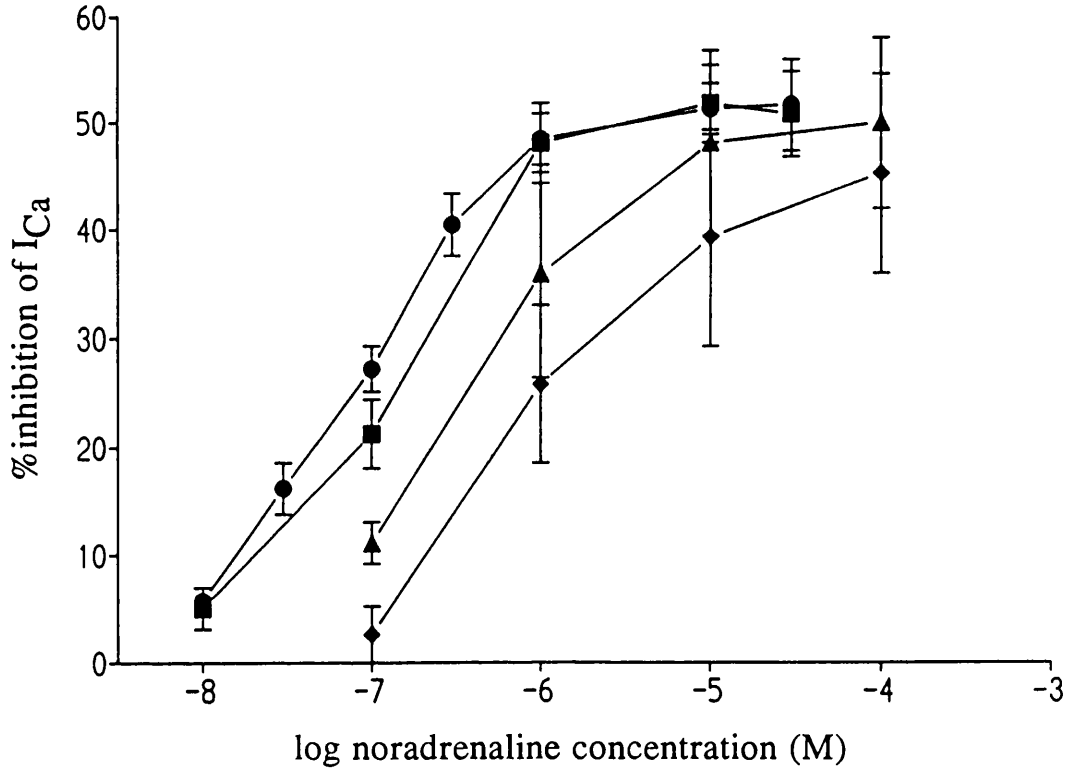
60
50
40
30
20
10
0
% inhibition of I_{Ca}
-8
-7
-6
-5
-4
-3
log noradrenaline concentration (M)

B.

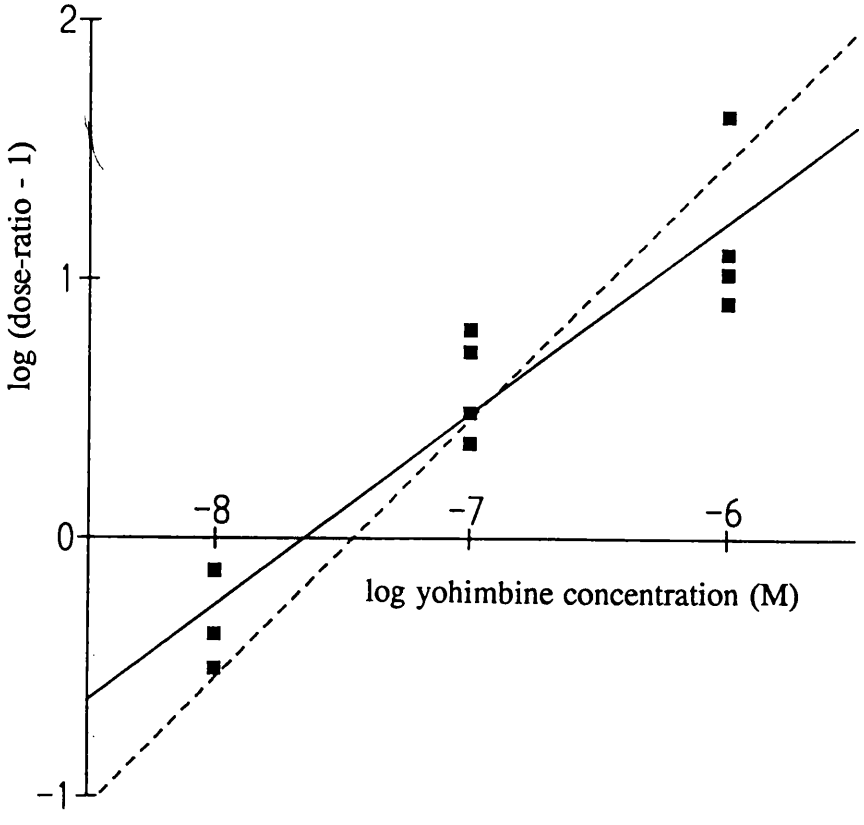
2
1
0
-1
log (dose-ratio - 1)
-8
-7
-6
log yohimbine concentration (M)

Fig. 4.8 Antagonism of noradrenaline's inhibition of I_{Ca} by high concentrations of prazosin.

A. Combined dose-response relationships for the inhibition of I_{Ca} by noradrenaline in the absence (●) and the presence of 1μM (n=3,■), 10μM (n=3,▲) and 30μM (n=3,◆) prazosin. Data represents mean ± s.e.m.

B. Schild analysis of the data shown above (see fig. 4.5 for details)

A.

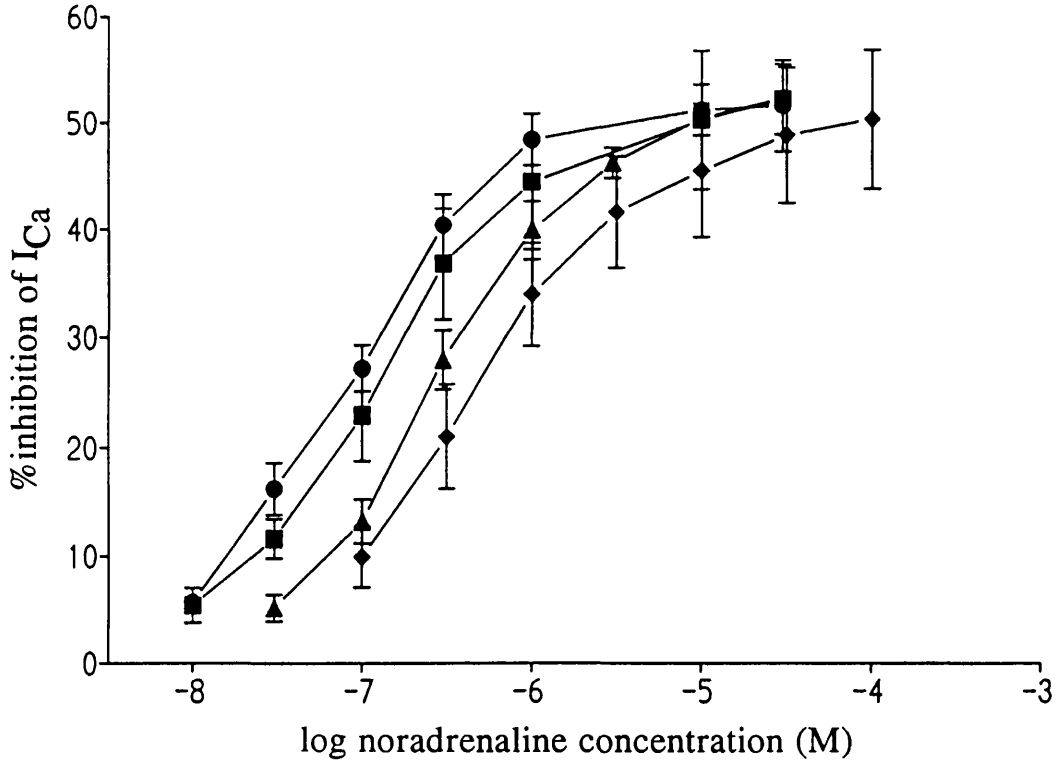
60
50
40
30
20
10
0
% inhibition of I_{Ca}
-8
-7
-6
-5
-4
-3
log noradrenaline concentration (M)

B.

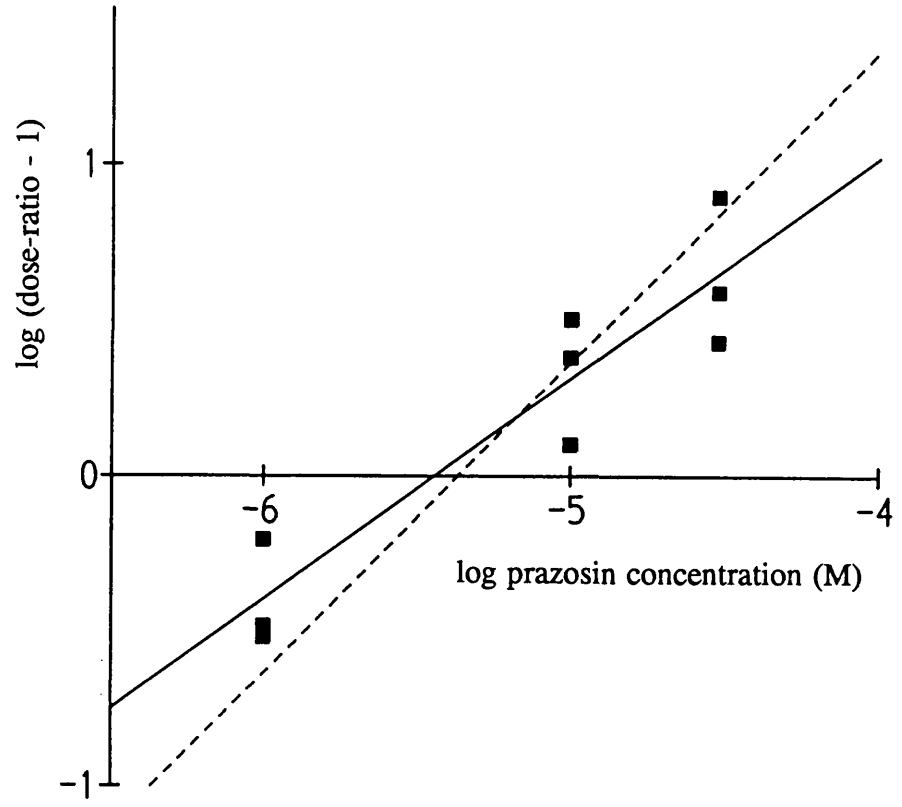
log (dose-ratio - 1)
1
0
-1
-6
-5
-4
log prazosin concentration (M)

Chapter 5.

Investigation of I_{AHP}.

Introduction.

The aim of this chapter is to investigate the current that generates the after-hyperpolarization (a.h.p.) of s.c.g. neurones, to determine the basic characteristics of the current, investigate the calcium dependence of the current, and to investigate the pharmacological properties of the current.

Methods.

Initial experiments were performed using intact s.c.g. neurones. Voltage-clamp recordings were made via an intracellular microelectrode (see chapter 2, Methods). Later experiments were performed on dissociated s.c.g. neurones, voltage-clamp recordings usually being made via a whole-cell patch electrode (chapter 2, Methods). In addition, a few experiments on dissociated neurones were performed using intracellular electrodes.

Neurones were voltage-clamped at constant holding potentials (usually -40 to -55mV) and currents evoked by depolarizing commands (usually to about 0mV and of 50ms in duration). The amplitude of the evoked current was generally measured 25ms after the end of the voltage command, the value obtained being used as peak amplitude in calculations, though occasionally I_{AHP} amplitude was measured at later times to make investigation of drug effects easier. Although the evoked current had partially decayed by 25ms, measurements of the current could not reliably be made before this time. Where appropriate, an approximate value for the rate of decay of the outward current was calculated as the time taken for the current to decay to half of its peak value. The rate of decay of current was also, when possible, more accurately estimated

by plotting log I_{AHP} amplitude against time to produce a linear decay, allowing calculation of the slowest component and curve-stripping to obtain faster components.

The effects of drugs were determined by recording currents in the absence and presence of each drug. Dose-response relationships were constructed using cumulative additions of drug, allowing the response to reach steady-state at each concentration. The effects of various drug treatments on I_{AHP} amplitude and time-constant are summarized in table 3.

Results.

A. Characterization of I_{AHP} in s.c.g. neurones

I_{AHP} in intact neurones.

Initial experiments were carried out using microelectrode recordings from intact s.c.g. neurones. Fig. 5.1A illustrates a typical example of the outward tail-current evoked by a depolarizing command in voltage-clamp. The current was maximal immediately following the end of the voltage-command, and slowly decayed back to the holding-current recorded prior to the command. Similar depolarizing voltage-clamp commands from holding potentials of around -50mV evoked slow outward tail-currents in many other cells. The peak amplitude of these outward currents (measured at 25ms after the end of the voltage-command) varied from 0.1 to 1nA (mean 0.723 $\pm$ 0.06nA from a sample of 38 neurones), and the total duration varied between 0.5 and 3s.

The pattern of decay of the outward current varied: many neurones showed slow tail-currents that could be fitted by either 1 or, more commonly, 2 exponentials. Currents obtained from a sample of 15 neurones exhibiting a 2-exponential decay yielded time constants of approximately 135 $\pm$ 11 ms and 441 $\pm$ 36 ms, calculated from semi-logarithmic plots. In some neurones the current showed a more complicated

time course that could not be fitted to an exponential decay (illustrated by non-linear semi-logarithmic plots). Because of this variability, kinetic analysis of recordings from large populations of neurones could not reliably be provided by the semi-logarithmic plots described above and was also provided by measurement of the time from peak current (measured at 25 ms after the command) to half-decay. This varied between 100 and 350ms (mean 197 ± 15ms; n=31).

The slow tail-current recorded here appears similar to I_{AHP} recorded in bullfrog neurones (Pennefather et al, 1985) and it seems reasonable, at this point, to similarly designate this slow outward tail-current in s.c.g. neurones as $\mathbf{I_{AHP}}$.

In addition to the slow outward tail-current following depolarizing pulses, a large rapidly-decaying outward tail was usually observed, superimposed on the early part of the slow tail. Using data obtained from the semi-logarithmic plots described above, a time constant of approximately 20ms was calculated. Since this fast tail decayed within 50ms of the end of the depolarizing pulse it did not hinder investigation of the decay of the slow tail-current beyond this period. However, this large fast component obscured any rising phase of the slow tail-current that might have otherwise been observable. Because of the difficulty in resolving this fast tail with the single-electrode voltage-clamp used, this current has not been investigated in detail.

The amplitude and time-course of the outward tail-currents in any one cell were generally constant with successive command pulses, though run-down of the peak amplitude of the current was frequently observed during longer experiments. Not all neurones showed slow tail-currents in response to depolarizing commands. Failure to record an evoked current was most commonly observed in neurones with low input resistances following damage during impalement.

I_{AHP} in dissociated neurones.

Most experiments using dissociated neurones were made via whole-cell patch

electrodes. Fig. 5.1B illustrates an example of the outward tail-current recorded from a dissociated neurone using a whole-cell electrode. The current observed appeared similar to that recorded from the intact ganglion although the peak amplitude of the current was smaller (0.307 $\pm$ 0.023nA, n=28). The current recorded from dissociated neurones also appeared to decay more slowly than the current recorded from intact neurones (time to half decay = 285 $\pm$ 17ms in 19 cells). Decay of I_{AHP} in dissociated neurones was more consistent than in intact neurones. Semi-logarithmic plots yielded a single exponential decay in most cells (illustrated in Fig. 5.2), with a mean time constant of 440 $\pm$ 34ms (n=22). Because of the greater consistency of decay in dissociated neurones the effect of drugs on the decay time constant could be investigated.

A few experiments using dissociated neurones were made with intracellular electrodes. Under these conditions, the mean amplitude of the I_{AHP} was 0.282 $\pm$ 0.029nA, and the time constant of decay was 345 $\pm$ 31 ms (n=9).

It was noticed that the size of I_{AHP} recorded from dissociated neurones increased during the first few days following dissociation and recordings made 1 or 2 days following dissociation often failed to show the presence of I_{AHP}. Recordings were therefore only made from neurones that had been dissociated at least four days previously, though neurones were generally not used beyond 1 week after dissociation. Run-down of I_{AHP} was frequently observed with whole-cell recordings, though there was little consistency between recordings with the current decaying within 10 minutes in some cells and maintaining a constant amplitude for at least 1 hour in others. No relationship between current run-down and pipette resistance was noticed.

Dependence on extracellular Ca^{2+}.

The Ca^{2+} dependence of I_{AHP} was shown by the removal of Ca^{2+} from the extracellular solution (Fig. 5.3A). On switching to nominal Ca^{2+} free solution, the slow outward tail-current representing I_{AHP} was very much reduced, although the initial fast component of the tail-current was less inhibited. The effect of a calcium

channel blocker, Cd^{2+}, on I_{AHP} was also investigated (Fig. 5.3B). Following addition of 500μM Cd^{2+} the slow tail-current was abolished and the fast tail substantially reduced.

Effect of membrane potential.

In intact neurones, the tail-current amplitude varied with holding potential in the manner shown in Fig. 5.4, and reversed between -80 to -95mV. The linear relationship between amplitude of I_{AHP} and membrane potential observed over the range -60 to -90mV suggests that the conductance was independent of voltage in this range. However in many cells the reversed inward current was very small, suggesting possible outward rectification. In addition, decay of the initial fast outward component following the command pulse frequently reversed at a more positive potential (-70 to -80mV) than the later I_{AHP}, possibly due to accumulation of K^+ in the extracellular space (see Belluzzi et al, 1985b). The duration of I_{AHP} remained constant at holding potentials of -40 to -110mV (Fig 5.4A), although measurement was difficult in many cells around and beyond reversal due to the small currents observed.

A similar voltage relationship was observed in dissociated neurones (using whole-cell recording) (Fig. 5.5). Again the relationship was linear between -60 and -90mV with reversal around -85mV. It was, however, noted that above -60mV I_{AHP} became maximal and then decreased with depolarized holding potentials. It is reasonable to assume that depolarized holding potentials will lead to inactivation of I_{Ca} and therefore reduce calcium entry during the command pulse. To avoid this, and investigate the voltage-dependence of I_{AHP} under conditions of constant Ca^{2+} entry, the holding potential prior to the command pulse was kept constant with different post-command voltages being applied (Fig. 5.6). As can be seen, I_{AHP} is approximately linear between -40 and -90mV, and not reduced at depolarized membrane potentials. The effect of the pre-command membrane potential was also recorded to investigate the effect of steady-state inactivation of I_{Ca} on I_{AHP}, and is shown in Fig 5.7. I_{AHP} amplitude decreases with

depolarized pre-pulse potentials in a manner similar to that observed with the steady-state inactivation of I_{Ca}.

Dependence of I_{AHP} on command potential.

The amplitude and time-course of I_{AHP} was dependent on the command potential. Fig. 5.8 illustrates a dissociated s.c.g. neurone subjected to increasing voltage commands. I_{AHP} is activated by commands above -30mV and reaches a maximal amplitude around +10mV. At higher potentials the peak amplitude of the current remains similar. The time-constant of current decay increases as command potential is raised above -30mV (τ = 317ms at a command potential of -16mV in this cell) and, like the amplitude, is maximal around +10mV (τ = 447ms). However, at higher potentials the decay time constant decreases (τ = 252ms at +42mV), the effect being that the appearance of I_{AHP} is considerably altered. The plot of time-constant against command potential is similar to the current-voltage relationship obtained for I_{Ca} (see Fig. 3.3), suggesting that the time-course of I_{AHP} decay is dependent upon the size of the calcium load (see later). The relatively consistent amplitude of I_{AHP} at command potentials above +10mV is possibly due to the early part of I_{AHP} decay being contaminated by $I_{K(DR)}$, which will be strongly activated by the large depolarizing commands.

Dependence of I_{AHP} on extracellular K^+.

Fig. 5.9A illustrates the effect of raised extracellular K^+ on I_{AHP} recorded at -58mV in an intact neurone. As K^+ is raised from 5 to 20mM, I_{AHP} amplitude is reduced and then reversed. Reversal of I_{AHP} became less negative as the external K^+ concentration was raised. Thus in one intact s.c.g. neurone (Fig. 5.9B) reversal occurred at -85mV in normal extracellular K^+ (4.8mM), decreasing to -48mV as K^+ was raised to 20mM. This reversal potential shift of 37mV compares well with an expected shift in reversal for a pure K^+ conductance of 36mV at 20°C. There was no noticeable

effect of varied external K^+ on the time-course of I_{AHP}.

Effect of altering temperature.

Fig. 5.10A illustrates the effect of temperature on I_{AHP}. Raising the temperature of the Krebs' solution perfusing the intact s.c.g. from 25 to 35°C caused a large increase in the amplitude of I_{AHP} (Q_{10} of up to 4) and slowed the decay rate. Fig 5.10B shows the record obtained at 25°C scaled up illustrating the change in the decay pattern. It was noticed that as the temperature of the preparation was raised, the command pulse became more difficult to clamp reliably, the actual potential attained being lower than the command potential. This was overcome as far as possible by continually adjusting the command pulse as the temperature was changed, so as to produce a constant depolarizing pulse in the cell.

B. Regulation of I_{AHP} by calcium.

Effect of varying external Ca^{2+} concentration.

Fig. 5.11 illustrates the effect of altering extracellular Ca^{2+} in intact neurones. Increasing extracellular Ca^{2+} from 2.5mM to 5mM (Fig 5.11A) caused an increase of both the peak amplitude and the time to half-decay. Using data from 15 neurones there was a mean increase of the time to half-decay of 15.0 ± 3.8 % but only an insignificant increase in the peak amplitude (3.9 ± 3.2 %). Increasing the extracellular Ca^{2+} further to 7.5mM produced no further consistent effect on the time to half-decay (+13.5 ± 4.3 % n=11 from control), and a slightly larger peak amplitude (+7.0 ± 4.8 %). However there was no consistent effect upon the total duration of I_{AHP}. Following return to normal extracellular Ca^{2+}, the time to half-decay and peak amplitude returned

to control values.

Decreasing extracellular Ca^{2+} (for example Fig 5.11B) had greater effect on I_{AHP} than was found with raising Ca^{2+}. Following reduction in extracellular Ca^{2+} from 2.5mM to 1.25mM (2.8mM Mg^{2+}), the time to half-decay decreased (-27 $\pm$ 1.5 % n=5) and peak amplitude was also reduced (-12.5 $\pm$ 2.3 %). There was no change to the total duration of I_{AHP}. It thus appeared from these experiments that the rate of decay of I_{AHP} (as measured by time to half decay) is more sensitive to the size of the Ca^{2+} influx than is the peak amplitude. However the effects described varied considerably between cells, and since alteration in the extracellular Ca^{2+} and Mg^{2+} concentrations might have effects other than just reduction of Ca^{2+} influx, further experiments were considered necessary.

Effect of varying pulse duration on I_{AHP}.

The size of the Ca^{2+} influx into the cell was also varied by altering the duration of the depolarizing command pulses. Fig. 5.12 illustrates records from an intact neurone with the duration of the command pulse varied from 1ms to 100ms. This resulted in I_{AHP}s of both increasing amplitude and time to half decay. The total duration of the I_{AHP}s also increased as the command was lengthened. With the longer commands it was noticed that the decay of I_{AHP} became more complex with an obvious slow component. It was also noticed that whilst a 2ms command evoked clearly evoked I_{AHP}, a 1ms command failed to evoke any current.

The relationship between pulse duration and I_{AHP} was investigated further in dissociated neurones. Fig. 5.13A shows records from an impaled dissociated neurone. Similarly to intact neurones, both amplitude and the time-course increased with increasing pulse duration. The decay was mono-exponential and thus allowed calculation of the decay time-constant in addition to measurement of amplitude (Fig 5.13B). Data from 9 impaled neurones was analysed and the results are shown in Table 2, with data

standardized to the values obtained at 10ms. Although it is obvious that increasing Ca^{2+} influx leads to increases in both I_{AHP} amplitude and time-course, the relationship between I_{AHP} and Ca^{2+} influx can not be directly deduced from the data shown since I_{Ca} will not be constant during the command. An approximate value for the Ca^{2+} charge influx for each pulse duration was calculated from I_{Ca} recordings (using neurones 1 day following dissociation). The relationship (plotted on a log-log scale) between Ca^{2+} charge, and I_{AHP} amplitude and time constant is shown in Fig. 5.14. Both I_{AHP} amplitude and time-course show a similar relationship to the size of the calcium load.

Table 2. Effect of command pulse-length on I_{AHP} parameters (standardized to 10ms).

Pulse-length (ms)	Amplitude	Time-constant	Q_{Ca} (pC)	n
2	0.305 ± 0.059	0.530 ± 0.064		5
5	0.700 ± 0.044	0.790 ± 0.033	17	9
10	1	1	31	9
20	1.330 ± 0.045	1.228 ± 0.071	75	9
50	1.957 ± 0.120	1.663 ± 0.097	125	9
100	2.534 ± 0.181	2.282 ± 0.148	208	9

Effect of cadmium on I_{AHP}.

High concentrations of cadmium (Cd^{2+}) cause an almost complete block of I_{AHP} (see earlier). Using dissociated neurones, lower concentrations of Cd^{2+} caused a dose-dependent block (Fig. 5.15A) with a dose-response relationship showing 50% of the current being blocked at 5μM (Fig 5.15B).

Since the effect of Cd^{2+} on I_{AHP} is likely to be due to its action as a calcium

channel blocker, it might be expected that Cd^{2+} would accelerate the decay of I_{AHP}. This was observed and the increase in rate of decay of I_{AHP} is illustrated in Fig 5.15A. Data from 10 cells show that 3μM Cd^{2+} caused a decrease in the time constant of decay from 396 $\pm$ 51ms to 270 $\pm$ 36ms (a decrease of 38%).

The effect of Cd^{2+} on I_{AHP} amplitude and I_{Ca} were compared. Fig 5.16A shows the dose-response curves for both inhibition of I_{AHP} and I_{Ca}, illustrating that inhibition of both currents is closely related. Fig 5.16B shows inhibition of I_{AHP} plotted against inhibition of I_{Ca} for each concentration of Cd^{2+}, and shows that the relationship is approximately linear. There is a small discrepancy between inhibition of I_{Ca} and I_{AHP} with a slightly higher proportion of I_{Ca} being blocked by each concentration of Cd^{2+} (Fig 5.16A), with 98% block of I_{Ca} corresponding with 84% block of I_{AHP} (100μM Cd^{2+}). This is reflected in the plot in Fig. 5.16B. The reason for this discrepancy is probably due to contamination of I_{AHP} by rapidly decaying currents following the command, which are Cd^{2+}-insensitive (such as $I_{K(DR)}$), and which have not completely decayed by the time that I_{AHP} is measured (25ms after end of the command).

Effect of Caffeine on I_{AHP}.

Caffeine prolongs the a.h.p. in rat s.c.g. neurones, possibly by the release of Ca^{2+} from intracellular stores (Kawai and Watanabe, 1989). In this study it was observed that caffeine greatly prolonged the a.h.p. recorded in current-clamp. However voltage-clamp experiments failed to demonstrate a corresponding increase in I_{AHP}, with only a small effect being observed. Since the main difference between the 50ms command pulse in voltage-clamp and the action potential is the very much greater duration of the command pulse, the effect of caffeine on I_{AHP} evoked by command pulses of different length was investigated. Fig 5.17A illustrates that 2mM caffeine caused a substantial increase in the duration of I_{AHP} evoked by short commands, but had a smaller effect on I_{AHP} evoked by longer commands. A similar effect was observed in 3 other neurones. It was also

noticed that caffeine often reduced the peak amplitude of I_{AHP}. In 2 neurones, another effect of caffeine was to cause an apparent slowing of the activation of I_{AHP} such that peak current occurred up to 100ms after the end of the command pulse (illustrated in Fig. 5.17B).

C. Pharmacological inhibition of I_{AHP}.

Tetraethylammonium

In the presence of tetraethylammonium (TEA) (5mM) an inward current (typically 0.05-0.1nA) was induced at the holding potential of -50mV. There was a clear inhibition of the initial fast outward tail-current, but only small and variable effects on the slow outward tail representing I_{AHP} (Fig. 5.18). In some cells a small increase was seen in the amplitude of the later part of I_{AHP} with a clear slowing of the decay (illustrated in Fig 5.18). This was possibly due to an improved clamp of the depolarizing command, because the outward current during the pulse was reduced (data not shown) and a consequential increase in Ca^{2+} entry. The reduction of the fast tail-current following voltage-commands made measurement of I_{AHP} easier and 5mM TEA was frequently added to the Krebs' solution during experiments for this reason.

D-tubocurarine.

D-tubocurarine (dTC) caused a reversible reduction of I_{AHP} in both intact and dissociated neurones. Fig. 5.19A illustrates the inhibition of I_{AHP} by dTC in dissociated neurones, and Fig. 5.19B shows the dose-response relationship for the inhibition in dissociated neurones, with 50% block of I_{AHP} occurred at about 30μM. Using intact neurones, higher concentrations of dTC (up to 1mM) resulted in a block of up to 77%. There was no change in the leak conductance, and no noticeable change in

holding current induced following addition of dTC suggesting that I_{AHP} does not contribute to the resting conductance.

The effect of 30μM dTC on both I_{AHP} amplitude and decay was investigated. Using data from 7 neurones, the amplitude of I_{AHP} was reduced by 58 $\pm$ 5% from control, but the time constant was unchanged (an increase of 1 $\pm$ 2%).

Inhibition of I_{AHP} by dTC occurred without effect on Ca^{2+} entry. The effect of 30μM dTC on I_{Ca} was tested in 3 neurones with no effect.

Apamin.

The effect of apamin on I_{AHP} was investigated in 3 dissociated neurones and Fig. 5.20 illustrates inhibition of I_{AHP} by 30nM apamin. The amplitude of I_{AHP} was substantially reduced (by 53.7 $\pm$ 3.9%) without effect on the time-course, but the inhibition by apamin was not reversible. The action of apamin appeared qualitatively similar to dTC, and since dTC was more readily available in a pure form as well as producing a reversible response, dTC was used in preference to apamin to investigate block of I_{AHP}.

4-Aminopyridine.

The effect of the potassium channel blocker 4-aminopyridine (4-AP) was investigated (Fig. 5.21). In 3 dissociated neurones 3mM 4-AP was without any observable effect, and was consequently not investigated further.

Noradrenaline.

The effect of noradrenaline was investigated in both intact and dissociated s.c.g. neurones. Addition of noradrenaline to intact neurones caused a reversible inhibition of I_{AHP} (Fig. 5.22A). The inhibition was dose-dependent from 0.03 to 100μM, and had a

mean half-maximal inhibition of I_{AHP} at 1μM (n=10; Fig 5.23A). The mean maximal block of the current was 58 $\pm$ 3%, though in some cells up to 65% of I_{AHP} could be blocked.

In dissociated patch-clamped neurones, noradrenaline also caused a reversible dose-dependent inhibition of I_{AHP} (Fig. 5.22B) with half-maximal inhibition at 0.4μM (n=4, Fig. 5.23B). However the maximal block of I_{AHP} by noradrenaline was only 13 $\pm$ 6 % (measured 50ms after the end of the voltage command). When measured 150ms after the end of the voltage command,inhibition increased to 27 $\pm$ 4%, still less than half the block achieved in intact neurones. The inhibition of I_{AHP} by noradrenaline in dissociated neurones was compared to the inhibition of I_{Ca}. Fig. 5.24A shows the dose-response relationships for both I_{AHP} (measured at 150ms) and I_{Ca}. Inhibition of I_{AHP} is obviously very much less, in contrast to the similar inhibition of both I_{AHP} and I_{Ca} by Cd^{2+} (see Fig. 5.16). However, when the data is standardized to the inhibition by 10μM noradrenaline. the curves appear similar (not shown). Fig. 5.24B shows a plot of inhibition of I_{AHP} against $\frac{\text{inhibition of } Q_{Ca}}{\wedge}$ for each concentration of noradrenaline, and also the data obtained for Cd^{2+} for comparison.

Assuming inhibition of I_{AHP} by noradrenaline to be due to the reduction in I_{Ca} then, in addition to a decrease in the peak amplitude of I_{AHP}, an increase in the rate of decay of I_{AHP} would be expected. This was observed: 10μM noradrenaline reduced the decay time constant by 31 $\pm$ 3% in 4 dissociated neurones (illustrated in Fig 5.22A). The rate of decay in intact neurones was also increased, though because of the variable kinetics of decay this had to be expressed in terms of the time to half-decay which was reduced by 18 $\pm$ 2% (n=10).

The pharmacology of noradrenaline's inhibition of I_{AHP} was qualitatively investigated. Clonidine and oxymetazoline showed no significant inhibition of I_{AHP}. However, the α_2-antagonist, yohimbine was also tested and was an effective antagonist. Fig. 5.25 illustrates the antagonism by yohimbine of noradrenaline's suppression of I_{AHP} in a dissociated neurone.

In many cells there was also an outward current induced following application of

noradrenaline with an associated increase in membrane conductance. In most cells this outward current was very small (>50 pA) and could not be reliably measured. It is likely that this current generates the hyperpolarization observed during extracellular recording from the intact s.c.g. preparation (Brown and Caulfield, 1979). One observation made on this current in an intact neurone was that dTC had no effect on it at concentrations which largely blocked I_{AHP} in the same neurone.

Muscarinic inhibition of I_{AHP}.

Muscarine (10μM) produced small and variable effects on I_{AHP} in intact neurones, and in the absence of any consistent inhibition by muscarine it seemed unlikely that I_{AHP} was coupled to muscarinic receptors. However the experiments were performed in the presence of 5mM TEA, a competitive antagonist of muscarinic receptors, and may therefore have prevented any inhibition which would otherwise have been observed. Consequently, muscarinic inhibition of I_{AHP} was considered further, and the effect of methacholine on I_{AHP} in dissociated cells was investigated. Methacholine reduced both peak amplitude and the decay time constant (Fig. 5.26A). In 7 cells, 10μM methacholine reduced I_{AHP} amplitude by 27 $\pm$ 5% and the decay time constant by 27 $\pm$ 4% from control. Recovery from methacholine was often poor. The reduction in the decay time constant suggested that methacholine suppressed I_{AHP} via inhibition of the preceding Ca^{2+} entry. Consequently, methacholine was tested against I_{Ca} and fig. 5.26B shows the inhibition of I_{Ca} by 10μM methacholine. The effect of methacholine was also directly compared to the inhibition caused by dTC and Cd^{2+}. Fig. 5.27 illustrates inhibition of I_{AHP} by 10μM dTC, 10μM Cd^{2+} and finally 10μM methacholine. Peak amplitude is reduced by each drug application, but only Cd^{2+} and methacholine reduce the decay time constant, illustrating that the effect of methacholine more closely resembles the effect of Cd^{2+} than dTC.

Table. 3. Effect of drug treatment on I_{AHP} parameters relative to controls in dissociated s.c.g. neurones.

Experiment	Amplitude (% ± s.e.m.)	time-constant (% ± s.e.m.)	n
Cd^{2+} (3μM)	71.9 ± 3.3	68.2 ± 3.4	10
d-Tubocurarine (30μM)	57.7 ± 4.6	100.8 ± 4.6	7
noradrenaline (10μM)	87.3 ± 5.6	69.3 ± 2.5	4
methacholine (10μM)	73.0 ± 4.8	73.0 ± 4.2	4
Reduced Ca^{2+}-influx (20ms command pulse)	68.0 ± 4.3	73.8 ± 3.9	9

All data measured 25ms after end of voltage command.

Discussion.

The experiments in this chapter describe some of the properties of the Ca^{2+}-dependent K^+ current that underlies the a.h.p. of rat s.c.g. neurones. The current showed the following basic properties:

(1) It was characterized as a small, slowly decaying outward current following depolarizing voltage-commands.

(2) The current was clearly Ca^{2+}-dependent and was affected by conditions that alter Ca^{2+} influx.

(3) The current appeared to be a pure K^+ current.

(4) The underlying conductance of the current was independent of membrane potential.

(5) The current was maximally activated by commands to around 0mV, and was reduced by depolarizing holding potentials prior to the command pulse.

(5) The current was blocked by low concentrations of dTC and apamin, but not by TEA or 4-AP.

(6) Noradrenaline and methacholine both reduced the current.

The current recorded in this study appears to share similar characteristics with the after-hyperpolarization current (designated I_{AHP}) observed in bullfrog sympathetic neurones (Pennefather et al. 1985) which likewise was Ca^{2+}-dependent, insensitive to membrane voltage, and blocked by low concentrations of dTC but not TEA. Because of this similarity, it is reasonable to refer to the current recorded in this study as I_{AHP}.

I_{AHP} was recorded from both intact and dissociated neurones, and showed similar characteristics using both preparations. The most noticeable difference was the smaller amplitude of I_{AHP} recorded from dissociated neurones. The appearance of I_{AHP} in dissociated cells was dependent upon the time in culture since dissociation, with I_{AHP} only being consistently recorded about 4 days following dissociation. The reason for this slow development of I_{AHP} is unclear since other membrane currents are readily observable in freshly dissociated cells. Another difference was the altered pattern of decay in that the time-course of decay was usually mono-exponential in dissociated neurones, whereas there were frequently two components of decay observed in intact neurones. This made analysis easier since the time-course could be fitted by a single exponential allowing accurate estimation of drug effects on the time-course of I_{AHP} decay. It does, however, leave open the question of whether there are two separate currents, only one of which was maintained in dissociated neurones, and whether direct comparison can be made between I_{AHP} recorded under the two conditions.

The variable pattern of decay of I_{AHP} in intact neurones does suggest that more than one current may contribute to I_{AHP}. The decay was frequently 2-exponential with times constants of approximately 135 and 440ms, but the effects of drug treatment upon the two components were very variable not allowing comparisons to be made. One observation suggesting multiple components was that TEA appeared to suppress the early part of I_{AHP} while leaving the later part unaffected (or even enhanced due to the improved clamp and consequent increase in Ca^{2+} entry). The suppression of the early I_{AHP} lasted over 200ms in some cells (not shown in Fig. 18), far longer than can be accounted for by the suppression of either I_C or $I_{K(DR)}$. The inference from this is that

there are two separate components to I_{AHP}, but in the absence of further information no conclusions can be reliably made. A 2-component I_{AHP} has been reported in bullfrog sympathetic neurones with time-constants of 50 and 250ms, the two components being pharmacologically distinct (Tanaka et al, 1986; Tanaka and Kuba, 1987). Other studies in bullfrog neurones have however failed to demonstrate the presence of 2-components (Pennefather et al., 1985; Goh and Pennefather, 1987), so clarification on the existence of separate I_{AHP} components is also needed in bullfrog neurones.

Not all cells showed I_{AHP} following the voltage-command protocol used to evoke currents, and the magnitude of I_{AHP} varied considerably from cell to cell. During experiments with intact neurones it was noticed that poor currents were often associated with a low input resistance, following damage during impalement. It has been suggested that the variability of I_{AHP} in bullfrog neurones is due to such damage, rather than representing different cell types (Lancaster and Pennefather, 1987). However there were some cells with high input resistances but which had a small I_{AHP}. Poor currents were also a frequent problem during whole-cell experiments, even immediately following whole-cell patch formation before intracellular proteins would have diffused into the pipette. I_{AHP} was also quite labile, with run-down being frequently observed during both intracellular and whole-cell recordings. This might reflect run-down of the calcium current, particularly with whole-cell recording of I_{AHP} since I_{Ca} showed a similar run-down (see chapter 3). Alternatively, this may be due to Ca^{2+} loading in the cell from impalement damage or from frequent stimulation resulting in permanent activation of I_{AHP}, though since dTC did not alter the holding current this seems unlikely.

I_{AHP} is distinguishable from other membrane currents present in s.c.g. neurones on the basis of its biophysical and pharmacological properties. Thus I_{AHP} is distinct from another Ca^{2+}-dependent K^+ current I_C, since I_C is strongly voltage-dependent (Galvan and Sedlmeir, 1984; Belluzzi et al. 1985b) and blocked by TEA (Marsh and Brown, 1991). I_M is activated by depolarizing commands and decays with a comparable time-course to I_{AHP} but can also be eliminated on the basis of its voltage-dependence (Constanti and Brown, 1981).

Although raising the temperature caused a large increase in the amplitude of I_{AHP}, there was no obvious change to the total duration of I_{AHP} although the shape of decay was altered. This is different from myenteric neurones, for example, where the Q_{10} of inactivation is approximately 3 (North and Tokimasa, 1983). Interpretation of the decay of I_{AHP} at raised temperature is however difficult because of the greatly enhanced amplitude of I_{AHP}. This may at least be partially due to an enhanced Ca^{2+} influx, taking longer to be sequestered possibly masking the faster kinetics of removal. Difficulty was also encountered in adequately clamping the command pulse at raised temperature which caused variable command potentials to be attained.

Calcium dependence of I_{AHP}.

Both amplitude and time-course of I_{AHP} were dependent upon the level of Ca^{2+} influx into the cell, as illustrated by the relationship between the rise in intracellular Ca^{2+} concentration, and I_{AHP} amplitude and time-constant. In addition to an increase in I_{AHP} amplitude, the time-constant of decay increases with calcium load, such that I_{AHP} takes much longer to decay. This suggests that the time-course of I_{AHP} reflects the removal of intracellular Ca^{2+}, as has been suggested in bullfrog sympathetic neurones (Goh and Pennefather, 1987), rather than the open time of individual channels. This view is supported by other experiments in bullfrog sympathetic neurones (Smith et al. 1983), which demonstrated that the kinetics of the post-tetanic hyperpolarization reflect the kinetics of the intracellular transient, indicating that the removal of Ca^{2+} is the rate limiting step in the decay of I_{AHP}. It was noted that a minimum pulse length of 2ms was necessary to generate I_{AHP}. It is possible that the failure of a 1ms pulse to generate I_{AHP} is due to a requirement for a minimum Ca^{2+} entry to 'prime' the I_{AHP} channels. Alternatively I_{Ca} may not be activated during a 1ms pulse, particularly since Ca^{2+} entry is likely to occur mainly during the falling phase of an action potential, as implied by computer modeling by Belluzzi and Sacchi (1989; 1991).

The inhibition of I_{AHP} by Cd^{2+} is consistent with dependence of I_{AHP} on

calcium load. Cd^{2+} both inhibits peak current and reduces the time constant of decay, further suggesting that I_{AHP} decay is dependent on the size of the Ca^{2+} load and the rate of removal of Ca^{2+}. In contrast dTC inhibited only the amplitude of I_{AHP} without any effect on the time-course of decay, and also did not block $I_{Ca}{}^{2+}$. It would therefore appear that drugs which inhibit I_{AHP} by reducing Ca^{2+} influx also increase the rate of decay, while drugs which inhibit I_{AHP} independently of I_{Ca} do not increase the rate of decay, as suggested for bullfrog neurones (Goh and Pennefather, 1987). This provides a simple method of determining whether a drug inhibits I_{AHP} directly or via inhibition of I_{Ca}.

Noradrenaline increased the rate of decay of I_{AHP} in both intact and dissociated neurones, an action consistent with its suppression of I_{Ca} (Chapter 3). There was a discrepancy between the intact and dissociated preparations in that noradrenaline showed a smaller inhibition of peak current in the dissociated neurones. This is difficult to interpret since noradrenaline still increased the rate of decay, such that a greater inhibition of current was observed 150ms after the end of the voltage-command. Noradrenaline inhibited I_{Ca} by approximately 50% in the dissociated neurones, so the small inhibition of I_{AHP} compared to intact neurones is unlikely to be due to receptor alteration following dissociation, unless the culture conditions resulted in receptors being altered or lost over the several days between dissociation and use for I_{AHP} recordings. It is possible that there is an early component to I_{AHP} in dissociated neurones that is resistant to suppression by noradrenaline. In addition, the relationship between I_{AHP} and I_{Ca} inhibition by Cd^{2+} was linear, whilst the relationship for inhibition by noradrenaline was both alinear and comparatively shallow. The shallow relationship is probably due to the comparatively low degree of inhibition of I_{AHP} by noradrenaline in dissociated neurones. One possible explanation for the non-linear relationship is that at higher concentrations noradrenaline blocks I_{AHP} directly. In contrast, methacholine showed a clear reduction of I_{AHP} amplitude. In addition, methacholine also increased the rate of decay of I_{AHP}, strongly implying that muscarinic suppression of I_{AHP} is via inhibition of I_{Ca}, confirmed by the observation that methacholine did block I_{Ca}. Interestingly, Goh

and Pennefather (1987) reported that muscarine did not increase the rate of decay of I_{AHP} in bullfrog neurones, concluding that muscarine did not suppress I_{AHP} via inhibition of I_{Ca}. The reason for this difference is not clear, but it may suggest a direct inhibition of I_{AHP} occurs in addition to inhibition of I_{AHP} via suppression of I_{Ca}.

The effect of caffeine was to prolong I_{AHP} evoked by short commands. A similar potentiation of the a.h.p. in s.c.g. neurones has been observed (Kawai and Watanabe, 1989; Kawai and Watanabe, 1991), and of I_{AHP} in bullfrog neurones (Goh et al, 1992b). The relationship between command-length and effect of caffeine was unexpected, showing that the effect of caffeine was greater on short commands. One possible explanation for this is that the longer voltage-commands caused a substantial release of Ca^{2+} from caffeine dependent stores such that caffeine produced little further release. Alternatively, the caffeine-sensitive stores may only be able to provide a small release of Ca^{2+} following a stimulus, such that the slow decay following long commands obscure the relatively small effect of caffeine. It is, however, possible that the effect of caffeine is to inhibit uptake of Ca^{2+} into caffeine-sensitive stores rather than to potentiate release. Assuming that the uptake is saturated by larger Ca^{2+} loads, such that uptake is proportionally greater for small loads, then block by caffeine would be expected to have a greater effect on I_{AHP} evoked by short commands. The importance of the mobilization of intracellular Ca^{2+} could be more closely investigated using ryanodine, which shortens the a.h.p. in rat s.c.g. neurones (Kawai and Watanabe, 1989; Kawai and Watanabe 1991) by depleting the caffeine-sensitive store (Fill and Coronado, 1988).

Since the rate of decay of I_{AHP} appears to be closely related to the calcium load, it is possible that I_{AHP} can provide a sensitive indication of the time-course of calcium signals. I_{AHP} was recorded after a calcium charge influx of 16pC during a 5ms command (probably less, since a 2ms command evoked I_{AHP} in some neurones, but measurement of Q_{Ca} from I_{Ca} traces was impractical for the 2ms command). However, this in itself is not necessarily meaningful since the measurement of the Ca^{2+} charge is across the whole cell and not just localized to the region containing I_{AHP} channels.

Experiments in GH_3 cells suggest a calcium sensitivity of 100-300nM (Lang and Ritchie, 1987), and this is probably a better measure of the dependence of I_{AHP} on Ca^{2+}. Since the basal level of Ca^{2+} in s.c.g. cells is approximately 80nM (Trouslard et al, 1993), it is likely that I_{AHP} channels can be activated by very small changes in intracellular Ca^{2+}.

Suppression of I_{AHP} by noradrenaline was antagonized by yohimbine, suggesting an α_2-receptor. Whilst quantitative evaluation was not undertaken, this is consistent with the α_2-block of I_{Ca} (Chapter 4) and is further evidence that noradrenaline exerts its effect on I_{AHP} via I_{Ca}.

In conclusion, the results in this chapter describe the basic properties of I_{AHP}. Both amplitude and decay kinetics are dependent on Ca^{2+} load, and it appears that control of I_{AHP} is provided by Ca^{2+}. In addition, neurotransmitters appear to exert their effect on I_{AHP} via inhibition of I_{Ca}. Finally the pharmacological properties of I_{AHP} recorded here suggest it to be analogous to the I_{AHP} recorded in bullfrog neurones.

It was noticed, however, that clonidine did not reduce I_{AHP}. The reason for this is not clear, but clonidine also had little effect on I_{Ca} in some neurones (chapter 4), and the failure of clonidine to inhibit I_{AHP} is likely to reflect a lack of effect on I_{Ca}.

Fig. 5.1 I_{AHP} recorded from intact and dissociated s.c.g. neurones.

Records illustrate the outward tail-currents recorded by 50ms depolarizing voltage commands in s.c.g. neurones.

A. Records were obtained from an intact neurone using an intracellular electrode. Holding potential was -49mV and the command potential was -3mV

B. Records obtained from a dissociated neurone using a whole-cell patch electrode. Holding potential was -48mV and the command potential was -5mV.

A.

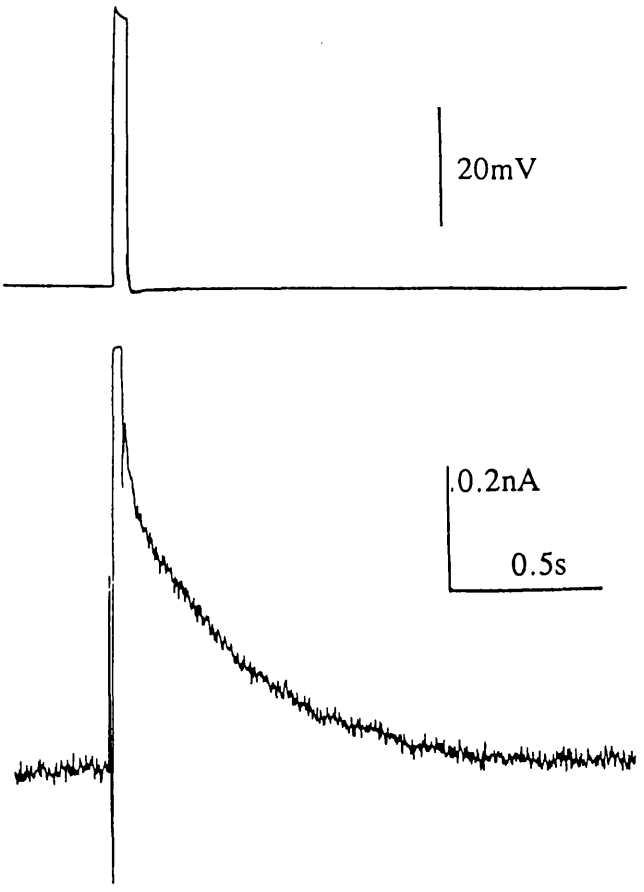

B.

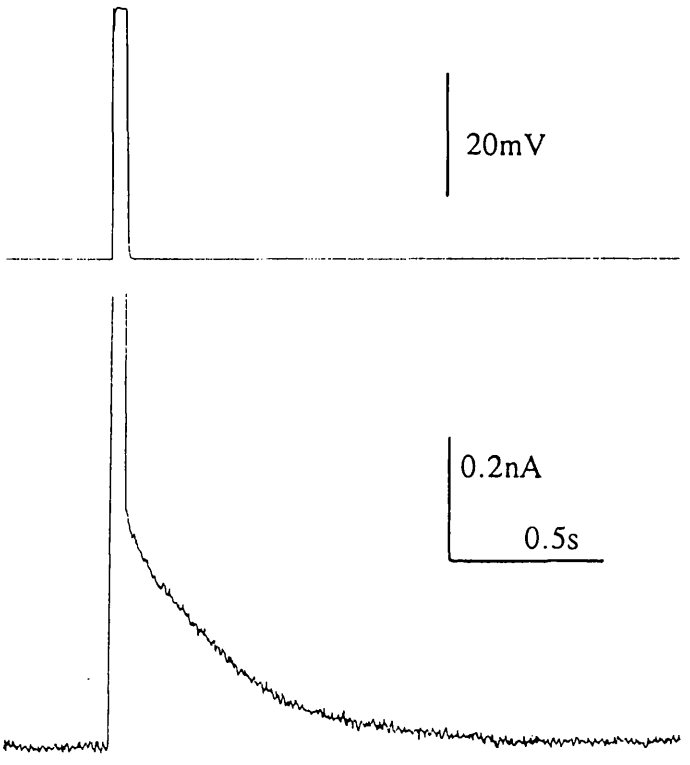

Fig. 5.2 Exponential decay of I_{AHP} in a dissociated neurone.

Plot of I_{AHP} amplitude . on a logarithmic scale against time for the dissociated neurone illustrated in Fig 1B. The decay time-constant (τ) was calculated as 329 ms. Zero-time on the plot represents the end of the command pulse.

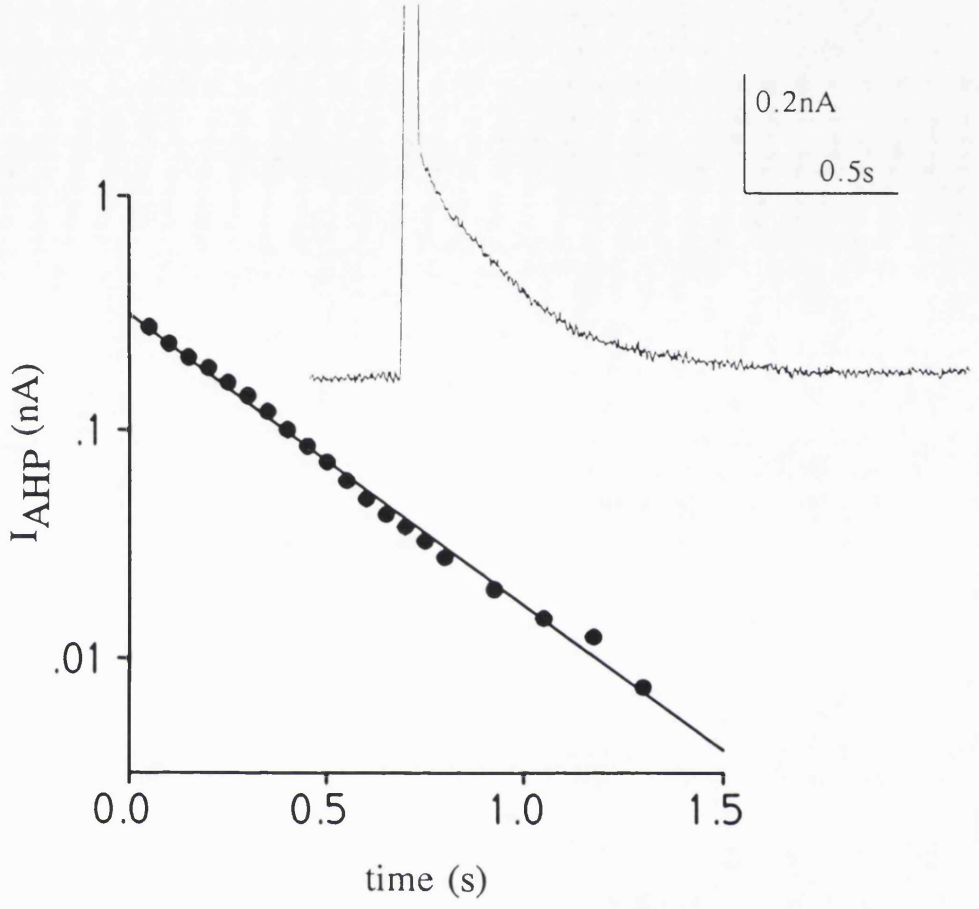
0.2nA
0.5s
1
.1
.01
I_{AHP} (nA)
0.0
0.5
1.0
1.5
time (s)

Fig. 5.3 Calcium dependence of I_{AHP} in intact neurones (different cells).

A. Records showing effect of a nominal Ca^{2+}- free Krebs' solution on I_{AHP} recorded from an intact neurone. Records were obtained by 50ms commands to -3mV from -51mV.

B. Records showing inhibition of I_{AHP} by 500μM Cd^{2+}. Currents were evoked by 50ms commands to -2mV from -50mV.

A.

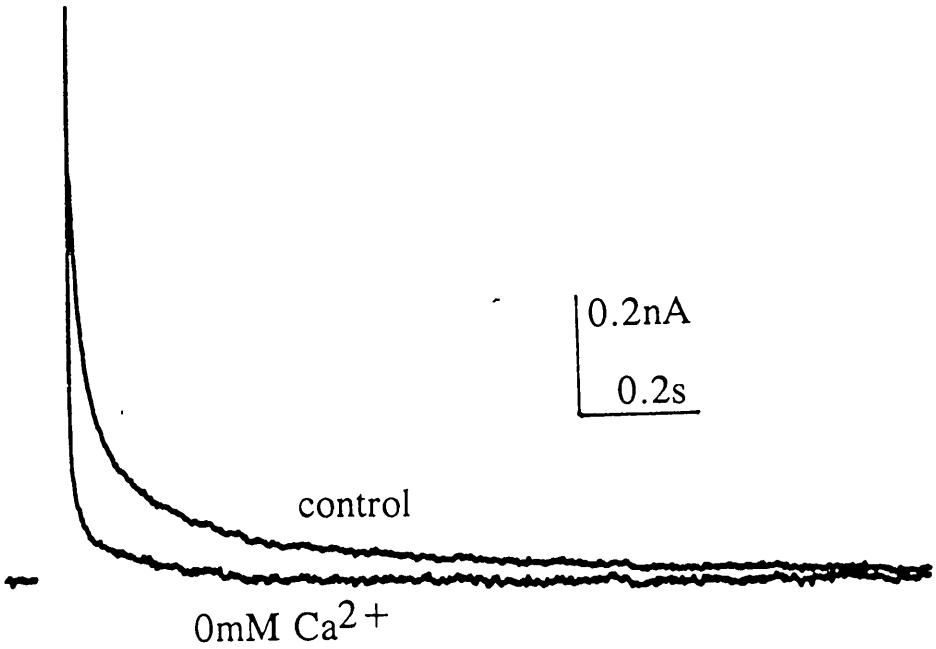

B.

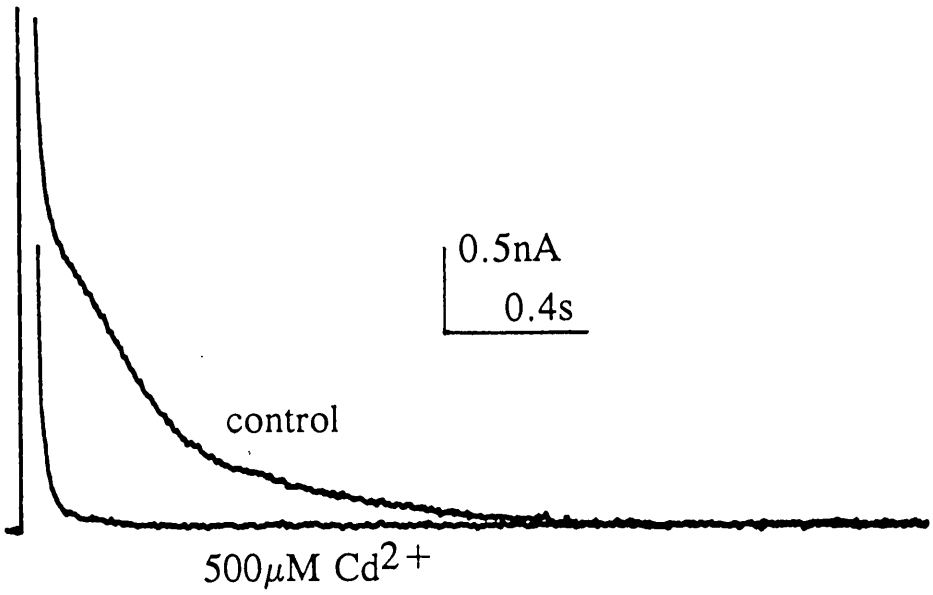

Fig. 5.4 Effect of holding potential on peak amplitude of I_{AHP} (intact s.c.g. neurone).

A. Shows superimposed outward tail-currents recorded at different holding potentials from an intact s.c.g. neurone. I_{AHP} was evoked by 50ms voltage commands to 0mV. The holding current at each potential is offset so that the currents can be easily compared.
Note that the fast component of the tail-current reverses at a more depolarized potential than the slow component.

B. Shows the relationship between peak current and holding potential.
In this cell reversal occurred at approximately -95mV.

A.

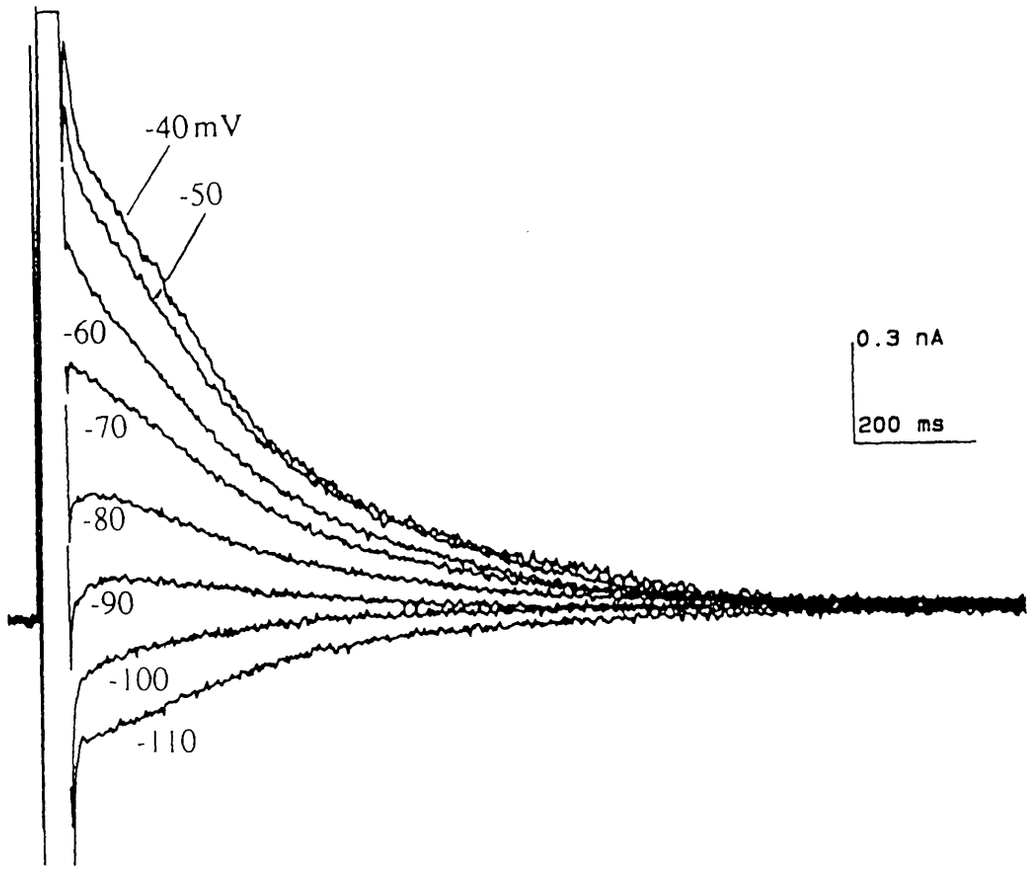
-40 mV
-50
-60
-70
-80
-90
-100
-110
0.3 nA
200 ms

B.

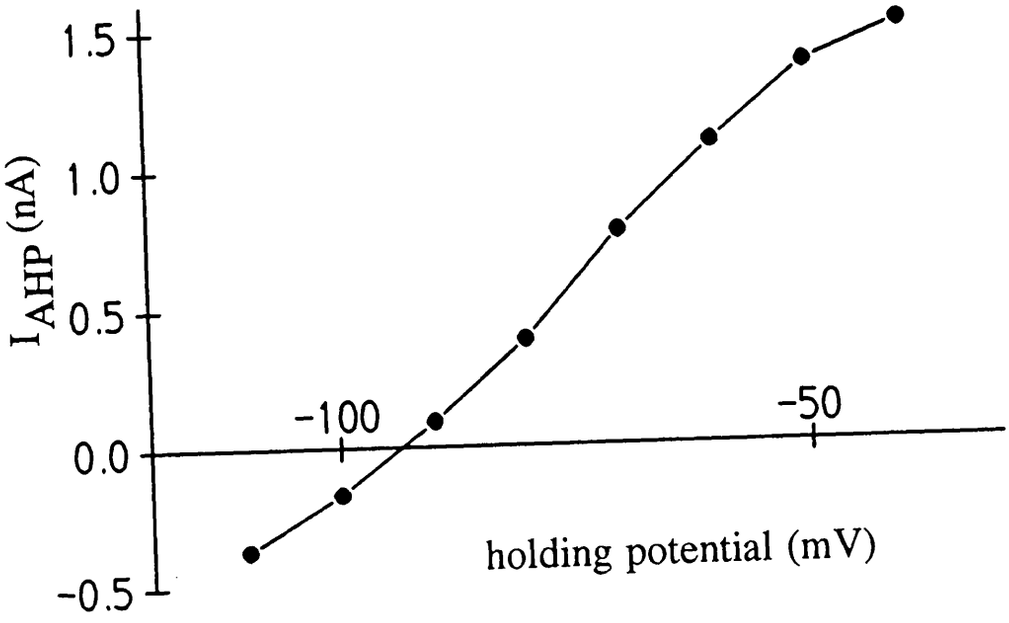
1.5
1.0
0.5
0.0
-0.5
I_{AHP} (nA)
-100
-50
holding potential (mV)

Fig. 5.5 Relationship between holding potential and I_{AHP} in a whole-cell voltage-clamped dissociated neurone.

A. Shows tail-currents evoked by voltage commands to -2mV from different holding potentials (same procedure as in Fig. 5.4).

B. Shows the relationship between I_{AHP} amplitude and holding potential. Reversal in this cell was approximately -85mV.

A.

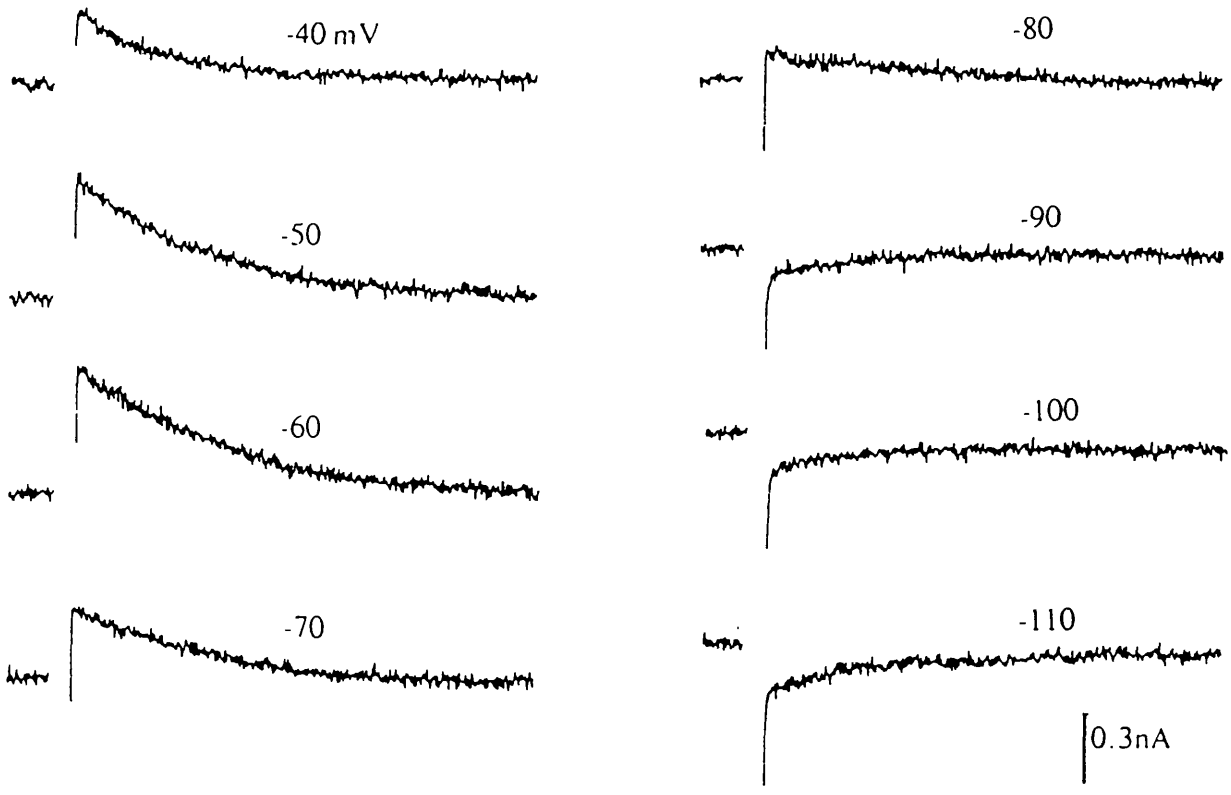

B.

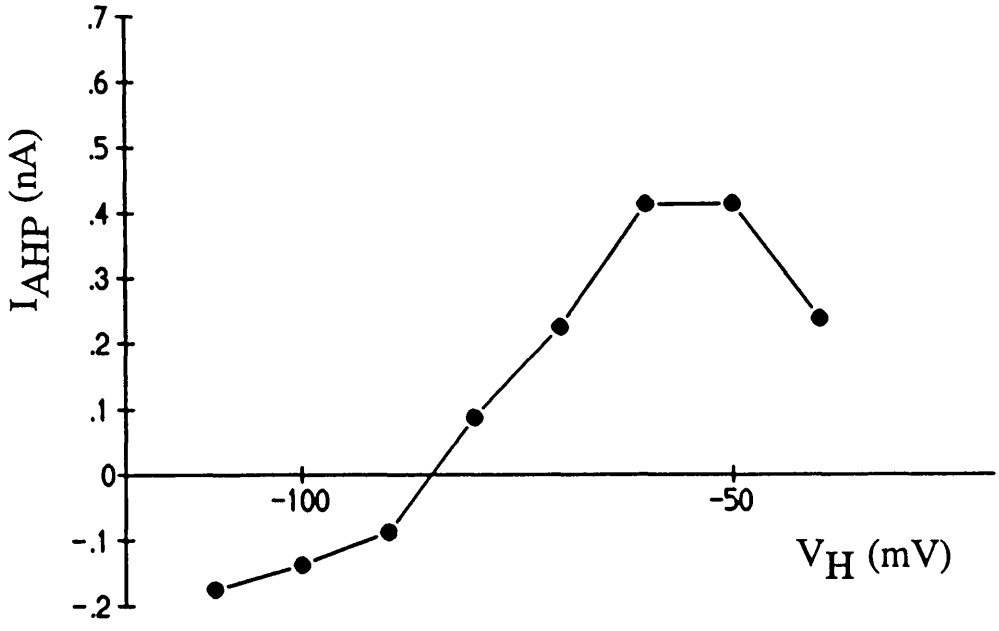

Fig. 5.6 Relationship between membrane potential and I_{AHP} when evoked from a constant holding potential.

A. Illustrates I_{AHP} evoked by 50ms voltage commands to -2mV from a holding potential of -50mV, and recorded at the post-command potentials indicated. Records show the difference current between the current evoked by the protocol described above, and records obtained without the command pulse, to minimise contamination by other currents. Same cell as previous figure.

B. Shows the relationship between peak current and membrane potential.

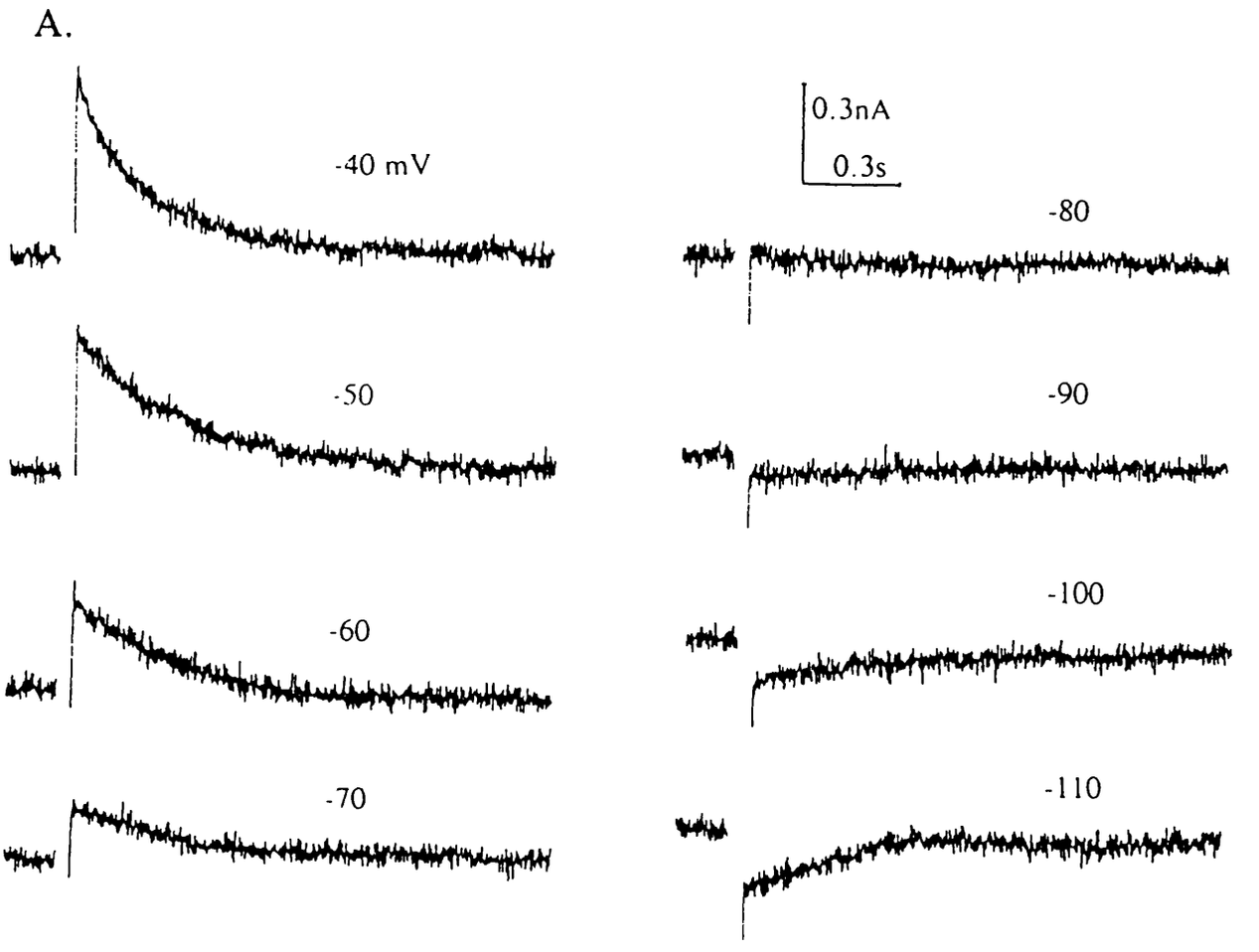
A.
0.3nA
0.3s
-40 mV
-50
-60
-70
-80
-90
-100
-110

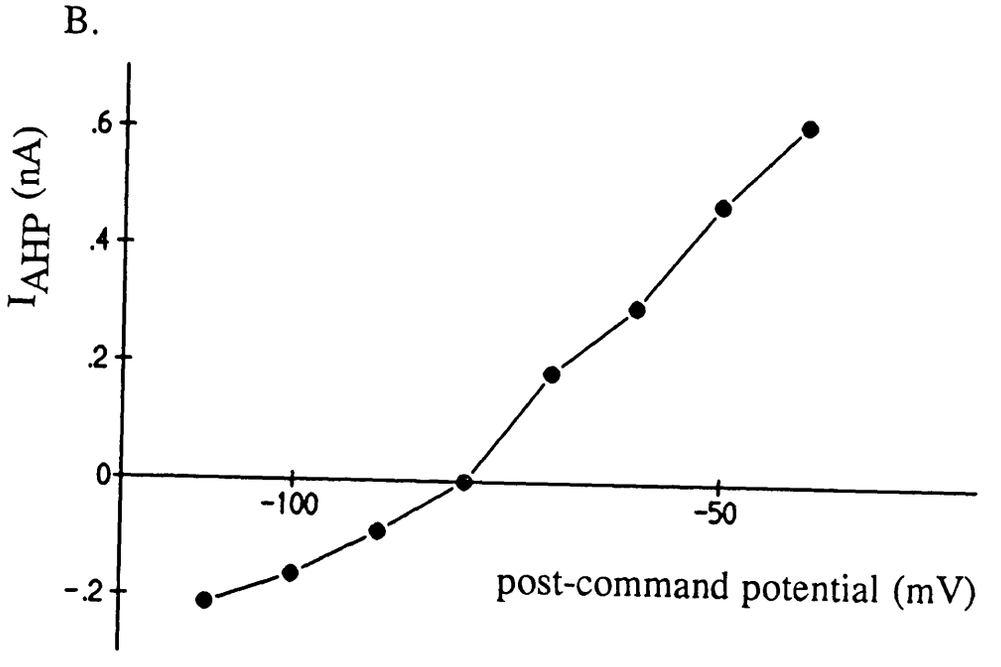
B.
I_{AHP} (nA)
.6
.4
.2
0
-.2
-100
-50
post-command potential (mV)

Fig. 5.7 Effect of altering the pre-command potential on I_{AHP} in a whole-cell voltage-clamped dissociated neurone.

A. Illustrates currents evoked by voltage commands to -2mV from the holding potentials indicated. Currents were recorded at -50mV and the records illustrated here show the difference current between the protocol described above, and records obtained without the command pulse to isolate the current evoked by the command.

B. Shows the relationship between the evoked current and pre-command potential.

A.

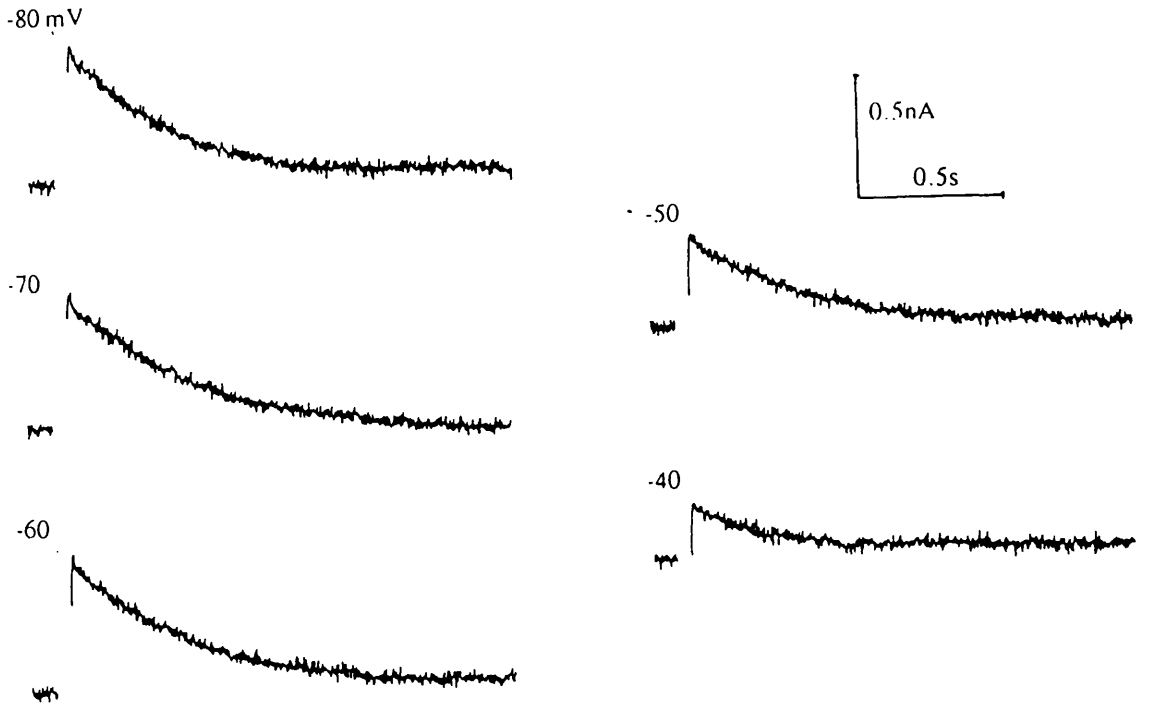
-80 mV
-70
-60
-50
-40
0.5nA
0.5s

B.

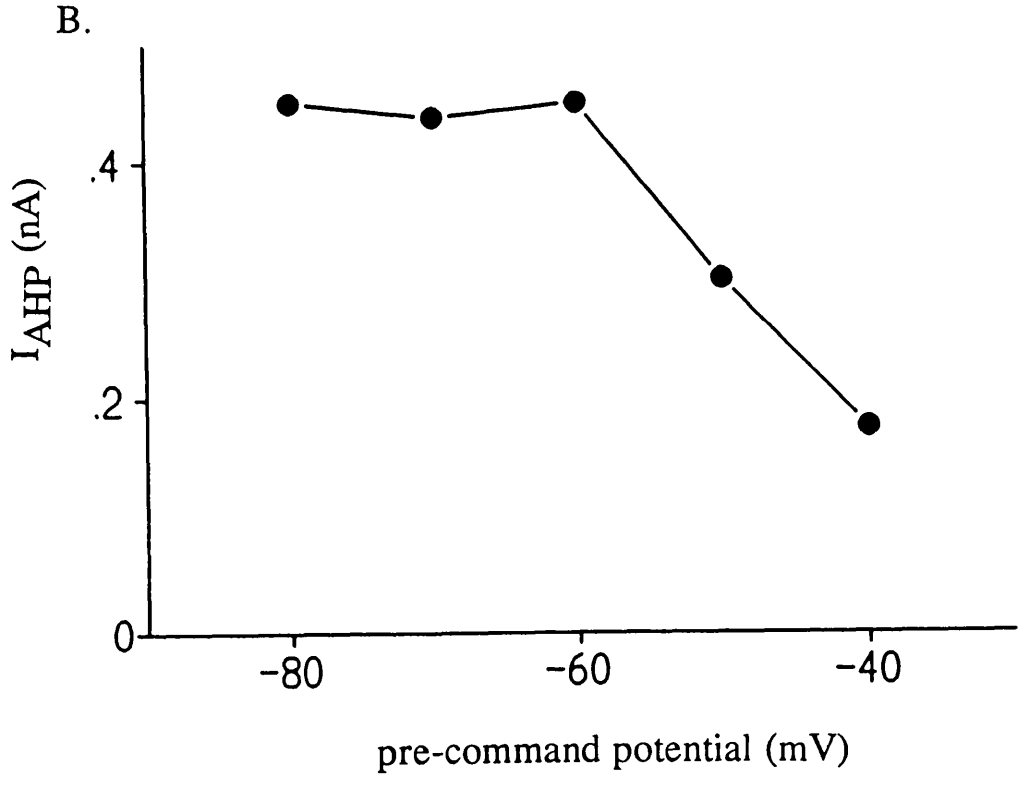
I_{AHP} (nA)
.4
.2
0
-80
-60
-40
pre-command potential (mV)

Fig. 5.8 Dependence of I_{AHP} on command potential in an whole-cell voltage-clamped dissociated neurone

A. Illustrates I_{AHP} evoked by 50ms commands to the potentials indicated.

B. Plot showing I_{AHP} amplitude (■) and decay time-constant (τ; ●) against command potential.

A.

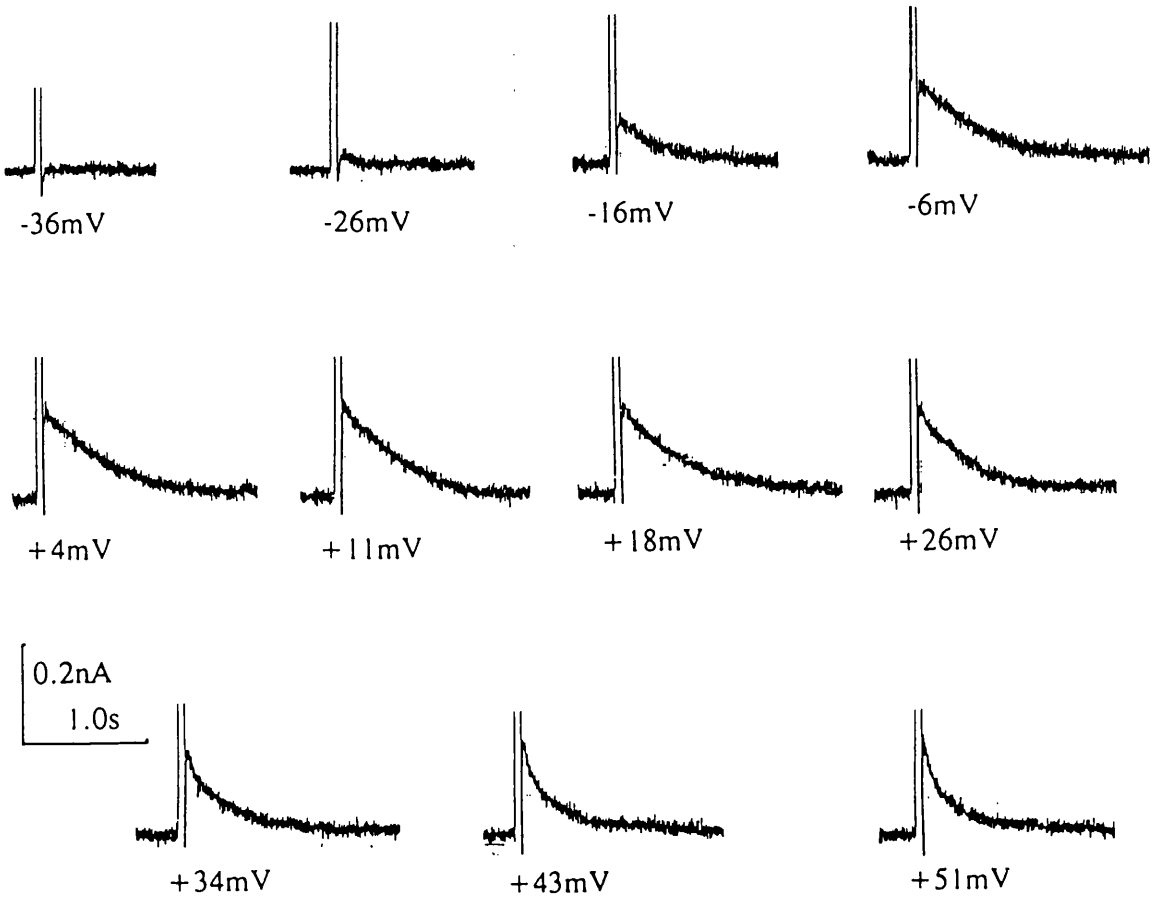
-36mV
-26mV
-16mV
-6mV
+4mV
+11mV
+18mV
+26mV
0.2nA
1.0s
+34mV
+43mV
+51mV

B.

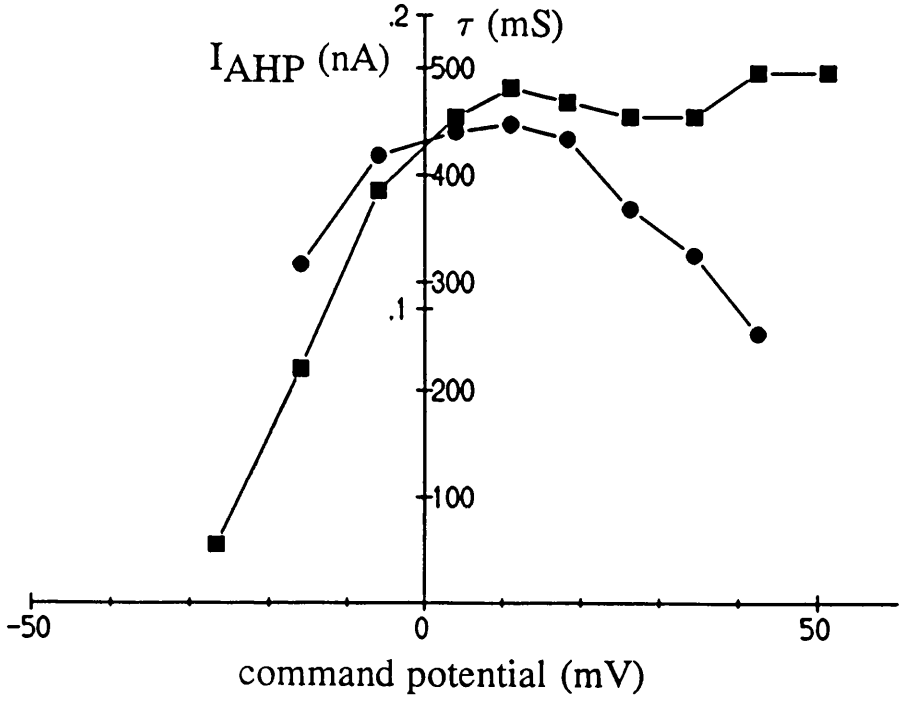
I_{AHP} (nA)
.2
.1
τ (mS)
500
400
300
200
100
-50
0
50
command potential (mV)

Fig. 5.9 Effect of high K^+ on I_{AHP}.

A. Voltage-clamp records (V_H=-58mV, V_C=0mV) from an intact s.c.g. neurone showing the effect of raising the concentration of KCl from 5mM (normal) to 12 and 20mM.

B. Plot showing the effect of altered K^+ concentration on I_{AHP} reversal. The reversal potential (mV) was plotted against K^+ concentration (on a logarithmic scale).
Same neurone as above.

A.

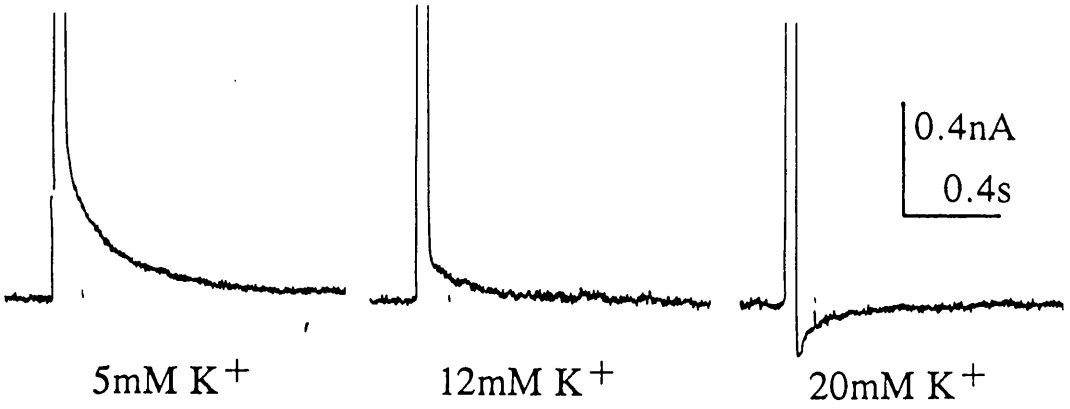
0.4nA
0.4s
5mM K+
12mM K+
20mM K+

B.

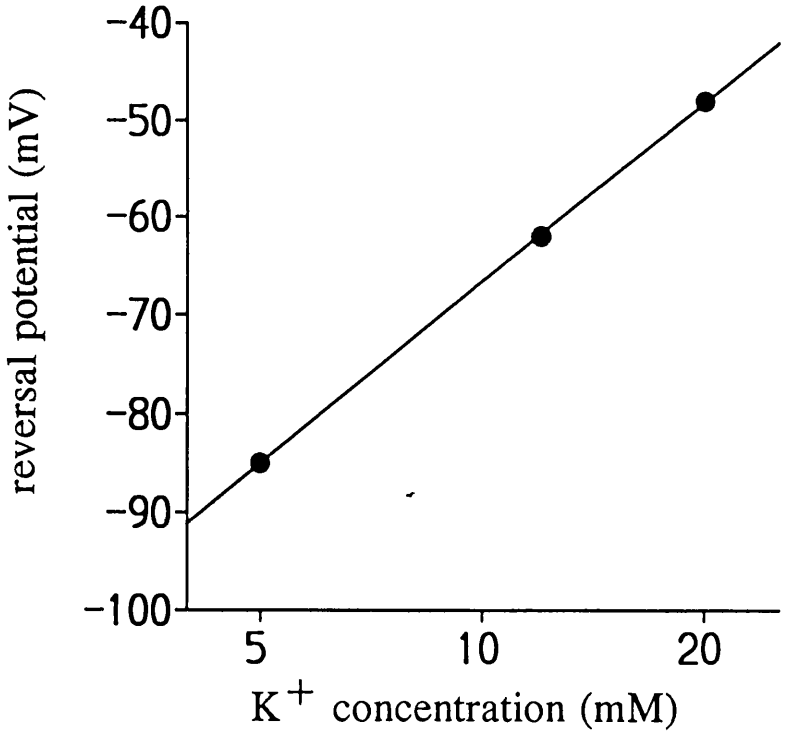
reversal potential (mV)
-40
-50
-60
-70
-80
-90
-100
5
10
20
K+ concentration (mM)

Fig. 5.10 Effect of temperature on I_{AHP}.

A. Records illustrate outward tail-currents obtained from a voltage-clamped intact s.c.g. neurone (V_H=-50mV, V_C=-10mV) at temperatures of 25, 30, and 35^{o}C.
1μM TTX and 5mM TEA were present in the Krebs' solution.
B. Illustrates the record obtained at 25^{o}C scaled up to compare the decay of current with the record obtained at 35^{o}C.

A.

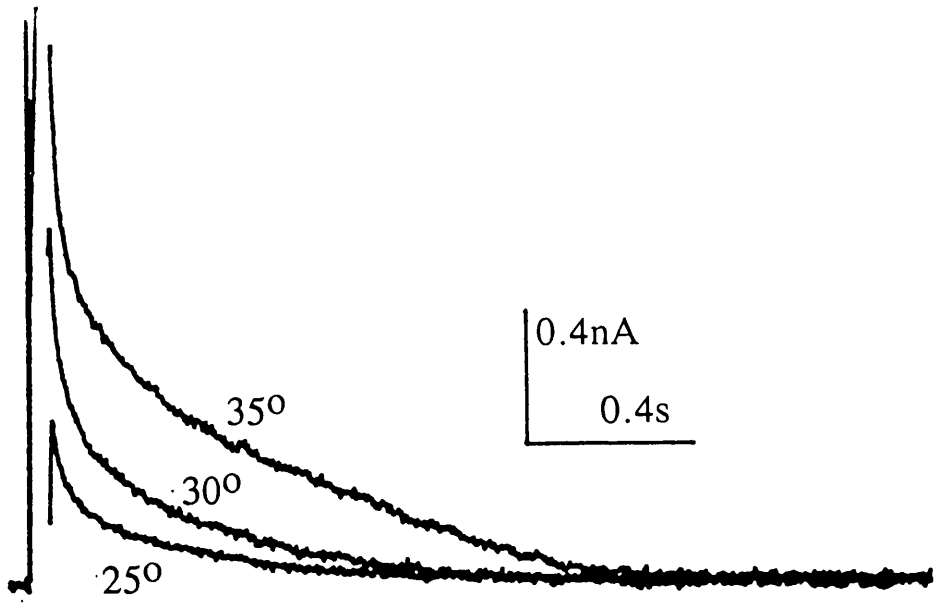

B.

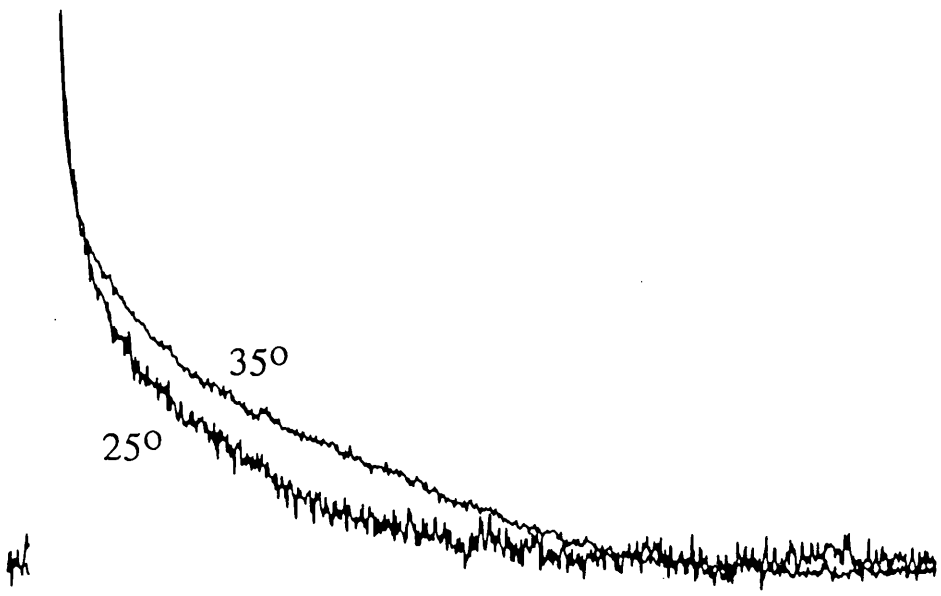

Fig. 5.11 Effect of altered external Ca^{2+} concentration on I_{AHP}.

A. Records obtained from an intact neurone (V_H=-50mV, V_C=-2mV) illustrating the effect of raising extracellular Ca^{2+} from 2.5 (normal) to 5mM.

B. Records obtained from another neurone (V_C= -50mV, V_C=0mV) showing the effect reducing extracellular Ca^{2+} from 2.5 to 1.25mM.
5mM TEA was present in the Krebs' solution.

A.

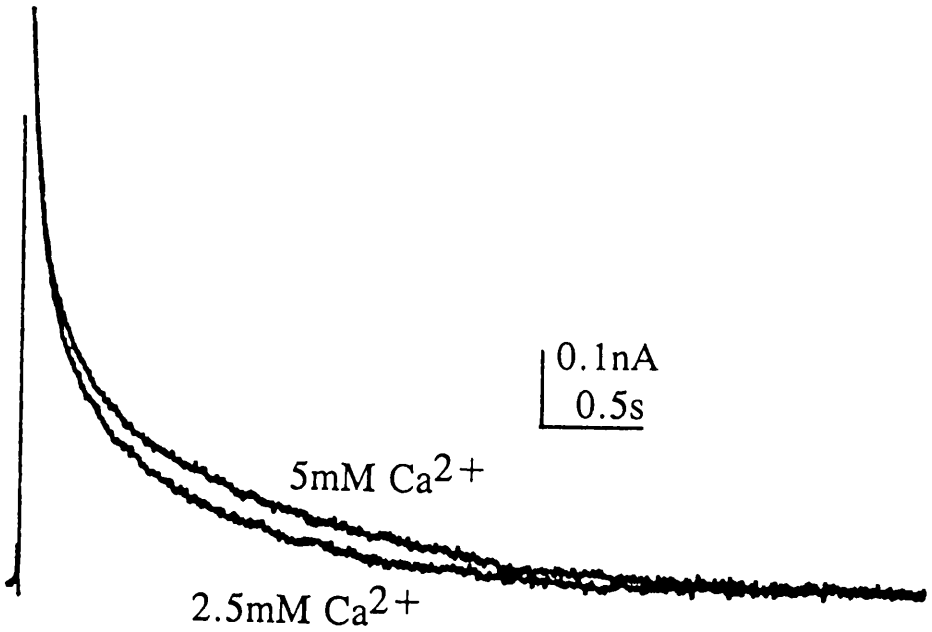

B.

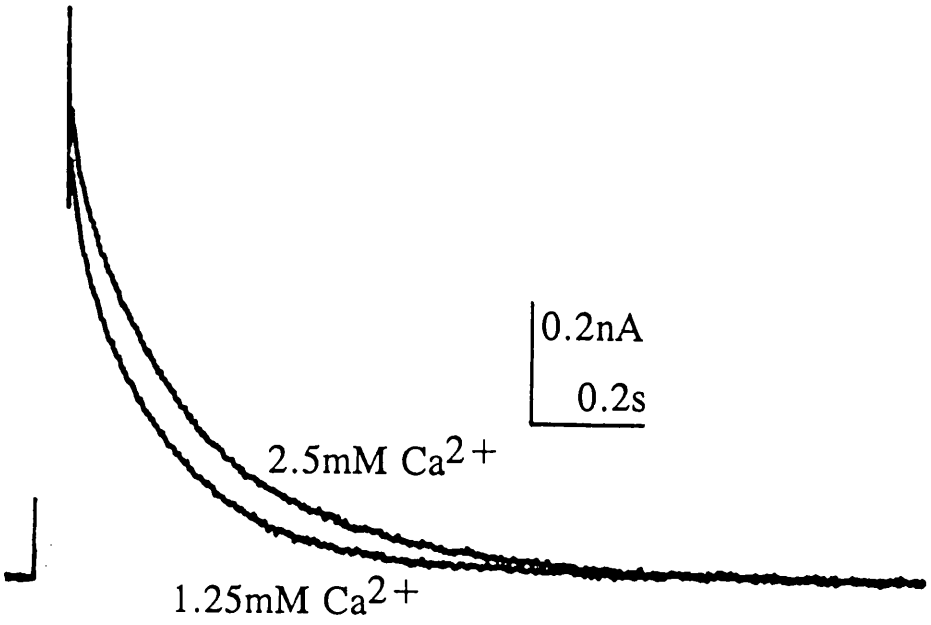

Fig. 5.12 Effect of different command pulse lengths on I_{AHP} in an intact neurone.

Records obtained from a voltage-clamped intact s.c.g. neurone following voltage commands (V_H=-50mV, V_C=-8mV) of increasing duration from 1 to 100ms.

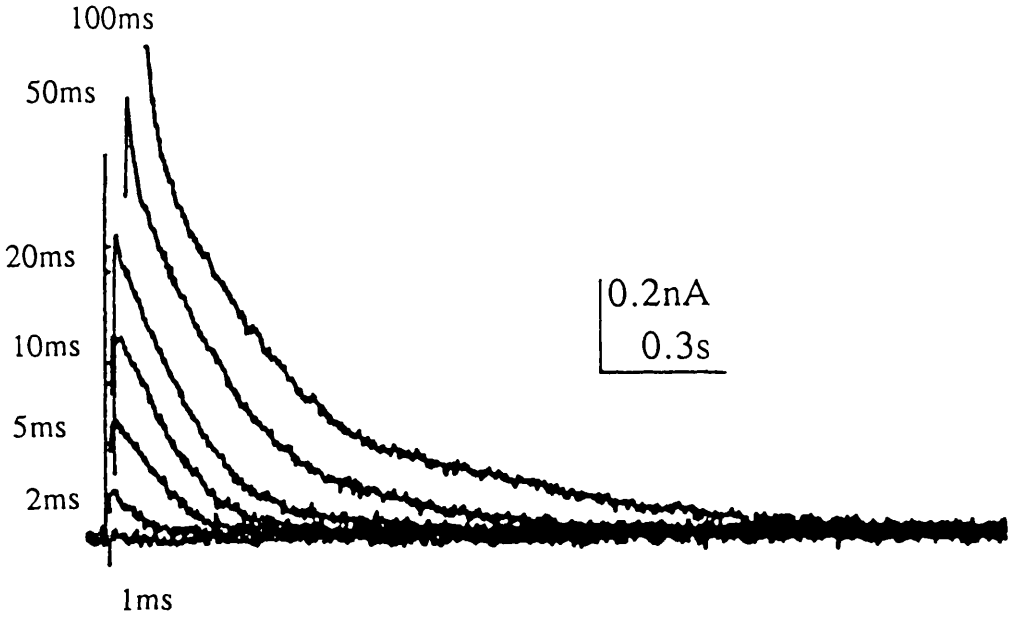
100ms
50ms
20ms
10ms
5ms
2ms
1ms
0.2nA
0.3s

Fig. 5.13 Effect of different command pulse lengths in an impaled dissociated neurone.

A. Records show I_{AHP} evoked by voltage commands (V_H=-55mV, V_C=-6mV) and of the duration indicated.

B. A plot of log I_{AHP} amplitude against time to illustrate the relationship between pulse duration and decay of I_{AHP}. The plot shows data obtained from 10ms (●; τ=169ms), 20ms (■; τ=227ms), 50ms (▲; τ=365ms) and 100ms (◆;τ=468ms) pulses. The plot for the 5ms pulse is omitted for clarity (τ was calculated as 162ms).

A.

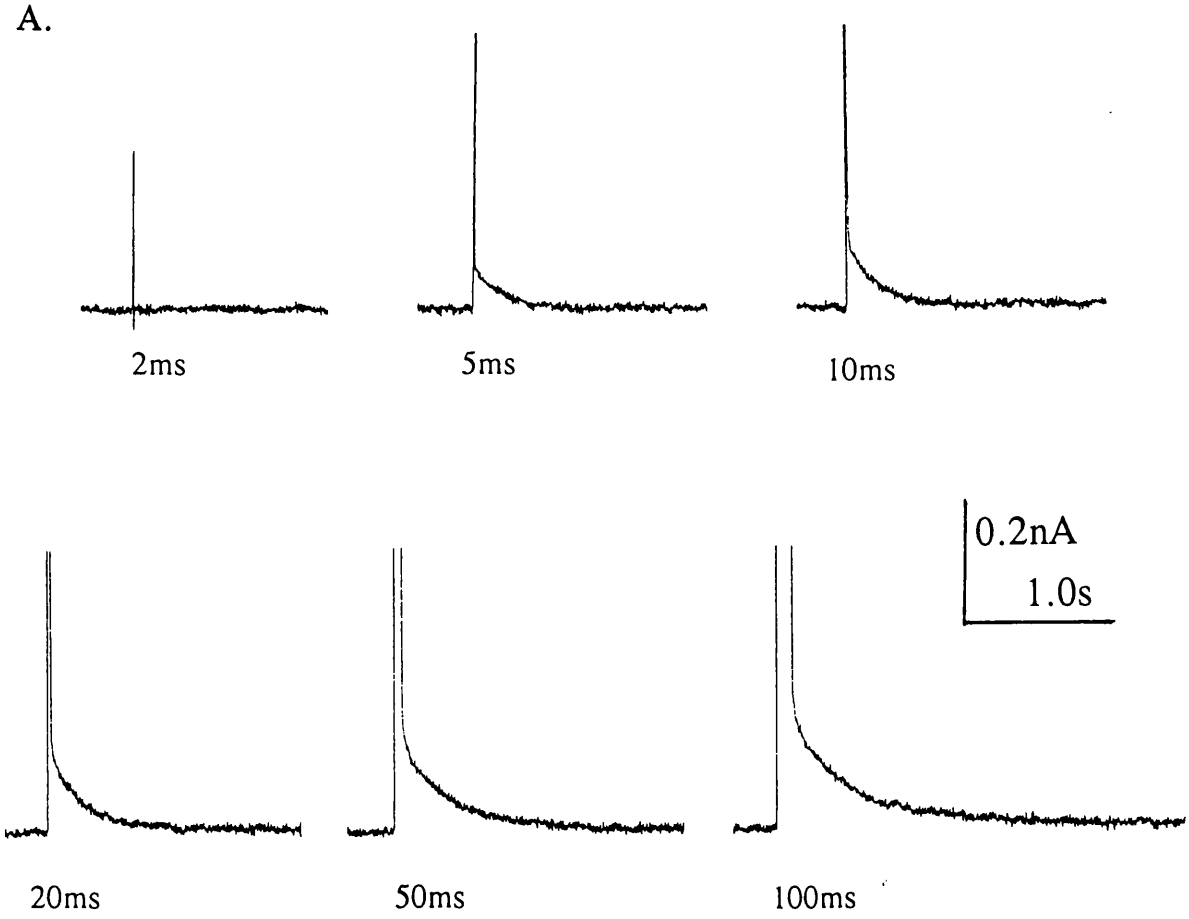

B.

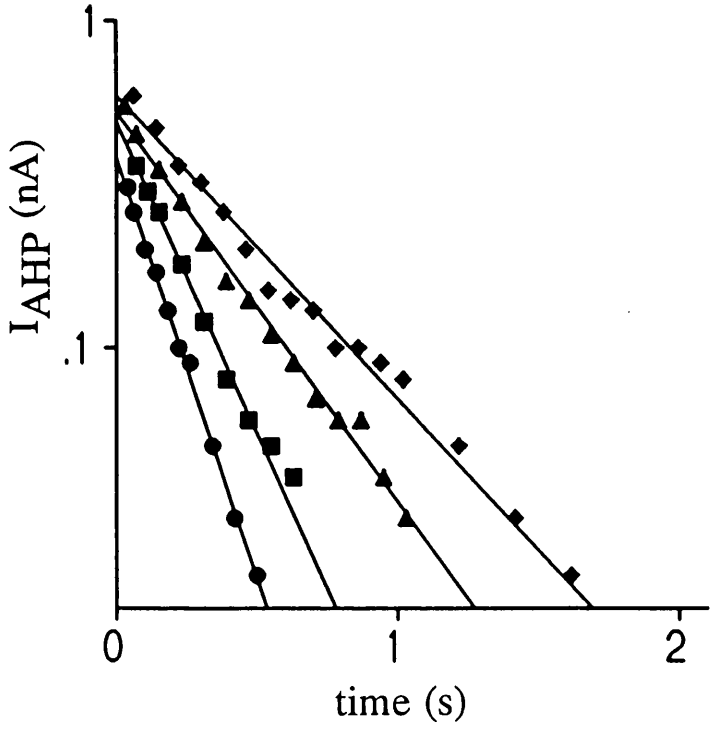

Fig. 5.14 Relationship between I_{AHP} and calcium load in dissociated neurones.

Plot showing I_{AHP} amplitude (■) and time-constant (τ; ●) against calcium charge (Q_{Ca}) entry during the voltage command (plotted on a log-log scale). Q_{Ca} was calculated from calcium current recordings (obtained from neurones 1 day following dissociation; n=4).

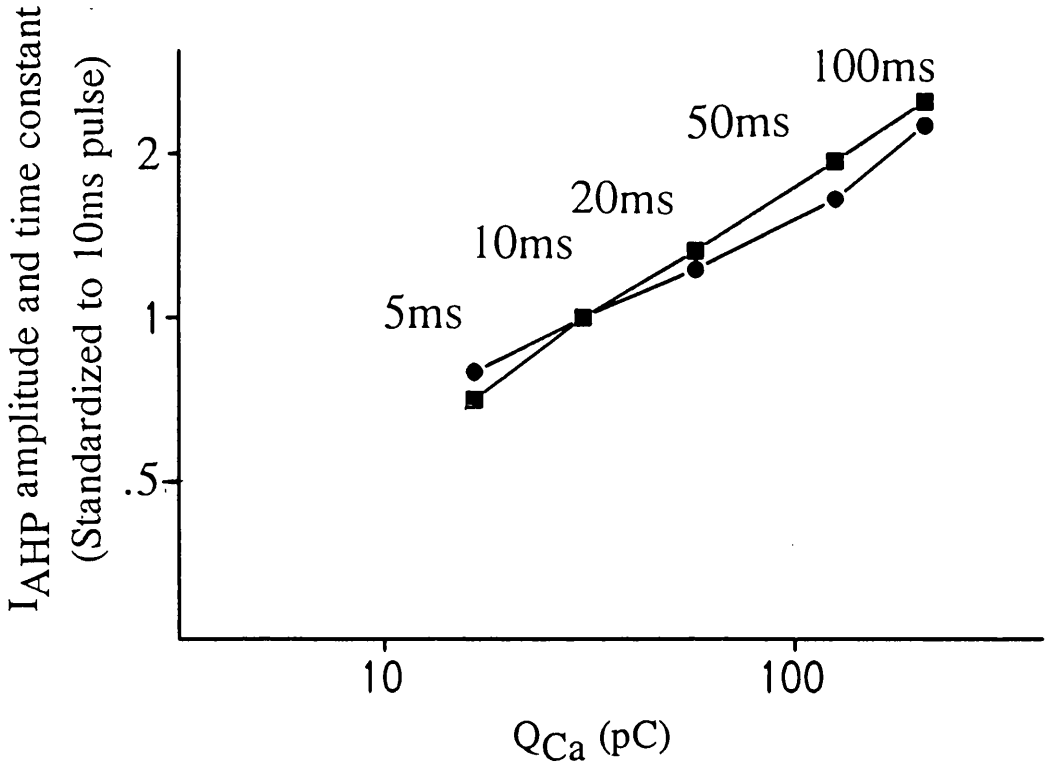
I_{AHP} amplitude and time constant
(Standardized to 10ms pulse)
2
1
.5
100ms
50ms
20ms
10ms
5ms
10
100
Q_{Ca} (pC)

Fig. 5.15 Effect of cadmium on I_{AHP}.

A. Whole-cell voltage-clamp records from a dissociated s.c.g. neurone showing I_{AHP} recorded in the absence and presence of 3 and 30μM Cd^{2+}. Currents were evoked by a 50ms command to 0mV from a holding potential of -49mV. Inset shows log I_{AHP} amplitude plotted against time for the records obtained for control (●; τ=675ms) and 3μM Cd^{2+} (■; τ=416ms) to illustrate the effect of Cd^{2+} on the rate of I_{AHP} decay.

B. Dose-response relationship for the block of I_{AHP} by Cd^{2+}. Data are expressed as mean ± s.e.m. (n=7).

A.

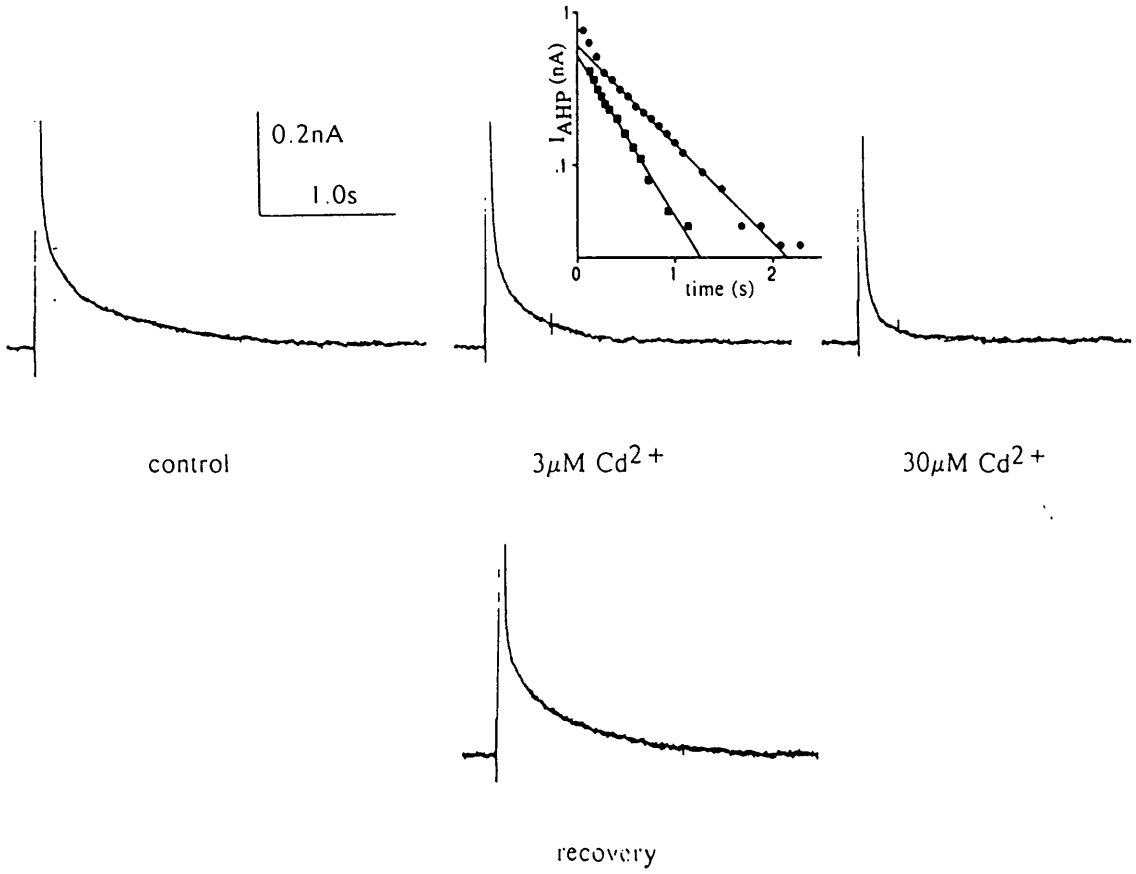
0.2nA
1.0s
I_{AHP} (nA)
time (s)
control
3μM Cd^{2+}
30μM Cd^{2+}
recovery

B.

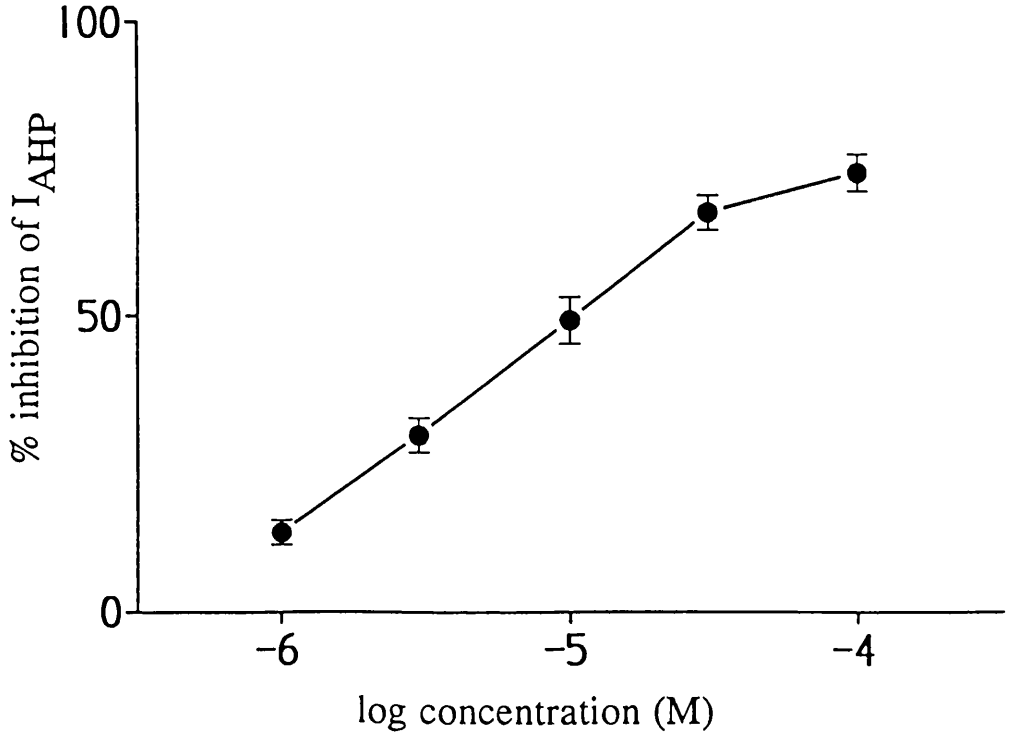
100
50
0
% inhibition of I_{AHP}
-6
-5
-4
log concentration (M)

Fig. 5.16 Comparison of the inhibition of I_{Ca} and I_{AHP} by Cd^{2+}.

A. Illustrates the dose-response relationships obtained for inhibition of I_{Ca} and I_{AHP} by Cd^{2+}.

B. Plot showing inhibition of I_{AHP} by Cd^{2+} against inhibition of I_{Ca} for each concentration of Cd^{2+}.

A.

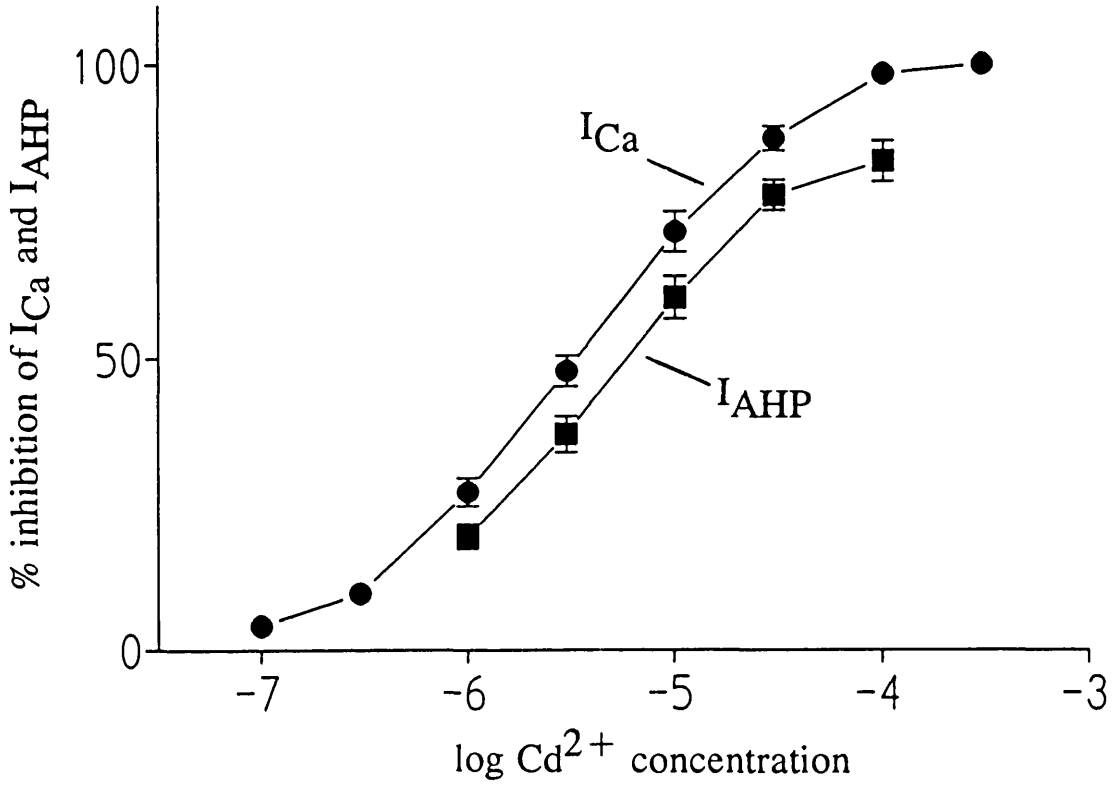
100
50
0
% inhibition of I_{Ca} and I_{AHP}
I_{Ca}
I_{AHP}
-7
-6
-5
-4
-3
log Cd^{2+} concentration

B.

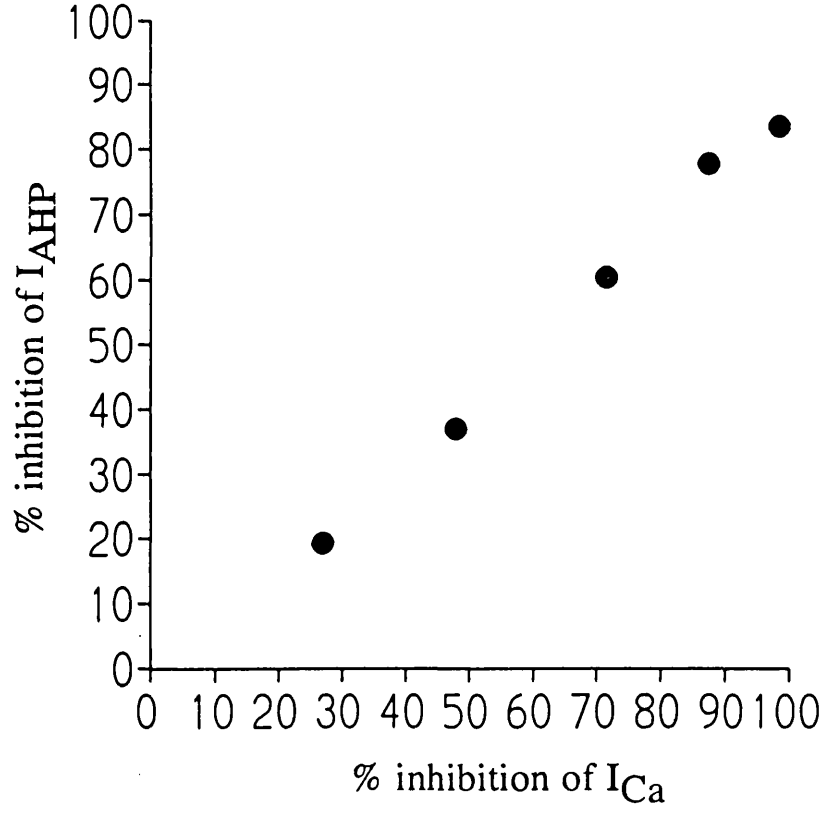
100
90
80
70
60
50
40
30
20
10
0
% inhibition of I_{AHP}
0 10 20 30 40 50 60 70 80 90 100
% inhibition of I_{Ca}

Fig. 5.17 Effect of caffeine on I_{AHP} in an impaled dissociated neurone.

A. Records show I_{AHP} (V_H=-55mV, V_C=-2mV) recorded in the absence (above) and presence (below) of 2mM caffeine for the command durations indicated.

B. Records show I_{AHP} (V_H=-52mV, V_C=0mV) in the absence and presence of 2mM caffeine to illustrate the apparent slowing of the activation of I_{AHP} by caffeine. Duration of command pulse was 10ms.

A.

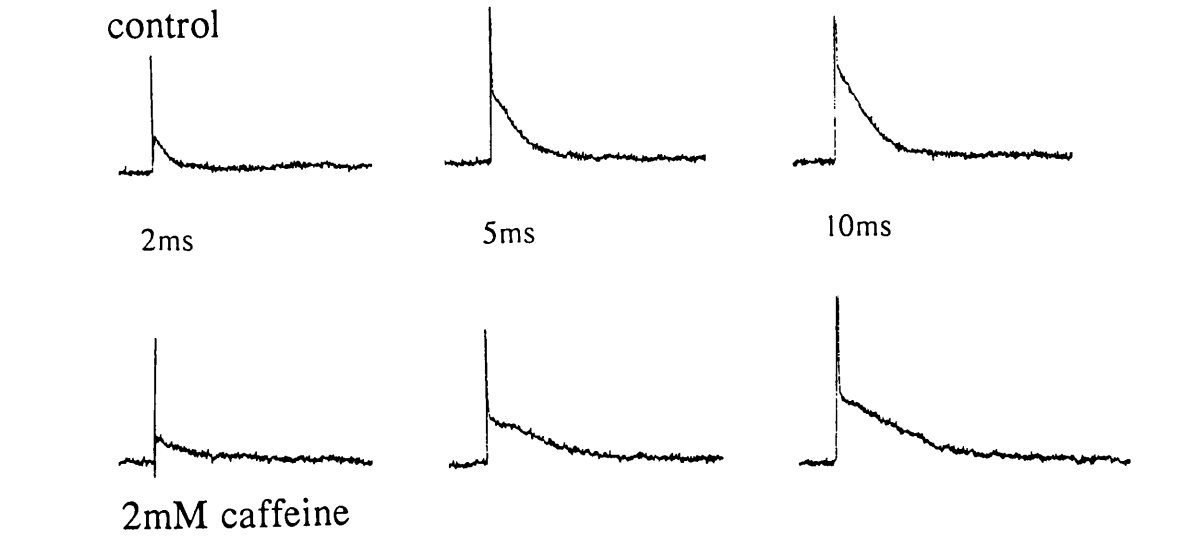
control
2ms
5ms
10ms
2mM caffeine

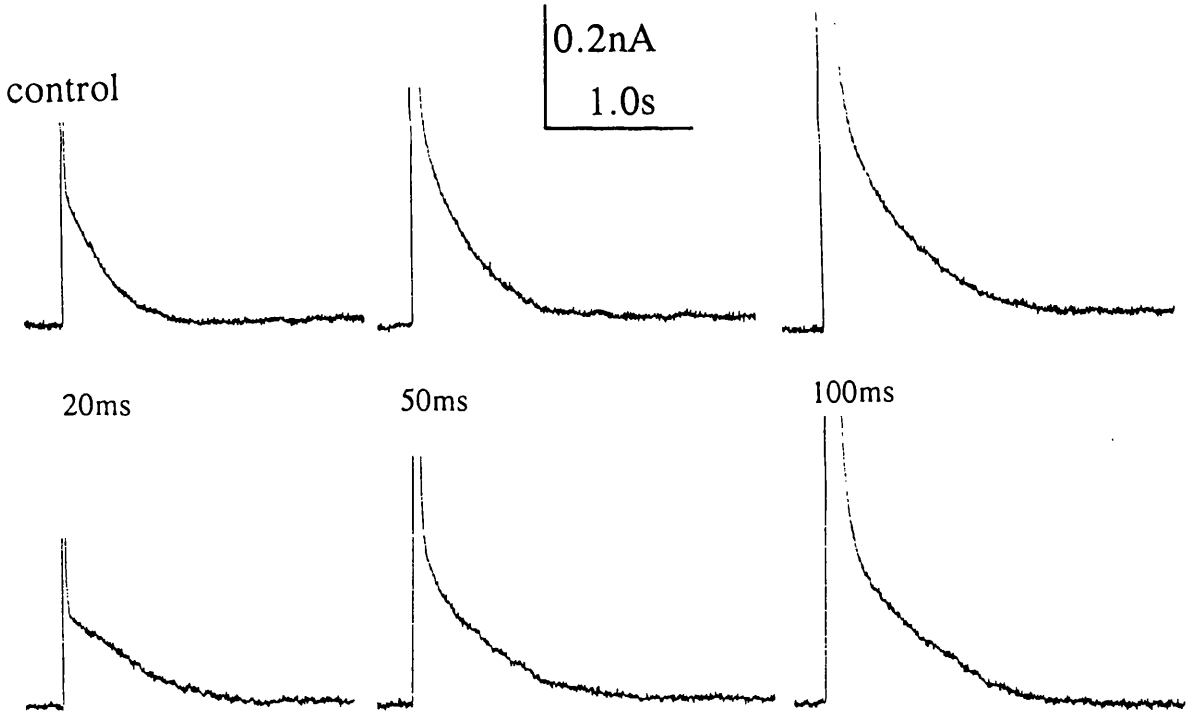
0.2nA
1.0s
control
20ms
50ms
100ms
2mM caffeine

B.

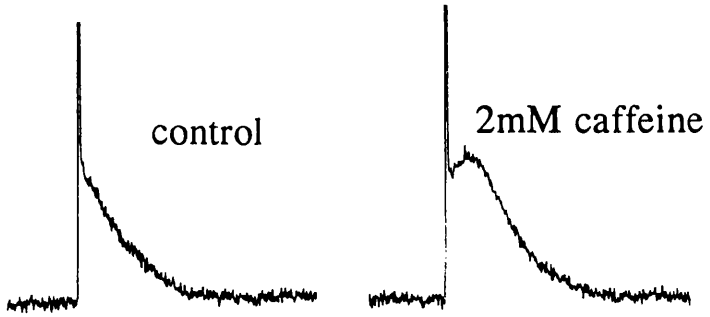
control
2mM caffeine

Fig. 5.18 Effect of tetraethylammonium (TEA) on I_{AHP}.

Currents recorded from an voltage-clamped intact neurone in the absence and presence of 5mM TEA. Currents were evoked by 50ms commands to -4mV from a holding potential of -50mV.

TEA inhibits the fast component of the tail-current, but increases the slow component (see text).

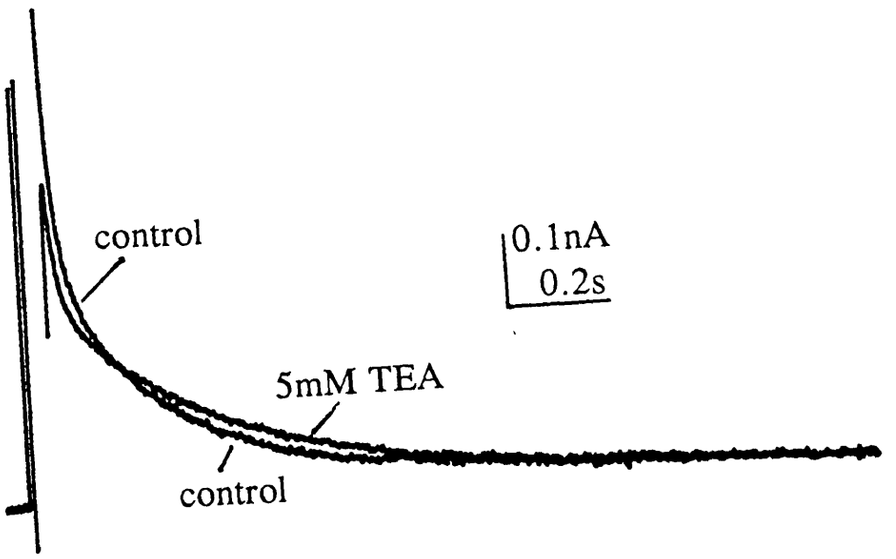
control
0.1nA
0.2s
5mM TEA
control

Fig. 5.19 Effect of d-tubocurarine (dTC) on I_{AHP}.

A. Whole-cell voltage-clamp records from a dissociated s.c.g. neurone showing inhibition by cumulative addition of dTC. The holding potential was -49mV and currents evoked by 50ms commands to -3mV. Also shown is a plot of log I_{AHP} amplitude aginst time for control (●; τ=410ms) and 10μM dTC (■; τ=423ms) to illustrate the lack of effect by dTC on the time course of I_{AHP} decay.

B. Dose-response curve for the block of I_{AHP} by dTC. Data are expressed as mean ± s.e.m. (n=5).

A.

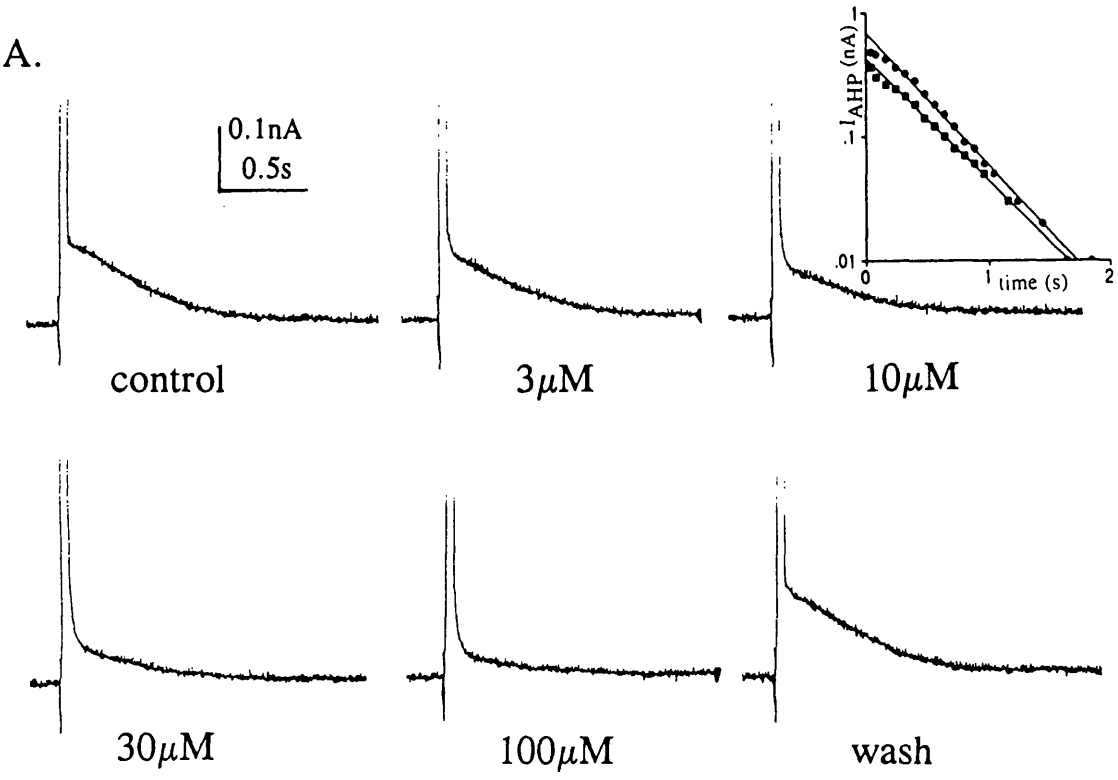
0.1nA
0.5s
control
3μM
10μM
30μM
100μM
wash
-I_AHP (nA)
.01
0
1
time (s)
2

B.

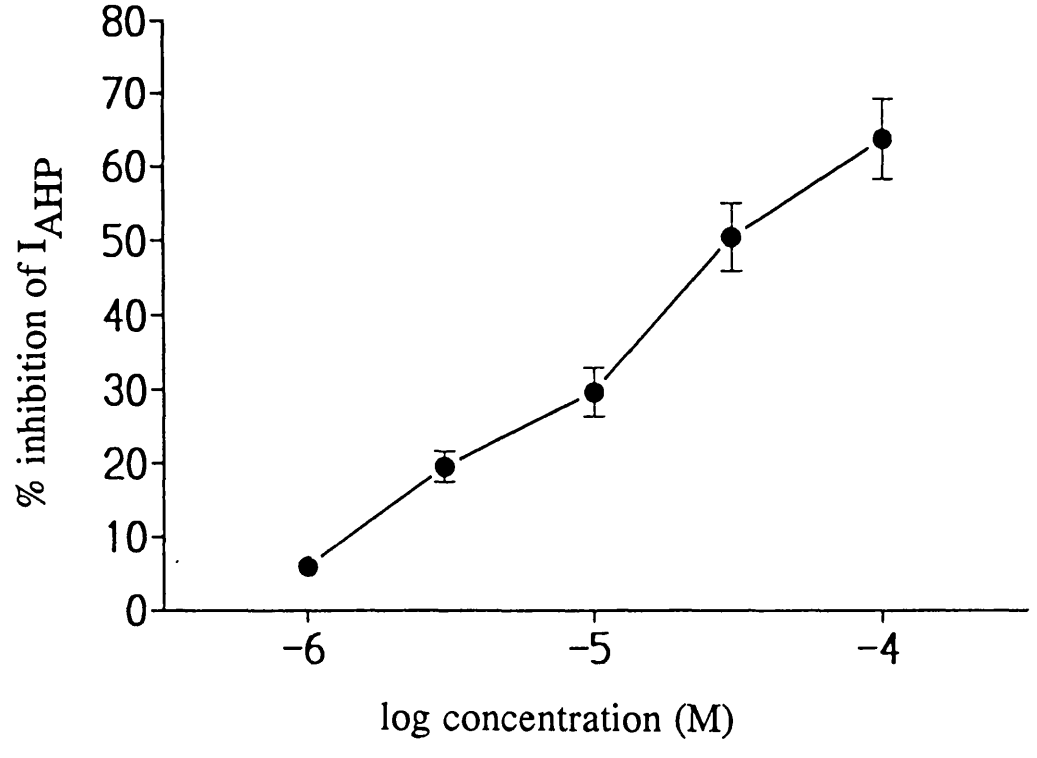
% inhibition of I_AHP
80
70
60
50
40
30
20
10
0
-6
-5
-4
log concentration (M)

Fig. 5.20 Effect of apamin on I_{AHP}.

Records illustrate I_{AHP} (V_H=-53mV, V_C=5mV) recorded from a whole-cell voltage-clamped dissociated neurone and obtained in the absence, and presence of 30nM apamin. There was no recovery.

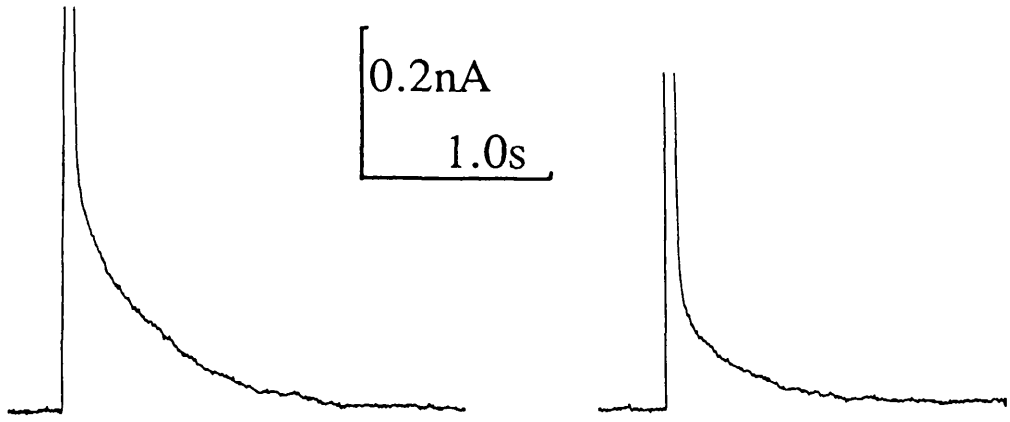

control

30nM apamin

Fig. 5.21 Effect of 4-aminopyridine (4-AP) on I_{AHP}.

Records illustrate I_{AHP} (V_H=-55mV, V_C=+1mV) recorded from a whole-cell voltage-clamped dissociated neurone and obtained before, during and after addition of 3mM 4-AP.

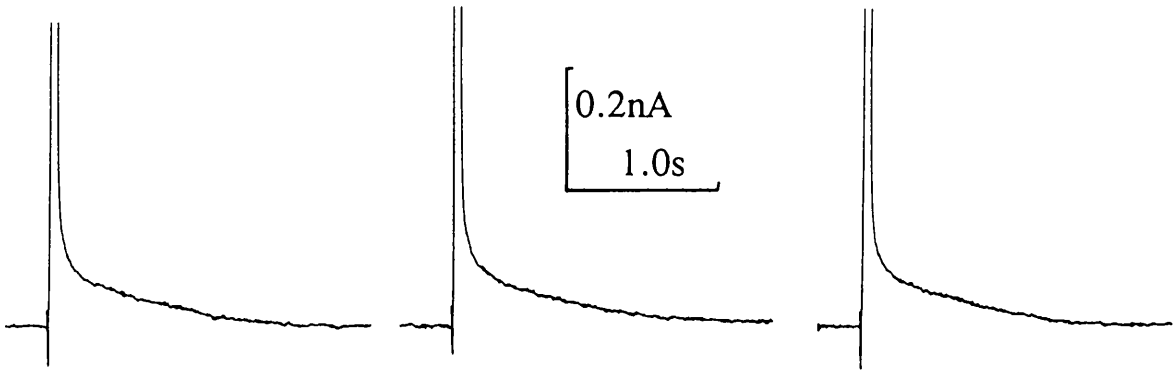
0.2nA
1.0s
control
3mM 4-AP
wash

Fig. 5.22 Effect of noradrenaline on I_{AHP}.

A. I_{AHP} recorded from a voltage-clamped intact s.c.g. neurone (a) before, and (b) following addition of 10μM noradrenaline to the Krebs' solution, and (c) following wash.
The holding-potential was -45mV and I_{AHP} was evoked by a 50ms command to -1mV.

B. Whole-cell voltage-clamp records from a dissociated s.c.g. neurone showing currents obtained (a) before, (b) during and (c) after addition of 10μM noradrenaline.
The holding-potential was -50mV and I_{AHP} was evoked by a 50ms command to -4mV.
Also shown is a plot of log I_{AHP} amplitude against time for the records for control (●; τ=724ms) and 10μM noradrenaline (■; τ=489ms) to illustrate the effect of noradrenaline on I_{AHP} decay.

A.

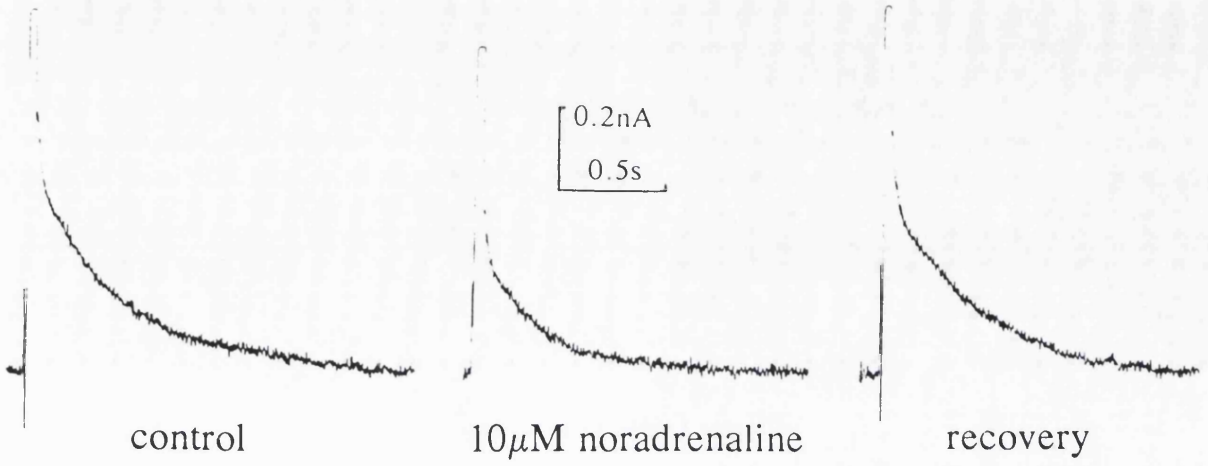
0.2nA
0.5s
control
10μM noradrenaline
recovery

B.

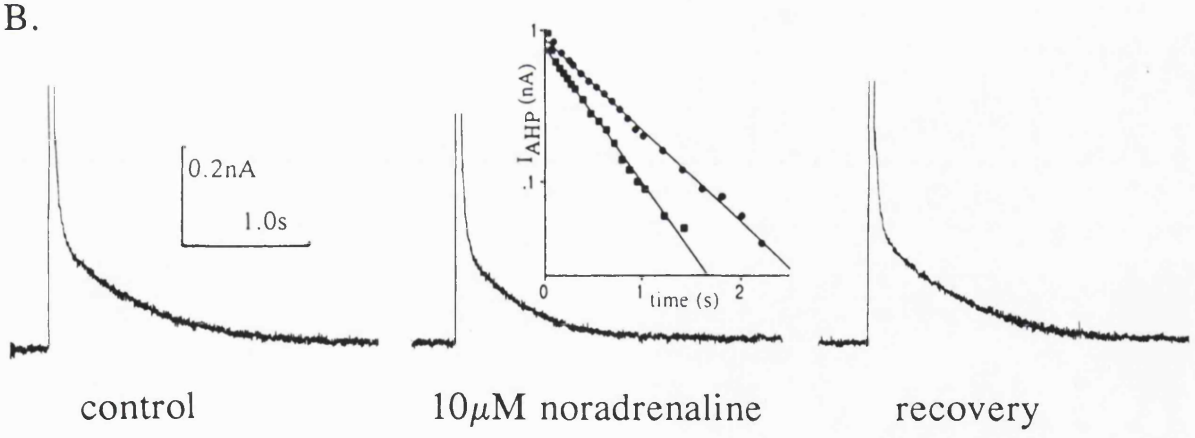
0.2nA
1.0s
$-I_{AHP}$ (nA)
1
0
1
2
time (s)
control
10μM noradrenaline
recovery

Fig. 5.23 Dose-response relationship for inhibition of I_{AHP} by noradrenaline.

Mean dose-response curves for the inhibition of I_{AHP} by noradrenaline using (A) intact neurones, and (B) dissociated s.c.g. neurones (whole-cell voltage-clamped). Data is expressed as mean $\pm$ s.e.m. (intact, n=10; dissociated, n=4) and experiments were performed using cumulative additions of noradrenaline.

Data from the dissociated cells was measured 150ms after the end of the voltage command.

A.

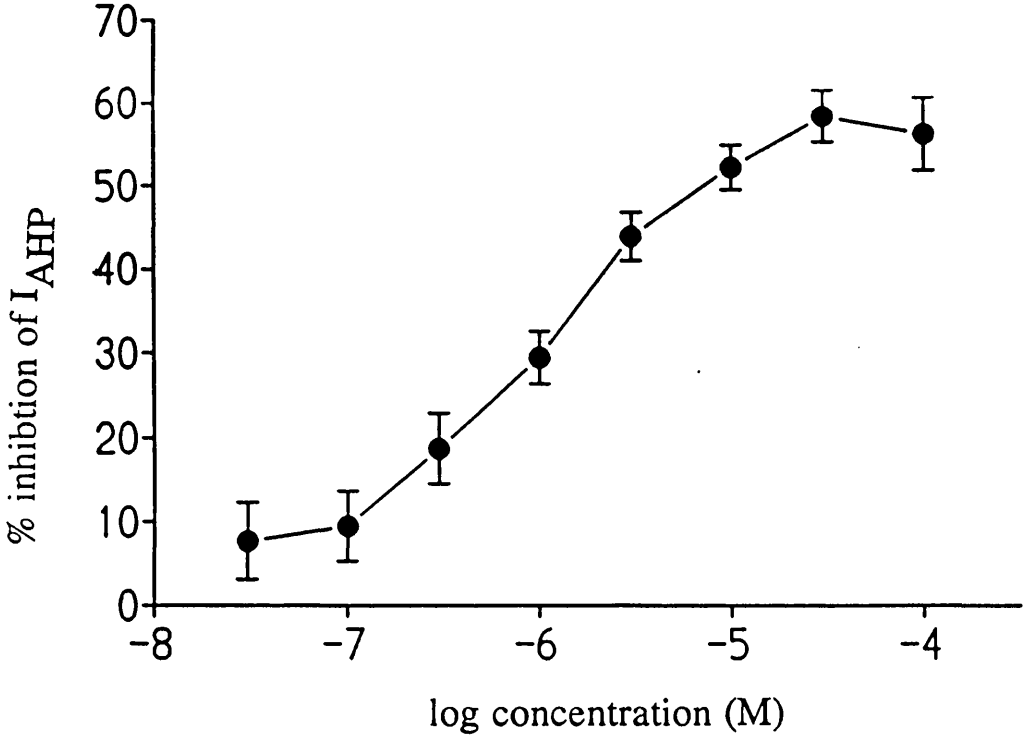
70
60
50
40
30
20
10
0
% inhibtion of I_{AHP}
-8
-7
-6
-5
-4
log concentration (M)

B.

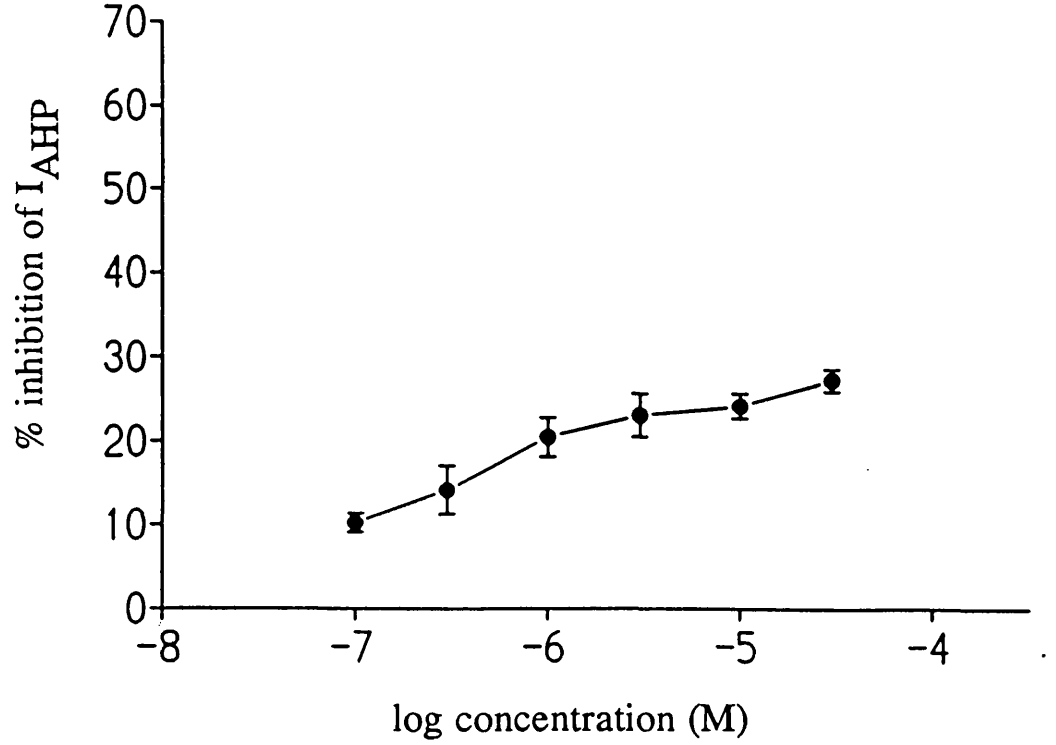
70
60
50
40
30
20
10
0
% inhibition of I_{AHP}
-8
-7
-6
-5
-4
log concentration (M)

Fig. 5.24 Comparison of noradrenaline's suppression of I_{AHP} and I_{Ca}.

A. Compares the dose-response relationships obtained for inhibition of I_{AHP} and I_{Ca} by noradrenaline in dissociated neurones.

B. Plot showing inhibition of I_{AHP} by noradrenaline against inhibition of Q_{Ca} for each concentration of noradrenaline (●). Q_{Ca} was calculated from I_{Ca} recordings and represents Ca^{2+} influx during a 50ms command. Q_{Ca} is used instead of I_{Ca} since noradrenaline alters I_{Ca} kinetics, such that measurement of peak I_{Ca} inhibition may not give an accurate estimation of the change in Ca^{2+} entry. Also shown for comparison is the plot obtained for Cd^{2+} (■; data taken from Fig. 5.16). The values for Cd^{2+} were not converted from I_{Ca} to Q_{Ca} since Cd^{2+} did not alter the shape of the recorded current.

A.

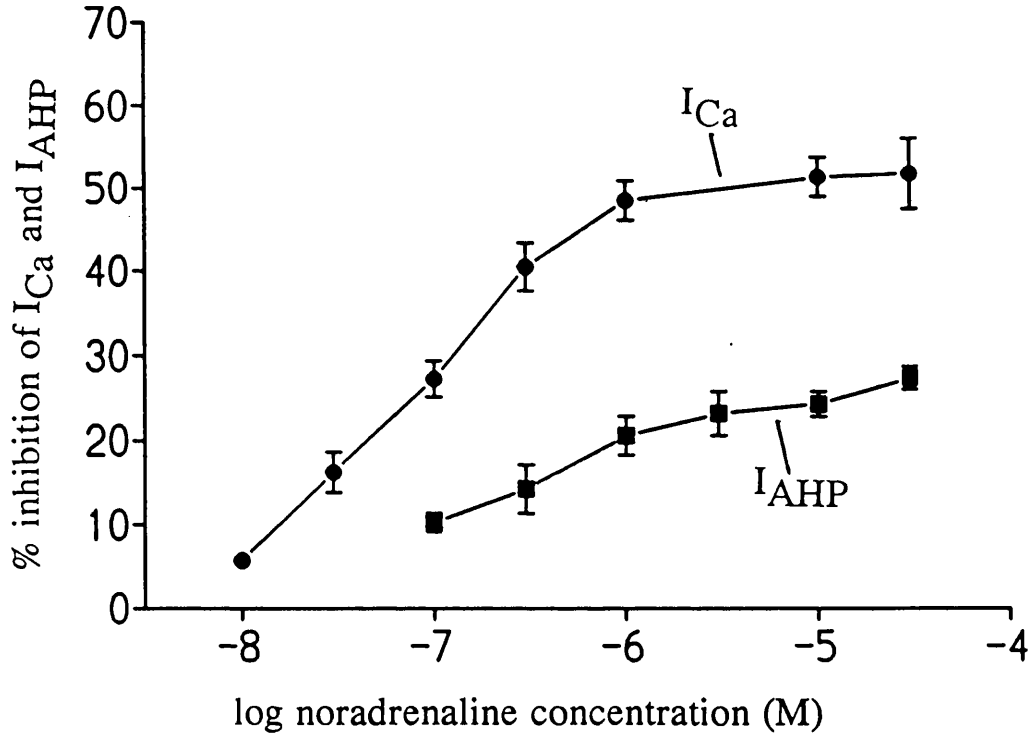
% inhibition of I_{Ca} and I_{AHP}
70
60
50
40
30
20
10
0
I_{Ca}
I_{AHP}
-8
-7
-6
-5
-4
log noradrenaline concentration (M)

B.

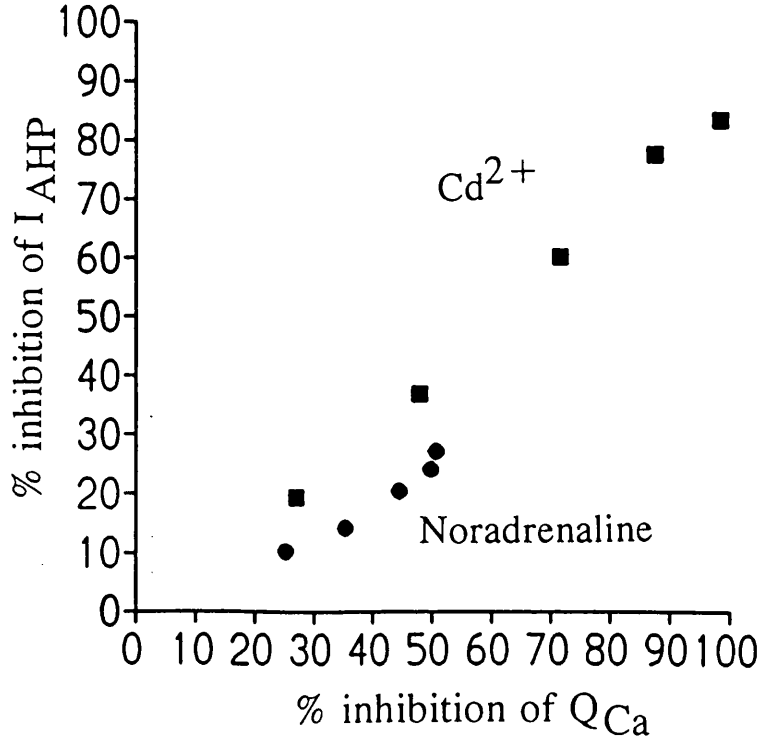
% inhibition of I_{AHP}
100
90
80
70
60
50
40
30
20
10
0
Cd^{2+}
Noradrenaline
0 10 20 30 40 50 60 70 80 90 100
% inhibition of Q_{Ca}

Fig. 5.25 Antagonism of noradrenaline's suppression of I_{AHP} by yohimbine.

Records show I_{AHP} (V_H=-52, V_C=-3mV) recorded before, during and after superfusion of 10μM noradrenaline (a) in the absence and (b) in the presence of 10μM yohimbine. Data obtained from a whole-cell voltage-clamped neurone.

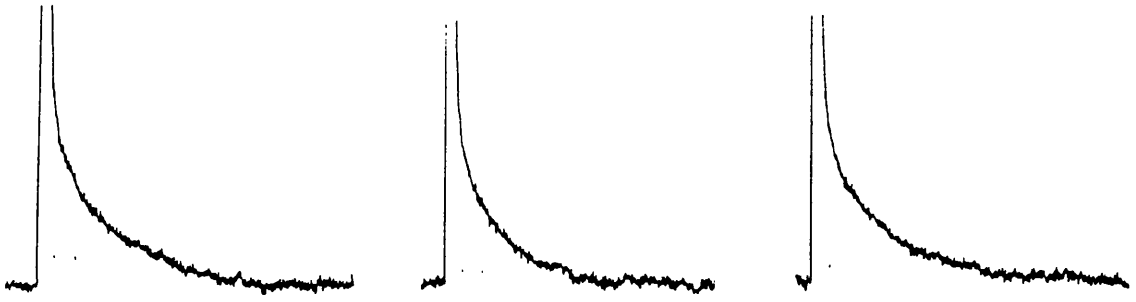

control　　10μM noradrenaline　　recovery

+10μM yohimbine

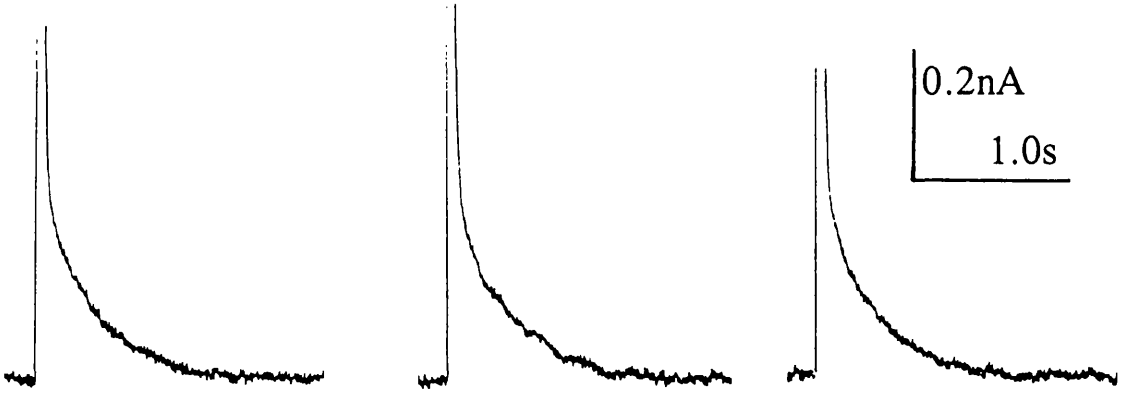

control　　10μM noradrenaline　　recovery

Fig. 5.26 Inhibition of I_{AHP} (and I_{Ca}) by methacholine in whole-cell voltage-clamped dissociated neurones.

A. Records show I_{AHP} (V_H=-55mV, V_C=-2mV) obtained in the absence and the presence of 10 and 100μM methacholine. There was only a poor recovery from the response. Also shown is a plot of log I_{AHP} decay against time for the records obtained for control (●; τ=387ms) and 10μM methacholine (■; τ=292ms).

B. Shows the inhibition of I_{Ca} by 10μM methacholine (V_H=-90mV, V_C=0mV; see chapter 3 for details of I_{Ca} recording).

A.

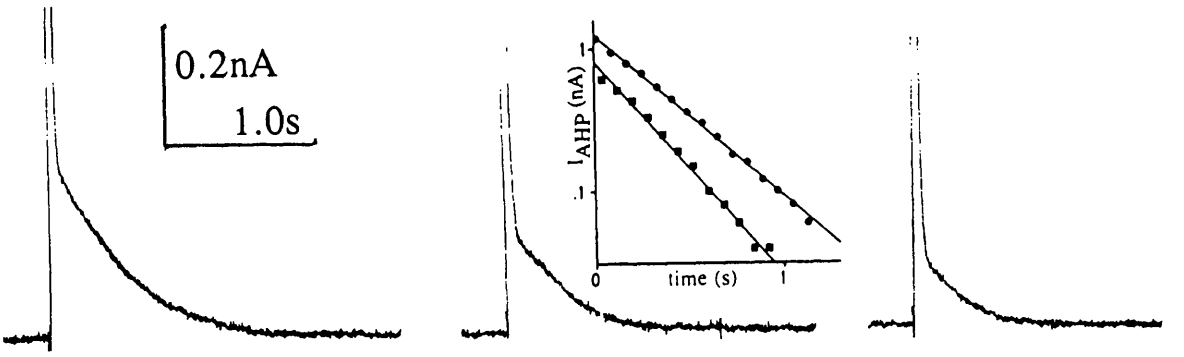

control 10μM methacholine 100μM methacholine

B.

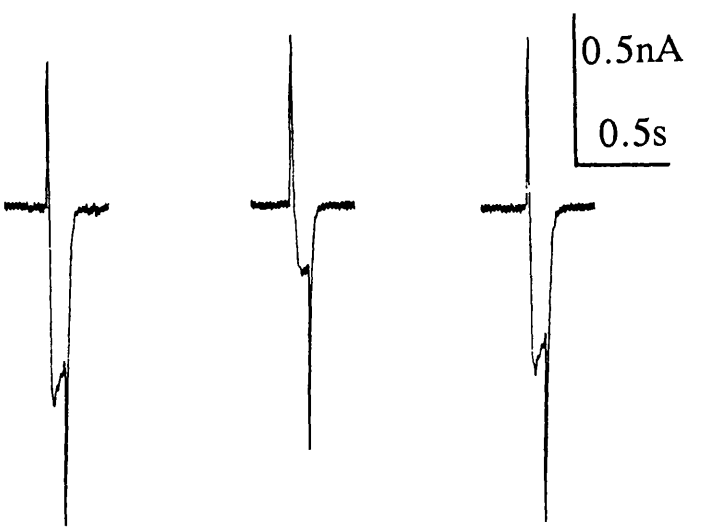

control 10μM methacholine wash

Fig. 5.27 Comparison of the suppression of I_{AHP} by methacholine with block by Cd^{2+} and dTC.

Illustrates the effects of methacholine, Cd^{2+} and dTC on I_{AHP} amplitude and time-course in the same whole-cell voltage-clamped neurone.

Records show I_{AHP} (V_H=-55mV,V_C=-4mV) recorded before, during and after application of (a) 10μM dTC, (b) 10μM Cd^{2+} and (c) 10μM methacholine. Also shown are plots of log I_{AHP} amplitude against time for the records obtained for each drug (■) and control records (●), to illustrate the effect of each drug on I_{AHP} decay.

Calculated values for time constant (τ) of I_{AHP} decay:-

(a) control, 521ms; 10μM dTC, 492ms.

(b) control, 502ms; 10μM Cd^{2+}, 287ms.

(c) control, 575ms; 10μM methacholine, 317ms.

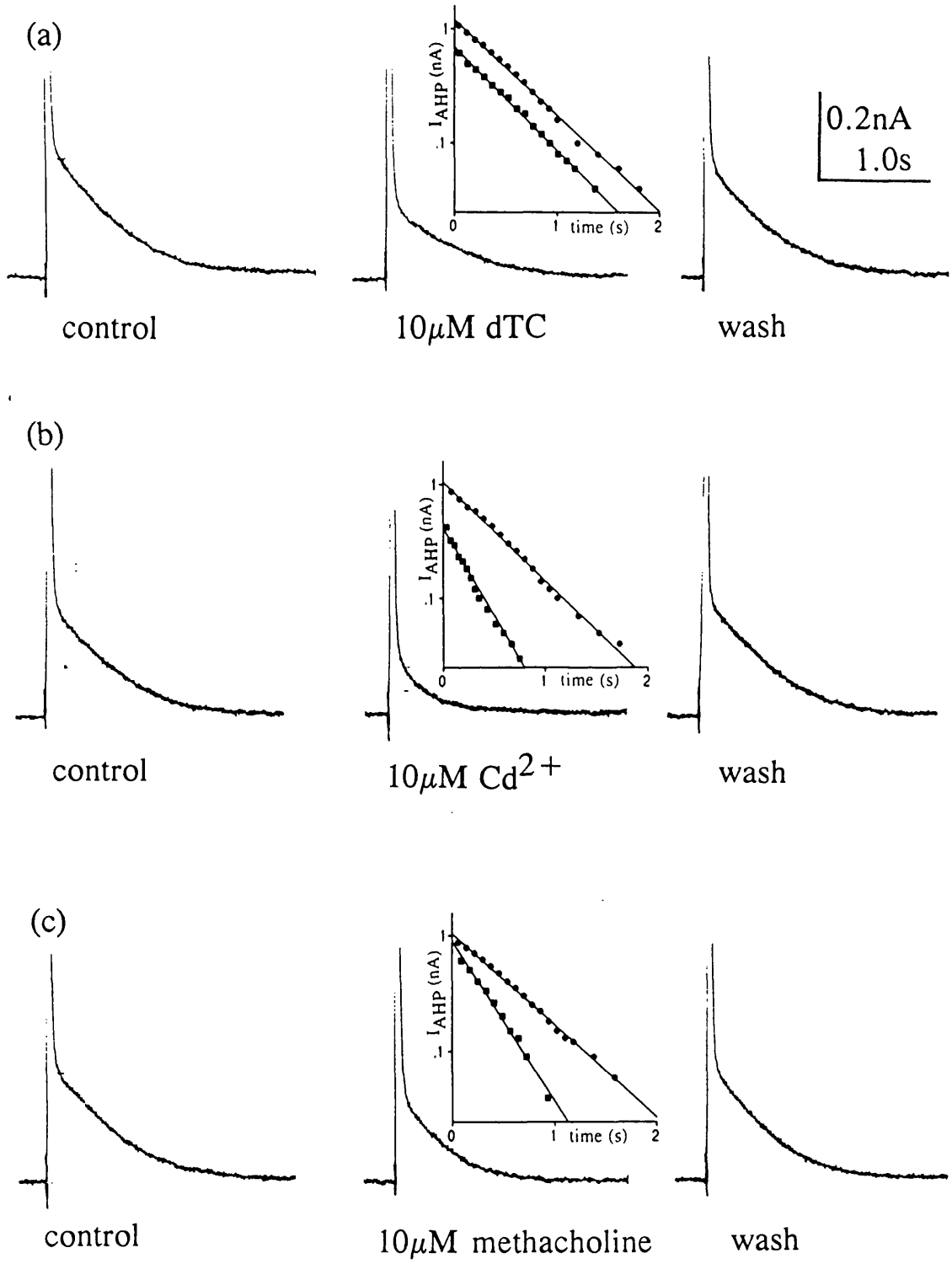
(a)
I_{AHP} (nA)
time (s)
0.2nA
1.0s
control
10μM dTC
wash
(b)
I_{AHP} (nA)
time (s)
control
10μM Cd^{2+}
wash
(c)
I_{AHP} (nA)
time (s)
control
10μM methacholine
wash

Chapter 6.

General discussion.

This study has investigated the membrane currents responsible for the generation of the long after-hyperpolarization (a.h.p.) of rat superior cervical ganglion (s.c.g.) neurones. The a.h.p. was generated by a potassium current, I_{AHP}, similar to the I_{AHP} of bullfrog sympathetic ganglion cells. I_{AHP} was shown to be calcium-dependent, independent of membrane potential and suppressed by neurotransmitters. It was blocked by d-tubocurarine and apamin, but insensitive to tetraethylammonium and 4-aminopyridine. The calcium necessary for activation of I_{AHP} originates primarily from influx through voltage-gated calcium channels, which showed a corresponding sensitivity to neurotransmitters. The size of the calcium load determined the decay kinetics of I_{AHP}, such that a decreased calcium load reduced the duration of the current. It also appeared that the inhibition of I_{AHP} by neurotransmitters was mediated via inhibition of I_{Ca}. Noradrenergic suppression was primarily investigated, and inhibition of I_{Ca} was mediated by α_2-receptors. Thus, some of the pharmacological properties of I_{AHP} in rat s.c.g. neurones have been characterized. The physiologically relevant question that now needs to be addressed clearly is, what is the functional role of I_{AHP} and in particular its inhibition by noradrenaline (and other neurotransmitters)?

The principle action of I_{AHP} in sympathetic neurones is the reduction of neuronal excitability following action potentials. Block of the a.h.p. decreases accommodation and increases repetitive firing during sustained depolarization (Kawai et al, 1985; Kawai and Watanabe, 1986), suggesting that the role of the a.h.p. is to suppress subsequent firing of postganglionic neurones following an initial action potential, thereby modulating ganglionic transmission (Kawai and Watanabe, 1986). It would therefore appear that I_{AHP} does play an important role in s.c.g. neurones, but is there also a functional significance for the suppression of I_{AHP} by neurotransmitters? It was noticed

during the course of this study that noradrenaline did increase repetitive firing during depolarizing current commands in current-clamp though the effect was small, presumably due to activation of I_M during the current command. This observation might suggest that a physiological action of catecholamines in the s.c.g. is to increase the excitability of postganglionic neurones via inhibition of I_{AHP}. However, the situation is much more complicated than this since noradrenaline exerts several actions in sympathetic ganglia (see below), and it is therefore necessary to consider the various actions of noradrenaline, in addition to inhibition of I_{AHP}, before a physiological significance to the suppression of I_{AHP} can be suggested. A role for noradrenaline in the s.c.g. is likely since there are small catecholamine containing cells (Eranko and Harkonen, 1963; Koslow, 1975; Eranko, 1976) in the ganglion, some of which function as interneurones (Williams et al, 1976; Elfvin et al, 1993). In addition, there is evidence that noradrenaline is released from the soma or dendrites of the postganglionic neurones (Reinert, 1963), though more recent evidence from cultured chick sympathetic neurones indicates that release of noradrenaline is from neurites and growth cones but not from cell bodies (Przywara et al, 1993).

One reported action of noradrenaline on postganglionic neurones is the α_2-mediated hyperpolarization (Brown and Caulfield, 1979). This hyperpolarization was inversely related to the external potassium concentration (Brown and Caulfield, 1979), consistent with an increased potassium conductance, and therefore reduced neuronal excitability. However, the hyperpolarization, measured using intracellular electrodes, is small (approximately 1mV) without a clear effect on the voltage-current relationship (Brown and Caulfield, 1981), so the modulating effect of this hyperpolarization on neuronal excitability may be minor. A more significant action of noradrenaline may occur in preganglionic neurones, where release of acetylcholine from terminals is reduced, with a consequent depression of ganglionic transmission (Brown and Caulfield, 1981), the action of noradrenaline being mediated by α_2-receptors. The reduction in transmitter release probably occurs as a result of the suppression of Ca^{2+} entry also observed in these neurones (Elliott et al, 1989). Other actions of noradrenaline in the s.c.g. are

excitatory and are demonstrated by a postganglionic depolarization, and an increase transmitter release from preganglionic neurones with a corresponding facilitation of ganglionic transmission (Brown and Dunn, 1983b), these actions being mediated by ß-receptors. It is therefore clear that noradrenaline exerts many actions in the s.c.g., both excitatory and inhibitory in nature. However the dominant overall effect in the intact ganglion seems to be inhibitory with presynaptic depression of ganglionic transmission (Lindl, 1979; Brown and Caulfield, 1981). Given these circumstances is there any significance to the suppression of I_{AHP} by noradrenaline? One possibility is that suppression of I_{AHP} becomes significant at high levels of sympathetic activity. Under such conditions ganglionic transmission will be suppressed by intraganglionic release of noradrenaline, such that only large, and important, stimuli will release sufficient acetylcholine from preganglionic neurones to cause firing of postganglionic neurones. Suppression of I_{AHP}, and the resulting shortening of the a.h.p., will allow more frequent firing of the postganglionic neurones in response to these important stimuli, thus providing a high safety factor for ganglionic transmission when accurate transmission of important messages is needed.

It is, however, possible that there is no significant physiological function for the suppression of I_{AHP} by noradrenaline, and that the suppression observed is merely a secondary consequence of the reduction of I_{Ca}. Suppression of transmitter release at nerve terminals is postulated to be mediated via α_2-autoreceptor inhibition of Ca^{2+} entry (Starke, 1987), and it is possible that a similar mechanism exists in the soma. However, noradrenaline release from cell bodies may be insignificant compared with release from terminals, as has been demonstrated in chick sympathetic neurones (Przywara et al, 1993), in which case suppression of I_{AHP} may be the main consequence of I_{Ca} suppression by noradrenaline in cell bodies.

Muscarinic inhibition of I_{AHP} is likely to have a similar effect on excitability of s.c.g. neurones, and combined with the simultaneous inhibition of I_M, it is likely that muscarinic receptor stimulation, by acetylcholine, produces a greater excitation of postganglionic neurones than that caused by noradrenergic stimulation. Other

neurotransmitters are likely to be involved in control of I_{AHP} in s.c.g. neurones. For example somatostatin, which has been suggested to be released by intraganglionic neurones (Leranth et al, 1980), suppresses I_{Ca} (Ikeda and Schofield, 1989) and will presumably also suppress I_{AHP}. Since various neurotransmitters exert multiple actions in the s.c.g. the precise functional role of I_{AHP} suppression remains to be determined.

It is possible that I_{AHP} plays a role in controlling transmitter release from sympathetic nerve terminals, where suppression of I_{AHP}, and the subsequent enhancement of excitability, could lead to an enhancement of noradrenaline release. However, it is not known whether I_{AHP} channels are expressed at the terminals. Investigation of synaptic transmission at the frog neuromuscular junction suggests that I_C, rather than I_{AHP}, modulates transmission, with charybdotoxin, but not apamin, enhancing transmitter release (Robitaille and Charlton, 1992). It has also been suggested that I_C channels are clustered at the transmitter release sites (Robitaille et al, 1993). The effect of apamin on transmitter release from sympathetic neurones has not been reported, and any possible role of I_{AHP} in sympathetic nerve terminals remains to be determined.

Although some of the properties of I_{AHP} in rat s.c.g. neurones have been described in this study, many questions remain. The single channels underlying I_{AHP} were not investigated, and there are no reports describing channels with the necessary properties to account for I_{AHP} in s.c.g. neurones. Small conductance channels underlying similar currents in other cell-types have been observed, for example in cultured rat skeletal muscle (Blatz and Magleby, 1986), GH_3 cells (Lang and Ritchie, 1987) and cultured hippocampal neurones (Lancaster et al, 1991). The large conductance channels underlying I_C have been characterized in the s.c.g. (Smart, 1987), though there was no report of smaller conductance Ca^{2+}-activated channels. It should be possible to record I_{AHP} in inside-out patches by observing channel activity following changes in intracellular Ca^{2+}, and to identify the channels as those generating I_{AHP} on the basis of voltage-independence and pharmacological characteristics.

The role of calcium in controlling the time-course of I_{AHP} needs to be investigated further. It would be interesting to determine whether the time-course of I_{AHP} decay reflects the decay of intracellular Ca^{2+} following Ca^{2+} entry. This could be attempted by simultaneous voltage-clamp recording and measurement of intracellular Ca^{2+} using a Ca^{2+}-indicator such as indo-1, though such techniques measure whole-cell Ca^{2+} when precise estimation of Ca^{2+} at the cell membrane is necessary. In addition, the mobilization of intracellular calcium needs to be investigated further. Although caffeine prolonged I_{AHP} evoked by short commands, this does not prove that intracellular release of Ca^{2+} contributes to I_{AHP}. If intracellular Ca^{2+} release does contribute to I_{AHP} then a shortening of I_{AHP} duration by ryanodine would be expected. This has been demonstrated for the a.h.p. in rat s.c.g. neurones (Kawai and Watanabe, 1989), though investigation of I_{AHP} in bullfrog neurones showed a lack of effect of ryanodine, suggesting that mobilization of intracellular Ca^{2+} does not contribute to I_{AHP} (Goh et al, 1992b). It is possible that this represents a difference in I_{AHP} between rat and bullfrog sympathetic neurones, though further work is needed to clarify this.

Another question that needs to be investigated further is the mechanism by which neurotransmitters suppress I_{AHP}. The conclusion that noradrenergic and muscarinic suppression of I_{AHP} is via inhibition of the preceding calcium current was made indirectly since I_{Ca} was necessary to activate I_{AHP}. It might be possible to record I_{AHP} independently of I_{Ca} by using a calcium ionophore, such as ionomycin (Beeler et al, 1979), to cause sufficient influx of Ca^{2+} into the cell to activate I_{AHP}. Ionomycin-induced Ca^{2+} entry has been successfully used as an alternative to voltage-activated Ca^{2+} entry, for example, in evoking acetylcholine release at frog motor nerve endings (Hunt and Silinsky, 1993). Assuming that ionomycin can activate I_{AHP} in s.c.g. neurones it will both allow investigation of I_{AHP} in isolation from I_{Ca}, and also allow direct investigation of the pharmacological inhibition of I_{AHP}.

Noradrenergic inhibition of I_{Ca} was suggested to be mediated via an α_2-receptor (chapter 4). In recent years it has, however, become increasingly apparent that α_2-receptors can be separated into distinct subtypes. The first suggestion that α_2-receptors

may show heterogeneity was by Bylund (1981) based on a comparison of [^{3}H]-clonidine and [^{3}H]-yohimbine binding in various tissues. Subsequent pharmacological studies have revealed the existence of four subtypes of α_2-adrenoceptor: α_{2A}, found in, for example, rabbit spleen (Michel et al, 1990) and human platelet cells (Bylund et al, 1988); α_{2B}, in rat kidney (Michel et al, 1990) and NG108-15 cells (Bylund et al, 1988); α_{2C}, in opussum kidney OK cells (Murphy and Bylund, 1988); α_{2D}, in bovine pineal gland (Simmoneaux et al, 91). Molecular cloning techniques have provided further evidence for α_2-receptor heterogeneity. Three clones were initially isolated from human DNA: α_2C10 (Kobilka et al, 1987); α_2C2 (Lomasney et al, 1990); α_2C4 (Regan et al, 1988). The pharmacology of these clones correspond with α_{2A}-, α_{2B}- and α_{2C}- receptors respectively (Bylund et al, 1992). Three clones have also been isolated from rat tissues: RNG (α_{2B}, Zeng et al, 1990); RG10 and RG20 (α_{2C} and α_{2D} respectively, Lanier et al, 1991), though it has also been suggested that the RG20 clone may correspond to the α_{2A} receptor (Harrison et al, 1991).

The question here is which subtype of α_2-receptor mediates the suppression of I_{Ca}? It is not possible from the small number of antagonists used in this study to answer this conclusively. However, the relatively low potency of yohimbine compared to phentolamine is consistent with the α_{2D}-subtype (Simonneaux et al, 1991) and the receptor encoded by RG20 (Lanier et al, 1991), both studies demonstrating phentolamine to be more potent than yohimbine in competition binding experiments. The other α_2-subtypes show the reverse order of potency for these two antagonists. It has also been suggested by Hill et al (1993) that the adrenoceptor modulating noradrenaline release from rat s.c.g. neurones is similar to the α_{2D}-subtype. Further investigation is necessary before the α_2-adrenoceptor subtype mediating inhibition of I_{Ca} in rat s.c.g. neurones can be conclusively identified.

References

Adams, P.R. (1981). The calcium current of a vertebrate neurone. In Salankin, J. (ed). Advances in physiological sciences, vol. 4, Proc. 28th Int. Congress Physiol. Sci., Akademiai Kiando, Budapest. pp 135-138.

Adams, P.R., Brown, D.A. & Constanti, A. (1982a). Pharmacological inhibition of the M-current. *J. Physiol.* **332**, 223-262.

Adams, P.R., Constanti, A., Brown, D.A. & Clark, R.B. (1982b). Intracellular Ca^{2+} activates a fast voltage-sensitive K^{+} current in vertebrate sympathetic neurones. *Nature* **296**, 746-749.

Adams, P.R. & Galvan, M. (1986). Voltage-dependent currents of vertebrate neurones and their role in membrane excitability. In Delgado, A.V., Ward, A.A., Woodbury, D.M. & Porter, R.J. (Eds). Advances in Neurology, vol. 44. Raven Press, New York. pp 137-157.

Ahlquist, R.P. (1948). A study of the adrenotropic receptors. *Am. J. Physiol.* **153**, 586-600.

Akasu, T., Tsurusaki, M. & Tokimasa, T. (1990). Reduction of the N-type calcium current by noradrenaline in neurones of rabbit vesical parasympathetic ganglia. *J. Physiol.* **426**, 439-452.

Anwyl, R. (1991). Modulation of vertebrate neuronal calcium channels by transmitters. *Brain Res. Rev.* **16**, 265-281.

Arunlakshana, O. & Schild, H.O. (1959). Some quantitative uses of drug antagonists. *Br. J. Pharmacol.* **14**, 48-58.

Bean, B.P. (1989a). Classes of calcium channels in vertebrate cells. *Annu. Rev. Physiol.* **51**, 367-84.

Bean, B.P. (1989b). Neurotransmitter inhibition of neuronal calcium currents by changes in channel voltage dependence. *Nature* **340**, 153-156.

Beech, D.J., Bernheim, L. & Hille, B. (1990). Muscarinic receptor coupling to calcium channels via a diffusible second messenger in acutely dissociated rat sympathetic neurones in vitro. *J. Physiol.* **434**, 36P.

Beech, D.J., Bernheim, L. & Hille, B. (1992). Pertussis toxin and voltage dependence distinguish multiple pathways modulating calcium channels of rat sympathetic neurones. *Neuron* **8**, 97-106.

Beech, D.J., Bernheim, L., Mathie, A. & Hille, B. (1991). Intracellular Ca^{2+} buffers disrupt muscarinic suppression of Ca^{2+} current and M current in rat sympathetic neurones. *Proc. Natl. Acad. Sci. USA* **88**, 652-656.

Beeler, T.J., Jona, I. & Martonosi, A. (1979). The effect of ionomycin on calcium fluxes in sarcoplasmic reticulum vesicles and liposomes. *J. Biol. Chem.* **254**, 6229-6231.

Belluzzi, O. & Sacchi, O. (1989). Calcium currents in the normal adult rat sympathetic neurone. *J. Physiol.* **412**, 493-512.

Belluzzi, O. & Sacchi, O. (1991). A five-conductance model of the action potential in the rat sympathetic neurone. *Prog. Biophys. molec. Biol.* **55**, 1-30.

Belluzzi, O., Sacchi, O. & Wanke, E. (1985a). A fast transient outward current in the rat sympathetic neurone studied under voltage-clamp conditions. *J. Physiol.* **358**, 91-108.

Belluzzi, O., Sacchi, O. & Wanke, E. (1985b). Identification of delayed potassium and calcium currents in the rat sympathetic neurone under voltage clamp. *J. Physiol.* **358**, 109-129.

Bernheim, L., Beech, D.J. & Hille, B. (1991). A diffusible second messenger mediates one of the pathways coupling receptors to calcium channels in rat sympathetic neurones. *Neuron* **6**, 859-867.

Bernheim, L., Mathie, A. & Hille, B. (1992). Characterization of muscarinic receptor subtypes inhibiting Ca^{2+} current and M-current in rat sympathetic neurones. *Proc. Natl. Acad. Sci. USA* **89**, 9544-9548.

Berthelson, S. & Pettinger, W.A. (1977). A functional basis for classification of α-adrenergic receptors. *Life Sci.* **21**, 595-606.

Besse, J.C. & Furchgott, R.F. (1976). Dissociation constants and relative efficacies of agonists acting on α-adrenergic receptors in rabbit aorta. *J. Pharmacol. Exp. Ther.* **197**, 66-78.

Biagi, B.A. & Enyeart, J.J. (1990). Gadolinium blocks low- and high-threshold calcium currents in pituitary cells. *Am. J. Physiol.* **259**, C515-C520.

Blatz, A.L. & Magleby, K.L. (1986). Single apamin-blocked Ca-activated K^+ channels of small conductance in cultured rat skeletal muscle. *Nature* **323**, 718-720.

Blaustein, M.P. & Goldman, D.E. (1968). The action of certain polyvalent cations on the voltage-clamped lobster axon. *J. Gen. Physiol.* **51**, 279-291.

Bley, K.R. & Tsien, R.W. (1990). Inhibition of Ca^{2+} and K^+ channels in sympathetic neurones by neuropeptides and other ganglionic transmitters. *Neuron* **2**, 379-391.

Blinks, J.R. (1967). Evaluation of the cardiac effects of several beta adrenergic blocking agents. *Ann. N.Y. Acad. Sci.* **139**, 673-685.

Brown, D.A., Adams, P.R. & Constanti, A. (1982). Voltage-sensitive K-currents in sympathetic neurones and their modulation by neurotransmitters. *J. Aut. Nerv. Syst.* **6**, 23-35.

Brown, D.A. & Caulfield, M.P. (1979). Hyperpolarizing 'α_2'-adrenoceptors in rat sympathetic ganglia. *Br. J. Pharmacol.* **65**, 435-445.

Brown, D.A. & Caulfield, M.P. (1981). Adrenoceptors in ganglia. In Kunos, G. (ed). Adrenoceptors and catecholamines action, vol. 1. John Wiley & Sons. pp 99-115

Brown, D.A., Constanti, A. & Adams, P.R. (1983). Ca-activated potassium current in vertebrate sympathetic neurones. *Cell Calcium* **4**, 407-420.

Brown, D.A. & Dunn, P.M. (1983a). Depolarization of rat isolated superior cervical ganglia mediated by $ß_2$-adrenoceptors. *Br. J. Pharmacol.* **79**, 429-439.

Brown, D.A. & Dunn, P.M. (1983b). Cyclic adenosine 3',5'-monophosphate and ß-effects in rat isolated superior cervical ganglia. *Br. J. Pharmacol.* **79**, 441-449.

Brown, D.A., Gahwiler, B.H., Marsh, S.J., & Selyanko, A.A. (1986). Mechanisms of muscarinic excitatory synaptic transmission in ganglia and brain. *Trends Pharmacol. Sci. Suppl. Muscarinic receptors II* 66-71.

Burlhis, T.M. & Aghajanian, G.K. (1987). Pacemaker potentials of sertogenic dorsal raphe neurones. Contribution of a low-threshhold Ca^{2+} conductance. *Synapse* **1**, 582-588.

Burton, H. & Bunge, R.P. (1975). A comparison of the uptake and release of ^{3}H-noradrenaline in rat autonomic and sensory ganglia in tissue culture. *Brain Res.* **97**, 157-162.

Bylund, D.B. (1981). Comparison of [^{3}H]clonidine and [^{3}H]yohimbine binding: possible subtypes of alpha-2 adrenergic receptors. *Pharmacologist* **23**, 215.

Bylund. D.B., Blaxall, H.S., Iversen, L.J., Caron, M.G. Lefkowitz, R.J. & Lomasney, J.W. (1992). Pharmacological characteristics of α_2-adrenergic receptors: comparison of pharmacologically defined subtypes with subtypes identified by molecular cloning. *Mol. Pharmacol.* **42**, 1-5.

Bylund, D.B., Ray-Prenger, C. & Murphy, T.J. (1988). Alpha-2A and alpha-2B adrenergic receptor subtypes: antagonist binding in tissues and cell lines containing only one subtype. *J. Pharmacol. Exp. Ther.* **245**, 600-607.

Canfield, D.R. & Dunlap, K. (1984). Pharmacological characterization of amine receptors on embryonic chick sensory neurones. *Br. J. Pharmacol.* **82**, 557-563.

Cannell, M.B. (1986). Effect of tetanus duration on the free calcium during the relaxation of frog skeletal muscle fibres. *J. Physiol.* **376**, 203-218.

Carbone, E. & Lux, H.D. (1984). A low voltage-activated calcium conductance in embryonic chick sensory neurones. *Biophys. J.* **46**, 413-418.

Carbone, E., Morad, M. & Lux, H.D. (1987). External Ni^{2+} selectively blocks the low-threshold Ca^{2+} current of chick sensory neurones. *Pflugers Arch.* **408**, R60.

Carbone, E. & Swandulla, D. (1989). Neuronal calcium channels: kinetics, blockade and modulation. *Prog. Biophys. molec. Biol.* **54**, 31-58.

Caulfield, M.P. (1978). Pharmacological characteristics of catecholamine receptors in rat sympathetic ganglia. Ph.D thesis, University of London.

Constanti, A. & Brown, D.A. (1981). M-currents in voltage-clamped mammalian sympathetic neurones. *Neurosci. Letts.* **24**, 289-294.

Cook, N.S. & Haylett, D.G. (1985) Effects of apamin, quinine and neuromuscular blockers on calcium-activated potassium channels in guinea-pig hepatocytes. *J. Physiol.* **358**, 373-394.

Crunelli, V., Lightowler, S. & Pollard, C.E. (1989). A T-type Ca^{2+} current underlies low-threshold Ca^{2+} potentials in cells of the cat and rat lateral geniculate nucleus. *J. Physiol.* **413**, 543-561.

Delcour, A.H., Lipscombe, D. & Tsien, R.W. (1993). Multiple modes of N-type channel activity distinguished by differences in gating kinetics. *J. Neurosci.* **13**, 181-194.

Delcour, A.H. & Tsien, R.W. (1993). Altered prevalence of gating modes in neurotransmitter inhibition of N-type calcium channels. *Science* **259**, 980-984.

Docherty, R.J. (1988). Gadolinium selectively blocks a component of calcium current in rodent neuroblastoma x glioma hybrid (NG108-15) cells. *J. Physiol.* **398**, 33-47.

Docherty, R.J. & McFadzean, I. (1989). Noradrenaline-induced inhibition of voltage sensitive calcium currents in NG108-15 hybrid cells. *Eur. J. Neurosci.* **1**, 132-140.

Dolphin, A.C. (1991). Regulation of calcium channel activity by GTP binding proteins and second messengers. *Biochim. Biophys. Acta.* **1091**, 68-80.

Dolphin, A.C. & Scott, R.H. (1987). Calcium channel currents and their inhibition by (-)-baclofen in rat sensory neurones: modulation by guanine nucleotides. *J. Physiol.* **386**, 1-17.

Dunlap, K. & Fischbach, G.D. (1978). Neurotransmitters decrease the calcium component of sensory neurone action potentials. *Nature* **276**, 837-839.

Eckert, R. & Lux, H.D. (1976). A voltage-sensitive persistent calcium conductance in neuronal somata of Helix pomatia. *J. Physiol.* **254**, 129-151.

Elfvin, L-G., Lindh, B. & Hokfelt, T. (1993). The chemical neuroanatomy of sympathetic ganglia. *Annu. Rev. Neurosci.* **16**, 471-507.

Elliott, P., Marsh, S.J. & Brown, D.A. (1989). Inhibition of Ca-spikes in rat preganglionic cervical sympathetic nerves by sympathomimetic amines. *Br. J. Pharmacol.* **96**, 65-76.

Elmslie, K.S. (1992). Calcium current modulation in frog sympathetic neurones: multiple neurotransmitters and G-proteins. *J. Physiol.* **451**, 229-246.

Elmslie, K.S., Zhou, W. & Jones, S.W. (1990). LHRH and GTP-τ-S modify calcium current activation in bullfrog sympathetic neurones. *Neuron* **5**, 75-80.

Endo, M. (1977). Calcium release from the sarcoplasmic reticulum. *Physiol. Rev.* **57**, 71-108.

Eranko, O. (1976). Histochemical demonstration of catecholamines in sympathetic ganglia. *Ann. Histochim.* **21**, 83-100.

Eranko, O. & Harkonen, M. (1963). Histochemical demonstration of fluorogenic amines in the cytoplasm of sympathetic ganglion cells of the rat. *Acta. Physiol. Scand.* **58**, 285-286.

Fatt, P. & Ginsborg, B.L. (1958). The ionic requirements for the production of action potentials in crustacean muscle fibres. *J. Physiol.* **142**, 516-543.

Fill, M. & Coronado, R. (1988). Ryanodine receptor channel of sarcoplasmic retculum. *Trends. Neurosci.* **11**, 453-457.

Finkel, A.S., & Redman, S. (1984). Theory and operation of a single microelectrode voltage clamp. *J. Neurosci. Meth.* **11**, 101-127.

Fischer, J.E. & Snyder, S.H. (1965). Disposition of norepinephrine-H^3 in sympathetic ganglia. *J. Pharmacol. Exp. Ther.* **150**, 190-195.

Forscher, P. & Oxford, G.S. (1985). Modulation of calcium channels by norepinephrine in internally dialysed avian sensory neurons. *J. Gen. Physiol.* **85**, 743-763.

Fox, A.P., Nowycky, M.C. & Tsien, R.W. (1987a). Kinetic and pharmacological properties distinguishing three types of calcium currents in chick sensory neurones. *J. Physiol.* **394**, 149-172.

Fox, A.P., Nowycky, M.C. & Tsien, R.W. (1987b). Single-channel recordings of three types of calcium channels in chick sensory neurones. *J. Physiol.* **394**, 173-200.

Furchgott, R.F. (1967). The pharmacological characterization of adrenergic receptors. *Ann. N.Y. Acad. Sci.* **139**, 553-570.

Furchgott, R.F. (1970). Pharmacological characteristics of adrenergic receptors. *Fed. Proc.* **29**, 1352-1361.

Galvan, M. & Adams, P.R. (1982). Control of calcium current in rat sympathetic neurones by norepinephrine. *Brain Res.* **244**, 135-144.

Galvan, M. & Sedlmeir, C. (1984). Outward currents in voltage-clamped rat sympathetic neurones. *J. Physiol.* **356**, 115-133.

Gardos, G. (1958). The function of calcium in the potassium permeability of human erythrocytes. *Biochim. Biophys. Acta.* **30**, 653-654.

Gater, P.R., Haylett, D.G. & Jenkinson, D.H. (1985). Neuromuscular blocking agents inhibit receptor mediated increases in the potassium permiability of intestinal smooth muscle. *Br. J. Pharmacol.* **86**, 861-868.

Geduldig, D. & Junge, D. (1968). Sodium and calcium conductance of action potentials in the Aplysia giant neurone. *J. Physiol.* **199**, 347-365.

Goh, J.W. & Pennefather, P.S. (1987). Pharmacological and physiological properties of the after-hyperpolarization current of bullfrog ganglion neurones. *J. Physiol.* **394**, 315-330.

Goh, J.W., Kelly, M.E.M., Pennefather, P.S., Chicchi, G.G., Cascieri, M.A., Garcia, M.L. & Kaczorowski, G.J. (1992a). Effect of charybdotoxin and leiurotoxin I on potassium currents in bullfrog sympathetic ganglion and hippocampal neurones. *Brain Res.* **591**, 165-170.

Goh, J.W., Sanches-Vives, M.V. & Pennefather, P.S. (1992b). Influence of Na/Ca exchange and mobilization of intracellular calcium on the time course of the slow afterhyperpolarization current (I_{AHP}) in bullfrog sympathetic ganglion neurones. *Neurosci. Letts.* **138**, 123-127.

Grant, J.A. & Scrutton, M.C. (1979). Novel α_2-adrenoceptors primarily responsible for inducing human platelet aggregation. *Nature* **277**, 659-661.

Grassi, F. & Lux, H.D. (1989). Voltage-dependent GABA-induced modulation of calcium currents in chick sensory neurones. *Neurosci. Letts.* **105**, 113-119.

Gray, R. & Johnston, D. (1987). Noradrenaline and ß-adrenoceptor agonists increase activity of voltage-dependent calcium channels in hippocampal neurones. *Nature* **327**, 620-622.

Hagiwara, N. & Byerly, L. (1981). Calcium channel. *Annu. Rev. Neurosci.* **4**, 69-125.

Hagiwara, N., Irisawa, H. & Kameyama, M. (1988). Contribution of two types of calcium currents to the pacemaker potentials of rabbit sino-atrial node cells. *J. Physiol.* **395**, 233-253.

Hamill, O.P., Marty, A., Neher, E., Sakmann, B. & Sigworth, F.J. (1981). Improved patch-clamp techniques for high resolution current recording from cells and cell-free membrane patches. *Pflugers Arch.* **391**, 85-100.

Hanbauer, I., Johnson, D.G., Silberstein, S.D. & Kopin, I.J. (1972). Pharmacological and kinetic properties of ^{3}H-noradrenaline uptake by rat superior cervical ganglia in organ culture. *Neuropharmacol.* **11**, 857-862.

Hancock, A.A., Bush, E.N., Stanisic, D., Kyncl, J.J. & Lin, C.T. (1988). Data normalization before statistical analysis: keeping the horse before the cart. *Trends Pharmacol. Sci.* **9**, 29-32.

Harrison, J.K., D'Angelo, D.D., Zeng, D. & Lynch, K.R. (1991). Pharmacological characterization of rat α_2-adrenergic receptors. *Mol. Pharmacol.* **40**, 407-412.

Hill, C.E., Powis, D.A. & Hendry, I.A. (1993). Involvement of pertussis toxin-sensitive and -insensitive mechanisms in α-adrenoceptor modulation of noradrenaline release from rat sympathetic neurones in tissue culture. *Br. J. Pharmacol.* **110**, 281-288.

Hirning, L.D., Fox, A.P., McCleskey, E.W., Olivera, B.M., Thayer, S.A., Miller, R.J. & Tsien, R.W. (1988). Dominant role of N-type Ca^{2+} channels in evoked release of norepinephrine from sympathetic neurones. *Science* **239**, 57-61.

Hirst, G.D.S., Johnson, S.M. & van Helden, D.F. (1985). The slow calcium-dependent potassium current in a myenteric neurone of the guinea-pig ileum. *J. Physiol.* **361**, 315-337.

Hirst, G.D.S. & Spence, I. (1973). Calcium action potentials in mammalian peripheral neurones. *Nature, New Biol.* **243**, 54-56.

Holz, G.G., Rane, S.G. & Dunlap, K. (1986). GTP-binding proteins mediate transmitter inhibition of voltage-dependent calcium channels. *Nature* **319**, 670-672.

Horn, J.P. & McAfee, D.A. (1979). Norepinephrine inhibits calcium-dependent potentials in rat sympathetic neurones. *Science* **204**, 1233-1235.

Horn, J.P. & McAfee, D.A. (1980). Alpha-adrenergic inhibition of calcium-dependent potentials in rat sympathetic neurones. *J. Physiol.* **301**, 191-204.

Hunt, J.M. & Silinsky, E.M. (1993). Ionomycin-induced acetylcholine release and its inhibition by adenosine at frog motor nerve endings. *Br. J. Pharmacol.* **110**, 828-832.

Ikeda, S.R. & Schofield, G.G. (1989). Somatostatin blocks a calcium current in rat sympathetic ganglion neurones. *J. Physiol.* **409**, 221-240.

Ikeda, S.R., Schofield, G.G. & Weight, F.F. (1987). Somatostatin blocks a calcium current in acutely isolated rat superior cervical ganglion neurones. *Neurosci. Letts.* **81**, 123-128.

Jahnsen, H. & Llinas, R. (1984). Ionic basis for the electroresponsiveness and oscillatory properties of guinea-pig thalamic neurones in vitro. *J. Physiol.* **349**, 227-247.

Jenkinson, D.H. (1991). How we describe competitive antagonists: three questions of usage. *Trends Pharmacol.* Sci. **12**, 53-54.

Jones, S.W. (1985). Muscarinic and peptidergic excitation of bull-frog sympathetic neurones. *J. Physiol.* **366**, 63-87.

Jones, S.W. & Marks, T.N. (1989a). Calcium currents in bullfrog sympathetic neurones: I. Activation kinetics and pharmacology. *J. Gen. Physiol.* **94**, 151-167.

Jones, S.W. & Marks, T.N. (1989b). Calcium currents in bullfrog sympathetic neurones: II. Inactivation. *J. Gen. Physiol.* **94**, 169-182.

Kameyama, M., Hofmann, F. & Trautwein, W. (1985). On the mechanism of ß-adrenergic regulation of the Ca channel in the guinea-pig heart. *Pflugers Arch.* **405**, 285-293.

Kasai, H. & Aosaki, T. (1989). Modulation of Ca-channel current by an adenosine analog mediated by a GTP-binding protein in chick sensory neurones. *Pflugers Arch.* **414**, 145-149.

Kasai, H., Aosaki, T. & Fukuda, J. (1987). Presynaptic Ca-antagonist conotoxin irreversibly blocks N-type Ca channels in chick sensory neurones. *Neurosci. Res.* **4**, 228-235.

Kater, S.B., Mattson, C., Cohan, C. & Connor, J. (1988). Calcium regulation of the neuronal growth cone. *Trends Neurosci.* **11**, 315-321.

Katz, B. (1969). The release of neural transmitter substances. Liverpool University Press.

Kawai, T., Oka, J. & Watanabe, M. (1985). Hexamethonium increases the excitability of sympathetic neurones by the blockade of the Ca^{2+}-activated K^{+} channels. *Life Sci.* **36**, 2339-2346.

Kawai, T. & Watanabe, M. (1986). Blockade of Ca-activated K conductance by apamin in rat sympathetic neurones. *Br. J. Pharmacol.* **87**, 225-232.

Kawai, T. & Watanabe, M. (1989). Effects of ryanodine on the spike after-hyperpolarization in sympathetic neurones of the rat superior cervical ganglion. *Pflugers Arch.* **413**, 470-475.

Kawai, T. & Watanabe, M. (1991). Ryanodine suppresses the frequency-dependent component of the spike after-hyperpolarization in the rat superior cervical ganglion. *Japan. J. Pharmacol.* **55**, 367-374.

Kobilka, B.K., Matsui, H., Kobilka, T.S., Yang-Feng, T.L., Francke, U., Caron, M.G., Lefkowitz, R.J. & Regan, J.W. (1987). Cloning, sequencing and expression of the gene coding for the human platlet α_2-adrenergic receptor. *Science* **238**, 650-656.

Koketsu, K. & Nishi, S. (1969). Calcium and action potentials of bullfrog sympathetic ganglion cells *J. Gen. Physiol.* **53**, 608-623.

Koslow, S.H. (1975). Mass fragmentographic analysis of SIF cells catecholamines of

normal and experimental rat sympathetic ganglia. In Eranko, O. (ed). SIF cells. pp 82-88.

Kuba, K. (1980). Release of calcium ions linked to the activation of potassium conductance in a caffeine-treated sympathetic neurone. *J. Physiol.* **298**, 251-269.

Kuba, K., Morita, K. & Nohmi, M. (1983). Origin of calcium ions involved in the generation of a slow afterhyperpolarization in bullfrog sympathetic neurones. *Pflugers Arch.* **399**, 194-202.

Kuba, K. & Nishi, S. (1976). Rhythmic hyperpolarizatioms and depolarization of sympathetic ganglion cells induced by caffeine. *J. Neurophysiol.* **39**, 547-563.

Lancaster, B. & Adams, P.R. (1986). Calcium-dependent current generating the afterhyperpolarization of hippocampal neurones. *J. Neurophysiol.* **55**, 1268-1282.

Lancaster, B. Nicoll, R.A. & Perkel, D.J. (1991). Calcium activates two types of potassium channels in rat hippocampal neurones in culture. *J. Neurosci.* **11**, 23-30.

Lancaster, B. & Pennefather, P. (1987). Potassium currents evoked by brief depolarizations in bull-frog sympathetic ganglion cells. *J. Physiol.* **387**, 519-548.

Lands, A.M., Arnold, A., McAuliff, J.P., Luduena, F.P. & Brown, T.G. (1967). Differentiation of receptor systems activated by sympathomimetic amines. *Nature* **214**, 597-598.

Lang, D.G. & Ritchie, A.K. (1987). Large and small conductance calcium-activated potassium channels in the GH_3 anterior pituitary cell line. *Pflugers Arch.* **410**, 614-622.

Langer, S.Z. (1974). Presynaptic regulation of catecholamine release. *Biochem. Pharmacol.* **23**, 1793-1800.

Langer, S.Z. (1981). Presynaptic regulation of the release of catecholamines. *Pharmacol. Rev.* **32**, 337-362.

Langer, S.Z. & Trendelenburg, U. (1969). The effect of a saturable uptake mechanism on the slopes of dose-response curves for sympathetic amines and on the shifts of dose-response curves produced by a competitive antagonist. *J. Pharmacol. Exp. Ther.* **167**, 117-142.

Lanier, S.M., Downing, S., Duzic, E. & Homcy, C.J. (1991). Isolation of rat genomic clones encoding subtypes of the α_2-adrenergic receptor. *J. Biol. Chem.* **266**, 10470-10478.

Lansman, J.B. (1990). Blockade of current through single calcium channels by trivalent lanthanide cations. *J. Gen. physiol.* **95**, 679-696.

Leranth, C.S., Williams, T.H., Jew, J.Y. & Arimura, A. (1980). Immuno-electron microscope identification of somatostatin in cells and axons of sympathetic ganglia in the guinea-pig. *Cell Tissue Res.* **212**, 83-89.

Lindl, T. (1979). Cyclic AMP and its relation to ganglionic transmission. A combined biochemical and electrophysiological study of the rat superior cervical ganglion in vitro. *Neuropharmacol.* **18**, 227-235.

Lipscombe, D., Kongsamut, S. & Tsien, R.W. (1989). α-Adrenergic inhibition of sympathetic neurotransmitter release mediated by modulation of N-type calcium-channel gating. *Nature* **340**, 639-642.

Lipscombe, D., Madison, D.V., Poenie, M., Reuter, H., Tsien, R.Y. & Tsien, R.W. (1988). Spatial distribution of calcium channels and cytosolic calcium transients in growth cones and cell bodies of sympathetic neurones. *Proc. Natl. Acad. Sci. USA* **85**, 2398-2402.

Lipscombe, D. & Tsien, R.W. (1987). Noradrenaline inhibits N-type Ca channels in isolated frog sympathetic neurones. *J. Physiol.* **390**, 84P.

Llinas, R. & Yarom, Y. (1981). Properties and distribution of ionic conductances generating electroresponsiveness of mammalian inferior olivary neurones in vitro. *J. Physiol.* **315**, 569-584.

Logothetis, D.E., Plummer, M.R., Hess, P. & Nadal-Ginard, B. (1989). Acetylcholine inhibits mostly a sustained rather than an inactivating component of the calcium current in rat sympathetic neurones. *Biophys. J.* **55**, 36a.

Lomasney, J.W., Lorenz, W., Allen, L.F., King, K., Regan, J.W., Yang-Feng, T.L., Caron, M.G. & Lefkowitz, R.J. (1990). Expansion of the α_2-adrenergic receptor family: cloning and expression of a human α_2-adrenergic receptor subtype, the gene for which is located on chromosome 2. *Proc. Natl. Acad. Sci.* USA **87**, 5094-5098.

MacDermott, A.B. & Weight, F.F. (1982). Action potential repolarization may involve a transient, Ca^{2+}-sensitive outward current in a vertebrate neurone. *Nature* **300**, 185-188.

Marchetti, C., Carbone, E. & Lux, H.D. (1986). Effects of dopamine and noradrenaline on Ca channels of cultured sensory and sympathetic neurones of chick. *Pflugers Arch.* **406**, 104-111.

Marrion, N.V., Smart, T.G. & Brown, D.A. (1987). Membrane currents in adult rat superior cervical ganglia in dissociated tissue culture. *Neurosci. Letts.* **77**, 55-60.

Marsh, S.J. & Brown, D.A. (1991). Potassium currents contributing to action potential repolarization in dissociated cultured rat superior cervical sympathetic neurones. *Neurosci. Letts.* **133**, 298-302.

Mathie, A., Bernheim, L. & Hille, B. (1992). Inhibition of N- and L-type calcium channels by muscarinic receptor activation in rat sympathetic neurones. *Neuron* **8**, 907-914.

Matsuda, Y., Yoshida, S. & Yonezawa, T. (1976). A Ca-dependent regenerative response in rodent dorsal root ganglion cells cultured in vitro. *Brain Res.* **115**, 334-338.

Mayer, M.L. (1985). A calcium-activated chloride current generates the after-depolarization of rat sensory neurones in culture. *J. Physiol.* **364**, 217-239.

McAfee, D.A., Henon B.K., Horn, J.P. & Yarowsky, P. (1981). Calcium currents modulated by adrenergic receptors in sympathetic neurones. *Fed. Proc.* **40**, 2246-2249.

McAfee, D.A. & Yarowsky, P.J. (1979). Calcium-dependent potentials in the mammalian sympathetic neurone. *J. Physiol.* **290**, 507-523.

McCleskey, E.W., Fox, A.P., Feldman, D.H., Cruz, L.J., Olivera, B.M., Tsien, R.W. & Yoshikami, D. (1987). Ω-Conotoxin: Direct and persistent blockade of specific types of calcium channels in neurones but not in muscle. *Proc. Natl. Acad. Sci.* USA **84**, 4327-4331.

Medgett, I.C., McCulloch, M.W. & Rand, M.J. (1978). Partial agonist action of clonidine on prejunctional and postjunctional α-adrenoceptors. *Naunyn-Schmiedeberg's Arch. Pharmacol.* **304**, 215-221.

Meech, R.W. (1978). Calcium-dependent potassium activation in nervous tissues. *Annu. Rev. Biophys. Bioeng.* **7**, 1-18.

Meech, R.W. & Strumwasser, F. (1970). Intracellular calcium injection activates potassium conductance in Aplysia nerve cells. *Fed. Proc.* **29**, 834a.

Michel, A.D., Loury, D.N. & Whiting, R.L. (1990). Assessment of imiloxan as a selective α_{2B}-adrenoceptor antagonist. *Br. J. Pharmacol.* **99**, 560-564.

Miller, R.J. (1987). Multiple calcium channels and neuronal function. *Science* **232**, 46-52.

Minota, S. & Koketsu, K. (1977). Effects of adrenaline on the action potential of sympathetic ganglion cells in bullfrogs. *Jap. J. Physiol.* **27**, 353-366.

Moore, G.E. & O'Donnell, S.R. (1970). A potent ß-adrenoceptor blocking drug 4-(2-hydroxy-3-isopropylaminopropoxy)indole. *J. Pharm. Pharmacol.* **22**, 180-188.

Morita, K. & Koketsu, K. (1980). Oscillation of $[Ca]_i$-linked K^+ conductance in bullfrog sympathetic ganglion cell is sensitive to intracellular anions. *Nature* **283**, 204-205.

Morita, K., North, R.A. & Tokimasa, T. (1982). The calcium-activated potassium conductance in guinea-pig myenteric neurones. *J. Physiol.* **329**, 341-354.

Murphy, T.J. & Bylund, D.B. (1988). Characterization of alpha-2 adrenergic receptors in the OK cell, an opossum kidney cell line. *J. Pharmacol. Exp. Ther.* **244**, 571-578.

Neering, I.R. & McBurney, R.N. (1984). Role for microsomal Ca storage in mammalian neurones? *Nature* **309**, 158-160.

Nohmi, M. & Kuba, K. (1984). (+)-Tubocurarine blocks the Ca^{2+}-dependent K^{+}-channel of the bullfrog sympathetic ganglion cell. *Brain Res.* **301**, 146-148.

Nohmi, M., Kuba, K. & Morita, K. (1983). Does intracellular release of Ca^{2+} participate in the afterhyperpolarization of a sympathetic neurone. *Brain Res.* **268**, 158-161.

North, R.A. & Tokimasa, T. (1983). Depression of calcium-dependent potassium conductance of guinea-pig myenteric neurones by muscarinic agonists. *J. Physiol.* **342**, 253-266.

North, R.A. & Tokimasa, T. (1987). Persistent calcium-sensitive potassium current and the resting properties of guinea-pig myenteric neurones. *J. Physiol.* **386**, 333-353.

Nowycky, M.C., Fox, A.P & Tsien, R.W. (1985). Three types of neuronal calcium channel with different calcium agonist sensitivity. *Nature* **316**, 440-443.

Olivera, B.M., McIntosh, J.M., Cruz, L.J., Luque, F.A. & Gray, W.R. (1984). Purification and sequence of a presynaptic peptide toxin from conus geographus venom. *Biochemistry* **23**, 5087-5090.

Pennefather, P., Lancaster, B., Adams, P.R. & Nicoll, R.A. (1985). Two distinct Ca-dependent K currents in bullfrog sympathetic ganglion cells. *Proc. Natl. Acad. Sci. USA* **82**, 3040-3044.

Perney, T.M., Hirning, L.D., Leeman, S.E. & Miller, R.J. (1986). Multiple calcium channels mediate neurotransmitter release from peripheral neurones. *Proc. Natl. Acad. Sci.* USA **83**, 6656-6659.

Plummer, M.R. & Hess, P. (1991). Reversible uncoupling of inactivation in N-type calcium channels. *Nature* **351**, 657-659.

Plummer, M.R., Logothetis, D.E. & Hess, P. (1989). Elementary properties and pharmacological sensitivities of calcium channels in mammalian peripheral neurons. *Neuron* **2**, 1453-1463.

Plummer, M.R., Rittenhouse, A., Kanevsky, M. & Hess, P. (1991). Neurotransmitter modulation of calcium channels in rat sympathetic neurons. *J. Neurosci.* **11**, 2339-2348.

Przywara, D.A., Bhave, S,V., Chowdhury, P.S., Wakade, T.D. & Wakade, A.R. (1993). Sites of transmitter release and relation to intracellular Ca^{2+} in cultured sympathetic neurones. *Neurosci.* **52**, 973-986.

Rafuse, P.E. & Smith, P.A. (1986). α_2-Adrenergic hyperpolarization is not involved in slow synaptic inhibition in amphibian sympathetic ganglia. *Br. J. Pharmacol.* **87**, 409-416.

Rall, W. (1977). Core conductor theory and cable properties of neurons. In Kandel, E.R. (Ed.) Handbook of Physiology, Section 1, The nervous system. Williams & Wilkins, USA. pp 39-97.

Rane, S.G., Holz, G.G. & Dunlap, K. (1987). Dihydropyridine inhibition of neuronal calcium current and substance P release. *Pflugers Arch.* **409**, 361-366.

Regan, J.W., Kobilka, T.S., Yang-Feng, T.L., Caron, M.G., Lefkowitz, R.J. & Kobilka, B.K. (1988). Cloning and expression of a human kidney cDNA for an α_2-adrenergic receptor subtype. (1988) *Proc. Natl. Acad. Sci.* USA **85**, 6301-6305.

Reinert, H. (1963). Role and origin of noradrenaline in the superior cervical ganglion. *J. Physiol.* **167**, 18-29.

Reuter, H. (1983). Calcium channel modulation by neurotransmitters, enzymes and drugs. *Nature* **301**, 569-574.

Reynolds, I.J., Wagner, J.A., Snyder, S.H., Thayer, S.A., Olivera, B.M. & Miller, R.J. (1986). Brain voltage-sensitive calcium channel subtypes differentiated by Ω-conotoxin fraction GVIA. *Proc. Natl. Acad. Sci. USA* **83**, 8804-8807.

Rittenhouse, A.R. & Hess, P. (1994). Microscopic heterogeneity in unitary N-type calcium currents in rat sympathetic neurones. *J. Physiol.* **474**, 87-99.

Robbins, J., Cloues, R. & Brown, D.A. (1992). Intracellular Mg^{2+} inhibits the IP_3-activated $I_{K(Ca)}$ in NG108-15 cells. [Why intracellular citrate can be useful for recording $I_{K(Ca)}$]. *Pflugers Arch.* **420**, 347-353.

Robitaille, R. & Charlton, M.P. (1992). Presynaptic calcium signals and transmitter release are modulated by calcium-activated potassium channels. *J. Neurosci.* **12**, 297-305.

Robitaille, R., Garcia, M.L., Kaczorowski, G.J. & Charlton, M.P. (1993). Functional colocalization of calcium and calcium-gated potassium channels in control of transmitter release. *Neuron* **11**, 645-655.

Romey, G. & Lazdunski, M. (1984). The coexistance in rat muscle cells of two distinct classes of Ca^{2+}-dependent K^{+} channels with different pharmacological properties and different physiological functions. *Biochem. Biophys. Res. Commun.* **118**, 669-674.

Sah, D.W.Y., Regan, L.J. & Bean, B.P. (1989). Calcium channels in rat neurones.: high threshold channels that are resistant to both Ω-conotoxin and dihydropyridine blockers. *Soc. Neurosci. Abstr.* **15**, 823.

Schild, H.O. (1949). pA_x and competitive drug antagonism. *Br. J. Pharmacol.* **4**, 277-280.

Schofield, G.G. (1990). Norepinephrine blocks a calcium current of adult rat sympathetic neurones via an α_2-adrenoceptor. *Eur. J. Pharmacol.* **180**, 37-47.

Schofield, G.G. (1991). Norepinephrine inhibits a Ca^{2+} current in rat sympathetic neurones via a G-protein. *Eur. J. Pharmacol.* **207**, 195-207.

Schofield, G.G. & Ikeda, S.R. (1988). Sodium and calcium currents of acutely isolated adult rat superior cervical ganglion neurons. *Pflugers Arch.* **411**, 481-490.

Schofield, G.G. & Ikeda, S.R. (1989). Potassium currents of acutely isolated adult rat superior cervical ganglion neurons, *Brain Res.* **485**, 205-214.

Schwartzkroin, P.A. & Slawsky, M. (1977). Probable calcium spikes in hippocampal neurones. *Brain Res.* **135**, 157-161.